Studies on CD40mAb-adjuvanted conjugate vaccines

Thesis Submitted by

Tessabelle Sultana

For

The degree of Doctor of Philosophy

Department of Infection & Immunity

Faculty of Medical School

November 2014

ACKNOWLEDGEMENTS

First and foremost, I would like to thank my supervisors, Professor Andrew W. Heath and Dr. Jennifer Carlring-Wright for the opportunity to read for this PhD, for their time and patience, as well as for always keeping me on my proverbial toes by constantly challenging me. I would also like to thank Ms. Catherine Cooke and Ms. Amy Lewis for technical support, Dr. Martina Daly and Dr. Pete Monk for scientific advice, Ms. Sue Newton and Ms. Kay Hopkinson for flow cytometry help, Dr. David Williams and Dr. Oliver Wilkinson for such an interesting time at the Chemistry Department and Dr. Simon Johnston for the time and effort invested in my microscopy work. I have learned a great deal from this PhD journey thanks to all of you. I am also very grateful for the constructive advice given by my thesis mentor, Dr. Kay Guccione and personal mentor Dr. Martin Nicklin. Last but not least I would like to show my gratitude to my very interesting colleagues and peers Dr. Jonathan Shaw, Dr. Sabela Balboa, Dr. Richard Jones, Ms. Magdalena Wierzbicka and Ms. Furaha Rooshie Asani.

Beyond science, I am blessed with the best support system anyone could ever hope for. My auntie Johanna Rizzo and my jolly Mexican friend Lorena Preciado Llanes are the pillars of my life. Your ambition and strong-will inspired me to work harder. Edwina Muscat, my non-blood sister, for her listening to my incessant complaining in stressful times, unfaltering support and proof reading science! You are the best. I would like to express my gratitude to my parents, Doris and Paul Sultana, for always blindly believing in me and for your financial support. Also, my sister Beverie Sultana, the strongest person emotionally and physically (!) I have the pleasure of knowing, for transferring some of her strength when times got very hard and my lovely, super-brother Nigel Sultana, for the best hugs in the world. I will always cherish our very grumpy brother-sister quality study-time in the basement! Finally, but definitely not in order of importance, I would like to thank my partner in crime, my source of positivity, Charlotte Evans. *Inħobbok b'qalbi kollha*. Thank you for your unceasing patience and understanding, and sticking by me through the past four years of this PhD.

“Everything is theoretically impossible, until it is done”

Robert A. Heilein

SUMMARY

The field of cancer vaccines has been investigated for decades, but it is still in the early stages of development. The slow progress can be partly attributed to shortcomings in vaccine design, which induced ineffective anti-tumour cytotoxic responses. An increasing number of adjuvants are currently being researched to overcome these shortcomings, but effective adjuvants are in most cases, unsafe and not well-tolerated. In fact the number of licensed adjuvants for human use are few.

The adjuvant of interest in this work was CD40mAb, which stimulates CD40 mimicking T cell help in the CD40-CD154 co-stimulatory pathway. Previous publications showed that conjugation of CD40mAb to antigen enhanced the immunogenicity of the antigen by up to a 1000-fold. The primary finding in this thesis showed that a low average molecular weight conjugate maximised the adjuvant potential of CD40mAb, and a strong trend of enhanced overall and median survival in a murine tumour model when administered as a prophylactic vaccine was observed.

Cancer vaccines that progressed to Phase III clinical trials include the B cell lymphoma therapeutic vaccines. Most B cell lymphoma patients are routinely treated with rituximab that depletes B cells. Thus, another aim was to identify if B cells or DCs are the primary target of the CD40mAb as an adjuvant. This would give valuable information in defining the optimal timing of the CD40mAb-Id therapy relative to other therapies such as rituximab. The work presented shows that CD40mAb conjugated to antigen targeted and activated both B cells and DCs *in vitro*. In addition, CD40mAb enhanced cross-presentation by both B cells and DCs *in vitro*.

A central finding of this thesis is that CD40mAb-adjuvanted vaccines directly enhanced $CD8^+$ cytotoxic T cell responses against the conjugated antigen in a murine system. The aforementioned results together with the knowledge that CD40mAb immunotherapy in human cancer trials is well-tolerated shows the great potential of CD40mAb as an adjuvant in therapeutic and prophylactic vaccines.

CONTENTS

LIST OF FIGURES

CHAPTER 1

CHAPTER 2

CHAPTER 3

CHAPTER 4

CHAPTER 5

LIST OF TABLES

ABBREVIATIONS

2ME	2-mercaptoethanol
AS	Adjuvant system
APC	Antigen presenting cell
BCG	Bacille Calmette-Guérin
BCR	B cell receptor
BM-DC	Bone marrow derived dendritic cells
BSA	Bovine Serum Albumin
CD40mAb	Anti-CD40 monoclonal antibody
cDC	Classical dendritic cell
CDP	Common dendritic cell precursors
CFSE	Carboxyfluorescein diacetate succinimidyl ester
ConA	Concavalin A
CSP	Circumsporozoite protein
CTL	Cytotoxic T lymphocyte
CTLA-4	Cytotoxic T lymphocyte-associated molecule-4
dH_2O	Ultrapure or de-ionised Water
DAMP	Damage-associated molecular pattern
DBCO	Dibenzylcyclooctyne-NHS ester
DC	Dendritic cell
DMF	Dimethylformamide
DMSO	Dimethylsulphoxide
FCA	Freund's complete adjuvant
FCS	Fetal calf serum
FITC	Fluorescein isothiocyanate
GC	Germinal centre
GM-CSF	Granulocyte-macrophage colony-stimulating factor
H_2O_2	Hydrogen peroxide
Hib	*Haemophilus influenza* type b
HbOC	Polyribosylribitol phosphate conjugated to CRM_{197}
HCV	Hepatitis C Virus
HPV	Human Papilloma Virus
ICAM-1	Intracellular adhesion molecule - 1
Id	Idiotype
IFN	Interferon
IFN-ϒ	Interferon (IFN)-ϒ
Ig	Immunoglobulin
IL	Interleukin

i.p.	Intraperitoneal
i.v.	Intravenous
IRF-3	Interferon-regulatory factor-3
ISQ	ISQAVHAAHAEINAGR peptide
ISQC	ISQAVHAAHAEINAGRC peptide
KLH	Keyhole limpet hemocyanin
LAL	Limulus Amebocyte Lysate
LP	Lymphoid-committed progenitors
LPS	Lipopolysaccharide
mAb	Monoclonal antibody
MDP	Macrophages, monocyte and DC precursors
MF59	Microfluidized emulsion 59
MHC	Major histocompatibility complex
MP	Myeloid-committed progenitors
MPL	Monophosphoryl lipid A
MW	Molecular weight
NEM	N-ethylmaleimide
NHS-PEG4-Azide	15-Azido-4,7,10,13-tetraoxa-pentadecanoic acid succinimidyl ester
NK cells	Natural killer cells
NOD	Nucleotide-binding and oligomerisation domain
NLR	Nod-like receptor
NLRPs	Nod-like pyrin domain-containing proteins
NF B cells	Naïve follicular B cells
O_2^-	Superoxide anion
OD	Optical density
OPD	*o*-Phenylenediamine dihydrochloride
OVA	Ovalbumin
PAMP	Pathogen-associated molecular pattern
PBS	Phosphate buffered saline
pDC	Plasmacytoid dendritic cell
PCD	Programmed cell death
PD	Programmed death
PE	R-Phycoerythrin
PE/Cy7	PE/Cyanine7
PLGA	Poly(d,l-lactic-co-glycolic acid) polymer
PMA	Phorbol 12-myristate 13-acetate
PRP	Polyribosylribitol phosphate
PRP-T	PRP conjugated to tetanus toxoid
PRP-OMP	PRP conjugated to conjugated to the *Neisseria meningitidis* group B strain outer membrane

PRR	Pathogen recognition receptor
QS-21	Quillaja saponaria-21
R1 medium	RPMI 1640 supplemented with 10% FCS, 2-ME, Penicillin and Streptomycin
R2 medium	R1 medium supplemented with GM-CSF and IL-4
RIH	Rig-I-like helicases
ROS	Reactive oxygen species
RT	Room temperature
SATA	N-Succinimidyl S-Acetylthioacetate
s.c.	Subcutaneous
Sulfo-SMCC	Sulfosuccinimidyl 4-[N-maleimidomethyl]-cyclohexane-1-carboxylate
TAA	Tumour-associated antigen
TAP	Transporter-associated with antigen processing
TCR	T-cell receptor
TD	T-cell dependent
T_H cell	T-helper cell or $CD4^+$ T cell
TI	T-cell independent
TI-1	T-cell independent type 1
TI-2	T-cell independent type 2
TipDC	Inflammatory DC
TLR	Toll-like receptor
TNF-α	Tumour necrosis factor-α
TNFRSF	Tumour necrosis factor receptor superfamily
TRAF	TNFR-associated factors
Treg	Regulatory T cell
VLP	Virus-like particle

CHAPTER 1

INTRODUCTION

1.1. Basic concepts of the immune response

The primary lines of defence against pathogens are the physical barriers of the host body, for example the skin, ciliated epithelia and mucous membranes. The first immune cells that pathogens come into contact with once they break the first line of defence are the phagocytic white blood cells like macrophages, which reside in different tissues and neutrophils that patrol the lymph and blood circulation. Both macrophages and neutrophils are able to rapidly and non-specifically phagocytose pathogens. Phagocytosis is the process by which pathogens are internalised into phagosomes where they are killed by the production of toxic compounds like hydrogen peroxide (H_2O_2) and superoxide anion (O_2^-). Tissue macrophages also release chemokines and cytokines upon pathogen encounter that lead to an inflammatory response. Another tissue-residing cell type, the dendritic cell (DC) is also efficient at antigen-uptake at the site of infection (Murphy et al., 2008). Immune cells are able to identify self from non-self by certain structures expressed by pathogens or transformed cells, and become activated. Activation of tissue-residing macrophages and DCs as well as mobile cells like neutrophils, natural killer (NK) cells and eosinophils lead to the release of cytokines like interleukins (IL) and tumour necrosis factor (TNF-α), and the rapid recruitment of more cells to the site of infection by means of enhanced permeability of vessels leading to inflammation (Moser and Leo, 2010). Inflammation could also be triggered by activation of the complement system, which activates phagocytes and mast cells to release granules containing histamine. The complement system consists of a number of plasma proteins that work collectively to opsonise pathogens to aid in the internalisation by phagocytes (Murphy et al., 2008).

In anti-tumour immunity, DCs at the tumour site sample tumour antigens, which could be (i) mutated protein typical of tumours, (ii) the products of non-mutated genes preferentially expressed by tumour cells, or (iii) differentiation antigen linked with tumour origin. DC activation, a step crucial to promote immunity, is supplied by signals from necrotic tumour cells (Sauter et al., 2000, Brusa et al., 2008). Tumour cells also express endoplasmic reticulum (ER) proteins like calreticulin on their plasma membrane that promote tumour cell phagocytosis (Mellman et al., 2011). Innate recognition of tumours is mediated by type I interferon (IFN), which is predominantly

secreted by a subset of DC at the site of the tumour (Cella et al., 1999). NK cells are activated by IFNs and target certain ligands expressed by malignantly transformed cells. NK cells also target cells that have lost surface molecules like major histocompatibility complex (MHC), making them crucial for early defence against tumours (Mocikat et al., 2003). NK cells mediate tumour-directed killing by binding to malignant cells and releasing cytotoxic granules and effector proteins that induce programmed cell death (Hayakawa et al., 2002, Murphy et al., 2008).

If the innate immune mechanisms are inefficient in clearing the tumour or infection, the second line of defence is induced, which directs a specific and long-lasting immune response against the pathogens or malignant cells. The adaptive immune response is not exclusively induced against antigens that escape the innate immune response. Vaccine antigens presented by migratory DCs (De Vries et al., 2003a, De Vries et al., 2003b, Lesterhuis et al., 2011, Mellman et al., 2011), also induce adaptive immunity.

The cellular backbones of the adaptive immune response are the B and T lymphocytes. Mature naive lymphocytes develop in the primary lymphoid organs, and are found circulating in the lymph and the blood as well as within the secondary lymphoid organs, such as the lymph nodes and spleen where the adaptive immune response is initiated. Both B and T lymphocytes become activated by engagement of their B cell (BCR) or T cell receptors (TCR) (respectively) to specific antigens (Moser and Leo, 2010). Antigen-specific naive $CD4^+$ (helper) T cells and $CD8^+$ (cytotoxic) T cells are found in low frequencies in the absence of antigen, but once encountering foreign antigen predominantly presented by migrating DCs, they undergo clonal expansion leading to the formation of effector and memory T cells. Antigen can also be presented to T cells by other antigen presenting cells (APCs) namely B cells or macrophages resident in the secondary lymphoid organs. Following activation, B cells undergo proliferation and differentiate into antibody-producing plasma cells as well as memory cells. These B and T memory cells together with antibody responses constitute the basis for protection against disease and infection. Immune memory is an important property of the adaptive immune response, and allows a rapid and more robust response once the host re-encounters the same pathogen (Moser and Leo, 2010).

1.1.1. Pattern recognition receptors of the innate immune system

DCs, macrophages and B cells have pattern recognition receptors (PRRs) that are able to identify a series of conserved molecular structures expressed by pathogens or malignant cells. The conserved molecular structures can be divided into two groups. The first group is the pathogen-associated molecular patterns (PAMPs) that include flagella and lipoproteins, and the second group is the damage-associated molecular patterns (DAMPs) that include heat shock proteins and extracellular ATP (Moser and Leo, 2010). Whilst PAMPs are molecules of exogenous nature found selectively on a group of microbes, DAMPs are molecules of endogenous nature released on tissue damage or cell lysis due to infection or tumour.

The cells of the innate immune system can therefore directly identify pathogens in an infectious event, a mechanism first described by Janeway and referred to as the Pattern Recognition Theory (Janeway, 1989b). Cell damage or stress resulting from infection or tumour can also be directly identified. The latter mechanism was described by Matzinger and referred to as the Danger Theory (Matzinger, 1994). The signals released from PAMPs or DAMPs are known as 'danger signals' characterised by the release of chemokines and cytokines from the cells of the innate immune system.

The most well-characterised PRRs include the membrane bound Toll-Like receptors (TLRs). Ten types have been recently discovered in humans and these have been classified according to the type of PAMPs they recognise and where they are localised (Table 1.1.) (Moser and Leo, 2010). TLRs also respond to some DAMP signalling (Sollinger et al., 2014). The activation of TLRs leads to the production of proinflammatory cytokines such as IL-6 and TNF-α, as well as to APC activation linking the innate response to the adaptive immune response.

Microbes express multiple PAMPs that lead to different TLRs being activated simultaneously. Since different TLRs respond to different adaptor proteins, the nature of the TLR being activated shapes the immune response. Different signalling pathways are induced depending on the PAMP stimulated, leading to the activation of transcription factors including activation protein (AP)-1, nuclear factor (NF)-$_{K}$B and interferon-regulatory factor (IRF)-3 (Krishnaswamy et al., 2013).

Stimulation of TLRs leads to the release of danger signals in response to microbes or altered endogenous molecules presented on the cell surface or in endosomal compartments. In contrast to TLR family members, two other families of PRRs, RIG-I-like helicases (RIHs) and Nod-like receptors (NLRs), recognise and respond to microbial components that escaped into the cytosol (Maisonneuve et al., 2014).

The innate immune response is not specific and does not provide immunological memory, which together with the lack of knowledge about PRRs were reasons why the innate immune response was taken for granted for vaccine development in the past. However, due to recent progress in immunology, the innate immune system is also considered a target of interest in vaccine design.

TLRs expressed on the cell surface		
TLR	**PAMP**	**DAMP**
1	lipopeptides, peptidoglycan	-
2	lipopeptides, zymosan, glycolipids, lipoteichoic acid	-
4	lipopolysaccharide, virus envelope protein, respiratory syncytial virus fusion protein, mouse mammary tumour, phosphorylcholine	defensin 2, hyaluronic acid, fibrinogen, heat shock protein, high-mobility group 1 protein
5	flagellin	-
6	lipopeptides	-
TLRs expressed in endosomal compartments		
TLR	**PAMP**	**DAMP**
3	small interfering RNA, double-stranded RNA	messenger RNA
7/8	imidaqzoquinoline, imiquidmod, resiquimod, single-stranded RNA	Autoantigens-containing immune complexes, U1 small nuclear RNA
9	CpG DNA	Chromatin complex
10	Unknown – but has been implicated in viral infections	

Table 1.1. Ten types of TLRs and their respective PAMPs and DAMPs which are expressed either on the cell surface or in endosomal compartments (Moser and Leo, 2010, Lee et al., 2014).

1.1.2. Dendritic cells connect the innate and adaptive immune response

DCs patrol peripheral organs in an antigen-sampling state characterised by high endocytic and phagocytic potential in the immature state. DCs take up pathogen- or tumour-derived antigens in the peripheral organs through pinocytosis, phagocytosis and receptor-mediated endocytosis (Reis e Sousa et al., 1993, Jiang et al., 1995, Sallusto et al., 1995). Upon uptake of antigen, DCs migrate to areas of secondary lymphoid organs that are T cell rich and mature into an antigen-presenting state by upregulating expression of MHC and co-stimulatory molecules such as CD40, CD80 and CD86 and adhesion molecules such as intracellular adhesion molecule (ICAM)-1 (Sallusto et al., 1995, Cella et al., 1997, Vermaelen et al., 2001, Henri et al., 2001). This mechanism is known as the Langerhans cell paradigm. The enhanced surface antigen expression make DCs better equipped to activate naive T helper (T_H) cells residing in the lymph node (Cella et al., 1996). The ability of DCs to migrate to the secondary lymphoid organs and differentiate marks a very important difference to macrophages that typically remain at the site of antigen-uptake. Macrophages are very efficient phagocytes of cellular debris, pathogens and dead cells, and rapidly break down internalised antigens into amino acids. In contrast, DCs retain internalised antigens in phagosomes for extended time periods and can still efficiently present the peptides to T cells (Turley et al., 2000).

1.1.2.1. DC subsets

DCs make up a heterogeneous group of efficient APCs that are phenotypically and functionally diverse. In spite of the great advances made in understanding DC subsets, deciphering between the different DC types is still a challenging task. DCs present in peripheral tissues and lymphoid organs are constantly being replenished from hematopoietic stem cells (HSCs) in the bone marrow (Liu et al., 2007). HSCs give rise to either lymphoid (LP) or myeloid (MP) committed progenitors. DCs could arise from either LP or MP origin, but a fate-mapping study showed that only a small proportion of DCs arise from LP progenitors (Schlenner et al., 2010). MPs lead to the generation of precursors of macrophages, monocytes and DCs (MDPs), which in turn generate common DC precursors (CDPs), monocytes and some subsets of macrophages. MDPs and CDPs are only found in the bone marrow (Liu et al., 2009).

CDPs can give rise to all subsets of DCs. DC subsets migrating to the spleen only do so via the blood, whilst DC subsets migrating to the lymph nodes do so via the blood as well as the lymphatic system (Jakubzick et al., 2008). DC subsets residing in the secondary lymphoid organs are classical or conventional DCs (cDCs), plasmacytoid DCs (pDCs) and DCs subsets arising from monocytes (Liu et al., 2007).

1.1.2.1.1. cDCs

The CDPs in the bone marrow develop into pre-cDCs that migrate through the blood stream to the secondary lymphoid organs where they further divide and differentiate (Liu et al., 2007, Liu et al., 2009). Therefore, in contrast to pDCs and monocytes, cDCs that are resident in the lymphoid tissues migrate out of the bone marrow as immature cells. Different cDCs are categorised according to their function, location and phenotypic surface markers.

There are two main types of cDC subsets in secondary lymphoid organs, namely (i) $CD8^{+}DEC205^{+}$ and (ii) $CD8^{-}33D1^{+}$ (Dudziak et al., 2007). In the spleen, the cDC subset $CD8^{+}DEC205^{+}$ can be found in the T cell zone and are specialised for uptake from apoptotic cells and cross-presenting the antigens to $CD8^{+}$ T cells (den Haan et al., 2000). In contrast, cDC subset $CD8^{-}33D1^{+}$ can be found in the pulp and marginal zone of the spleen and is specialized for presentation of antigen to $CD4^{+}$ T cells (Dudziak et al., 2007). Both $CD8^{+}$ and $CD8^{-}$ cDC subsets have a short half-life and are continuously replaced from the bone marrow precursors via a FMS-related tyrosine kinase 3 ligand (Flt3L)-dependent mechanism (Waskow et al., 2008).

Another two subsets of cDCs can be found in non-lymphoid tissues including the skin, lung and liver. These include $CD103^{+}CD11b^{low}$ and $CD103^{-}CD11b^{high}$ DCs (Ginhoux et al., 2009). In the skin, $CD103^{+}$ cDCs are very similar to $CD8^{+}$ cDCs, and also specialize in cross-presentation of antigens (Bedoui et al., 2009). In a steady state skin-derived cDCs account for 20% of DCs in the lymph nodes (Jakubzick et al., 2008), a percentage which rises dramatically in the presence of inflammation (Jakubzick et al., 2008), mechanical or chemical stress (Tomura et al., 2014).

It is worthy to mention that the maturation status of the cDC subsets residing in lymphoid and non-lymphoid tissues is variable. cDCs residing in the peripheral organs

are phenotypically immature which mature prior to migration to the lymphoid organs conforming with the Langerhans cell paradigm. However, in contrast to the paradigm cDCs in the secondary lymphoid organs were also found to be relatively immature (Wilson et al., 2003, Wilson et al., 2004, Dudziak et al., 2007).

1.1.2.1.2. pDCs

The pDC subset in contrast to the cDC subset, matures in the bone marrow and migrates to the secondary lymphoid organs also via the bloodstream. pDCs are a $CD11c^{lo}CD11b^{-}CD45RA^{hi}$ population (O'Keeffe et al., 2003) that could be distinguished from cDCs by their characteristic spherical appearance similar to antibody-bearing plasma cells (Cella et al., 1999). In addition, pDCs also express the surface markers; bone marrow stromal cell Ag 2 (BST2) (Blasius et al., 2006) and Siglec-H (Zhang et al., 2006) in murine systems and BDCA2 (Dzionek et al., 2001) in human systems. pDCs respond to oligonucleotides containing CpG motifs in culture (O'Keeffe et al., 2003) and viral infection (Cella et al., 1999) by producing type I IFN, which maintains a prolonged T cell response and crucial anti-viral and anti-tumour immunity.

1.1.2.1.3. Monocyte-derived DCs

Monocytes are blood mononuclear cells that express F4/80 and CD11b in mice and CD11c, CD11b and CD14 in humans (Geissmann et al., 2003). Murine monocytes in the blood derived from MDPs in the bone marrow, do not differentiate to cDCs or pDCs (Liu et al., 2007) but into $Gr1^{+}CX3CR1^{low}CCR2^{+}$ monocytes that in turn give rise to DCs during inflammation caused by infection (Serbina et al., 2003, Geissmann et al., 2003). The inflammatory DC subset is called TipDCs that produce mediators of inflammation like iNOS, TNF and reactive oxygen species (Serbina et al., 2003). The TipDC subset is only present in the spleen following systemic infection. The human equivalents of the inflammatory monocyte subset are of the phenotype $CD14^{low}CD16^{+}$ (Geissmann et al., 2003).

In vitro, murine and human DCs can be generated from bone marrow-derived monocytes in culture using the cytokines GM-CSF and other cytokines for example IL-4 (Sallusto and Lanzavecchia, 1994, Son et al., 2002, Galea-Lauri et al., 2004). Similar to cDCs, DCs generated *in vitro* display an immature phenotype after a specified time in

culture that develop a mature phenotype after stimulation. However, the corresponding *in vivo* DC subset is still unclear.

1.1.3. $CD4^+$ T lymphocytes

Naive T helper lymphocytes (T_H cells) express CD4 surface marker and only become activated to form cytokine-producing effector cells, when they recognise antigens in the form of particular peptides on the surface of the MHC class II harboured by APCs (Interactions between T cells and APCs, *see* Section 1.1.6.). Effector lymphocytes do not circulate in the blood or lymph like naive lymphocytes, instead they either migrate to the site of infection via the blood or remain in the secondary lymphoid organs. A sign of T_H cell activation is IL-2 production (Morgan et al., 1976, Taniguchi et al., 1983). A defining characteristic of antigen-specific T_H cells is that post-activation, effector T_H cells can develop into different subsets including T_H1, T_H2, T_H17 and regulatory T cells (Treg), shaping the immune response according to the invading pathogen or transformed cells.

The T cell subtypes, T_H1 and T_H2, were first discovered in mice by Mossman and Coffman in 1986 (Mosmann et al., 1986). T_H cell polarisation into the T_H1 subtype is induced by intracellular pathogens and driven by the cytokine IL-12 (Seder et al., 1992). T_H1 cells produce IFN-γ that leads to (i) inflammation and macrophage activation (Nathan et al., 1983), as well as (ii) $CD8^+$ T cell-directed killing (Whitmire et al., 2005), for an anti-bacterial, anti-viral and anti-tumour response. T_H1 cells are therefore specialised for cell-mediated responses and phagocyte-dependent inflammation for clearance of intracellular pathogens. The T_H2 response is driven by the cytokine IL-4 (Seder et al., 1992) and is characterised by the cytokines IL-4, IL-5 and IL-13 that promote the humoral immune response. T_H2 cells are the main T_H cells that provide help for the production of isotype class-switched antibodies by B cells, especially IgG1 (Vitetta et al., 1985) and IgE (Kaplan et al., 1996, Coffman et al., 1986), and are important for the clearance of parasites (Collins et al., 1995). Due to induction of proinflammatory IgE isotype-class switch, T_H2 cells also contribute to the pathological response in asthma (Wong et al., 2001). Once naïve T_H cells commit to a

particular T_H subset lineage, cytokines produced by one pathway inhibit cytokines produced by another pathway. For example, IFN-γ production blocks T_H2 differentiation (Whitmire et al., 2005). The T_H17 subset is characterised by the production of IL-17 and IL-22, important for the protection against extracellular bacterial and fungal diseases (Aujla et al., 2008, Hernández-Santos et al., 2013). The cytokines IL-17 and IL-22 can however, also play a pathogenic role in autoimmune disease (Nakae et al., 2003). The development of T_H17 is driven by mainly tumour-growth factor (TGF)-β (Veldhoen et al., 2006) as well as IL-6 (Bettelli et al., 2006), and maintained by maintained by IL-23 (Park et al., 2005). The Treg subset, as their name implies are regulatory T cells with a lead role in immune and inflammatory response suppression, maintenance of self-tolerance and prevention of autoimmunity. Tregs produce TGF-β and IL-10, which induce isotype-switching to IgG4 and IgA and suppress IgE production (respectively) (Taylor et al., 2006).

1.1.3.1. DC influence on T cell differentiation

Mice with depleted DCs fail to mount an appropriate adaptive response (Phythian-Adams et al., 2010), indicating that DCs are fundamental in $CD4^+$ T cell priming. DCs of the innate immune response could be regarded as a converter station that identifies and translates pathogen input signals into output signals that have a direct effect on T_H cell polarisation. An example of an input signal is PRR stimulation. The output DC signals are (i) co-stimulatory molecule expression, (ii) antigen presentation and (iii) cytokine production (Walsh and Mills, 2013).

DCs expressing high levels of co-stimulatory molecules tend to activate T_H1, T_H2 and T_H17 subsets, whilst Tregs only become activated by immature or partially mature human DCs (Jonuleit et al., 2000). Tregs upregulate negative regulator molecules such as for example cytotoxic T lymphocyte–associated molecule 4 (CTLA-4) which binds to the CD80 and CD86 molecules instead of CD28. This inhibits T cell stimulation that leads to immunosuppression. Therefore, DCs presenting peptide in a steady state promote tolerance by driving Treg differentiation.

The extent of peptide presented by the DCs as well as the strength of the TCR binding to the peptide influences the functional differentiation of T_H subsets. A low concentration of peptide presented and a weak affinity to TCR tends to skew towards a T_H2 phenotype whilst a high concentration of peptide presented and a strong affinity to TCR skews towards a T_H1 phenotype (Constant et al., 1995, Tao et al., 1997).

TLRs play an important role in DC driven T_H differentiation. As summarised in Table 1.1, different TLRs expressed by different cells, respond to different adaptor proteins. This means the nature of the TLR activated, shapes the immune response, which is influenced by cytokine production. For example, TLR4 stimulation by lipopolysaccharide (LPS) leads to IL-12 production which predominantly induces the T_H1 response (Krummen et al., 2010). Furthermore, TLR4 stimulation also leads to IL-23 production which maintains T_H17 differentation (Abdollahi-Roodsaz et al., 2008). TLR2 knockout mice show impaired IL-10 production and reduced Treg numbers, which means that TLR2 stimulation has a role in the induction of Treg subsets (Netea et al., 2004).

Specific DC subsets also have a role in influencing the T_H polarisation (Figure 1.1). The lymphoid $CD8^+$ DC subsets have been reported to have the highest potential to produce IFN-y when stimulated with IL-12 (Ohteki et al., 1999). The $CD103^+CD11b^{low}$ (*see* Section 1.1.2.1.1.) subset being the migratory non-lymphoid complementary subset of $CD8^+$ DCs also demonstrates a role in driving T_H1 responses, however they have been reported to also produce IL-17, the characteristic cytokine of the T_H17 response (King et al., 2010). Conversely, $CD103^-CD11b^{high}$ (*see* Section 1.1.2.1.1.) induced T_H2 responses that in turn were an important mediator of allergic inflammation caused by the dust mite antigen (Plantinga et al., 2013, Zhou et al., 2014). The TNF-α and nitric oxide producing TipDCs have been shown to have a role in early innate immune responses at the site of infection (Serbina et al., 2003) however, TipDCs have been also implicated in T_H1 responses in a Leishmania experimental model (León et al., 2007).

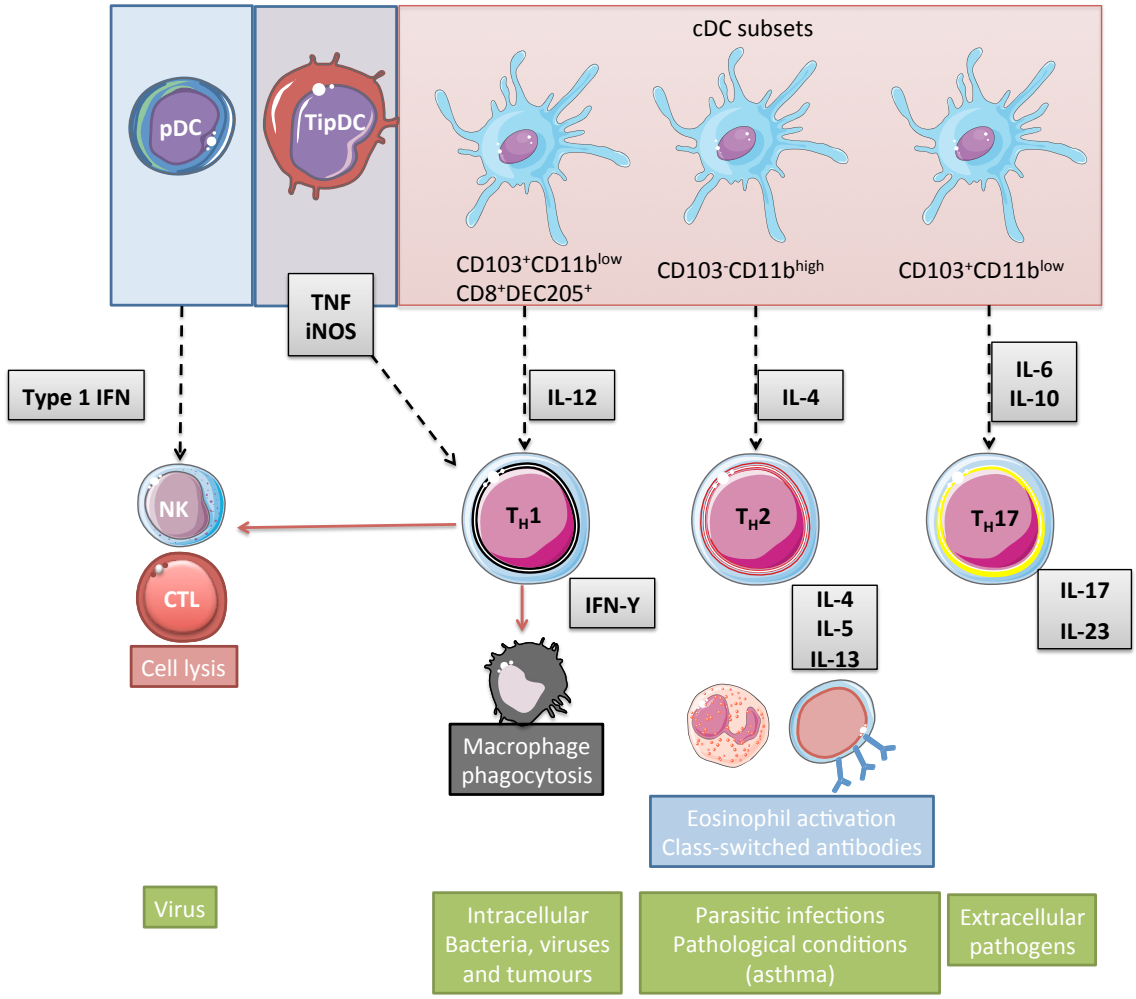

Figure 1.1. The influence of DC subsets on priming T cell responses and shaping the immune response. Different DC subsets influence T_H cell polarisation into T_H1, T_H2 or T_H17 amongst others. T_H cell subsets produce cytokines that lead to specific immune responses against the foreign antigens through other cells of the innate and adaptive immune response.

CTL = Cytotoxic T lymphocyte; T_H = T helper lymphocyte; pDC = Plasmacytoid dendritic cell; cDC = Classical dendritic cell; NK = Natural killer cell; TipDC = Inflammatory dendritic cell.

The described involvement of DCs in linking the innate and the adaptive immune response shows that DC subsets and their PRRs are an important target for more defined vaccine development.

1.1.4. $CD8^+$ T lymphocytes

Cytotoxic T cells express the CD8 surface marker ($CD8^+$ T cells) and are known as killer cells because of their effector functions. $CD8^+$ T cells carry out this effector function by releasing cytolytic proteins, like perforin that cause the release of the intracellular proteases or granzymes which causes the cell to become apoptotic (Chowdhury and Lieberman, 2008). TCR recognition of endogenous peptide on the MHC class I complex leads to the death of the malignant or infected cells. Exogenous antigens could also be presented to $CD8^+$ T cell in context of the MHC class I complex of professional APCs (*see* Section 1.1.6.). Similar to $CD4^+$ T cells, naive antigen-specific $CD8^+$ T cells undergo proliferation and differentiation upon antigen encounter, however the efficiency of this process is different for the two lymphocytes. $CD8^+$ T cells tend to proliferate sooner and at a faster rate than their $CD4^+$ expressing counterpart (Seder and Ahmed, 2003).

1.1.5. B Lymphocytes

B lymphocytes are APCs that are able to produce antibodies that neutralise the pathogen effects directly, or indirectly through opsonisation of the microorganism promoting efficient complement-mediated killing or phagocytosis. Antibody production is inarguably the most crucial effector function of B lymphocytes. The concept of the ability of certain B cell subsets to drive T_H1, T_H2 or Treg cell differentiation is still relatively new and controversial (Lund and Randall, 2010).

1.1.5.1. Antibody types

Antibodies are proteins composed of two light chains and two heavy chains linked together by disulphide bonds (Amzel and Poljak, 1979), which are secreted by effector B lymphocytes known as plasma cells. Each chain is composed of a variable region –

important for binding antigen and a constant region – important for the effector function involved in the elimination of bound antigen. There are five kinds of antibody isotypes that are determined by their heavy chains μ – IgM, δ – IgD, γ – IgG, α – IgA and ε – IgE. Each antibody isotype has a particular function (Murphy et al., 2008).

As the B cells develop in the bone marrow, the BCR normally consists of the IgM isotype. However, once the B cells leave the bone marrow they start to express IgD (Pernis et al., 1966, Geisberger et al., 2006). IgM antibodies are the first secreted in the primary immune response on first encounter with foreign antigen because they are produced without class-switching. IgG is the principal antibody isotype found in the extracellular fluid and blood, and have four subclasses named in order of abundance called IgG1, IgG2, IgG3 and IgG4. IgG antibodies are secreted in large quantities on second encounter of foreign antigen in the secondary humoral response. IgA antibodies can form dimers and are the principal antibody isotype found in body secretions like saliva, milk and tears. IgA antibodies are divided in two subclasses, IgA1 and IgA2. IgE antibodies are present in low levels in the extracellular fluid or blood. Secreted IgE antibodies bind to the surface of mast cells and basophils, by means of their constant regions (Fc portions) (Murphy et al., 2008).

1.1.5.2. B cell response to antigen

B cells residing in the secondary lymphoid organs encounter antigens in two ways. Naive B cells residing in the B cell follicles could directly encounter antigens of low molecular weight (<70kDa) that drain to the lymph nodes or the spleen (in the case of systemic infection) (Pape et al., 2007, Roozendaal et al., 2009). Otherwise, antigens are delivered on the surface of subcapsular sinus macrophages (Junt et al., 2007), peripheral DCs that have migrated to the secondary lymphoid organs (Bergtold et al., 2005) or stromal cells called follicular DCs that as their name implies reside within the follicles were they are specialised to trap-antigen (Suzuki et al., 2009).

Once activated, B cells differentiate into plasmablasts located outside the B-cell follicles, which secrete IgM antibodies. This occurs 2-12 days after antigen encounter. Isotype switching to IgG and affinity maturation occurs within 9-20 days after antigen encounter in specialised anatomical structures namely germinal centres. Finally, B cells residing in the germinal centres differentiate into plasma cells and memory cells

harbouring high-affinity Igs on their surface. Memory cells have a long life span, and become plasma cells upon antigen re-encounter. However, plasma cells only have a short life span ranging from a few days up to a few months (Jacob et al., 1991, Jacob and Kelsoe, 1992, Elgueta et al., 2009). Some plasma cells remain in the spleen and lymph nodes, but most migrate to and reside in the bone marrow, from where they secrete antibodies into the blood (Murphy et al., 2008).

B cells could be directly activated by T-cell independent (TI) antigens, such as polysaccharide antigens, by extensive cross-linking of antibodies on the cell surface, in absence of $CD4^+$ T cell help. However, for this type of immune response no class-switching occurs and the predominant antibody secreted is IgM type, and no memory cells are produced. This means that on second encounter of the same antigen, the secondary immune response to a TI antigen would be poor, whilst an immune response to a T-cell dependent (TD) antigen would be fast-developing and mostly made up of IgG antibodies (Moser and Leo, 2010).

1.1.6. Interactions between APCs and T lymphocytes

Macrophages, DCs and B cells are able to identify pathogens and malignant cells by means of PRRs, and uptake antigens by different mechanisms. Internalised antigens are cleaved into peptides by proteases in different cellular compartments. Proteins are broken down into a myriad of different epitopes capable of binding to MHC molecules, but T cells only respond to a limited number of these epitopes, called the immunodominant epitopes (Sercarz et al., 1993). The peptide-MHC complex is trafficked to the cell surface. Prior to interaction with T cells, APCs upregulate surface co-stimulatory molecules ready for interaction with T cells.

1.1.6.1. Antigen uptake by APCs

DCs patrol the peripheral tissues as well as the secondary lymphoid organs, and can internalise antigen non-specifically at each location. Naive B cells are circulating in the blood and lymphatic system, and are also found in the follicles of secondary lymphoid organs. Due to their anatomical locations, DCs are more efficient APCs. Both B cells and DCs are able to internalize antigen non-specifically by three distinct pathways,

namely clathrin-mediated endocytosis, phagocytosis and macropinocytosis (Parra et al., 2012, Gao et al., 2012, Blum et al., 2013). However, B cells are most efficient at antigen-specific uptake, and the major pathway for B cell uptake is through the BCR (Avalos and Ploegh, 2014). In fact, antigen recognition and uptake through BCR enhances their $CD4^+$ T cell stimulatory capacity by 10^3-10^4 fold (Lanzavecchia, 1985). In addition, B cells become increasingly better APCs when the amount of soluble or particulate antigen is low (Malynn et al., 1985). Published work shows that in B cell depleted mice, B cells are dispensable APCs when the antigen load is high but necessary when the amount of antigen is limited (Bouaziz et al., 2007).

Clathrin-mediated endocytosis mediates the internalisation of clusters of cell surface receptor-ligand complexes, soluble macromolecules and membrane proteins into endosomes. This pathway allows capture of antigens by means of cell-surface receptors that include BCR, Fc receptor, C-type lectin receptor DEC205 as well as CD40 co-stimulatory molecule (Davidson et al., 1990, Bonifaz et al., 2004, Chatterjee et al., 2012). In fact some of these receptors (DEC205, CD40) were targeted in vaccine development studies (Bonifaz et al., 2004). The CD40 receptor was found less efficient at internalisation compared to the DEC205 receptor, however, it was the most efficient at presenting antigen to $CD8^+$ T cells (Chatterjee et al., 2012). Once internalised, antigens are trafficked into early endosomes (weakly acidic, pH 6.8-5.9), late endosomes (pH 6.0–4.8) and lysosomes (pH 4.5) harbouring microenvironments of decreasing pH (Murphy et al., 1984, Maxfield and Yamashiro, 1987). Concentrated amounts of MHC class II molecules (Harding et al., 1990), but limited amounts of MHC class I molecules are detected in the late endosomes (Peters et al., 1991), where peptide loading occurs.

Phagocytosis is the process by which whole pathogens as well as apoptotic or necrotic cells are engulfed, usually mediated by opsonisation with the complement system. This mechanism is mediated by surface receptors. Phagocytosed antigens are trafficked into a phagosome containing proteases, reactive oxygen species (ROS) and anti-microbial agents to increase the efficiency of pathogen removal (Ramachandra et al., 2009). Phagosomes containing phagocytosed antigens fuse with lysosomes to form phagolysosomes. Phagolysosomes also have a low pH ranging from 4 to 4.5, which is

the environment at which the proteases called cathepsins work at their optimum. Published work shows that phagosomes contain both MHC class I and II molecules (Harding and Geuze, 1992, Harding, 1995, Ackerman et al., 2003).

Macropinocytosis is the capture of large quantities of extracellular materials into vesicles called pinosomes, not by surface receptors in this case, but by means of membrane folding (Hewlett et al., 1994). Innate immune stimuli, for example TLR stimulation in DCs promotes rapid macropinocytosis stimulating antigen presentation preferentially to either MHC class I or II molecules (West et al., 2004).

1.1.6.2. Antigen processing and presentation of peptide-MHC complexes

The MHC is polygenic and is located on chromosome 6 or 17, in humans or mice respectively. MHC genes are called human leucocyte antigen (HLA) genes in humans and H-2 genes in mouse (Murphy et al., 2008). Structurally MHC class I and II molecules possess a similar antigen-presenting groove made up of two domains, α1 and α2 or α1 and β1 respectively (Bjorkman et al., 1987, Fremont et al., 1992). However, certain unique structural features lead to each molecule binding peptides of different lengths.

Peptides presented by MHC class I are 8-9 amino acids long (Falk et al., 1991). The peptide-binding groove stabilises the peptide at both ends by hydrogen bonding with residues on the amino and carboxyl ends of the peptide known as anchor residues. Longer peptides can bind to the MHC class I however, they are cleaved by exopeptidases in the ER, which is the location were the peptide binds to the peptide-binding groove (Murphy et al., 2008, Blum et al., 2013). Peptides presented by MHC class II are more heterogeneous in size with 15 amino acids being the average peptide length (Hunt et al., 1992, Chicz et al., 1992). In contrast to MHC class I binding, peptides are not bound via their N- or C- termini, but by interactions along the length of the peptide (Murphy et al., 2008, Blum et al., 2013).

Generally, peptides presented by MHC class I molecules are derived from endogenous antigens like viruses or transformed cells and degraded by a large, multicatalytic proteinase complex, the proteasome. The generated peptides are translocated into

the ER by means of a transporter associated with antigen processing (TAP) and are bound to MHC class I molecules (Oancea et al., 2009). Peptide-binding is essential, otherwise the MHC class I molecule and/or unbound peptide are translocated back into the cytosol from the ER and are degraded by the proteasome. Only stable peptide:MHC complexes are transported to the cell surface (Grommé and Neefjes, 2002). In some cases, exogenous antigens are also presented on MHC class I molecules, by a mechanism known as cross-presentation, and it allows APCs to directly prime naive $CD8^+$ T cells (Moore et al., 1988, Kurts et al., 1996). Exogenous antigens can escape from endosomes or phagolysosomes into the cytosol were they are degraded by proteasome and bound to newly synthesised MHC class I in the ER (Grommé and Neefjes, 2002).

Internalised exogenous antigens are generally presented on MHC class II molecules by APCs (Chicz et al., 1992, Hunt et al., 1992). MHC class II molecules are synthesised in the ER, but full functional maturation occurs in the endosomal vesicles, which contain fragmented peptides (Villadangos, 2001). It is noteworthy that exogenous peptides need to compete for MHC class II binding with endogenous peptides present in the endosomal/lysosomal compartments being trafficked to the lysosomes to be degraded. Therefore, to ensure that exogenous peptides are presented, the MHC class II molecules are designed to accommodate diverse lengths and sequences of peptides. In this way, APCs present a huge variety of peptides, increasing the chance for one to be detected by T cells (Villadangos, 2001). Endogenous proteins get trafficked intro the different cellular compartments explained in Section 1.1.6.1. Vesicles of low pH containing peptide fragments fuse with newly synthesised MHC class II-containing vesicles. Endogenous peptides can also be presented on MHC class II molecules (Nuchtern et al., 1990).

1.1.6.3. Mechanism of co-stimulation

For an efficient immune response to be mounted APCs and T lymphocytes need to receive two signals. The first signal is termed as antigen specific and is delivered by the antigen itself when it binds to the receptor on the surface of the cell; TCR on T cells, BCR on B cells. The second signal is termed as co-stimulation, and is not antigen

specific. It is delivered by activated APCs to T cells, or by T_H cells for the activation of APCs (Huet et al., 1987, Schwartz, 1990, Barr et al., 2006). The TCR must engage both the presented peptide antigen and the co-stimulatory molecules on the same APCs. In the absence of either stimulus the naive T lymphocyte will enter a state of anergy (Murphy et al., 2008). Co-stimulation is crucial for an efficient immune response and for tolerance of self-antigens. There are multiple co-stimulatory molecules and the principal ones are illustrated in Figure 1.2.

The TCR is composed of a complex of membrane proteins and is also known as the TCR-CD3 complex. The TCR-CD3 complex is composed of the three CD3 signalling molecules, namely γε, δε, and ζζ and, ligand-sensing subunits that determine affinity for the antigens (Garboczi et al., 1996, Call et al., 2002). The TCR-CD3 complexes cluster on the T cell surface in order to be in close proximity with the MHC molecules on APC upon antigen presentation. Simultaneously, the co-receptors CD4 and CD8 bind to either MHC class II or MHC class I respectively, resulting in a stable MHC-antigen-TCR structure (Maroun and Julius, 1994). Furthermore, the adhesion molecule (ICAM-1) is another crucial molecule for the interaction of APCs and naive T lymphocytes. Activated T cells binds to the adhesion molecule ICAM-1 that is upregulated on activated APCs, through LFA-1 (Dustin and Springer, 1989).

The most important co-stimulatory molecules for the work conducted in this thesis are CD40 and its cognate ligand CD154. The cell surface molecule CD40 is a 48kDa phosphorylated transmembrane glycoprotein (previously known as Bp50), first identified in 1985 (Clark and Ledbetter, 1986). CD40 is a member of the tumour necrosis factor receptor (TNF-R) superfamily and is expressed by DCs, macrophages and B cells. However, the CD40 receptor is also expressed on hematopoietic progenitors, endothelial cells and epithelial cells (van Kooten and Banchereau, 2000). The CD154 (CD40L, gp39, T-BAM or TRAP) molecule belonging to the TNF family, was first discovered in 1992 by the Immunex group in Seattle and is mainly expressed on activated $CD4^+$ T cells (Armitage et al., 1992). However, it is also expressed on other cell types for example $CD8^+$ T cells, human basophils, mast cells and eosinophils (Gauchat et al., 1993). $CD4^+$ T cells only upregulate their CD154 expression after antigen-TCR ligation binding. CD154 expression on activated T cells is tightly regulated

and occurs in two phases. First, the $CD4^+$ T cells are activated within five minutes of the interaction between CD40 and their CD154 ligand, which lasts for two hours and is then down-regulated. At this stage the second phase of expression occurs, were *de novo* synthesis of the ligand is seen in $CD4^+$ T cells. This expression peaks within six hours and is sustained for more than twenty hours (Casamayor-Palleja et al., 1995). Activated T cells do not only express cell-membrane associated CD154 but also soluble forms of the ligand, which can also potentially bind to CD40, and deliver biological signals (Graf et al., 1995).

Other APC co-stimulatory molecules are CD80 (B7-1) and CD86 (B7-2), which belong to the B7/CD28 family and have a role in both T cell activation and inhibition. The two T cell molecules, CD28 (Linsley et al., 1991a) and CTLA-4 (Linsley et al., 1991b) bind to the B7 ligands. In contrast to CD28 that is expressed on 50% of the $CD8^+$ T cells and the majority of $CD4^+$ T cells (Linsley et al., 1991a, Lenschow et al., 1996), CTLA-4 is only expressed on activated $CD4^+$ T cells (Linsley et al., 1991b). CD28 binding provides positive signals and leads to T cell proliferation, cytokine production (in particular IL-2) and enhanced survival. In contrast, CTLA-4 binding dampens T cell-responses in order to guard against autoproliferative and autoimmune disease. In fact, CTLA-4 binds to B7 ligands with a higher affinity than CD28, and has a role in a negative feedback mechanism by blocking CD28 ligation, and limiting physical contact between APCs and T cells (Linsley et al., 1991b, Linsley et al., 1991a, Rudd et al., 2009).

Other members of the B7 family called programmed death (PD)-L1 (B7-H1) and PD-L2 (B7-DC) also have a role in T cell fate by binding to the PD-1 expressed by T cells. Whilst PD-L2 is only expressed by APCs, many different cell kinds express PD-L1. Both PD-L2 and PD-L1 binding to PD-1 block T cell proliferation by inhibiting the cell cycle (Latchman et al., 2001). PD-1 is a powerful modulator in blocking T cell activation and proliferation when the immune response is ineffective. The PD-L1 molecule is also expressed by tumour cells (Dong et al., 2002). Agonistic antibodies against PD-1 blocking the binding to PD-L1, enhance T cell response against the tumour cells (Iwai et al., 2002, Topalian et al., 2012).

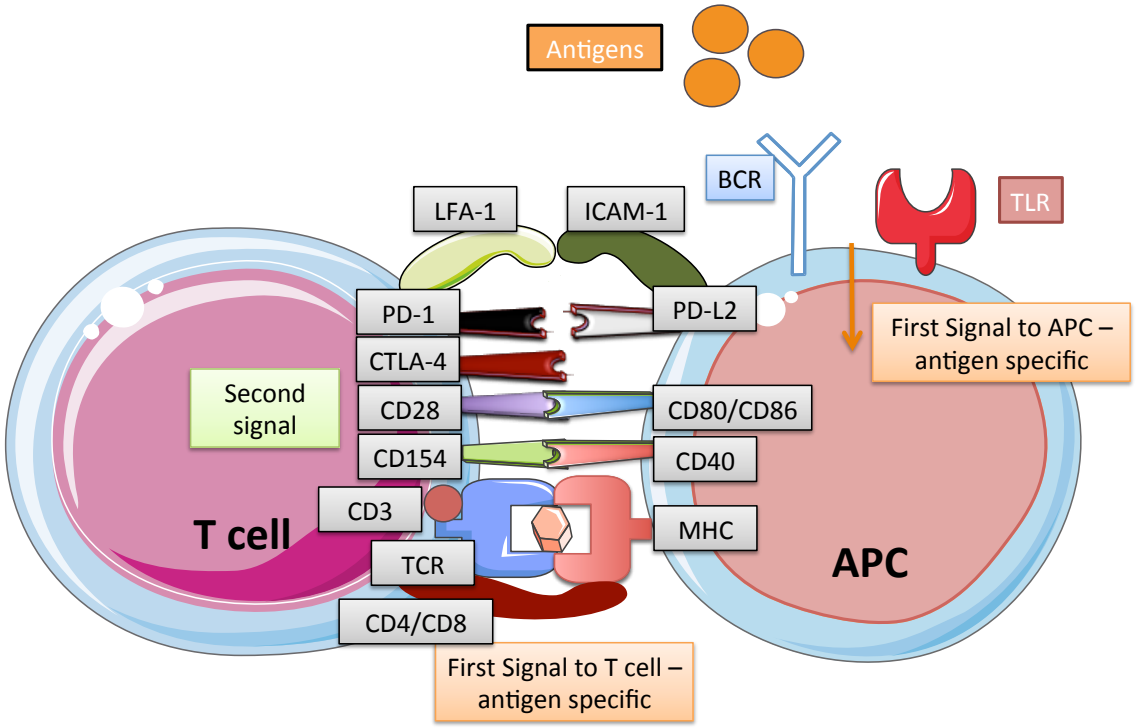

Figure 1.2. Cross-talk between APCs and T cells illustrating the principal contributing co-stimulatory molecules. The first signal to the B cell is released on antigen internalisation. The first signal to the T cell is released on TCR-CD3 complex recognition of MHC-peptide complex on APC. The second signal is released leading to T cell proliferation once the CD154, CD28 and LFA-1 on the T cell surface bind to CD40, CD80/CD86 and ICAM-1 (respectively) on the APC surface. T cell proliferation is blocked when CD80/CD86 bind CTLA-4 and PD-L2 binds to PD-1.

1.1.7. CD40-CD154 co-stimulatory pathway

The CD40-CD154 pathway is crucial for the generation of an effective adaptive immune response. The importance of the CD40-CD154 interaction in T-cell dependent B cell responses has been demonstrated by a condition characterised by a mutation in the CD154 gene called X-linked hyper IgM syndrome (H1GM1). The CD154 impairment leads to (i) autoimmunity, (ii) neutropenia, (iii) normal or elevated levels of IgM, (iv) low or absent IgG, IgA and IgE, (v) normal numbers of recirculating B cells and (vi) susceptibility to bacterial and opportunistic infections (Ramesh et al., 1994, Callard et al., 1993). In other words, the immune response resulted in poor isotype-switching and no B cell memory. Similar phenotypes to patients with X-linked hyper IgM syndrome were observed in mice deficient of the CD154 ligand (Xu et al., 1994). Mice immunised with CD40 monoclonal antibody (CD40mAb, rat IgG2a antibody) were able to enhance primary antibody responses against the Fc part of the CD40mAb, enhance *ex vivo* T cell proliferation to rat IgG2a and also delayed-type hypersensitivity responses (Carlring et al., 2004).

CD40 ligation also plays a significant role in the $CD8^+$ CTL response. This can also be observed in patients with X-linked hyper-IgM syndrome, who have an increased risk for malignancies (particularly lymphomas) and carcinomas (Schneider, 2000). In addition, CD40-deficient mice have an increased tumour susceptibility when compared to healthy mice (Mackey et al., 1997).

1.1.7.1. CD40 function on B cells

CD40-CD154 engagement on B cells leads to activation, sustained antigen-specific B cell proliferation (Clark and Ledbetter, 1986), affinity maturation, germinal centre formation and progression (Foy et al., 1994), isotype switching as well as the generation of memory B cells and plasma cells (Foy et al., 1994) which are the characteristic hallmarks of the adaptive humoral immune response. CD40 signalling has an effect on each aforementioned stage of B cell development.

The use of an agonistic murine anti-CD40 antibody directed against B cells showed that the CD40 signal leads to B cell activation. This is marked by upregulation of MHC II, co-stimulatory molecules such as, CD23 and CD86 as well as adhesion molecules like ICAM-1 (Hasbold et al., 1994, Heath et al., 1994) and increase in cell volume (Vallé et al., 1989). The use of human or murine CD40mAb also showed the importance of the CD40 signalling in B cell proliferation (Heath et al., 1994), which is enhanced by the addition of IL-4 cytokines (Vallé et al., 1989). It is of great interest that amongst the two clones of CD40mAb (1C10 and 4F11) used in a study conducted by Heath et al. (1994), only 1C10 induced B cell proliferation. This suggested that the two mAbs bound to different functional epitopes, and 1C10 bound epitopes within the binding site of CD154 which was confirmed by a later study (Barr and Heath, 2001). Furthermore, CD40mAb require co-engagement of their Fc domain with the inhibitory FcγRIIB receptor for immune co-stimulatory and anti-tumour activity (Li and Ravetch, 2011). The ligation of CD40 by activated T cell inhibits programmed cell death (PCD). PCD is a protective response that prevents B cell activation in response to TD antigens in the absence of T cell help and sentences the cells to apoptotic death (Sarma et al., 1995, Garrone et al., 1995).

CD40 signalling plays a critical role in different stages of B cell differentiation. On encounter of TD antigens, animal systems with defective CD40 receptor or the CD154 receptor are not capable of forming germinal centres or producing class-switched antibodies after immunisation (Xu et al., 1994, Castigli et al., 1994, Kawabe et al., 1994). In contrast there was no difference in the immune response to TI antigens in the absence of CD40 signalling, indicating the necessity of the CD40-CD154 interaction in response to TD antigens for the differentiation into plasmablasts.

Even though antibody class switching is initiated by CD40-CD154 engagement, cytokines have the main role in the determination of the specificity of the isotype. For example, whilst the use of human recombinant CD154 *in vitro* demonstrated B cell proliferation and antibody secretion, IL-2 and IL-10 were specifically required to enhance IgG1, IgA and IgM production, and IL-4 was required for the production of IgE and IgG4 (Armitage et al., 1993).

B cells localised in the germinal centres differentiate into either antigen specific antibody-producing plasma cells or long-lasting memory cells. CD40 signal drives differentiation of B cells into memory cells, but actively prevents formation of antibody-producing plasma cells (Arpin et al., 1995, Randall et al., 1998). However, upon disruption of the CD40-CD154 interaction the antibody-producing function is retrieved (Randall et al., 1998). Randal et al. (1998) also show that the use of CD154-transfected cells inhibited B cell differentiation, however monoclonal or polyclonal CD40 antibodies did not, showing that the type of trigger of the CD40 receptor has an effect on the CD40 signal produced. B cell fate is also determined by the amount of CD154 expressed on the $CD4^+$ T cell and therefore the strength of the CD40 signal. The use of transgenic mice showed that high CD154 expression on activated T cells induced higher antibody IgG titres of high affinity, compared to the wild type controls (Pérez-Melgosa et al., 1999).

1.1.7.2. CD40 function on DC

The initial studies carried out on the CD40-CD154 pathway were conducted on B cells, and it was only after a decade of research that attention shifted towards other cells expressing the CD40 receptor, like DCs, due to their important function in linking the innate and adaptive immune response.

The CD40 signal leads to DC maturation by upregulation of accessory molecules like CD54 (ICAM-1), CD58 (LFA-3), CD80, CD86 and MHC class II (Caux et al., 1994). CD40 ligation also supports DC survival (Björck et al., 1997), and secretion of macrophage-inflammatory protein 1-α, TNF-α IL-1, IL-6, IL-8 and IL-12 (Mutini et al., 1999). Even though similar to B cells, CD40-CD154 engagement leads to DC activation, it is noteworthy that different cell types respond in different ways to the CD40 signal. For example, high levels of IL-12 were produced by the DCs after stimulation via CD154 (Cella et al., 1996), therefore showing the ability to skew the immune response to a T_H1 response. Therefore, CD40 cross-linking on DCs drives these cells to perform functions that B cells are not able to do as efficiently.

1.2. History of vaccine development

In the past century, vaccination has been a very useful tool to reduce morbidity and mortality caused by infectious disease. Vaccination has led to the control of various threatening diseases including tetanus, pertussis, yellow fever, diphtheria, measles, mumps, rubella, rabies, typhoid and *Haemophilus influenzae* type b (Plotkin and Plotkin, 2008). Smallpox is the only human disease that has been certified eradicated (Breman and Arita, 1980, Fenner et al., 1988), however, poliomyelitis cases have fallen by 99%, and in 2014 the only countries that remain polio-endemic are Nigeria, Pakistan and Afghanistan (WHO, 2014).

The first vaccine developed was for smallpox and this was produced by Edward Jenner in 1796 (Jenner, 1798). During Jenner's time, pathogens were only thought to result as a consequence of death, but not to cause it. It was almost 100 years after Jenner's discovery, in 1876, that Robert Koch made the connection between pathogens and disease due to his research on anthrax bacilli. This information led to the concept of pathogens rendered non-pathogenic as prophylactic vaccines, which are called live-attenuated vaccines today was postulated by Louis Pasteur in 1881. He found that on prolonged culture of *Pasteurella multocida* (Plotkin, 2005) the cause of chicken cholera in non-human cells lose their pathogenicity in human cells. Pasteur hypothesized that this loss in pathogenicity was due to environmental factors like high temperature, chemicals and oxygen and described the vaccine as "live atmosphere-attenuated" (Pasteur, 1880). He proved this hypothesis by his ensuing work on anthrax, and developed an anthrax vaccine using a high temperature of 42-43°C (Pasteur, 1881). Pasteur developed the first therapeutic vaccine produced, using a new attenuation method involving the use of chemically dried nervous tissue (Pasteur, 1885). This was developed for the simple reason that the attenuation technique used for cholera, which is caused by bacteria, was not effective for rabies as it is a viral disease. This vaccination strategy was used for ten years (Smith, 2012). Between 1930 and 1980 a number of live-attenuated vaccines for viral diseases were developed because the cell culture technique was optimised for viruses (Plotkin, 2005). It is worth noting however, that certain pathogens are difficult to culture *in vitro* and therefore alternative vaccine strategies are required. For example it is only recently that the technique for hepatitis

C (HCV) (Wakita et al., 2005) and human papilloma virus (HPV) (Aaltonen et al., 1998) growth in culture have been developed and therefore, the use of a live-attenuated vaccine for these pathogens has not yet been evaluated.

Live-attenuated vaccines administered by different routes (nasal, oral or intramuscular) cause a long-lasting and durable immune response similar to a natural infection that leads to both humoral and cell-mediated responses against the pathogen without the need for multiple boosters. Some examples of live-attenuated vaccines include the Bacille Calmette-Guérin (BCG) tuberculosis vaccine (Calmette, 1931), oral polio vaccine (OPV) (Sabin et al., 1954) as well as the measles (Schwartz, 1990), mumps (Hilleman et al., 1968) and rubella vaccines (Plotkin et al., 1969). Despite all the advantages of live-attenuated vaccines, they have the disadvantage that the virus might revert to a more virulent strain, as was the case with the OPV (Guillot et al., 1994) and the live flavivirus vaccines (Seligman and Gould, 2004). Due to the risk of disease, live-attenuated vaccine administration is restricted to healthy individuals.

The next breakthrough in vaccine development was the use of whole-killed pathogen based vaccines. The whole-killed pathogens were killed through denaturation by heat or by chemical treatment. The first whole-killed vaccines developed were for typhoid (Wright and Semple, 1897) and cholera (Kolle, 1896) in the 1890s, followed by the development of hepatitis A (Wiedermann et al., 1990, Iino et al., 1992), and the inactivated polio (Salk type) vaccine (Salk, 1955, Salk et al., 1981) in the twentieth century. Toxoid vaccines made up of inactivated toxins, were also developed in the 1920s against extracellular toxins produced by bacteria as in the case diphtheria and tetanus diseases (Plotkin, 2005). Whole-killed vaccines have inherent immune-potentiating properties due to the bacterial or viral components and impurities they contain. However as they are incapable of replication, multiple large doses have to be administered, leading to the problem of reactogenicity.

Over the years, vaccine design has been further refined, and the use of well-characterised antigens, rather than whole-killed or attenuated pathogens, has gained in popularity. Vaccines developed using only specific components from the pathogen, are known as subunit vaccines and include (i) protein-based vaccines such as HBV vaccine (Dupont et al., 2006), (ii) polysaccharide-based vaccines such as *Haemophilus*

influenzae type b (Hib) vaccine (WHO., 2013) or (iii) peptide/T-cell epitope based such as malaria vaccines (Vreden et al., 1991) or cancer vaccine (Nestle et al., 1998) respectively. The subunit vaccine approach, (i) significantly enhances vaccine safety, (ii) improves lot-to-lot consistency, (iii) targets the immune response to particular epitopes and (iv) allows non-refrigerated storage and transport as the vaccines can be freeze-dried (Moyle and Toth, 2013). The challenge with these vaccines is that they are less immunogenic than traditional vaccines. In addition they need to achieve immunity in an immunogenetically heterogeneous population. In the case of traditional vaccines this is realised by the broad range of diverse epitopes of the pathogen in the vaccine. On utilising better-characterised subunit vaccines like synthetic peptide- and epitope-based vaccines, the benefit of increased specificity towards the disease might not always outweigh the cost. That is, that subunit vaccines might not induce a protective vaccine-associated immune response in every individual (Zepp, 2010). The subunit vaccine approach therefore requires the incorporation of immunostimulatory components like adjuvants to shift the balance to a beneficial one.

1.3. Overcoming limitations of Novel Vaccines

The slow progress in subunit vaccine development demonstrates that this is a difficult process. However, some subunit vaccines for example Engerix-B® (GlaxoSmithKline, 2012) and Recombivax® (Merck, 2011b) targeting HBV as well as Cervarix-B® (GlaxoSmithKline, 2011), and Gardasil® (Merck, 2011a) targeting HPV are licensed for human use, showing that this approach is not fruitless. However, it is interesting to note that all aforementioned vaccines are based on virus-like particles (VLP), which due to their repetitive structures and size are more immunogenic compared to peptides or soluble antigens. A substantial amount of effort has been directed against diseases like, HIV and malaria (Rappuoli and Aderem, 2011), but still no vaccines have yet been licensed for human use against these diseases, because novel vaccines are unable to develop a long-lasting, sustained T_H1 response, which to date has only been realised with live attenuated vaccines (Seder and Ahmed, 2003).

Vaccines against non-infectious diseases like cancer are gaining in popularity. However, while immunotherapies like rituximab have shown great success for decades (Miller et al., 1982, Kwak et al., 1992), most cancer vaccines do not advance out of Phase III clinical trials. In most cases this is due to the induction of ineffective anti-tumour cytotoxic responses. In fact the only two effective prophylactic cancer vaccines include the HBV vaccine in prevention of HBV-associated hepatocarcinoma (Lim et al., 2009), and the HPV vaccine in prevention of HPV-associated cervical carcinoma (Wright et al., 2006). Not considering therapeutic immunotherapies involving monoclonal antibody drugs like rituximab, the only therapeutic vaccine licensed for human use is sipuleucel-T (Provenge^{TM}, Dendreon), against advanced metastatic prostate cancer (Higano et al., 2009). Dendreon's Provenge^{TM} is a cell-based therapy that is time-consuming and expensive to produce (Buonaguro et al., 2013).

For the unmet requirements of vaccines to be fulfilled three important factors need to be considered (i) conjugation chemistry, (ii) the roles of, and (iii) the mechanism of action of traditional and novel adjuvants in vaccine formulations.

1.3.1. Refining vaccine formulations by bioconjugation

One feature of bioconjugation is to improve immunogenicity of antigens by covalent coupling of the antigens with highly immunogenic foreign carrier molecules, a strategy first adopted for *Haemophilus influenzae* type b (Hib) in the 1980s (Schneerson et al., 1980), using diphtheria toxoid as a carrier. The polysaccharide capsule found in bacterial organisms like *H. influenzae*, leads to a T-independent immune response when administered alone. However, covalent coupling of the polysaccharide capsule to highly immunogenic foreign carrier molecules alters the poor T-independent response to a strong T-dependent immune response (Schneerson et al., 1980). Since the 1980s, advances in bioconjugation led to production of three other licensed vaccines for this disease. These include the conjugation of the capsular polysaccharide of Hib namely polyribosylribitol phosphate (PRP) to tetanus toxoid (PRP-T) (Schneerson et al., 1980, Schneerson et al., 1986), mutant non-toxic diphtheria toxin CRM_{197} (HbOC) (Anderson, 1983) or the outer membrane protein from a *Neisseria meningitides* group

B strain (PRP-OMP) (Vella et al., 1992). The four vaccines differed in the (i) type of carrier protein, (ii) conjugation chemistry and (iii) size of PRP the carrier protein was conjugated to. The vaccine composition affected the immunogenicity of each vaccine all requiring different doses and frequency of doses to be effective. The PRP-OMP vaccine stimulates higher antibody production after two doses compared to the other vaccines (Decker et al., 1992). In contrast, PRP-T and HbOC vaccines are more immunogenic after the third dose than the PRP-OMP vaccine. Conjugation strategies are getting more refined, causing vaccines deemed successful in the past, to become obsolete. In fact, in spite of its success in the beginning, the vaccine using diphtheria toxoid carrier, was recently removed from the market (WHO, 2006).

The protein carriers CRM_{197} or OMP, used for *H. influenzae* vaccines, have been successful in enhancing the humoral immune response. $CD8^+$ T cell as well as antibody responses are crucial anti-tumour effectors that should be targeted by cancer vaccines. This is the reason why keyhole limpet hemocyanin (KLH), a protein carrier of high molecular mass obtained from the giant keyhole limpet *Megathura crenulata* marine mollusc which has the ability to induce both types of immune responses (Harris and Markl, 1999), is the protein carrier of choice for cancer vaccines. Keeping this in mind, the immunogenicity and efficacy of the vaccine does not just rely on the carrier protein or adjuvant, the method of conjugation also plays a very significant role. The research currently being conducted on therapeutic cancer vaccines against B cell lymphomas is a recent example of the fact that the optimal conjugation strategy is the product of exhaustive experimental validation.

Conjugation of KLH to specific peptides or antigens has shown promise in tumours including metastatic breast cancer (Theratope® vaccine) (Miles et al., 2011, Ibrahim et al., 2013) and lymphoma (Kwak et al., 1992, Bendandi et al., 1999, Betting et al., 2008, Kafi et al., 2009). Malignant B cell lymphomas express a unique immunoglobulin idiotype (Id), which when used alone is poorly immunogenic, and so it is conjugated to KLH to enhance its immunogenicity. Conjugation of the lymphoma-Id to KLH (KLH-Id) is traditionally performed using glutaraldehyde, and showed encouraging results in murine models (Campbell et al., 1987, Kaminski et al., 1987, Campbell et al., 1988). Successful Phase I/II clinical trials, led this vaccine to be investigated in three Phase III

clinical trials in patients with follicular lymphoma (Levy et al., 2008, Freedman et al., 2009, Schuster et al., 2009). One trial in which the vaccine was given only to patients that had received cytotoxic chemotherapy showed statistically improved disease-free survival. The other two Phase III clinical trials failed to reach their primary endpoints. Bendandi (2009) discussed that the failure of KLH-Id vaccination could have been due to the design of the clinical trials. However, Timmerman (2009) suggested that alternative strategies, involving different conjugation techniques could be the 'missing link' required to improve the humoral and cell-mediated immune responses necessary to protect against tumours.

KLH was therefore conjugated to Id using maleimide coupling instead of traditional methods using glutaraldehyde treatment. In a murine setting the novel method showed increased efficacy when compared to glutaraldehyde conjugated vaccines (Betting et al., 2008, Kafi et al., 2009). The authors proposed that this occurred because the reaction is limited to reduced cysteine sulphydryl groups. Alternatively, glutaraldehyde treatment causes extensive cross-linking potentially destroying valuable epitopes. Further refining of the lymphoma Id vaccine involved conjugation of Id to the adjuvant CD40mAb that also demonstrated enhanced median and overall survival in an A20 murine model compared to the KLH-Id lymphoma vaccines made by traditional methods (Carlring et al., 2012).

1.3.2. Adjuvants and their roles

An adjuvant can be described as any substance which, when administered with an antigen, enhances or modifies the immune response to that antigen. The late Charles Janeway Jr (Janeway, 1989b) described adjuvants as 'immunology's dirty little secret'. Adjuvants were described as 'dirty' because the addition of crude extracts like mycobacteria, aluminium hydroxide and mineral oil was required to allow the antigen to be of sufficient immunogenicity. Other technologies for example live vector technology (Galen et al., 2010, Wang et al., 2013) have been utilised instead of adjuvants, however for the purpose of this thesis the focus will be on adjuvants.

The most widely used adjuvants are aluminium salts or alum, which were discovered in the early 1920s by Glenny and colleagues whilst the group was investigating diphtheria toxin (Glenny et al., 1923). They were the only adjuvants used in humans for 80 years. It is only recently that other adjuvants have been introduced in vaccine formulations. This slow development could be attributed to the empirical approach carried out by researchers. In the mid-1950s, Freund tested different parts of the mycobacterial cell walls for adjuvant activity (Freund, 1956) and this is how Freund's complete adjuvant (FCA), which is a mixture of inactivated bacteria and mineral oil, was identified. FCA is very potent and used in animal models, however it causes serious side-effects like pain, swelling and fever, due to its reactogenicity and is therefore considered unsafe for use in humans. Smaller bacterial cell wall compounds were subsequently made for example muramyl dipeptide (MDP) (Ellouz et al., 1974). Lipopolysaccharide (LPS) was found to be an adjuvant with potent activity, but because of its toxicity it was dismissed for use as a vaccine adjuvant (Johnson et al., 1956). The cause of the toxicity and adjuvant properties was the lipid A portion of LPS (Galanos et al., 1985, Takada and Kotani, 1989). However, on removal of a residue from the phosphate group residing in the lipid A portion of LPS, the molecule became 100-to 1000-fold less toxic without losing its adjuvant properties (Takayama et al., 1981, Takayama et al., 1984). This derivative was later further refined and was called monophosphoryl lipid A (MPL) (Myers et al., 1990), which is one of the most successful adjuvants recently licensed for human use.

In the past the antibody responses were considered the predominant means to develop an immune response, and in fact vaccination successes were mediated by the production of protective antibodies (Plotkin, 2010). Diseases like cancer also require a cell-mediated response to achieve an effective vaccine-mediated immune response against the inoculated antigen. Therefore, traditional adjuvants like alum are not useful as they preferentially promote an antibody-based immune response (Brewer et al., 1999). Furthermore, cells of the innate immune response that behave as vessels by which the pathogenic or dangerous self-antigens like tumour antigens get transported to the secondary lymphoid organs need to be targeted and activated. In fact, a reason

behind ineffective cancer vaccines in the past decade is the lack of a DC-activating adjuvant.

Peptides immunised alone tend to be cleared by the immune system prior to being internalised or loaded onto DCs. In addition, targeting DCs is not enough, because if DCs are not activated, peptide-loaded DCs will remain in a steady state and promote tolerance (De Vries et al., 2003a, De Vries et al., 2003b, Lesterhuis et al., 2011, Kastenmüller et al., 2014). The immune stimulant IL-2 was recently co-administered with a short peptide in advanced melanoma patients, and resulted in enhanced anti-tumour responses and prolonged tumour progression-free survival in certain conditions when compared with the use of IL-2 alone (Schwartzentruber et al., 2011).

The use of peptide vaccines has potential in improving therapeutic efficiency if applied in the right way. This is the reason why novel adjuvant development is no longer empirical. In fact, novel vaccine formulations include adjuvants with particular roles to achieve the appropriate vaccine-mediated immune response against vaccine antigen. Particular adjuvant roles and examples are tabulated in Table 1.2.

Adjuvant Role	Example	Reference
To enhance effector T cell responses	**MPL:** Enhanced T_H1 response when co-delivered with hepatitis B virus core antigen in PLGA nanoparticle compared to non-adjuvanted vaccine	(Chong et al., 2005)
To enhance duration of response – induce generation of memory cells	**AS04 adjuvant:** Generated protective memory $CD8^+$ T cell responses against influenza A challenge	(MacLeod et al., 2011)
To enhance rapidity of immune response	**AS04 adjuvant:** Reduced dose-regimen from 3 doses to 2 in combination with recombinant hepatitis B antigen	(Levie et al., 2002)
To broaden the immune response	**TLR4 and TLR7 encapsulated in synthetic nanoparticles:** Displayed higher neutralisation titres as well as antibodies with high avidity to the vaccine-antigen compared to in the absence of the nanoparticles	(Kasturi et al., 2011)
To activate cells of the innate immune system	**AS01 adjuvant:** Higher numbers of activated antigen-presenting DCs in the draining LN were observed after injection with AS01-adjuvanted vaccine compared to injection with antigen alone	(Didierlaurent et al., 2014)
Antigen dose-sparing	**CAF01 (composed of cationic liposomes):** Allowed for a 10 times dose sparing when used in formulation with IPV	(Dietrich et al., 2014)

Table 1.2. Roles of adjuvants.
PLGA = Poly(d,l-lactic-co-glycolic acid) polymer, AS04 = adjuvant system containing MPL and alum, AS01 = adjuvant system containing Quillaja saponaria (QS)-21, MPL and liposomes.

Due to the knowledge of the importance of DCs in the immune response and their effect on T cell responses, current vaccines are now designed differently. In fact early stage trials have been investigating the targeting of DC receptors like DEC-205 by monoclonal antibodies coupled to peptides in the presence of adjuvants. In a study comparing receptor targeting of DEC205, CD11c, mannose receptor 1 and CD40 molecule using LPS as an adjuvant, targeting of the CD40 molecule led to best cross-presentation to $CD8^+$ T cells (Chatterjee et al., 2012). Other receptors on DCs that have been targeted extensively are the TLRs (Cho et al., 2000). One reason for this is that

TLRs recognise specific pathogen sequences and sequentially tailor the immune response according to the invading pathogen.

Novel adjuvants like TLR-agonists and vaccine antigens were later conjugated aiming to co-deliver the adjuvant and the vaccine antigen to the same APC, and reducing side-effects like induction of tolerance, autoimmune responses or undesired cytokine release. The success of conjugation of a TLR-agonist adjuvant to a vaccine antigen was first demonstrated with the use of TLR9-agonist CpG linked to ovalbumin antigen in mouse studies (Cho et al., 2000), which demonstrated $CD8^+$ T cell activity and T_H1-bias, compared to a vaccine consisting of the uncoupled counterparts. It is worthy to note that B cells also express TLRs, which means that TLR-agonists could also be acting directly on B cells especially if conjugated to antigen (Shirota et al., 2002). The work in our group in fact aims to target CD40 molecules on APCs by coupling of agonistic monoclonal antibodies to the vaccine peptides or antigen (Barr et al., 2003, Hatzifoti and Heath, 2007, Carlring et al., 2012).

Several vaccine conjugates of TLR-agonists with vaccine antigens were tested *in vivo* in mice in the context of different disease settings like tumour, allergy and infection (Cho et al., 2000, Tighe et al., 2000, Jackson et al., 2004). All conjugates produced a stronger immune response than the mixtures of the vaccine antigen and adjuvant. However, only one of these thus far proceeded to studies in non-human primates (Wille-Reece et al., 2005).

1.3.3. Mode of action of traditional and novel adjuvants

Novel and traditional adjuvants can be broadly classed in three groups according to their mode of action namely (i) immunopotentiators - direct activation of certain receptors of the innate immune system (for example TLR-agonists), (ii) delivery systems - delivery of antigen of interest leading to enhanced antigen presentation to the immune system (for example emulsions), or (iii) a combination of both (i) and (ii) (for example adjuvant system 04 or AS04) (Reed et al., 2013).

Alum adjuvants are the most widely used and are incorporated in tetanus, diphtheria, pertussis, HAV and HBV vaccines (Leroux-Roels, 2010). However, alum adjuvants

preferentially induce a T_H2 response, and has minimal or no effect on T_H1 and cytotoxic cell responses (Grun and Maurer, 1989, Brewer et al., 1996, Brewer et al., 1999). Despite the years of research only a few adjuvants have been licensed for human use in Europe and/or the US. These include oil-in-water emulsions; MF59 and AS03 (Vesikari et al., 2009, Andrews et al., 2011), AS04 (MPL co-administered with alum) (Levie et al., 2002) and virosomes (Moser et al., 2007, Bovier, 2008, Herzog et al., 2009). The previously mentioned licensed adjuvants as well as some examples of other adjuvants in pre-clinical and clinical development are listed in Table 1.3.

The putative mode of action of mounting an adjuvant-mediated immune response requires activation of T_H cells with the help of components of the innate immune response. Four signals are required to mount an immune response; signal 0 - activation of innate immune cell by for example TLR stimulation, signal 1 - antigen-presentation, signal 2 - co-stimulation and signal 3 - immune modulation by cytokine release (Janeway, 1989a). This is another way to classify adjuvants.

Understanding which of these signals adjuvants provide or enhance will give a better way to cleverly tailor vaccines to mount a specific immune responses and target particular pathways. Some examples are illustrated in Figure 1.3.

Adjuvant name	Receptor or Mechanism	Immune response	Some examples of vaccine targets		References
Immunopotentiators					
Lipid A analogues (MPL*)	**TLR4**	**Ab, T_H1, $CD8^+$ T cells, activates DCs**	**Pollinex Quattro™**	**Allergy**	(Richards et al., 1998, Ismaili et al., 2002, Johansen et al., 2003, Baldrick et al., 2007)
Imidazoquinolines (imiquimod*)	**TLR7 and TLR8**	**Ab, T_H1, $CD8^+$ T cells (when conjugated)**	**Aldara™**	**HPV, HIV (pre-clinical)**	(Owens et al., 1998, Wenzel et al., 2005, Wille-Reece et al., 2005)
CpG ODN	**TLR9**	**Ab, T_H1 (enhanced when conjugated), $CD8^+$ T cells**	**Phase III (Hepislav™),**	**HBV**	(Shirota et al., 2000, Miconnet et al., 2002, Shirota et al., 2002, Eng et al., 2013)
Particulate formulation or delivery systems					
Emulsions (AS03*, AF03, MF59*)	**Recruitment of immune cells, antigen uptake**	**Ab, T_H1, T_H2**	**Fluad™, Pandemrix™**	**Influenza, Pandemic flu**	(Vesikari et al., 2009, Andrews et al., 2011, Moris et al., 2011, Calabro et al., 2011)
Aluminium salts*	**Antigen delivery, NLRP3 inflammasome**	**Ab, T_H2**	**Havrix™, Engerix-B™, Infantrix™**	**HAV, HBV, DTaP**	(Grun and Maurer, 1989, Brewer et al., 1996, Brewer et al., 1999, Leroux-Roels, 2010, Kool et al., 2008)
Virosomes	**Antigen delivery**	**Ab, T_H1, T_H2**	**Epaxal™, Inflexal V™**	**Influenza, HAV**	(Bungener et al., 2002, Bovier, 2008, Herzog et al., 2009)
Adjuvant systems (a combination of immunopotentiators and particulate formulation)					
AS01 contains QS21, MPL, liposomes	**TLR4**	**Ab, T_H1, $CD8^+$ T cells, activates DCs**	**Phase III (RTS,S)**	**Malaria**	(Agnandji et al., 2011, Agnandji et al., 2012, Didierlaurent et al., 2014)
AS04* contains aluminium salt, MPL	**TLR4**	**Ab, T_H1, $CD8^+$ T cells, activates DCs**	**Cevarix™, Fendrix™**	**HPV, HBV**	(Levie et al., 2002, Giannini et al., 2006, Didierlaurent et al., 2009)

Table 1.3 Licensed and late-stage tested adjuvants classified as immunopotentiators, particulate formulations or delivery systems, or adjuvant systems
***licensed for human use.** ODN - oligodeoxynucleotides

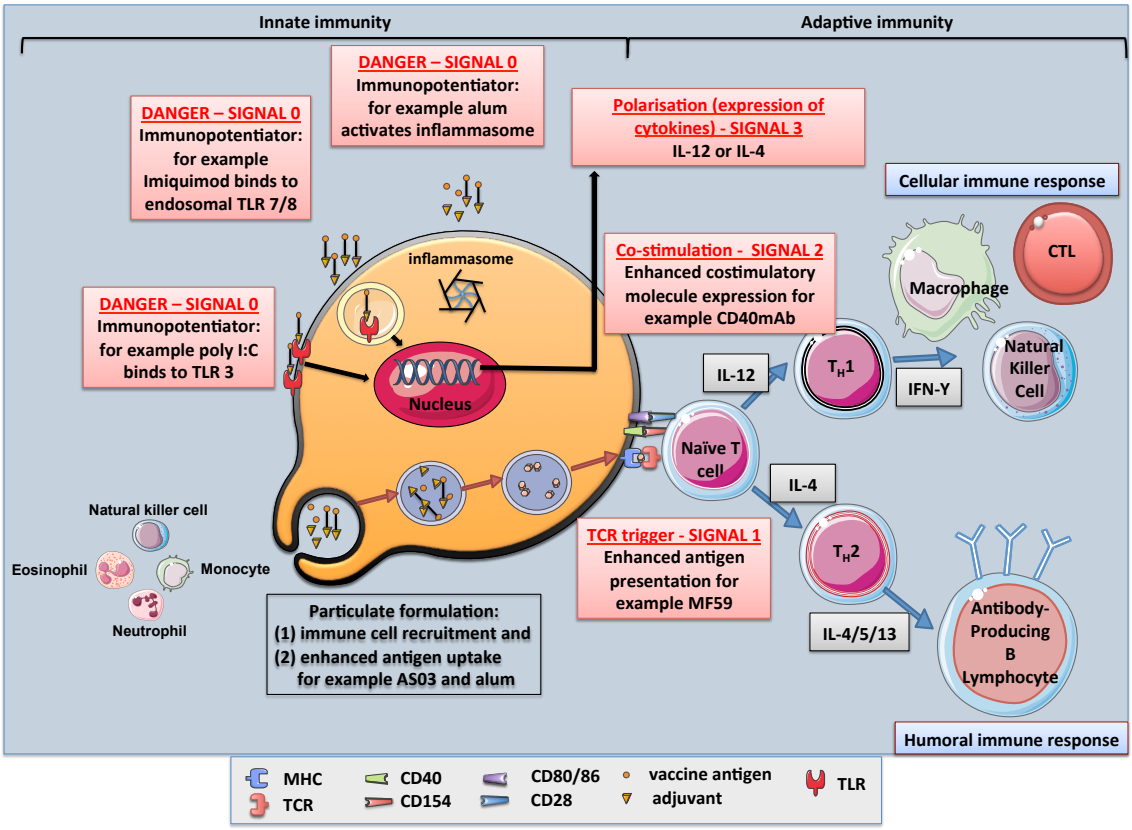

Figure 1.3. Mechanisms of action of adjuvants. Signal 0 and signal 1 are signals to APCs. Signals 1, 2 and 3 are signals to T cells. Adapted by permission from Macmillan Publishers Ltd: Nature (Reed et al., 2013), copyright 2013.

Immunopotentiators or immunodulatory molecules directly activate APCs by means of surface receptors. This could occur via mimicking a PAMP recognised by a pattern recognition receptor (PRR) such as a TLR on the APC. Recognition leads to the release of so-called 'danger signals' which the immune system can quickly respond to. Examples of these include TLR-agonists like MPL, Immunostimulatory sequences (ISS) of microbial DNA (CpG-rich motifs), Imidazoquinolines and heat shock proteins. Otherwise, co-stimulatory agonists like CD40mAb target co-stimulatory molecules. **Immunodulatory molecules** also activate the inflammasome complex via NLRP3 protein for example aluminium salts.

Delivery systems recruit immune cells and target antigen presentation via MHC to the TCR. Examples include aluminium hydroxide, liposomes and oil emulsions. **Delivery systems** could also direct the adjuvant and the vaccine antigen to the same cell. Examples include some TLR-agonists chemically conjugated to the vaccine antigen (CpG ODN conjugated to vaccine antigen).

1.3.3.1. Delivery systems

The purpose of delivery systems, as their name suggests, is to deliver the vaccine antigen, immunomodulatory molecule or both to the APC. This class of adjuvants normally enhance persistence of vaccine antigen at the site of vaccine inoculation, a theory coined by Glenny and his colleague in the 1920s, known as depot formulation (Glenny and Pope, 1925). Furthermore, due to the fact that these adjuvants are in particulate form, they enhance APC uptake leading to enhanced presentation by these cells (Ott et al., 1995, Dupuis et al., 1998, Calabro et al., 2011), and thus prolong signal 1. An example of a delivery system adjuvant licensed for use is the influenza vaccine, Inflexal^{TM}, introduced in the Swiss market in 1997 (Crucell, http://www.crucell.com). Virosomes (approximately 150nm in diameter) are able to induce B and T cell responses as they present vaccine antigen in the context of both MHC class I and II (Bungener et al., 2002). The adjuvant function of this vaccine is mediated via the haemagglutinin portion of the envelope binding to the cell receptors leading to pH-dependent fusion and stimulation of the cell (Wilschut, 2009). Another delivery-based adjuvant licensed for human use is the oil-in-water emulsion MF59, used in the vaccine Fluad^{TM} (also an influenza vaccine). This adjuvant has been found efficacious and safe even in young children (Vesikari et al., 2009). It has been compared to alum, and is a more effective adjuvant, as it (i) induces more potent antibody responses, (ii) allows antigen dose-sparing and fewer immunisations, (iii) generates memory cells and (iv) drives the immune response to a mixed T_H1 and T_H2 phenotype (Ott et al., 1995). This increased efficacy could be due to the fact that MF59 has a direct effect on immune cells and promotes recruitment of granulocytes, DCs, as well as differentiation of monocytes into DCs (Seubert et al., 2008, Calabro et al., 2011), in addition to enhanced antigen uptake by DCs (Dupuis et al., 1998).

Alum is still one of the commonly used adjuvants in humans. This adjuvant has a delivery role, due to its particulate nature. Alum adjuvant is made up of vaccine antigen adsorbed to precipitates of aluminium phosphate or aluminium hydroxide (Glenny et al., 1923, Glenny and Pope, 1925). Alum induces antibody responses in the absence of TLR-signalling (Gavin et al., 2006), and enhances the T_H2 pathway (Brewer et al., 1999). For years, alum was thought to just create a depot effect and enhance

uptake by APCs. However, it is now known that antigen depot is not required for adjuvanticity (Hutchison et al., 2012). It is apparent that alum is able to recruit immune cells to the site of infection (Calabro et al., 2011) and stimulate the cells of the immune response, leading to enhanced antigen-presentation (Ghimire et al., 2012). The NLRP3 inflammasome, has been shown to have a role in this mechanism (Kool et al., 2008, Franchi and Núñez, 2008, Wang et al., 2012). Alum might be inducing antigen uptake after interaction with DCs by means of cell membrane lipid reordering. However, alum is not taken up by the DCs (Flach et al., 2011). Studies show that alum induces danger signals via necrotic cell DNA release (Marichal et al., 2011), uric acid production (Kool et al., 2008) or heat shock protein 70 (Wang et al., 2012). Franchi et al. (2008) shows in NLRP3 deficient mice that the IgG antibody response is still enhanced in the presence of alum adjuvant. This demonstrates that the NLRP3 inflammasome has a role and is not indispensible for the IgG adjuvant activity.

1.3.3.2. Immunomodulatory molecules

The immunopotentiators encompass a broad class of adjuvants, for example saponins like QS-21 (mechanism unknown) (Skene and Sutton, 2006), co-stimulatory molecule agonists (CD40mAb) as well as ligands of the innate immune response including NLRs, C-type lectins, TLRs and RIG-I-like receptors (Maisonneuve et al., 2014). As illustrated in Figure 1.3, immunomodulatory molecules have a direct effect on APCs (signal 0). There are many immunomodulatory molecule-based adjuvants that are licensed for human use or have proceeded to late-stage clinical trials (Table 1.3). One of these has recently completed Phase III clinical trial is the TLR-agonist (TLR-9) CPG ODN used in a HBV vaccine (Hepislav^{TM}) (Eng et al., 2013). Another TLR-agonist, based on the TLR4 ligand, MPL is currently tested in multiple clinical trials for different applications, and is used in two licensed vaccines Cervarix^{TM} (Didierlaurent et al., 2009) and Fendrix^{TM} (Kundi, 2007, Didierlaurent et al., 2009) together in a formulation with alum. The adjuvant formulation is classed as a combination system (*see* Section 1.3.3.3.).

1.3.3.3. Combination systems

Most novel vaccines contain a combination of delivery as well as immunostimulatory adjuvants. In fact, certain adjuvants are physically adsorbed or chemically conjugated to the vaccine antigen in order to co-deliver the stimulation and antigen to the same target cell (Demento et al., 2011). The TLR-agonist CpG adjuvant was found to enhance both B cell (Shirota et al., 2002) and DC driven (Shirota et al., 2002) antigen-specific T_H1 responses when conjugated to the antigen compared to the unconjugated form. Furthermore, using a formulation of CpG and antigen encapsulated into a delivery system enhanced $CD8^+$ T cell responses compared to the CpG and antigen alone (Beaudette et al., 2009).

The licensed HBV vaccine, used to consist of only recombinant hepatitis B surface antigen (HBsAg) adsorbed to aluminium salts. However the addition of the adjuvant AS04, consisting of the MPL (together with alum) enhanced protective antibody levels and made the new vaccine (Fendrix™, GlaxosmithKline) effective in 2 doses rather than the 3 doses required with the original vaccine (Levie et al., 2002, Kundi, 2007, Didierlaurent et al., 2009). The adjuvant AS04 was also used in the HPV vaccine (Cervarix™, GlaxosmithKline) that also showed significantly enhanced anti-HPV antibody titres compared to the use of aluminium salts alone (Giannini et al., 2006). Alum adjuvants are delivery systems able to generate antibody and T_H2-type helper T cell responses but these are not enough to achieve a protective and long-lasting immune response. Upon addition of the TLR4 agonist, the required T_H1-type of helper T cell response is also enhanced achieving the desirable effect (Didierlaurent et al., 2009). Therefore, the use of MPL and alum as an adjuvant system is the perfect example of filling an unmet vaccine requirement due to better understanding of the adjuvants' roles and the type of immune response initiated.

In theory, certain combinations of adjuvants or different formulations should work together to achieve vaccine protection. However, the aim is not always fulfilled. An example of this is the RTS,S malaria vaccine candidate. Immunisation with RTS,S vaccine formulated with AS02 (MPL, QS-21 and emulsions), AS03 (emulsion only) or AS04 (alum and MPL) together with the same circumsporozoite protein fused to HBsAg gave largely variable results. The use of AS02 formulation protected 6 out of 7

individuals, whilst the use of AS03 and AS04 led to 7 from 8 and 5 from 8 to become infected by malaria (Stoute et al., 1997). Even though in the aforementioned study the primary dose was well tolerated, the second dose with AS03 and AS04 produced adverse reactions, with four individuals demonstrating pain, malaise, headache, myalgias and fever. To further improve the effectiveness of the vaccine, the formulation AS02 was switched to AS01, which contained the same adjuvants but in liposomes not emulsions. The difference in adjuvant in the AS01 formulation greatly enhanced immunogenicity of RTS,S vaccine (Stewart et al., 2006). Both of the previous formulations were well tolerated.

1.3.4. Effective versus successful adjuvants

There are multiple effective novel adjuvants in pre-clinical and clinical development (Table 1.3) that can induce cell-mediated responses, humoral responses as well as target and activate DCs. O'Hagan and De Gregorio (2009), define successful adjuvants as ones that have been included in a licensed vaccine product. With this definition, many novel adjuvants are unsuccessful as approval of adjuvants for human use has been slow.

The reasons why adjuvants are unsuccessful are several fold, (i) complex synthetic pathway, meaning that they are difficult to scale-up, (ii) difficulty to obtain raw materials due to expense or purity, (iii) non-biodegradable, which poses a problem at the site of administration (iv) vaccine formulation not optimal and (v) incompatibility with different antigens, which makes conjugation and use in adjuvant systems problematic (O'Hagan and De Gregorio, 2009). However, the crucial reason why certain adjuvants are unsuccessful is safety, tolerability and the risk of triggering autoimmune diseases, due to the direct stimulation of receptors of cells of the innate immune system (Coffman et al., 2010).

1.4. CD40mAb co-administered with antigen as an adjuvant. Current experimental progress.

CD40 stimulation plays an important role in T cell immunity both via B cells and DCs in humoral (Ramesh et al., 1993, Xu et al., 1994) and cell-mediated immune responses (Mackey et al., 1997, Schneider, 2000). This is a critical point for adjuvanticity. Stimulation via the co-stimulatory molecule CD40 could: (1) employ signal 1 or signal 2 by-passing TLRs and associated side-effects and (2) initiate both T_H1 and T_H2 immune responses which is not the case for traditional adjuvants. Certain novel adjuvants fail Phase III clinical trials due to safety reasons. To date, four different CD40mAbs have been explored as immunotherapy in human cancer clinical trials: lucatumumab (Novartis) (Fanale et al., 2014), CP-870, 893 (Pfizer and VLST) (Vonderheide et al., 2007), dacetuzumab (Seattle Genetics) (Khubchandani et al., 2009) and Chi Lob 7/4 (University of Southampton, Southampton, UK) (Johnson et al., 2010). The different CD40mAbs are heterogeneous and show a variety of activities ranging from antagonism (lucatumumab) to agonism (CP-870,893). CD40mAb treatments have all been well tolerated in clinic with only mild to moderate cytokine release syndrome as side-effects, showing that the use of this treatment is a step in the right direction.

CD40mAb has been studied by members of the Heath laboratory not for its application alone in immunotherapy, but for its potential to boost the immune response against co-administered antigens in therapeutic and prophylactic vaccines.

1.4.1. CD40mAb co-administered with TI antigens

The effectiveness of CD40mAb as an adjuvant was first investigated in a study conducted by Dullforce *et al*. (1998). When CD40mAb was co-administered with a TI-2 antigen (type 3 pneumococcal capsular polysaccharide, PS3) *in vivo*, an enhanced IgG-type isotype switched antibody responses, that were protective against *Streptococcus pneumonia* (Dullforce et al., 1998) were generated. This is not normally observed with TI-2 antigens. The authors came up with the hypothesis that CD40mAb is working by direct CD40 receptor stimulation, bypassing T cell help, which is not initiated by TI-

antigens. However, it is noteworthy that the doses of antibodies used in the aforementioned study were as high as 500μg, which was shown by other studies to stimulate $CD8^+$ T cell responses in the absence of T cell help (French et al., 1999, Tutt et al., 2002). This response was probably due to overstimulation of CD40 receptor bearing APCs (Bennett et al., 1998, Schoenberger et al., 1998), which is the very reason high doses are very impractical for vaccination (Barr et al., 2005).

In a subsequent study, co-administration of CD40mAb with LPS, a TI-1 antigen, was investigated in a *Salmonella* infection model (Barr and Heath, 1999). TI-2 antigens have multiple highly repetitive epitopes and only activate B lymphocytes, unlike TI-1 antigens that activate B lymphocytes through TLR signalling (Dintzis et al., 1983, Mond et al., 1995). Enhanced production of protective antibodies against the antigen was again observed, further demonstrating the effectiveness of the CD40mAb adjuvant. The same mode of action was again proposed. Another group that investigated the antibody responses on co-administration of CD40mAb and TI-1 antigen showed that IgG3-type antibodies were predominant (Garcia de Vinuesa et al., 1999), which is characteristic of a TI-2 response together with the absence of memory B cells or GC. Due to their results, they disagreed that CD40mAb works by replacing T-cell help but rather mimicking T cell help, and proposed that CD40mAb works via APC stimulation.

1.4.2. CD40mAb co-administered with TD antigens

CD40mAb targeting CD40 receptor has also been shown to lead to the formation of memory T cells, as well as enhanced T cell responses when immunised in mice. However, in this case the adjuvant effect was achieved against the Fc region of the CD40mAb itself, considered as a TD antigen (Carlring et al., 2004). Barr et al. (2005), showed that CD40mAb does not work by replacing T-cell help, as in CD4 depleted mice antibody responses against the Fc region were not enhanced when compared to the isotype control, even on the simultaneous administration of recombinant IL-4. These results conform to the previous study by Carlring et al. (2004) that demonstrated that T cells are as important as B cells for the adjuvant effect. Interestingly, in CD154 deficient mice, CD40mAb immunised mice enhanced antibody responses compared to the isotype control, showing that the CD40mAb replaces the CD154 stimulus to B cells

which is absent (Barr et al., 2005). The previous two studies therefore show that CD40mAb could directly stimulate antigen-specific B cells, in addition to enhancing antigen-presentation to T cells, leading to improved T-cell help. It is however noteworthy that CD40 receptor is expressed by other APCs including macrophages and DCs and these cell types could have a role in the mode of action of CD40mAb.

CD40mAb admixed with influenza A virus nucleoprotein CTL epitope (NP-366-374) encapsulated in liposomes administered prophylactically in virus challenged mice, induced protective $CD8^+$ cytotoxic T cell immunity (Ninomiya et al., 2002). To confirm the requirement of $CD8^+$ cytotoxic T cell immunity, MHC class I, or MHC class II deficient mice prophylactically immunised with the adjuvant formulation were also infected with influenza. Results showed that there was no protection from the disease in either group of mice, demonstrating that both $CD8^+$ and $CD4^+$ T cells are important for clearing the virus. The fact that protection was achieved when the adjuvant formulation was administered intranasally but not subcutaneously showed that the route of administration is a factor to consider. Other studies have shown enhanced $CD8^+$ cytotoxic T cell responses with the use of liposomal peptide co-administered with CD40mAb (Ito et al., 2000a, Ito et al., 2000b, Hatzifoti et al., 2008). Interestingly, the CD40mAb and the CTL peptide alone do not induce a cytotoxic response in the absence of liposomes (Ito et al., 2000b). This indicates that co-delivery of the antigen and the CD40mAb is essential for an optimal vaccine efficacy. Heat-killed *Listeria monocytogenes* (HKL)-based vaccines are ineffective and very poorly immunogenic. However, immunisation together with CD40mAb induced T_H1 and $CD8^+$ CTL responses which led the mice to survive a normally lethal dose of the pathogen (Rolph and Kaufmann, 2001).

The combination of CD40mAb with TLR-agonists co-administered with antigen has also shown success *in vitro* (Ahonen et al., 2004). The use of these two adjuvants together aimed to target two separate pathways and would exemplify filling the unmet need of a vaccine as TLR stimulation was found important for improving CD40-induced responses. In fact, the use of CD40mAb and TLR agonists co-administered with tumour antigen showed promise for both therapeutic and prophylactic vaccines in murine studies (Llopiz et al., 2008).

1.5. CD40mAb conjugated to antigen as an adjuvant. Current experimental progress.

Since CD40 receptor is widely expressed, it is likely that administration of CD40mAb adjuvant could result in activation of non-antigen specific cells, or more alarmingly, self-reactive B cells. In fact high doses of the antibody induced widespread APC activation giving rise to side-effects like splenomegaly and polyclonal antibody production. This problem was elegantly by-passed by conjugation of CD40mAb to the vaccine antigen (Barr et al., 2003).

CD40mAb chemically conjugated to vaccine antigen (TD antigen) showed between a 100-fold to a 1000-fold increase in antibody responses against the conjugated antigen compared to the CD40mAb/antigen mixture (Barr et al., 2005). This adjuvant effect was achieved even at the very low dose of 1µg. Thus, the problem of toxicity was overcome (Barr et al., 2003). An antibody response could be observed within just 7 days of immunisation (Bhagawati-Prasad et al., 2010). Liposomal encapsulation with CD40mAb also showed success and gave another potential route for the production of a more immunogenic multivalent vaccine (Hatzifoti et al., 2008).

CD40mAb was conjugated to three influenza vaccine antigens to produce (i) B and T cell epitope (from virus haemagglutinin)-based vaccine (subunit vaccine), (ii) whole-killed influenza virus vaccine and (iii) detergent split virus vaccine. Immunogenicity of all three vaccines was enhanced when compared to the respective isotype control conjugates. Interestingly, the different vaccine antigens enhanced antibody production to different degrees, with the weakest vaccine antigen being the epitope-based vaccine (Hatzifoti and Heath, 2007). Furthermore, the detergent split virus vaccine was found to enhance splenic lymphocyte proliferation *ex vivo* against the vaccine antigen.

A CD40mAb conjugated to lymphoma Id vaccine was evaluated for therapeutic and prophylactic anti-tumour efficacy in a murine tumour model. A conjugation strategy (based on sulphydryl-thiol chemistry) used by our lab for the past decade was used to link the CD40mAb and the antigen. Prophylactic immunisation with the CD40mAb conjugate vaccine enhanced median and overall survival of mice compared to

lymphoma Id conjugated to KLH carrier protein, made by traditional techniques (Carlring et al., 2012).

Murine survival was further enhanced in a prophylactic setting and tumour progression was retarded in a therapeutic setting, on co-administration of lymphoma Id-CD40mAb vaccine with the TLR-agonist MPL, confirming the assumptions of possible synergy between CD40mAb co-stimulatory molecules and TLR-agonists. $CD8^+$ and $CD4^+$ depletion studies on A20-CD40mAb+MPL immunised mice demonstrated that $CD8^+$ T cells were the major effector cells in inhibiting tumour growth, however, $CD4^+$ T cells have an indirect role.

1.5.1. Mode of action of CD40mAb-adjuvanted conjugates

THESIS RATIONALE

The precise mode of action of CD40mAb-adjuvanted conjugate vaccines remains unknown. One of the main aims of this project was to evaluate CD40mAb as an adjuvant for T cell responses against conjugated antigen, which is hypothesised to work by:

1. Enhanced delivery of antigen to APCs (B cells or DC) leading to increased antigen on MHC class II, or class I
2. Enhanced activation of APCs (B cells or DC) leading to better co-stimulation
3. Both of the above

The work in this thesis presents first a novel conjugation strategy aiming to refine the conjugation technique to maximise the potential of CD40mAb as an adjuvant, in CD40mAb-adjuvanted conjugates (Chapter 3).

The experimental work shown in Chapter 4 and Chapter 5 is heavily focused on identifying whether B cells or DCs (or both) are involved in the mechanism of action of CD40-mAb-adjuvanted conjugate vaccines. The latter was also investigated in the context of downstream $CD4^+$ and $CD8^+$ T cell responses. A summary of the hypothesised mechanisms of how CD40mAb possibly works as an adjuvant for $CD4^+$ and $CD8^+$ T cell responses against conjugated antigen (investigated in this thesis) are illustrated in Figure 1.4.

The knowledge of which APC is crucial in the mechanism of action, and also the type of immune response elicited will allow better prophylactic application of the vaccine, or therapeutic use together with or relative to other cancer immunotherapies.

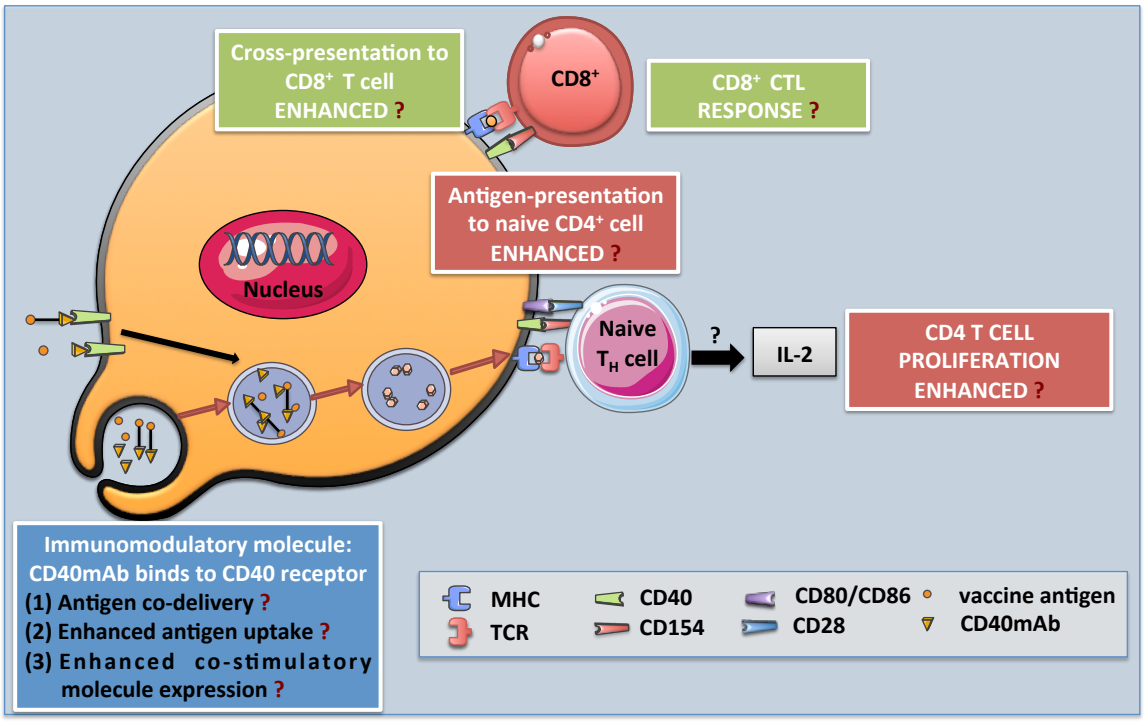

Figure 1.4. Hypothesised mechanism of action of CD40mAb as an adjuvant for T cell responses against conjugated antigen, investigated in this work. CD40mAb-antigen conjugates could work by delivery of antigen to B cells and/or DCs, or both, leading to more peptide loading on MHC class I and/or II. CD40mAb-antigen conjugates could activate B cells and/or DC leading to enhanced co-stimulatory molecule expression, possibly enhancing antigen presentation to naive $CD4^+$ and/or $CD8^+$T cells. CD40mAb-antigen conjugates could enhance $CD4^+$ T cell proliferation against conjugated antigen. CD40mAb-antigen conjugates could enhance $CD8^+$ cytotoxic T cell responses against conjugated antigen.

CHAPTER 2

MATERIALS AND METHODS

2.1. Materials

2.1.1. General Materials

Ultrapure or de-ionised Water (dH_2O)

A Millipore deionising unit was used to de-ionise water. De-ionised water was autoclaved at 121°C for 15 minutes before use.

Phosphate Buffered Saline (PBS)

PBS (supplied by Oxoid, Basingstoke, UK) was prepared by dissolving 1 tablet in 100ml dH_2O. PBS was autoclaved at 121°C for 15 minutes before use.

Buffers

The buffers used for click chemistry conjugation, sodium dodecyl sulphate polyacrylamide gel electrophoresis (SDS PAGE) and Western blotting were prepared as follows. The pH of each buffer was adjusted. Each buffer was autoclaved (as above) and stored at room temperature (RT) unless stated otherwise.

Tris (1.5M) buffer pH 8.8

Tris Base (Fisher Scientific, Loughborough, UK)	18.2g
dH_2O volume up to:	100ml

Tris (1.0M) pH 6.8 (for SDS PAGE) and pH 8.0 (for conjugation)

Tris HCl (Melford Laboratories Ltd., Suffolk, UK)	15.76g
dH_2O volume up to:	130ml

10% Sodium dodecyl sulphate (SDS)

Electrophoresis grade SDS (BDH Biochemical, Poole, UK)	10g
dH_2O volume up to:	100ml

10X Erythrocyte lysis buffer, pH 7.3 (all chemicals purchased from Sigma-Aldrich), stored at 4°C

Ammonium chloride	89.9g
Potassium Hydrogen Carbonate	10g
Tetrasodium EDTA	370mg
dH_2O volume up to:	1000ml

2X Loading buffer, pH 6.8, stored at -4°C

Tris-HCl	12g
SDS	2g
Dithiothreitol (DTT, Sigma-Aldrich)	5g
Glycerol (BDH Laboratory supplies)	15g
Bromophenol blue (Biorad)	0.04g
dH_2O volume up to:	100ml

SDS-PAGE Running buffer and WB transfer buffer compositions

	Company	Running (1X)	Transfer (1X)
Tris-base	Fisher Scientific	1.515g	1.515g
Glycine	Sigma-Aldrich	9.5g	9.5g
SDS	BDH Biochemical	1g	--
Methanol	VWR international Ltd.	--	100ml
dH_2O volume up to:	--	500ml	500ml
pH	--	8.8	8.8

Table 2.1. Preparation of 1X running and transfer buffer for SDS PAGE and Western blotting respectively

Preparation of SDS PAGE gel

	Resolving gel (10ml)			Stacking gel (4ml)
	6%	10%	15%	5%
dH_2O	5.3ml	4.0ml	2.3ml	2.7ml
30% Acrylamide mix*	2.0ml	3.3ml	5.0ml	0.67ml
1.5M Tris (pH 8.8)	2.5ml	2.5ml	2.5ml	--
1.0M Tris (pH 6.8)	--	--	--	0.5ml
10% SDS	0.1ml	0.1ml	0.1ml	0.04ml
10% ammonium persulphate**	0.1ml	0.1ml	0.1ml	0.04ml
TEMED**	0.008ml	0.004ml	0.004ml	0.004ml

Table 2.2. Preparation of SDS PAGE resolving and stacking gel. ***purchased from Geneflow Ltd., Lichfield, UK** ****purchased from Sigma-Aldrich***

Western blotting buffers

Wash buffer

0.1% Tween-20 (Fisher Scientific, UK)	0.5 ml
PBS volume up to:	500 ml

Blocking buffer

Non-fat milk powder	3g
Wash buffer volume up to:	100ml

ELISA buffers

ELISA plates were washed after each incubation step with the following wash buffer:

0.05% Tween-20	5 ml
PBS volume up to:	10,000 ml

ELISA plates are blocked either with the western blotting blocking buffer or:

5% bovine serum albumin (First Link Ltd., UK)	5 ml
PBS volume up to:	100 ml

The blocking buffer used is indicated in the methods section.

Protein quantification assay

Protein quantification was carried out using the bicinchoninic acid (BCA) Protein Assay kit purchased from Pierce, IL, USA.

Endotoxin assay

The Chromogenic Limulus Amebocyte Lysate (LAL) kit purchased from Biowhittaker, Lonza, UK, was used to test for endotoxin contamination.

General non-reusable materials

Product	Company
10ml, 25ml Stripette pipettes	Corning incorporated, Pittsburgh, USA
20, 50ml Universal Tubes	Sarstedt, Nümbrecht, Germany
1ml, 5ml and 60ml syringes	BD Plastipak™, Oxford, UK
21-gauge needle	BD Microlance 3, Fraga, Spain
Sterile Petri Dishes	Bibby Sterilin, Nottingham, UK
0.1% Trypan Blue	Sigma-Aldrich, Steinheim, Germany
Trypsin-Versene®	Biowhittaker, Lonza, UK

Table 2.3. General non-reusable materials

2.1.2. Monoclonal antibodies, reagents and materials used for conjugation

Product	Company
General Materials	
30kDa and 100kDa molecular-weight cut-off (MWCO) centrifugal filter units	Amicon® Ultra-4, EMD Millipore, Billerica, MA, USA
MACSMix tube rotator	Miltenyi Biotec GmbH, Germany
Dimethylsulphoxide (DMSO) Hybri-Max™	Sigma-Aldrich, Steinheim, Germany
Dimethylformamide (DMF)	Pierce, IL, USA
Sodium azide	Sigma-Aldrich, Steinheim, Germany
Sulphydryl-maleimide coupling (Standard method)	
N-ethylmaleimide (NEM)	Sigma-Aldrich, Steinheim, Germany
***N*-Succinimidyl *S*-acetylthioacetate *(*SATA)**	Pierce, IL, USA
Sulfosuccinimidyl-4-(*N*-maleimidomethyl) cyclohexane-1-carboxylate *(*SMCC)	Pierce, IL, USA
Hydroxylamine hydrochloride	BDH Laboratory supplies, Poole, England
L-cysteine hydrochloride	Sigma-Aldrich, Steinheim, Germany
Click chemistry coupling (CLICK method)	
Dibenzylcyclooctyne-NHS ester (DBCO) linker	Jena Bioscience, GmbH, Germany
15-Azido-4,7,10,13-tetraoxa-pentadecanoic acid succinimidyl ester (NHS-PEG4-Azide) linker	Jena Bioscience, GmbH, Germany

Table 2.4. Reagents and materials used for conjugation

Product	Company
Chicken Egg Albumin (OVA)	Sigma-Aldrich, Steinheim, Germany
Imject™ Maleimide-activated OVA	Pierce, IL, USA
A20-Idiotype (A20 antibody) (mouse IgG2a)	Antibody resource centre (ARC). University of Sheffield, UK.
CD40mAb; clone 1C10 (rat IgG2a)*	Antibody resource centre. University of Sheffield, UK.
Isotype mAb; GL117mAb* (rat IgG2a, which recognises *E.coli* β-galactosidase).	Antibody resource centre. University of Sheffield, UK.
CD40mAb; clone 10C8 (rat IgG1)*	Antibody resource centre. University of Sheffield, UK.
Isotype mAb; 20C2 mAb* (rat IgG1 which recognises human IL-12, CRL-2382™, ATCC)	Antibody resource centre. University of Sheffield, UK.
SIINFEKLC peptide (>95% purity)	Genecust, Dudelange Luxembourg
ISQAVHAAHAEINAGRC (ISQC) peptide (>95% purity)	Genecust, Dudelange Luxembourg
EZ-Link Sulfo-NHS-Biotin	Pierce, IL, USA
NHS-Fluorescein	Pierce, IL, USA
DyLight 650 NHS Ester	Pierce, IL, USA

Table 2.5 Monoclonal antibodies and OVA used for conjugation
Hybridomas were grown in bioreactors and antibodies were purified from tissue culture supernatants (Heath et al., 1994, Presky et al., 1996, Barr and Heath, 2001), by protein G affinity

2.1.3. ELISA and Western blotting reagents and antibodies

2.1.3.1. ELISA reagents and antibodies

ELISA antibodies shown in Table 2.6 were diluted in PBS and added to the 96-well plate in a volume of 100µl, unless suggested otherwise. The ELISA experiments were carried out in 96-well flat-bottomed plates (without lid) and purchased from Corning inc.

Murine recombinant IL-2 purchased from eBioscience was used as a standard in the IL-2 detecting ELISA. A20-Id Fab fragments used for the CD40-specific ELISA were generated in-house and used at a concentration of 2.5µg/ml. A20-Id Fab fragments were diluted in 0.1M sodium bicarbonate (BDH Laboratory supplies) buffer (pH 9.4).

Specificity	Conju-gate	Type	Application and WD	Source
OVA-specific ELISA or Western blot				
Rat IgG	none	Polyclonal goat anti-rat IgG (mouse adsorbed)	ELISA: 1/500	Serotec
OVA	none	Polyclonal rabbit (IgG) anti-OVA	ELISA: 1/5000 WB: 1/10,000	Abcam
Rabbit IgG whole molecule	HRP	Polyclonal goat anti-rabbit IgG	ELISA: 1/5,000 WB: 1/10,000	Sigma-Aldrich
A20-Id-specific ELISA or Western blot				
Rat IgG	none	Polyclonal goat anti-rat IgG (mouse adsorbed)	ELISA: 1/500	Serotec
Mouse Ig	HRP	Polyclonal goat anti-mouse (multiple adsorbed)	ELISA and WB: 1/2000	Pharmingen
CD40-specific ELISA or WB				
Human IgG (Fc specific)	none	Goat anti-human (mouse and rat adsorbed) IgG	ELISA: 1/200	Sigma-Aldrich
Mouse CD40	none	Recombinant mouse fusion protein between mouse CD40 and human IgG1 Fc (CD40/Fc chimera)	ELISA: 1/1000	R&D Systems
Mouse Ig	HRP	Polyclonal goat anti-mouse (multiple adsorbed)	ELISA and WB: 1/2000	Pharmingen
Rat IgG (mAb)-specific WB				
Rat IgG	**HRP**	Polyclonal goat anti-rat (H+L) IgG	WB: 1/1000	Biosource
Biotinylated conjugate by WB				
Biotin	**HRP**	HRP-labelled Streptavidin	WB: 1/2000	Vector Labs
Antibodies used for detection of IL-2 by ELISA				
Mouse IL-2	none	Purified rat anti-mouse IgG2	ELISA: 1/250	eBioscience
Mouse IL-2	none	Biotinylated rat anti-mouse IgG2b	ELISA: 1/500	eBioscience
Biotin	HRP	HRP-labelled Streptavidin	ELISA: 1/2000	Vector Labs

Figure 2.6. The antibodies used for ELISA and/or Western blotting experiments.
WD- working dilution; WB – Western Blot; HRP – Horseradish Peroxidase

The ELISA substrate used was SIGMA*FAST*™ OPD (*o*-Phenylenediamine dihydrochloride) purchased from Sigma-Aldrich. This consisted of two tablets; one OPD tablet and one urea hydrogen peroxide/buffer tablet. The two tablets were dissolved in 20ml of dH_2O obtaining a ready-to-use substrate.

2.1.3.2. Western Blotting reagents and antibodies

ECL Western blotting substrate purchased from Pierce (IL, USA) was used. Detection reagents 1 and 2 were mixed at a 1:1 ratio, added to the GE Healthcare Amersham™ Protran™ Premium NC Nitrocellulose Membrane (Pittsburgh, USA) of pore size 0.45µm and incubated for 1 minute in the dark. The excess reagent was drained. The membrane was either exposed to an X-ray film, placed in developer solution (Ilford Phenisol, Harman technology Ltd, Cheshire, UK) for few minutes and then dipped in fixer solution (Ilford Hypam Rapid Fixer, Harman technology Ltd, Cheshire, UK), otherwise the membrane was imaged using the ChemiDoc™ XRS+ System (Biorad), using the Image Lab™ acquisition and analysis software (Biorad).

2.1.4. Flow cytometry instrument, reagents and antibodies

2.1.4.1. Flow cytometry instrument

All samples for this thesis were analysed on an LSRII™ flow cytometer, (BD Biosciences). The BD LSRII™ has 4 lasers, as shown in Table 2.4. Table 2.4 also shows the settings at the BD LSRII™ Core Flow Cytometry facility at the University of Sheffield. BD FACSDiva™ (BD Biosciences) and/or FlowJo™ (Tree Star, San Carlos, California) software were used to analyse results (overlaid histograms were produced using FlowJo™).

Laser	Excitation channel (nm)	Filters
Red	633	780/60 730/45 660/20
Blue	488	780/60 695/40 660/20 610/20 575/26 530/30
Violet	405	525/50 450/50
UV	355	530/30 450/50

Figure 2.7. The four laser settings of the BD LSRII™ cytometer

2.1.4.2. Flow cytometry buffers, reagents and antibodies

FACS buffer was made using sterile PBS containing 0.1% BSA. This was refrigerated at 4°C and kept on ice during sample preparation. Paraformaldehyde purchased from Sigma-Aldrich, was frozen at a stock solution of 4% in sterile PBS buffer.

A cell viability dye LIVE/DEAD® Fixable Blue Dead Cell Stain control (Molecular Probes, Invitrogen, UK) was used with each experiment. The dye penetrates damaged membranes of dead cells and binds to free amines inside and outside the cells. In contrast, the dye does not permeate live cell membranes and therefore binds to the extracellular amines (Perfetto et al., 2006) resulting in dim staining. For dye reconstitution, 50µl of DSMO was added to the vial and small aliquots were stored at -4°C in the dark for future use.

Carboxyfluorescein diacetate succinimidyl ester (CFSE, Molecular Probes, Invitrogen, UK) was used in lymphocyte proliferation cell assays. CFSE is an NHS-ester that only becomes fluorescent when the succinimidyl ester group is hydrolysed by intracellular esterases. On reaction with the intracellular amines, the dye is retained within the cells and divides between each daughter cell upon proliferation (Lyons and Parish, 1994). CFSE allows the monitoring of cell divisions even up to 10 generations (Lyons, 2000). A 10mM stock solution of CFSE was prepared with 90µl of sterile DMSO and frozen in aliquots, as per manufacturer's instructions (Molecular Probes, Invitrogen,

UK).

The fluorochrome-conjugated antibodies that were used in this study are shown in Table 2.8. All antibodies shown are anti-mouse antibodies, unless stated otherwise. Cells stained by multiple fluorochromes were compensated for by the use of anti-rat and anti-hamster Ig compensation beads, BD™ CompBead (BD Biosciences).

Specificity (volume = 200µl)	Clone number	Fluorochrome	Channel	Source and type
CD11c (0.2µg)	N418	R-Phycoerythrin (PE)	Blue 575/26	Biolegend, Armenian Hamster IgG2a
CD19 (0.1µg)	eBio1D3 (1D3)	eFluor-450	Violet 450/50	eBioscience, Rat IgG2a
CD19 (0.1µg)*	6D5	PE	Blue 575/26	Biolegend, Rat IgG2a
CD80 (0.2µg)	16-10A1	Fluorescein isothiocyanate (FITC)	Blue 530/30	Biolegend, Armenian Hamster IgG
CD86 (0.02µg)	GL-1	Allophycocyanin conjugate (APC)	Red 660/20	Biolegend, Rat IgG2a
F4/80 (0.2µg)	BM8	APC	Red 660/20	Biolegend, Rat IgG2a
Gr-1 (0.02µg)	RB6-8C5	PE	Blue 575/26	eBioscience, Rat IgG2b
CD4 (0.02µg)	RM4-5	PE/Cyanine7 (PE-Cy7)	Blue 780-60	eBioscience, Rat IgG2b
H-2K^{b} bound to SIINFEKL (0.2µg)	eBio25-D1.16	PE-Cy7	Blue 780-60	Biolegend
CD40 (0.5µg)	1C10	FITC	Blue 530/30	Southern Biotech, Rat IgG2a
CD40 (1µg) labelled in-house	1C10	Dylight 650 NHS-ester	Red 730-45	Pierce, Rat IgG1
CD16/CD32 (0.5µg)	2.4G2	**N/A**	**N/A**	Pharmingen, Rat IgG2b
OVA (4µg)	**N/A**	**N/A**	**N/A**	Abcam, Rabbit IgG
Rabbit IgG (2µg)	**N/A**	FITC	Blue 530/30	Southern Biotech, Goat IgG
A20 (mouse IgG2a) (0.2µg)	R19-15	FITC	Blue 530/30	BD Biosciences, Rat IgG2a

Figure 2.8. Antibodies used for flow cytometry

*PE-labeled CD19 was only used for positive B cell selection and related experiments

2.1.5. Tissue culture media and reagents

2.1.5.1. Tissue culture media, supplements and culture conditions

Tissue culture media, RPMI 1640 and DMEM were both purchased from BioWhittaker (Lonza, UK), and in all cases supplemented with 10% fetal calf serum (FCS) and 50µM 2-mercaptoethanol (2-ME). FCS was purchased from Nalgene Bioclear (Wiltshire, UK) and 2-ME from Sigma-Aldrich (Steinheim, Germany). Normal culture conditions includes incubation in a humidified atmosphere at 37°C, in the presence of 5% CO_2. The plasticware used for tissue culture is shown in Table 2.9.

For primary cell culture, RPMI 1640 was also supplemented with the antibiotics Penicillin and Streptomycin (100 U/ml, Sigma-Aldrich). This will be referred to as R1. For generation of bone marrow derived dendritic cells (BM-DCs) the growth factors GM-CSF (20ng/ml) and IL-4 (10ng/ml), both purchased from Peprotech Inc. (London, UK), were also added. This will be referred to as R2.

Plasticware for tissue culture

Product	Company
6-well/96-well cell culture plates with lid (flat-bottomed)	Corning Incorporated, Costar, Pittsburgh, USA
48-well cell culture plate	Greiner Bio-One GmbH, Frickenhausen, Germany
1.5ml Cryogenic vials	Nalge Nunc International, New York, USA
0.22µm Millex-GP Syringe Filter Unit	Millex, Bedford, MA, USA
Cell strainer (70µm Nylon)	BD Falcon, New Jersey, USA

Table 2.9. Plasticware used for tissue culture

2.1.5.2. T cell activation reagents and LPS

Concanavalin A (ConA), phorbol 12-myristate 13-acetate (PMA) and Ionomycin (Ion.) were obtained from Sigma-Aldrich and stored at -20°C. Bacterial LPS from *Escherichia coli* (serotype 026:B6) was obtained from Sigma-Aldrich. LPS was prepared on the day of use in sterile PBS or tissue culture media.

2.1.5.3. B cell positive selection

B cell positive selection from the spleen was carried out using anti-PE MultiSort MicroBeads, MACS® Separator and MS columns (which can hold up to 2 x 10^8 cells) all purchased from Militenyi Biotech. For this procedure an EDTA-containing buffer was used (PBS pH 7.2, 0.5% BSA and 2mM EDTA).

2.1.6. Cell lines

2.1.6.1. CD40L929 cell line

CD40L929 is a an L929 fibroblast cell line stably transfected with murine CD40 (Randall et al., 1998) used to determine the functional activity of CD40mAb. This was a kind gift of DNAX Research Institute, Palo Alto, CA. This cell line is an adherent cell line grown in DMEM culture medium supplemented with the selective antibiotic geneticin or G418 (0.5mg/ml) purchased from Sigma-Aldrich.

2.1.6.2. T cell hybridoma cell lines

Two T cell hybridoma lines were used. Both cell lines were grown in supplemented RPMI-1640. The DO11.10 cell line (a kind gift from Dr. Philippa Marrack, National Jewish Health Center, Denver) is a $CD4^+$ T cell hybridoma which recognises the C-terminal epitope $OVA_{323-339}$ with the amino acid sequence **I**SQAVHAAHAEINAGR (referred to as ISQ peptide, in this thesis), presented on both I-A^d and I-A^b (Robertson et al., 2000b). The B3Z cell line (a kind gift from Dr. Eleanor Cheadle, Paterson Institute for Cancer research, Manchester, UK) is a $CD8^+$ T cell hybridoma that expresses a T cell receptor (TCR) specific for $OVA_{257-264}$ with the amino acid sequence SIINFEKL, presented on the murine H-$2K^b$ MHC class I molecule (Sanderson and Shastri, 1994). C57Bl/6 splenocytes incubated with SIINFEKL peptide (Cambridge Bioscience) stimulate B3Z hybridoma cells, whilst BALB/c splenocytes incubated with ISQ peptide (Cambridge Bioscience) stimulate DO11.10 hybridoma T cells. On activation both DO11.10 and B3Z cell lines produce IL-2, measured in this thesis by means of ELISA.

2.1.6.3. A20 tumour cell line

The BALB/c B cell lymphoma cell line used for tumour studies is the A20 cell line that is originally derived from a spontaneous reticulum cell neoplasm (ATCC) (Kim et al., 1979). Cells are a suspension cell line maintained in culture in RPMI-1640 medium supplemented with 10% FCS, 2mM *L*-glutamine (Sigma-Aldrich) and 50µM 2-ME and incubated at 37°C, 5% CO_2.

2.1.7. Animals

Female BALB/c mice between 6-12 weeks old were used to evaluate antibody responses to immunisation with the antigen-mAb conjugate vaccines. Female C57Bl/6 mice of 6 weeks old were used for the *in vivo* cytotoxicity assay. Mice were purchased from Harlan, UK.

BALB/c and C57Bl/6 mice of both sexes and of age older than 6 weeks were used for organs utilised in *in vitro* tests, as well as for the *in vivo* conjugate-tracking experiments. The previously mentioned mice were donated from different groups in the Medical School, University of Sheffield.

2.2. Methods

2.2.1. Conjugation of antigen to mAbs by different methods

All materials, reagents and antibodies used for conjugation are shown in Section 2.1.2. mAbs for these procedures refers to CD40mAb and isotype control mAb.

2.2.1.1. Conjugation of A20 antibody to mAbs using Sulphydryl-maleimide coupling (Standard method)

To introduce sulphydryl groups into monoclonal antibodies (mAbs, MW approximately 150kDa) SATA was added at a 19.25 molar excess. SATA was prepared immediately before use according to the manufacturers' instructions by adding DMSO to a concentration of 52mM, and 10µl SATA was thereafter added to 1 ml of mAb of concentration 4mg/ml (27µM). SATA was reacted with the mAbs at RT for 30 minutes on a MACSMix tube rotator. To remove excess unbound SATA, the SATA-treated mAb was buffer-exchanged against PBS using a 30-kDa MWCO spin filter at 1400rcf three times with 4ml following manufacturer's instructions. Sulphydryl groups introduced into mAbs were de-protected by adding 100µl of 0.5M hydroxylamine buffer (25mM EDTA in PBS, pH 7.2-7.5) to 1ml of SATA-treated mAb at 1mg/ml. This reaction was incubated for 2 hours at RT on the MACSMix tube rotator.

To introduce maleimide groups into the A20 antibody (MW approximately 150kDa), Sulfo-SMCC was added at a 35 molar excess. Sulfo-SMCC solution was prepared immediately before use according to the manufacturers' instructions by adding dH_2O at a concentration of 7.56mM, and 60µl of this solution was incubated with 1ml of A20 antibody of concentration 2mg/ml (13µM). Sulfo-SMCC was reacted with the A20 antibody at RT for 1 hour on a MACSMix tube rotator. The maleimide-activated A20 antibody was buffer exchanged three times with 4 ml PBS using a 30-kDa MWCO spin filter at 1400rcf.

The maleimide-activated A20 antibody (13µM) was incubated with SATA-treated mAbs (13µM) in a molar ratio of 1:1 at 4°C on MACSMix tube rotator overnight. To stop the reaction a final concentration of 50mM L-cysteine (prepared fresh) was

added and incubated for 15 minutes. The conjugates were filtered three times with 4ml PBS using a 30-kDa MWCO spin filter at 1400rcf, and were stored at 4°C in 1ml of PBS containing 0.01% sodium azide.

2.2.1.2. Conjugation of OVA to mAbs using the Standard method

The mAbs were functionalised with SATA as described in Section 2.2.1.1.

To block sylphydryls and prevent disulphide formation, 3mg/ml ovalbumin (OVA, MW of 45kDa) (66.67µM) in PBS was treated with the equivalent amount of N-ethylmaleimide (NEM) for two hours at RT on the MACSMix tube rotator. To maleimide activate OVA, 7.56mM Sulfo-SMCC was prepared prior to use and 60µl (7 molar excess of Sulfo-SMCC to OVA) was incubated with 1ml OVA antigen (66.67µM) solution for 1 hour at RT on the MACSMix tube rotator. The maleimide-activated OVA antigen was buffer exchanged three times with 4 ml PBS using a 30-kDa MWCO spin filter as described in Section 2.2.1.1.

Maleimide-activated OVA at a concentration of 22.2µM was incubated with SATA-treated mAbs at a concentration of 3.33µM (resulting in a 7:1 molar ratio of OVA to mAb) at 4°C on the MACSMix tube rotator overnight, and the reaction was stopped as in Section 2.2.1.1.

2.2.1.3. Conjugation of Imject™ maleimide-activated OVA to mAbs using the Standard method

The mAbs were functionalised with SATA as described in Section 2.2.1.1.

The Imject™ maleimide-activated OVA was reconstituted in 200µl dH_2O for a concentration of 10mg/ml. The maleimide-activated OVA antigen (22.22µM) was incubated with SATA-treated mAbs (6.67µM) in a molar ratio of 3:1 (OVA:mAb) at 4°C on MACSMix tube rotator overnight, and then treated as explained in Section 2.2.1.1. A 100-kDa MWCO spin filter was used instead of a 30-kDa MWCO spin filter for conjugate buffer exchange, for this experiment.

2.2.1.4. Conjugation of biotinylated and non-biotinylated peptide to mAbs using the Standard method

2.2.1.4.1. ISQC peptide biotinylation

ISQC peptide (MW of 1877Da) was reconstituted in PBS and 200µg was added to 3.3mg EZ-Link Sulfo-NHS-Biotin (MW of 443.43Da) in a total volume of 700µl in PBS (equating to 50-fold molar excess of Biotin – as advised by the manufacturer). EZ-Link Sulfo-NHS-Biotin was prepared immediately before use according to the manufacturers' instructions by adding dH_2O to the desired concentration.

This was incubated for 30 minutes at RT on a MACSMix tube rotator. The excess unconjugated EZ-Link Sulfo-NHS-Biotin and non-biotinylated ISQC were not removed by buffer exchange because of their low MW, and potential loss of valuable sample. The sample was refrigerated for at least 1 week before conjugation to the mAbs (this ensured that the excess EZ-Link Sulfo-NHS-Biotin reagent was hydrolysed and does not also conjugate to antibody). Therefore, EZ-Link Sulfo-NHS-Biotin solution reconstituted on the day of peptide biotinylation was labelled and refrigerated to be used as an internal control during conjugation on a later date.

2.2.1.4.2. SIINFEKLC peptide biotinylation

SIINFEKLC peptide (MW of 1066Da) was reconstituted in dH_2O, and 200µg was added to 5.8mg EZ-Link Sulfo-NHS-Biotin (443.43Da) in a total volume of 700µL dH_2O (equating to 50-fold molar excess of Biotin – as advised by the manufacturer), and incubated for 30 minutes at RT on a MACSMix tube rotator. The rest of the procedure is as described in Section 2.2.1.4.1.

2.2.1.4.3. Conjugation of mAbs to biotinylated peptide or non-biotinylated peptide

Sulfo-SMCC (7.6mM) was reconstituted in dH_2O, and 25µl Sulfo-SMCC solution was added to 500µl mAb (40µM in PBS) at 10-fold molar excess. After 1 hour incubation at RT on a MACSMix tube rotator, the solution was buffer exchanged three times

with 4ml PBS using a 30-kDa MWCO spin filter at 1400rcf as described in Section 2.2.1.1, to remove lower MW materials.

Maleimide-activated mAbs (1mg in 1ml, 6.67µM) were mixed with 0.09mg of biotinylated or non-biotinylated ISQC peptide (47.5µM), as well as 0.05mg of biotinylated or non-biotinylated SIINFEKLC peptide (47µM) at a 1 to 7 molar ratio of mAb to peptide in a total volume of 1ml PBS and incubated overnight at 4°C on a rotator.

Maleimide-activated mAbs (1mg) were also mixed with 0.02mg of hydrolysed biotin* reagent (reconstituted on the day of peptide biotinylation, Section 2.2.1.4.1.) in a total volume of 1ml PBS, and incubated overnight at 4°C on a rotator. This served as an internal control to ensure that the NHS-Biotin in the biotinylated peptide solution had hydrolysed and was not also conjugating to the mAbs. Stopping the conjugation reaction and the remainder of the procedure was the same as in Section 2.2.1.1.

**to ensure that the biotin is hydrolysed and non-reactive, at least a week was left between peptide biotinylation and conjugation.*

2.2.1.5. Conjugation of SIINFEKLC$_{FAM}$ peptide to mAbs$_{Dylight}$ using the Standard method

2.2.1.5.1. Labelling of SIINFEKLC peptide with NHS-Fluorescein (FAM)

The NHS-Fluorescein (will be referred to as FAM) was reconstituted fresh at a concentration of 20mg/ml by addition of 50µl DMF and 50µl dH_2O to 2mg. SIINFEKLC (200µg) peptide was added to FAM (1.8mg) in a total volume of 700µL dH_2O (equating to 20-fold molar excess of FAM), and incubated for 30 minutes at RT on on a MACSMix tube rotator. The rest of the procedure is as described in Section 2.2.1.4.1.

2.2.1.5.2. Labelling of mAbs with Dylight 650 NHS-ester

The Dylight 650 NHS-ester (will be referred to as Dylight) was prepared at a concentration of 1mg/ml by reconstitution of 1mg in 100µl DMF and 900µl PBS. Four sets of mAbs were prepared at a concentration of 2mg/ml. The mAbs (13.3µM) were

incubated with a molar excess of 7 (93.1µM), 3.5 (46.55µM), 1.5 (19.95µM) or 0.75 (10µM) Dylight (MW of 1066Da) for 1 hour at RT. The labelled mAbs were filtered extensively with 4ml PBS using a 100-kDa MWCO spin filter as described in Section 2.2.1.1 and stored at 4°C in PBS.

2.2.1.5.3. Conjugation of mAbs or Dylight-labelled mAbs to FAM-labelled SIINFEKL

$mAb_{Dylight}$ and unlabelled mAbs were maleimide-activated with Sulfo-SMCC as explained in Section 2.2.1.4.3. with the alteration that, the mAbs (3.33µM) was treated with an 80-fold molar excess of Sulfo-SMCC. This was performed because of the low concentration of the mAbs, as was recommended by the manufacturer.

To make $SIINFEKL_{FAM}$-mAb conjugates, maleimide-activated mAb (0.5mg in 1ml, 3.33µM) was mixed with 0.022mg $SIINFEKLC_{FAM}$ (20µM) in a 1 to 7 molar ratio in a total volume of 1ml PBS and incubated overnight at 4°C on a MACSMix tube rotator, and treated as in Section 2.2.1.1. To make $SIINFEKL_{FAM}$-$mAb_{Dylight}$ conjugates, maleimide-activated $mAb_{Dylight}$ (0.5mg) was mixed with 0.022mg $SIINFEKLC_{FAM}$ in a 1 to 7 molar ratio in a total volume of 1ml PBS and incubated overnight at 4°C on a MACSMix tube rotator, and treated as in Section 2.2.1.1.

Maleimide-activated mAbs (0.5mg) were also mixed with 0.02mg of hydrolysed FAM* (reconstituted on the day of peptide labelling, Section 2.2.1.5.1.) in a total volume of 1ml PBS, and incubated overnight at 4°C on a MACSMix tube rotator. This served as an internal control to ensure that the FAM in the $SIINFEKL_{FAM}$ solution had hydrolysed and is not also conjugating to the mAbs. Stopping the conjugation reaction and the remainder of the procedure is the same as in Section 2.2.1.1.

**to ensure that the FAM is hydrolysed and non-reactive, at least a week was left between peptide labelling and conjugation.*

2.2.1.6. Conjugation of A20 antibody to mAbs using click chemistry

mAbs were prepared at a concentration of 6mg/ml (40µM) in buffer (20mM $NaPO_4$, 150mM NaCl, pH 7.35), and were functionalised with DBCO. DBCO was prepared in DMSO at a concentration of 10mM and 90µl was added to of the antibodies (in a

total volume of 1800µl, 12.5 molar excess of DBCO) and incubated at RT for 30 minutes. The reaction was stopped by the addition of a quenching buffer (1M Tris-HCl, pH 8.0) to a final concentration of 50mM Tris.

The A20 antibody was prepared at a concentration of 6mg/ml (40µM) in PBS and was functionalised with 90µl of freshly prepared 10mM NHS-PEG4-Azide reagent. The reaction was allowed to proceed for 30 minutes at RT and stopped by the addition of a quenching buffer (1M TRIS-HCl, pH 8.0) to a final concentration of 50mM TRIS. The functionalised A20 antibody was buffer exchanged three times with 4ml PBS using a 30-kDa MWCO spin filter at 1400rcf.

The NHS-PEG4-Azide-functionalised A20 antibody (37µM) was incubated with DBCO-functionalised mAbs (37µM) at a 1:1 molar ratio at 4°C on MACSMix tube rotator overnight. The conjugates were filtered three times with 4ml PBS using a 30-kDa MWCO spin filter at 1400rcf, and were stored at 4°C in 1ml of PBS containing 0.01% sodium azide.

2.2.1.7. Conjugation of OVA to mAbs using click chemistry

The functionalisation of mAbs with DBCO, and OVA with NHS-PEG4-Azide was carried out as in Section 2.2.1.6. It is noteworthy that OVA concentration was 6mg/ml (133µM), and a 4 molar excess of NHS-PEG4-Azide was added. The NHS-PEG4-Azide functionalised OVA (110µM) was incubated with the DBCO-treated mAbs (37µM) in a molar ratio of 3:1 (OVA to mAb) at 4°C on MACSMix tube rotator overnight and then treated as in Section 2.2.1.2.

2.2.2. Fractionation of conjugates using HPLC

The click chemistry conjugates were separated by size-exclusion high-performance liquid chromatography (HPLC) into several fractions. The HPLC buffer (25mM sodium phosphate, 0.1% TFA, 20% methanol, pH 6.7) that was degassed using Nalgene filter of pore size 0.22µm prior to use and HPLC conditions were optimised by Dr. Oliver Wilkinson (Chemistry Department, University of Sheffield).

To remove possible sample precipitate the sample was centrifuged at 16,000rcf for 15 minutes after which the supernatant was transferred into a new tube. The size-exclusion chromatography column (Phenomenex®, CA, USA) was screwed tightly to the HPLC (Gilson Preparative HPLC system) instrument. Using a program previously optimised by Dr. Oliver Wilkinson, a sample amount of 50µg was injected, and a print out of the data trace was obtained. The sample fractions of interest were collected. The different fractions were then buffer exchanged three times with 4 ml PBS using a 30-kDa MWCO spin filter at 1400rcf, to remove any traces of methanol, and were stored at 4°C in 1ml of PBS containing 0.01% sodium azide.

2.2.3. Quantification of antigen-mAb conjugates by BCA Protein Assay

A BCA Protein Assay kit was used to determine the concentration of conjugates. An ampule containing BSA (2 mg/ml) supplied with the kit was used as a reference to determine the protein concentration. A series of dilutions of known concentrations were made starting at 2mg/ml according to manufacturer's instructions (Table 2.10).

µg/ml protein	Vial	Volume + Source of BSA
2000	A	Stock BSA
1500	B	75µl stock + 25µl PBS
1000	C	55µl stock +55µl PBS
750	D	30µl vial B + 30µl PBS
500	E	55µl vial C + 55µl PBS
250	F	55µl vial E + 55µl PBS
125	G	45µl vial F + 45µl PBS
25	H	12µl vial G + 48µl PBS
0	I	PBS only

Table 2.10. Serial dilution of Bovine serum albumin for use as standard curve

A 25µl volume of each standard and sample were added to a 96 well plate and tested in replicates of two. A 200µl working solution prepared from reagents A and B (at a ratio of 50:1 respectively) available from the kit were added to the well containing the standard dilutions and the conjugates. The plate was incubated in the dark at 37°C for 30 minutes, and the absorbance was read at 562nm on an ELx808™ Absorbance Microplate Reader (Bio Tek). The concentration of the conjugates was determined by comparison with the standard curve.

2.2.4. Verification of antigen-mAb conjugate composition

2.2.4.1. Verification of antigen-mAb conjugate composition by reducing and non-reducing SDS PAGE

The composition of the antigen-mAb conjugates were analysed using reducing SDS-PAGE (BioRad) using a 6%, 10% or 15% gel. An amount of 1-10µg (according to the sample being tested) of conjugates and controls was prepared in a 1:1 ratio with 2X loading buffer which contained DTT and denatured the proteins via reduction of disulphide bonds. The samples were also heated to 99°C for 5 minutes, using a heating block, to further denature proteins. A volume of 20µl of each sample and a volume of 5µl protein ladder (PageRuler™ Prestained Protein Ladder, Fermentas) ranging from 10-170kDa, was loaded onto the gel and run for 80 minutes at 120V. The gel was stained using InstantBlue (Expedeon) for 2-24 hours, and subsequently washed and stored in dH_2O at RT. The composition of the antigen-mAb conjugates was also analysed using non-reducing SDS-PAGE (BioRad). The alterations in procedure include the use of a 2X loading buffer that does not contain any reducing agent, and the direct addition of the samples to the gel, thus missing the heating step.

2.2.4.2. Verification of antigen-mAb conjugate composition by Western Blotting

Detection of rat IgG, mouse A20 IgG, biotinylated peptides and OVA in the particular antigen-mAb conjugates was carried out using the antibodies mentioned in Table 2.6. The substrate was re-constituted and added as explained in 2.1.3.2.

The composition of the conjugates was confirmed by Western blotting. The rat IgG (mAb) portion of the conjugate was detected with an HRP labelled anti-rat IgG antibody. The OVA portion was detected using a rabbit (IgG) anti-OVA antibody and an HRP-conjugated anti-rabbit IgG antibody. The A20 antibody portion was detected with an HRP-conjugated polyclonal anti-mouse Ig antibody. The biotinylated peptides portion was detected with HRP-conjugated streptavidin.

SDS PAGE gel apparatus was disassembled and the gel was positioned onto nitrocellulose membrane and placed between two filter papers soaked in 1X transfer buffer. The apparatus was placed in the electrophoresis tank filled with 1X transfer buffer and was run for 60 minutes at 100V. The nitrocellulose membrane was then placed into block buffer and was incubated for 1 hour at RT on an orbital shaker.

2.2.4.2.1. Rat IgG, Mouse IgG or Biotin-specific Western blotting

The detection antibody HRP-conjugated anti-rat IgG (CD40mAb and isotype mAb detection), HRP-conjugated polyclonal anti-mouse Ig (A20 antibody detection) or HRP-conjugated streptavidin (biotinylated peptide detection) were diluted in blocking buffer and added to the nitrocellulose membrane containing the transferred samples. Incubation was allowed to continue for two hours at RT. The blocking buffer was drained and the nitrocellulose membrane was incubated with 10ml wash buffer for 10 minutes at RT on the orbital shaker. The previous step was repeated three times. After addition of the substrate, the nitrocellulose membrane was left to expose to the X-ray film for 30 minutes in the case of HRP-conjugated anti-rat IgG and 1-2 minutes in the case of HRP-conjugated polyclonal anti-mouse Ig. For the biotinylated samples, the membrane was imaged using the ChemiDoc™ XRS+ System (Biorad) after exposure for less than a minute.

2.2.4.2.2. OVA-specific Western blotting

Rabbit (IgG) anti-OVA antibody was diluted in blocking buffer, added to the nitrocellulose membrane and incubated overnight at 4°C. The nitrocellulose membrane was washed with wash buffer for 10 minutes at RT on the orbital shaker for three times. Goat HRP-conjugated anti-rabbit IgG was thereafter added to the nitrocellulose membrane in block buffer and incubated at RT for 2 hours on the orbital shaker. The washing steps and the addition of substrate was the same as in Section 2.2.4.2.1, however, in this case the nitrocellulose membrane was left to expose to X-ray film for only 5-10 seconds.

2.2.4.3. Verification of antigen-mAb conjugates by sandwich Enzyme-Linked Immunosorbent Assay (ELISA)

The ELISA procedures were carried out using the antibodies demonstrated in Table 2.6, Section 2.1.3.

2.2.4.3.1. Rat IgG and OVA antigen – specific ELISA

ELISA 96-well plates were coated with goat anti-rat IgG in PBS and incubated overnight at 4°C. The plates were washed with PBS (with 0.05% Tween-20) and blocked for 1 hour at RT (with 5% BSA) on an orbital shaker. After washing, a series of double dilutions of conjugates or controls in PBS were added to the plate and incubated for 1 hour at RT on an orbital shaker. The plate was washed, the primary antibody – rabbit anti-OVA IgG in PBS was added and incubated for an hour at RT on an orbital shaker. After a further washing step, the secondary antibody – HRP-labelled goat anti-rabbit IgG in PBS was added and incubated under the same conditions. Finally the SIGMA*FAST*™ OPD substrate was added and incubated for 10-15 minutes at RT on an orbital shaker until the development of colour. The optical density (OD) was then read using ELx808™ Absorbance Microplate Reader (Bio Tek) at 450nm. A diagrammatic representation of this procedure is shown in Figure 2.1.

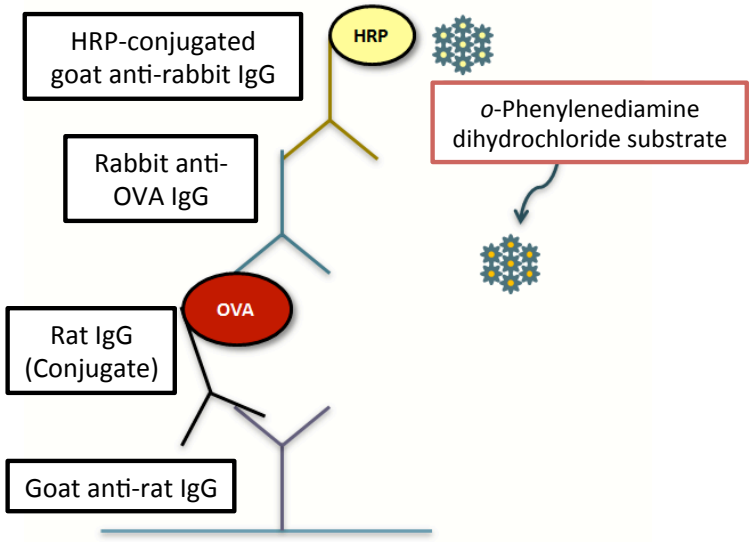

Figure 2.1. Diagrammatic representation of the main steps of the ELISA assay used to confirm the conjugation of OVA to mAb.

2.2.4.3.2. Rat IgG and Mouse Ig (A20 antibody) – specific ELISA

Goat anti-rat IgG was adsorbed to ELISA 96-well plates and incubated overnight at 4°C. The remainder of the procedure is the same as in Section 2.2.4.3.1, except that after the conjugates and controls were added to the plate and incubated, HRP-conjugated polyclonal anti-mouse Ig was added to the plate for detection (after washing).

2.2.4.3.3. CD40mAb-specific ELISA

ELISA 96-well plates were coated with goat anti-human IgG in PBS and incubated overnight at 4°C. After a washing step with PBS (with 0.05% Tween-20), recombinant mouse CD40/Fc chimera was added in PBS and incubated for 1 hour at RT. After washing, the plates were blocked for 1 hour at RT on an orbital shaker. After washing a series of double dilutions of conjugates or controls in PBS were added to the plate and incubated for 1 hour at RT on an orbital shaker. The remainder of the procedure was the same as 2.2.4.3.2.

2.2.4.4. General flow cytometry procedure

Samples and controls were incubated with 1 x 10^6 cells in 200µl FACS buffer for 30-60 minutes at 4°C. Controls included: cells alone and cell viability control using a UV LIVE/DEAD dye. After centrifugation at 400rcf for 5 minutes at 4°C, the labelled cells were washed twice with ice-cold FACS buffer. Subsequently cells were incubated with the primary antibody for 30-60 minutes at 4°C. The cells were then washed twice with FACS buffer (as above) and the samples were stained with secondary antibody (when indicated). After incubation the cells were washed twice with cold FACS buffer by centrifuging at 400rcf for 5 minutes at RT (as above). Cells were fixed in 1% paraformaldehyde and analysis was performed using the LSR II flow cytometer.

2.2.4.4.1. Verification of antigen-mAb conjugates by flow cytometry

All antibodies and reagents used for flow cytometry can be found in Section 2.1.4.

To determine the functional activity of CD40mAb, the ability of OVA-CD40mAb, A20-CD40mAb, $SIINFEKL_{FAM}$-$CD40mAb_{Dylight,}$ $SIINFEKL_{FAM}$-CD40mAb conjugates and $CD40mAb_{Dylight}$ to bind to CD40 expressed by the CD40L929 cell line was investigated by flow cytometry (Table 2.11).

CD40L929 fibroblast cells are an adherent cell line that requires trypsinisation for subculture. Trypsinisation involved primarily washing the cells with PBS, and subsequently adding 2ml of pre-warmed Trypsin to the cells and incubation of the flask in normal culture conditions for 15 minutes. A volume of 10ml of DMEM supplemented with 10% fetal calf serum (FCS), 50µM 2-ME and the selective antibiotic geneticin or G418 was then added to the dislodged cells and centrifuged at 400rcf for 5 minutes at 4°C. Cell pellet was resuspended in 1ml, and cells were counted.

The different conjugates were added to the 10^6 CD40L929 cells using the procedure explained in 2.2.4.4. FITC-labelled CD40 antibody was used in all cases as a positive control, to ensure that CD40L929 cells are all expressing CD40. FITC-labelled anti-mouse IgG2a and FITC-labelled goat anti-rabbit IgG were also added to the CD40L929 cells in the absence of the respective conjugate (Table 2.11), as a negative control.

Conjugate	Primary antibody	Secondary antibody
A20-mAb	Anti-mouse IgG2a (FITC)	N/A
OVA-mAb	Rabbit (IgG) anti-OVA (no label)	Goat anti-rabbit IgG (FITC)
$mAb_{Dylight}$	**N/A**	**N/A**
$SIINFEKL_{FAM}$-mAb	**N/A**	**N/A**
$SIINFEKL_{FAM}$-$mAb_{Dylight}$	**N/A**	**N/A**

Table 2.11. Functional capacity of the CD40mAb-portion of the different conjugates produced.

2.2.5. Culture, maintenance and activation of cell lines

A further explanation of the cell lines used can be found in Section 2.1.6.

2.2.5.1. Retrieving, subculturing and freezing of cell lines

Cell lines retrieved from liquid nitrogen storage were quickly thawed in a 37°C water bath using aseptic techniques. Once thawed the cell suspension was transferred to 10ml of pre-warmed cell culture medium and centrifuged for 5 minutes at 400rcf at 4°C, to remove DMSO. The cell pellet was resuspended in 10ml media and cultured in normal culture conditions. To maintain stocks of healthy cells, 1ml ice-cold media supplemented with 40% FCS and 10% DMSO was added to the cell pellet, which was first transferred to a -80°C freezer and subsequently to liquid nitrogen for long term storage.

2.2.5.2. Cell counting using the hemocytometer

A volume of 1ml cell suspension was thoroughly mixed and 10µl was added to 90µl 0.1% trypan blue. A volume of 10µl was added to haemocytometer and using 10x focusing cells in each of the 4 grids were counted. For calculating cells per ml:

$$(\text{Count in 4 grids} / 4) \times \text{dilution factor} \times 10^4$$

2.2.5.3. Specific and non-specific T cell activation

The functional activity of T cell hybridoma cell lines, B3Z and DO11.10 cells, was tested by OVA-specific stimulation using OVA peptide-pulsed splenocytes. Both cells lines were also tested by non-specific stimulation using PMA and Ionomycin.

2.2.5.3.1. Peptide-specific stimulation

A final concentration of 2µg/ml of peptide was added to 1 x 10^7 splenocytes in 1ml R1 culture medium and incubated for 2 hours under normal cell culture conditions. For co-culture, 10^5 peptide-pulsed spleen cells were co-cultured with 10^5 T cell hybridomas for 24-48 hours in 200µl (96-well plate).

2.2.5.3.2. PMA and Ionomycin stimulation

PMA at a final concentration of 50ng/ml and Ionomycin at a final concentration of 1µM were added to 1 x 10^5 hybridoma T cells per well in 200µl (96-well plate) and incubated for 24-48 hours.

2.2.6. Primary cell culture techniques

All materials, media and reagents utilised in tissue culture are shown in Section 2.1.5.

2.2.6.1. Organ harvesting

Organs were collected after mice were culled by cervical dislocation. The surface of the mouse was sterilised by spraying with 70% methylated spirit. The lymph node (excised by Professor Andrew Heath) and/or spleen were picked using sterile forceps and transferred to sterile PBS on ice. For the generation of DCs from bone marrow progenitors, the tibia and femur of both legs of the mouse were excised.

2.2.6.2. Isolation of Mouse Peritoneal cavity cells

Cell lines that required cloning by double dilution required growth with mouse feeder cells or mouse peritoneal cells until ready for first passage. Eight millilitres of R1 medium (RPMI supplemented with 10% FCS, 50µM 2ME and 100 U/ml Penicillin and Streptomycin) was injected into the peritoneal cavity. The peritoneum was lightly pressed to bring the cells into suspension. The abdominal skin was dissected open to expose peritoneum. The mouse was turned on its side and medium was aspirated using a 21-gauge needle. This procedure was performed by Dr. Jennifer Carlring-Wright. The immune cells collected were centrifuged at 400rcf for 5 minutes at a temperature of 4°C and the cell pellet was resuspended in 10ml R1 medium. The cell suspension was plated into a 96-well plate in a volume of 100µl per well and left over-night ready for the cloning of hybridoma T cells.

2.2.6.2.1. Limited dilution cloning of hybridoma cell lines

Hybridoma cell lines were re-cloned to maintain a homogeneous population of cells. Cell suspensions of concentration 100 cells/ml, 30 cells/ml, 10 cells/ml and 3 cells/ml were made. The 96-well plates seeded with mouse feeder cells 24-hours prior this experiment were divided into 2, half a plate for each of the aforementioned cell concentrations. Plates were incubated undisturbed for 5 days, after which they were examined microscopically daily. Wells that clearly only contained one clone were transferred to 48 well plates and cultured for another 2 days. After microscopic analysis, cells were transferred to 6 well plates and subsequently to T25 flasks containing 5 ml media. Clones were screened by their ability to produce IL-2 in the supernatant, detected by IL-2 ELISA assay.

2.2.6.3. Generation of bone marrow-derived dendritic cells

The tibias and femurs were placed in 70% ethanol for 5 minutes and rinsed with sterile PBS for 2 minutes. Using sterile forceps and scissors the bone was incised at both ends. The marrow was flushed out using a 1ml syringe and 25-gauge needle. The cell clusters in the bone marrow suspension were broken down via vigorous pipetting. The cells were resuspended thoroughly and centrifuged for 5 minutes at 400rcf at 4°C. The cell pellet was resuspended in 1ml PBS and erythrocytes were lysed by incubation with 14ml 1X erythrocyte lysing buffer (made-up in dH_2O fresh from a stock solution of 10x erythrocyte lysing buffer on the day of use, Section 2.1.1) for 5 minutes at 4°C. Subsequently the cells were washed by centrifuging twice in PBS and counted using 0.1% trypan blue. The bone-marrow progenitors were cultured in R2 medium, RPMI supplemented with 10% fetal calf serum (FCS), 50µM 2-ME, the growth factors GM-CSF (20ng/ml) and IL-4 (10ng/ml). On day 0, each Petri dish was seeded at 2 x 10^6 cells in 10ml medium and incubated under normal culture conditions. On day 3, 10ml of R2 media was added, and incubated until day 6. On day 6, 10ml of medium was aspirated, and centrifuged at 400rcf for 5 minutes at 4°C. Care was taken not to disturb adherent cells. The pellet was resuspended in 10ml fresh medium and plated back into the original plate. On day

10, non-adherent and semi-adherent cells were harvested by slowly aspirating the supernatant containing cells and media.

2.2.6.3.1. Maturation of bone marrow-derived dendritic cells using LPS

Ten-day old BM-DC were seeded at a concentration of 5 x 10^6cells/ml of 10ml R1 medium containing LPS (1µg/ml). After 48-hour incubation, the cells were scraped off the bottom of the Petri dish using a cell scraper, and analysed by flow cytometry.

2.2.6.3.2. Staining for Flow cytometric analysis

BM-DCs were prepared for flow cytometry as explained in Section 2.2.4.4. The antibodies against CD11c, CD40, F4-80 and Gr-1 used for staining are demonstrated in detail in Table 2.8. The Fc receptors were blocked using rat anti-mouse CD16/CD32 antibody (Rat IgG2b).

2.2.6.4. Preparation of murine lymph nodes cells

The lymph nodes were transferred to a cell strainer present in a Petri dish containing PBS. Using sterile forceps the tissue was teased apart until the cells formed a single cell suspension. The cells were transferred to a centrifuge tube, and centrifuged for 5 minutes at 400rcf at 4°C. Excess PBS was discarded and the pellet was resuspended in 1 ml PBS and counted using 0.1% trypan blue.

2.2.6.5. Preparation of murine splenocytes

The resected spleen was washed in sterile PBS, and transferred to a cell strainer present in a Petri dish containing PBS. Using sterile forceps the tissue was teased apart until the cells formed a single cell suspension. The cells were transferred to a centrifuge tube, and centrifuged for 5 minutes at 400rcf at 4°C. Excess PBS was discarded and the pellet was resuspended in 1 ml PBS. This cell suspension was

incubated with 14ml 1X erythrocyte lysing buffer for 10 minutes at 4°C. The cells were washed twice with PBS and counted using 0.1% trypan blue.

2.2.6.5.1. Purification of $CD19^+$ B cells from murine splenocytes using positive magnetic cell sorting

To purify $CD19^+$ B cells from splenocytes the cell population was labelled with 0.5µl CD19 PE-conjugated antibody per 10^7 total cells in 100µl EDTA-containing buffer (Section 2.1.5.). Tubes were mixed well and incubated in the dark for 10 minutes at 4°C. Unbound antibody was removed by the addition of 1-2ml buffer per 10^7 cells, and centrifuged for 5 minutes at 400rcf at 4°C and subsequently removing the supernatant. The previous step was repeated. After carefully removing all supernatant, the cell pellet was resuspended in 90µl buffer and incubated with 10µl anti-PE MultiSort MicroBeads for 15 minutes at 4°C. The unbound antibodies were removed by the addition of 1-2ml buffer per 10^7 cells, centrifuging for 5 minutes at 400rcf at 4°C and subsequently removing the supernatant. The previous step was performed twice. The cell pellet was resuspended in 500µl buffer. The MS column was placed in the magnetic field of MACS® Separator following the manufacturer's protocol. Briefly, the column was rinsed with 500µl of EDTA buffer and the cell suspension was applied to the column. The column was rinsed three times with 500µl buffer. The effluent was collected and 100µl was kept for flow analysis, whilst the rest was run through the column again. The column was again washed three times with buffer. The effluent was collected and analysed by flow cytometric analysis. The column was then removed from the cell separator and placed in a suitable collection tube. One millilitre of buffer was added to the syringe and labelled cells were flushed out by firmly applying the plunger supplied with the MS column and the sample was analysed by flow cytometry. To determine the percentage expression of CD19 by splenocytes prior to CD19 positive B cell sorting, 1 x 10^6 splenocytes were incubated with PE-labelled CD19 antibody (for more details about the antibody *see* Table 2.8) as described in Section 2.2.4.4.

2.2.6.6. *In vitro* culture of APCs in the presence of antigen-mAb conjugates

The BM-DC or splenocyte population was seeded in a 48-well plate at a concentration of 1 x 10^6 cells in 1 ml of R1 medium. The cells were cultured for 24 hours in the absence and presence of stimuli. The stimuli included 10µg/ml of antigen-CD40mAb, antigen-isotype control mAb conjugates as well as antigen alone (negative control) and 200ng/ml LPS (positive control). Cells were prepared for flow cytometry as explained in Section 2.2.4.4. Antibodies against CD11c, CD80 and CD86 were used to label the splenocytes or BM-DCs (for more details about the antibody *see* Table 2.8). The gating strategy for this experiment involved excluding debris and doublets, followed by gating on live cells based on UV LIVE/DEAD staining and subsequently on $CD11c^+$ or $CD19^+$ cells. The median fluorescence intensity (MFI) of the $CD11c^+CD80^{+/-}$, $CD11c^+CD86^{+/-}$, $CD19^+CD80^{+/-}$ and/or $CD19^+CD86^{+/-}$ was recorded using DIVA software. The gating strategy for the analysis of BM-DC co-stimulatory expression of CD80 and CD86 is shown as an example in Figure 2.2.

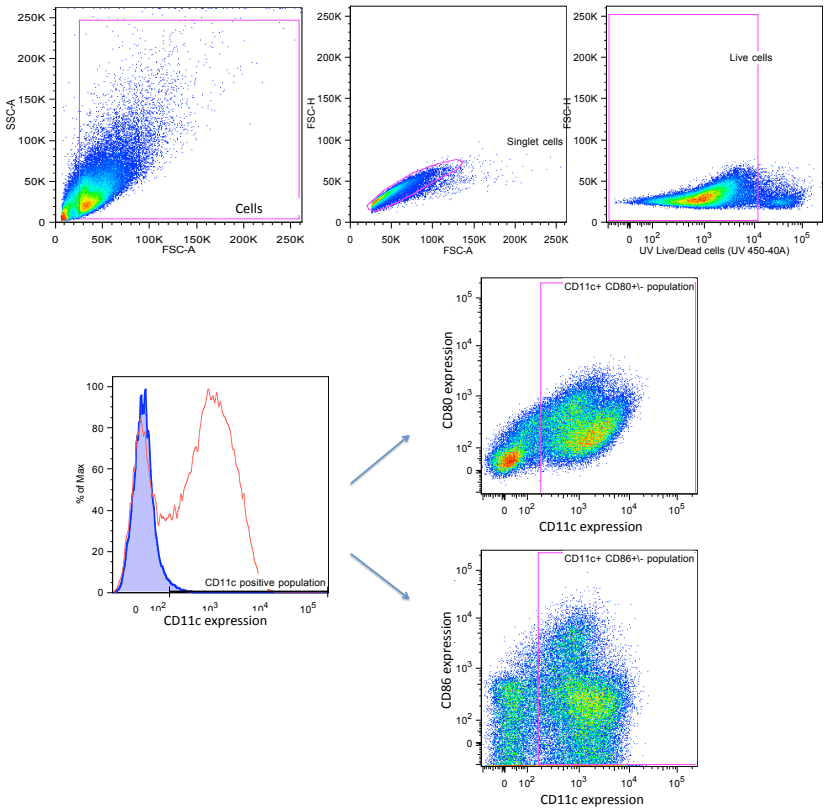

Figure 2.2. Gating strategy for the flow cytometric analysis of the expression of co-stimulatory molecules CD80 and CD86 on BM-DCs (as an example) is shown.

2.2.6.7. *In vitro* targeting of APCs by SIINFEKL$_{FAM}$-mAb$_{Dylight}$ conjugates

A total of 3 x 10^5 BM-DCs and splenocytes were cultured *in vitro* for 5 minutes or 1 hour in the presence of 10µg/ml of SIINFEKL$_{FAM}$-CD40mAb$_{Dylight}$, SIINFEKL$_{FAM}$-GL117$_{Dylight}$, SIINFEKL$_{FAM}$-CD40mAb, SIINFEKL$_{FAM}$-GL117, CD40mAb$_{Dylight}$ or GL117$_{Dylight}$, in a 96-well plate (total volume 100µl). The cells from each well were carefully aspirated and collected into flow cytometry tubes. PBS (500µl) was added to the tubes and the cells were centrifuged at 400rcf for 5 minutes at 4°C. This centrifugation step was repeated to ensure that any excess unbound fluorophore was removed. The cells were then fixed by the addition of 100µl 4% paraformaldehyde for 10 minutes at RT.

Prior to fixation step, splenocytes were first incubated with eFluor-450 labelled CD19 antibody in FACS buffer for 30 minutes at 4°C prior to fixation. This was performed in order to identify the B cell population. Two centrifugation steps were carried out using 500µl FACS buffer to ensure that excess unbound fluorophore was removed.

The fixed BM-DCs and splenocytes were then cytospun onto glass slides, by the addition of 100µl to the cytospin wells and spun at 30rcf for 5 minutes. Once dry, the slides were blocked with 50mM ammonium chloride (Sigma-Aldrich) for 10 minutes.

BM-DCs were labelled with Rhodamine Phalloidin (146nM, a kind gift from Dr. Simon Johnston, Department of Infection and Immunity, University of Sheffield), by over-night incubation at 4°C. This dye served as a cellular stain (staining actin), which was only necessary for BM-DCs, as B cells were already stained with the cell surface marker CD19 antibody. Coverslips were mounted onto the slides with 5µl mowiol and antifade (p-phenyldiamine).

2.2.6.7.1. Microscopy imaging

The presence of Dylight (red stain) and FAM (green stain) co-localised in the cell or on the cell surface was determined by epiflourescent microscopy on Ti (Nikon) with NEO camera (Andor) using NIS Elements AR software (Nikon). In the case of B cells, only co-localisation observed on cells stained for CD19 (efluor-450) was taken into

consideration. Fluorescence images were captured using CFP, GFP and Cy7 excitation filters**.** Forty z-sections every 0.5µM were captured. Six to eight fields of view using a 20x (BM-DC) or a 40x (splenocytes) objective were recorded. This work was kindly conducted by Dr. Simon Johnston (Department of Infection and Immunity, University of Sheffield).

2.2.6.7.2. Scoring of cells with co-localised $SIINFEKL_{FAM}$ and $mAb_{Dylight}$

Images were processed using NIS elements AR software (Nikon). The control samples stimulated with $SIINFEKL_{FAM}$-CD40mAb, $SIINFEKL_{FAM}$-GL117, $CD40mAb_{Dylight}$ and $GL117_{Dylight}$ were used to exclude autofluorescence and ensure reliable cell scoring. The cells stimulated with $SIINFEKL_{FAM}$-$CD40mAb_{Dylight}$ and $SIINFEKL_{FAM}$-$GL117_{Dylight}$ for 5 minutes and 1 hour were scored. The number of co-localised mAb and SIINFEKL were counted on 20 different BM-DCs per field (in a total of 6 fields). Since the number of B ($CD19^{+}$) cells in each field was less, the number of cells counted per field ranged from 10-20 cells.

2.2.6.8. *In vitro* co-culture of T cell hybridomas with APCs

Splenocytes (1×10^5), BM-DCs (3×10^4) or positively-selected B cells (3×10^4) were incubated with different concentrations of stimulants (specified in Chapter 5, Section 5.5) in a 100µl volume R1 medium and incubated for 2, 4, 18 or 24 hours (specified in Chapter 5). After the specified incubation, 1×10^5 B3Z cells in 100µl media was added to the stimulated APCs in the 96-well plate. After 24-hour co-culture with B3Z under normal culture conditions, the supernatants were collected and frozen (for subsequent IL-2 testing). Splenocytes were also stimulated with peptides (*see* Section 2.2.5.3.1.) and the T cell hybridomas were stimulated with PMA and Ionomycin (*see* Section 2.2.5.3.2.) as positive controls.

2.2.6.8.1. ELISA to detect IL-2 from co-culture supernatant

Antibodies used for this ELISA procedures are demonstrated in Table 2.6, Section 2.1.3.

ELISA 96-well plates were coated with purified rat anti-mouse IL-2 IgG2 and incubated overnight at 4°C. The plates were washed with PBS (with 0.05% Tween-20) and blocked for 1 hour at RT with PBS (with 5% BSA) on an orbital shaker. After washing, a series of double dilutions of standard recombinant murine IL-2 was made in separate eppendorf tubes. 100µl of each standard was added in duplicate to the 96-well test plate. 100µl of the sample supernatants were also added and incubated for 1 hour at RT on an orbital shaker. The plate was washed and biotinylated anti-mouse IL-2 IgG2b was added and incubated for an hour at RT on an orbital shaker. After a further washing step, HRP-labelled streptavidin antibody was added and incubated under the same conditions. The remainder of the procedure was the same as 2.2.4.3.1. The concentration of the unknowns was determined using a polynomial curve, using GraphPad Prism^{TM} software version 6.0 (GraphPad Software, Inc. CA, USA).

2.2.6.8.2. Flow cytometric analysis of APCs in co-culture presenting SIINFEKL peptide

Splenocytes in co-culture with B3Z hybridoma cells were collected and were prepared for flow cytometry as explained in Section 2.2.4.4. The anti-mouse antibodies against CD11c, CD19 (eFluor-450), CD80, CD86 and SIINFEKL bound to H-2K^{b} of MHC class I were used for staining (Table 2.8). SIINFEKL-pulsed splenocytes *in vitro* were used to compensate for anti-mouse SIINFEKL bound to H-2K^{b} of MHC class antibody. The MFI of the CD11c^{+}CD86^{+}SIIN$^{+/-}$, and/or CD19^{+}CD86^{+}SIIN$^{+/-}$expression of lymph nodes harvested from only C57Bl/6 were recorded using DIVA software. The gating strategy for the analysis of activated CD19^{+} cells presenting SIINFEKL is shown as an example in Figure 2.3.

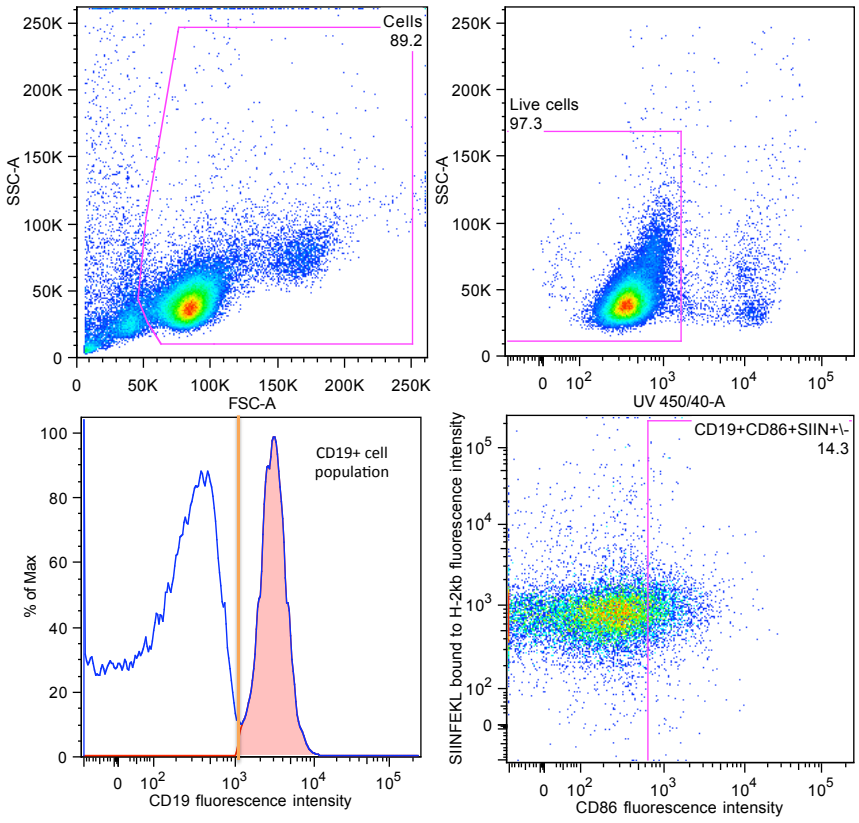

Figure 2.3. Gating strategy for the flow cytometric analysis of the expression of SIINFEKL presented by MHC I of activated CD19$^+$ cells is shown as an example.

2.2.7. *In vivo* experimentation

All animal techniques were performed in accordance with the Animals and Scientific Procedures Act (1986). Mice were immunised by intravenous (i.v.) (performed by Professor Andrew W. Heath), intraperitoneal (i.p.) or subcutaneous (s.c.). injection (Table 2.12). For blood collection the animal was placed in an incubator set at a temperature of 30°C for 5-10 minutes. Blood was then collected from the immunised animals by making a small nick in the tail dorsal vein using a scalpel blade.

Injection type	Syringe used	Volume	Immunisation
i.p.	25-gauge needle	200µl	Peritoneal cavity
s.c.	25-gauge needle	100µl	Beneath the skin on mouse flank
i.v.	25-gauge needle	200µl	Into the dorsal vein

Table 2.12. Immunisation routes utilised.

2.2.7.1. Immunisation schedule for A20-mAb conjugates

In vivo work using A20-mAb conjugates was conducted by Ms. Amy Lewis. Prophylactic tumour studies involved immunising a group of 10 naive BALB/c female mice with 10µg A20-CD40mAb conjugates subcutaneously in the left flank. This was performed on day -28 and mice were boosted on day -14. The mice were bled from the dorsal tail vein on day -1. The blood samples collected were incubated overnight at 4°C. Samples were centrifuged at 16,000rcf for 10 minutes, and sera were separated from the clotted blood and stored at -20°C. The anti-A20 specific antibodies in the mice sera were analysed by ELISA.

The mice were challenged with tumour cells two weeks after boosting on day 0. A lethal dose of 1 x 10^5 A20 cells in 50µl was administered s.c. in the right flank. The mice were monitored for tumour development every weekday for a period of 63 days. Tumours were measured using calipers along the shortest and longest diameter. The United Kingdom Coordinating Committee on Cancer Research Guidelines were followed that allow a maximum tumour size of 12mm (Workman et al., 2010), and mice with tumours reaching a diameter of 12mm were culled. The tumour volume was measured by the use of the formula: $((\text{short} + \text{long})*0.25)^3*4/3\pi$ were short refers to the shortest measured diameter and long refers to the longest measured diameter.

2.2.7.1.1. Anti-A20 antibody responses

A20-Id Fab fragments (2.5µg/ml generated in-house) in 0.1M sodium bicarbonate buffer (pH 9.4) was adsorbed to ELISA 96-well plates overnight at 4°C. The plates were washed with PBS (containing 0.05% Tween) and blocked for 1 hour at RT with 5% skimmed milk powder in PBS. Sera from immunised mice groups were added to the plate at a ten-fold starting dilution, double diluted across the plate in blocking buffer and incubated for an hour at RT on an orbital shaker. The remainder of the procedure is the same as in Section 2.2.4.3.2. The end-point titre was plotted.

2.2.7.2. Immunisation schedule for OVA-mAb conjugates

Five female naive BALB/c mice were immunised with 10µg OVA-mAb conjugate per group**,** via the i.p. route on day 1 and boosted on day 14. Mice were bled on day 13 and day 28. Blood samples were incubated overnight at 4°C. Consequently, samples were centrifuged at 16,000rcf for 10 minutes, and sera were collected. The anti-OVA antibody titres in the mice sera were analysed by ELISA.

2.2.7.2.1. Anti-OVA antibody responses

The blood samples collected were processed as in 2.2.7.1. Anti-OVA antibody end-point titres in the mice sera were analysed by ELISA. OVA antigen (10µg/ml in PBS) was adsorbed to ELISA 96-well plates overnight at 4°C. The plates were washed with PBS (containing 0.05% Tween-20) and blocked for 1 hour at RT with 5% skimmed milk powder in PBS. Sera from immunised mice groups were added to the plate at a ten-fold starting dilution, double diluted across the plate in blocking buffer and incubated for an hour at RT on an orbital shaker. The remainder of the procedure is the same as in Section 2.2.4.3.2. The end-point titre was plotted.

2.2.7.3. Lymphocyte proliferation in response to stimulus *ex vivo*

2.2.7.3.1. Immunisation schedule for antigen-mAb conjugates

Five BALB/c mice were immunised, on day 0 and were boosted on day 14, with 10µg CLICK OVA-CD40mAb, Standard OVA-CD40mAb, Standard OVA-GL117mAb per group via the i.p. route. Control groups included 5µg sOVA and 5µg CD40mAb (Mixture), 5µg sOVA antigen and PBS. Blood samples were incubated overnight at 4°C. Consequently, samples were centrifuged at 16,000rcf for 10 minutes, and sera were collected. The anti-OVA antibody titres in the mice sera were analysed by ELISA.

2.2.7.3.2. Immunisation schedule for ISQC-mAb conjugates

This procedure is the same as Section 2.2.7.3.1 with the alteration of the immunogens. BALB/c mice were immunised with 10µg ISQC-CD40mAb conjugate and ISQC-GL117mAb conjugate via the intraperitoneal route. Control groups included; 0.8µg ISQC and 9.2µg CD40mAb (Mixture) and PBS.

2.2.7.3.3. Staining with CFSE and lymphocyte culture

In order to quantify $CD4^+$ T cell proliferation, a protocol utilizing CFSE was carried out. All materials and reagents utilised are shown in Section 2.1.4. Splenocytes from immunised mice were harvested (as explained in Section 2.2.6.5.). Care was taken to keep the splenocytes on ice at all times to minimise cell death and clumping. CFSE was prepared on day of use, from stock aliquots by diluting to a concentration of 0.1mM in PBS. A concentration of 2×10^7 cells in 2 ml PBS were incubated at 37°C for 15 minutes with 2µM CFSE. Unbound dye was quenched with 2ml heat inactivated FCS and incubated at RT in the dark for 10 minutes. The cells were centrifuged three times in R1 medium for 5 minutes at 400rcf (4°C) and the cell pellet was resuspended each time in R1 medium. The CFSE labelled cells were seeded in a 48-well plate at a concentration of 1×10^6 cells in 1 ml. The cells from each immunised mouse group were incubated in normal cell culture conditions in the presence and absence of antigen or peptide for 72 hours. Prior to incubation the labelled CFSE cells were checked on the flow cytometer to observe whether the cells were labelled appropriately.

2.2.7.4. Staining for Flow cytometric analysis

Cells were prepared for flow cytometry as explained in Section 2.2.4.4. The antibodies CD19 (eFluor-labelled) and CD4 were used (Table 2.8). In this experiment a cell control with only CFSE staining was included, and the cultured cells were used for compensation.

2.2.7.5. Cytotoxicity assay

2.2.7.5.1. Immunisation schedule

A total of 8 C57Bl/6 mice per group were immunised on day 0 with 40µg SIINFEKLC-CD40mAb conjugate or SIINFEKLC-GL117 conjugate via the i.p. route. Control groups included 2µg SIINFEKLC and 40µg CD40mAb mixture (or MIX) and PBS. On day 6, spleens from naive C57Bl/6 mice were harvested and processed as explained in Section 2.2.6.5. Care was taken to keep splenocytes on ice at all times to minimise cell death and clumping. All media used in this section was R1 media (Section 2.1.5.).

2.2.7.5.2. Staining splenocyte populations with CFSE dye

The splenocytes were divided into three populations; (i) Population A was cultured in media with 1µg/ml (1µM) SIINFEKL peptide per 10^7 cells for one hour (to be stained with 0.2µM CFSE), (ii) Population B was cultured in medium only (to be stained with 2µM CFSE) and (iii) Population C was cultured in medium only and was used as an *in vitro* control for background staining (not stained with CFSE). As the SIINFEKL peptide used was dissolved in 70% ethanol, this was added to Populations B and C using the same volume of SIINFEKL peptide used in (i). This served as an internal control, to ensure that the 70% ethanol is not having a detrimental effect on the cells. All splenocyte populations were pelleted by centrifugation at 400rcf for 5 minutes at a temperature of 4°C. The pellet was resuspended in PBS.

CFSE was prepared to a concentration of 0.1mM in PBS (as explained in Section 2.2.7.3.3.). Population A was stained with 0.2µM CFSE ($CFSE^{LOW}$) whilst Population B was stained with 2µM CFSE ($CFSE^{HIGH}$) in PBS. CFSE staining was carried out as explained in Section 2.2.8. After CFSE staining, the cells in each population were counted. Population A and B were mixed in a 1:1 ratio. A number of cells from each population, as well as the mixed population (5 x10^5 cells) were checked for CFSE staining prior to immunisation by flow cytometric analysis. After ensuring the presence of both populations, a total number of cells ranging from 1 x 10^6 – 1 x 10^7 were immunised per mouse i.v. via the dorsal tail vein. An *in vitro* control of 1 x 10^6 of the mixed population of cells was incubated in R1 media overnight.

2.2.7.5.3. Flow cytometric analysis of splenocytes

After 18 hours of i.v. immunisation, the spleens from all the immunised mice were harvested as in Section 2.3.6.5. Cells were centrifuged twice for 5 minutes at 400rcf (4°C) and the cell pellet was resuspended first in FACS buffer and second in 1% paraformaldehyde. Cells were analysed by flow cytometric analysis on the LSRII. At least 1 million events (gated on the splenocyte population) were collected per sample.

2.2.7.5.4. Percentage lysis calculation

The percentage lysis of each group was calculated by the following formulae:

Formula 1: $r = \frac{\text{number CFSE}^{HIGH} \text{ population events collected}}{\text{number CFSE}^{LOW} \text{ population events collected}}$

Formula 2: $\text{Percentage lysis} = (1 - (r^{\text{PBS group}}/r^{\text{immunised groups}})) \times 100$

2.2.7.6. *In vivo* tracking SIINFEKL-mAb conjugates

2.2.7.6.1. Immunisation schedule for SIINFEKL-mAb conjugates

A group of 5 naïve C57Bl/6 mice and 3 BALB/c mice were immunised subcutaneously with 10µg (in a 200µl volume) SIINFEKLC-CD40mAb (right flank) and SIINFEKLC-GL117mAb (left flank) conjugate, per group. After 24 hours the inguinal draining lymph nodes were excised and processed. The spleen was also harvested for flow cytometric single cell staining.

2.2.7.6.2. Flow cytometric analysis of APC presenting SIINFEKL

Lymph nodes were processed as explained in Section 2.2.6.2. Flow cytometric analysis of lymph node derived B cells and DCs was performed as explained in Section 2.2.6.8.2.

2.2.8. Other techniques and analysis

2.2.8.1. Endotoxin Assay

To determine endotoxin levels of conjugates, antibodies and OVA the Endpoint Chromogenic LAL test was carried out. Prior to the assay all glass tubes to be used were rendered endotoxin-free by heating at 250°C for at least 2 hours. Reagents were prepared according to the manufacturer's instructions**.** Briefly, the LAL reagent was reconstituted right before use, by the addition of 1.4ml endotoxin-free reagent water to the reagent vial. The lyophilised chromogenic substrate was reconstituted by the addition of 6.5ml of LAL endotoxin-free reagent water yielding a concentration of approximately 2mM. This was kept protected from light. The lyophilized endotoxin was reconstituted by the addition of 1.0ml reagent water (warmed to RT). The actual concentration of the endotoxin standard was determined from the certificate of analysis. Prior to preparation of the standards, the solution was vigorously vortexed continuously for 15 minutes to prevent endotoxin attaching to the glass. The standards were prepared as shown in Table 2.13.

Endotoxin Concentration (EU/ml)	Endotoxin stock solution	Endotoxin Standard solution 1EU/ml	LAL endotoxin-free reagent water
1.0	0.1 ml	--	(X-1)/10ml
0.5	--	0.5ml	0.5ml
0.25	--	0.5ml	1.5ml
0.1	--	0.1ml	0.9ml

Table 2.13. Preparation of standards for the endotoxin assay

X = endotoxin concentration of the vial

Samples were prepared at 10µg in 50µl (final concentration of 200µg/ml) endotoxin-free reagent water in glass tubes. Four endotoxin standards were used in duplicate, namely 1.0 EU/ml, 0.5 EU/ml, 0.25 EU/ml and 0.1 EU/ml (Table 2.13). A blank sample that consisted of 50µl endotoxin-free reagent water only was also used per test. The order of addition of reagents from vessel to vessel and the rate of pipetting was kept consistent from sample to sample at each step. Freshly reconstituted LAL (50µl) was

added to the reaction vessel. Timing was started as soon as the reagent was added to the sample. Each sample was thoroughly mixed. After 10 minutes incubation, 100µl of chromogenic substrate solution (pre-warmed to 37°C prior to addition) was added to the sample, thoroughly mixed, and incubated at 37°C for 6 minutes. To stop the reaction 100µl of 10% SDS was added, and 200µl of each sample was transferred to a sterile individually wrapped 96-well plate. The absorbance was quickly read at 405nm using ELx808™ Absorbance Microplate Reader. The concentration of the unknown samples was determined using a standard curve.

2.2.8.2. Statistical Analysis

All statistical analysis was performed using GraphPad Prism 6 software. The values having a $p<0.05$ were deemed significant from controls and marked with an asterisk. Data was expressed as mean +/- standard deviation (SD). To determine the statistical significance between two groups an unpaired or paired, two-tailed Student t test was performed. A Mann-Whitney test was used for sample data not normally distributed. To determine the statistical significance between more than two groups an unpaired, one-way ANOVA was used together with either Dunnett's post-test (compares every mean to a control mean), Tukey's post-test (compares every mean with every other mean) or Sidak's post-test (comparisons between means of selected groups) was performed. An unpaired Dunn's (non-parametric) multiple comparison test was used to determine statistical significance for sample data not normally distributed. Kaplan-Meier survival analysis was carried out to determine the overall survival between groups using a log-rank test.

CHAPTER 3

COMPARISON BETWEEN NOVEL AND STANDARD CONJUGATION STRATEGIES FOR CD40MAB-ADJUVANTED VACCINE PRODUCTION

3.1. Introduction

The impact of bioconjugation in vaccine development and design is substantial. The importance of vaccine design and composition should not be underestimated because the immunogenicity and efficacy of the vaccine does not just rely on the carrier protein or adjuvant, the method of conjugation also plays a significant role. As a consequence novel vaccines are developed using more refined conjugation techniques. One example includes the conjugation strategies used to link lymphoma-specific antigen to carrier proteins.

B cell lymphomas express a unique Ig, referred to as an idiotype (Id), which is considered a tumour-specific antigen (Stevenson and Stevenson, 1975). Lymphoma-Id is not immunogenic enough when injected alone, so it is generally linked to KLH (KLH-Id), using glutaraldehyde conjugation, which was tested in phase III clinical studies (Bendandi, 2009). More recently, KLH-Id conjugation was performed using maleimide coupling, which was found to dramatically enhance vaccine efficacy in a murine lymphoma model (Betting et al., 2008). The authors suggested that the conjugation strategy was possibly superior because the reaction is limited to reduced cysteine sulphydryl groups, resulting in less precipitation and the formation of fewer high MW complexes (Kafi et al., 2009). Alternatively, glutaraldehyde treatment causes extensive cross-linking of the tumour antigen that may potentially destroy valuable epitopes. Furthermore, sulphydryl-maleimide coupling of CD40mAb to lymphoma-Id is superior to the use of KLH in a murine lymphoma model (Carlring et al., 2012).

Sulphydryl-maleimide coupling of the adjuvant CD40mAb to antigen has been the method of choice in our lab for making CD40mAb vaccine conjugates (Figure 3.1A) for more than a decade (Barr et al., 2003, Carlring et al., 2004, Hatzifoti and Heath, 2007, Carlring et al., 2012). Briefly, sulphydryl-maleimide coupling consists of the use of the heterobifunctional molecules Sulfosuccinimidyl 4-[N-maleimidomethyl]-cyclohexane-1-carboxylate (Sulfo-SMCC), which introduces a maleimide group to the antigen via amines and the N-Succinimidyl S-Acetylthioacetate (SATA), which

introduces sulphydryl groups to the antibody via amines. The maleimide activated protein reacts with sulphydryls on the antibody to form a stable thioether bond.

Early studies conducted in our laboratory using sulphydryl-maleimide coupling showed that CD40mAb, when chemically conjugated to the model antigen OVA enhanced primary antibody responses against OVA, compared to OVA antigen alone or a mixture of CD40mAb and OVA antigen (Barr et al., 2003). This showed the potential of CD40mAb-adjuvanted conjugates as vaccine candidates. Despite the advantages of using sulphydryl-maleimide coupling, CD40mAb conjugates made by this method are poorly defined and heterogeneous. This means that a conjugate will consist of more than one antigen molecule linked to one antibody molecule and vice versa, leading to a mixture of high and low molecular weight (MW) products.

It is known that CD40mAb works better as an adjuvant in a monomeric state (Heath and Laing, 2004). We therefore hypothesised that CD40mAb conjugates of lowest MW and greatest CD40mAb accessibility would make the most efficient vaccines. This led us to assess the cutting-edge technology click chemistry (Kolb et al., 2001) to further refine conjugates of CD40mAb and antigen. The name 'Click Chemistry' was created by Kolb and colleagues in the early 21st century to describe a high yielding, very specific reaction with by-products that could be easily removed (Kolb et al., 2001). Click chemistry has been applied in conjugation of heterogeneous polysaccharides to vaccine antigens or carriers, for example the non-toxic cross-reacting material of diphtheria toxin (CRM_{197}) (Crotti et al., 2014), chicken serum albumin (Lipinski et al., 2011) and tetanus toxoid (Lipinski et al., 2013, Wu et al., 2013) refining polysaccharide-based conjugate vaccines. Click chemistry has also been applied in lymphoma immunotherapy research (Patel and Swartz, 2011), in conjugation of the cytokine GM-CSF, the immunostimulatory molecule CpG DNA and lymphoma-Id to VLPs. Click chemistry conjugation allowed more control over the ratio of the molecules conjugated to VLPs.

The click chemistry method (Figure 3.1B) used in this study involves a reaction between a dibenzylcyclooctyne-NHS ester (DBCO-NHS) linker and an 15-Azido-4,7,10,13-tetraoxa-pentadecanoic acid succinimidyl ester (NHS-PEG4-Azide) linker (in a copper free system). These reagents are very narrowly reactive only to each other

leading to very efficient and specific linkage between the proteins even in the presence of other functional groups such as amine and sulphydryl groups, producing a less heterogeneous conjugate. The use of a copper-free reaction also known as strain-promoted alkyne-azide cycloaddition, overcomes the problem of possible copper toxicity.

In this chapter, two CD40mAb-adjuvanted conjugates made using sulphydryl-maleimide coupling (**Standard conjugates**) and click chemistry (**CLICK conjugates**) (Figure 3.1.) were evaluated. Firstly, CD40mAb was conjugated to A20 murine B cell lymphoma Id, referred to as the A20 antibody (A20-mAb conjugates), by both methods. The two methods were compared by prophylactic murine immunisation and subsequent challenge with A20 lymphoma cells in a mouse model. Secondly, CD40mAb was conjugated to the model antigen OVA (OVA-mAb conjugates) by both methods and the immunogenicity of the conjugates was compared. OVA antigen has been chosen as a model because it allows convenient testing of $CD4^+$ and $CD8^+$ T cell responses due to the readily available OVA-specific reagents, which would not be possible if A20-CD40mAb conjugates are used.

To test our hypothesis, HPLC was used to isolate the A20-CD40mAb and OVA-CD40mAb conjugates of lowest average MW made by click chemistry. The unfractionated CLICK conjugates as well as the highest and lowest average MW conjugates were compared to Standard conjugates and characterised primarily *in vitro* and subsequently investigated *in vivo* in murine systems.

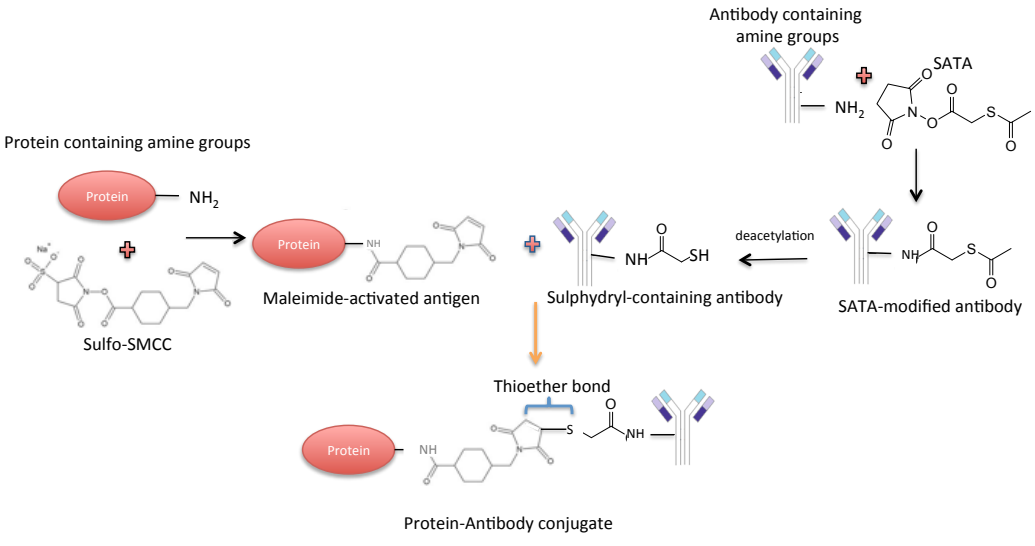

A.

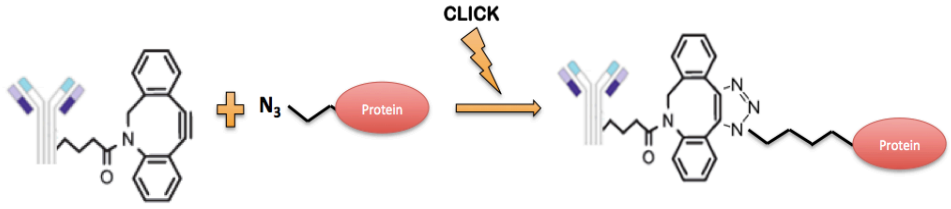

B.

Figure 3.1. Schematic representation of the two conjugation strategies used in this chapter: sulphydryl-maleimide chemistry (A) and click chemistry (B).

A. **Sulphydryl-maleimide chemistry or Standard method**. OVA or A20 antibody are maleimide-activated with heterobifunctional agent Sulfo-SMCC. Antibody is functionalised with SATA to introduce protected sulphydryl groups, by forming a stable amide bond with amines on the antibody. The addition of hydroxylamine results in the de-protection of the sulphydryl groups. Maleimide-activated OVA antigen or A20 antibody are mixed with the functionalised antibody. The maleimide group obtained from SMCC reacts with sulphydryl on the antibody to form a stable thioether bond.

B. **Click chemistry method**. CD40mAb is functionalised on lysine residues with DBCO-NHS and reacted with NHS-PEG4-Azide functionalized antigen (OVA antigen or A20 antibody) to form a stable triazole between the two.

Antibody = CD40mAb or corresponding isotype control mAb (20C2mAb); Protein = A20 antibody or OVA; SMCC = Succinimidyl 4-[N-maleimidomethyl]-cyclohexane-1-carboxylate; SATA = N-Succinimidyl S-Acetylthioacetate; DBCO = Dibenzylcyclooctyne-NHS ester; Azide = 15-Azido-4,7,10,13-tetraoxa-pentadecanoic acid succinimidyl ester.

3.2. Efficacy of a lymphoma antigen and CD40mAb conjugate as a prophylactic vaccine in a murine lymphoma model

3.2.1. Fractionation of A20-mAb conjugates by HPLC

A20 antibody was conjugated to CD40mAb and the isotype control antibody, 20C2mAb using the standard method (*see* Section 2.2.1.1.), and the click chemistry method (*see* Section 2.2.1.6.).

To determine whether the A20-CD40mAb conjugate consisted of a mixture of conjugates ranging from very high to very low average MW, as well as free unconjugated CD40mAb and A20 antibody, the conjugates were analysed by HPLC. The sample buffer and the conditions under which the samples were run were optimised by Dr. Oliver Wilkinson (Department of Chemistry, University of Sheffield), as described in Materials and Methods (*see* Section 2.2.2).

In order to accurately investigate the composition of the heterogeneous A20-CD40mAb conjugate, standards of sizes ranging from 13.7kDa to 660kDa were separated by HPLC (Figure 3.2). The highest MW standard was observed first (7.2 minutes) whilst the lowest MW standard was observed last (11.4 minutes) on the HPLC chromatogram.

In addition to the standards, the antibody alone as well as the antibody functionalised with DBCO-NHS or NHS-PEG4-Azide were analysed as part of the optimisation process (Figure 3.3). The A20 antibody peak was observed at 8.578 minutes whilst CD40mAb and the isotype control antibody, 20C2mAb were observed at 9.2 and 9.24 minutes respectively (Figure 3.3A). This means that the A20 antibody is of higher MW than the other two antibodies. When functionalised with NHS-PEG4-Azide the A20 antibody peak was observed slightly earlier at 8.541 minutes. When functionalised with DBCO-NHS the CD40mAb was observed at 9.2 minutes, whilst the isotype control antibody was observed at 9.206 minutes (Figure 3.3B). Conjugation with NHS-PEG4-Azide-linker or DBCO-NHS-linker only slightly affected the time at which the peaks were observed. This information allowed us to more informatively identify the conjugate fractions of interest in the A20-CD40mAb conjugates.

A 50µg sample of CLICK and Standard A20-CD40mAb conjugates were analysed on the HPLC size-exclusion column (SEC), and by comparing to the MW standards (Figure 3.2), the CLICK conjugate fractions of interest could be identified (Figure 3.4). Considering that the standard of MW 660kDa emerged around 7 minutes, the peak observed at 5 minutes would be with high probability a conjugate of the highest average MW. Furthermore, as the results showed that the free unconjugated antibodies, as well as the NHS-PEG4-Azide or DBCO-NHS functionalised antibodies emerged after 8.2 minutes (Figure 3.3), we assumed that a peak emerging just before would correspond to a conjugate containing one CD40mAb conjugated to one A20 antibody.

On comparing the conjugates made by the two different methods (Figure 3.4), the peaks appeared at similar times, however, Standard A20-CD40mAb conjugate contains mostly higher average MW proteins (5-6 minutes), whilst CLICK A20-CD40mAb conjugate contained more lower average MW proteins (6-8 minutes) observed after the 5 minute peak. Once the fractions of interest were identified the CLICK conjugates were centrifuged to remove precipitates and the samples were analysed on the HPLC SEC to be separated. Four fractions were collected from A20-CD40mAb conjugates (Figure 3.5), and these are tabulated in Table 3.1. Respective fractions from CLICK A20-istoype control antibody conjugates were also collected (Figure 3.5).

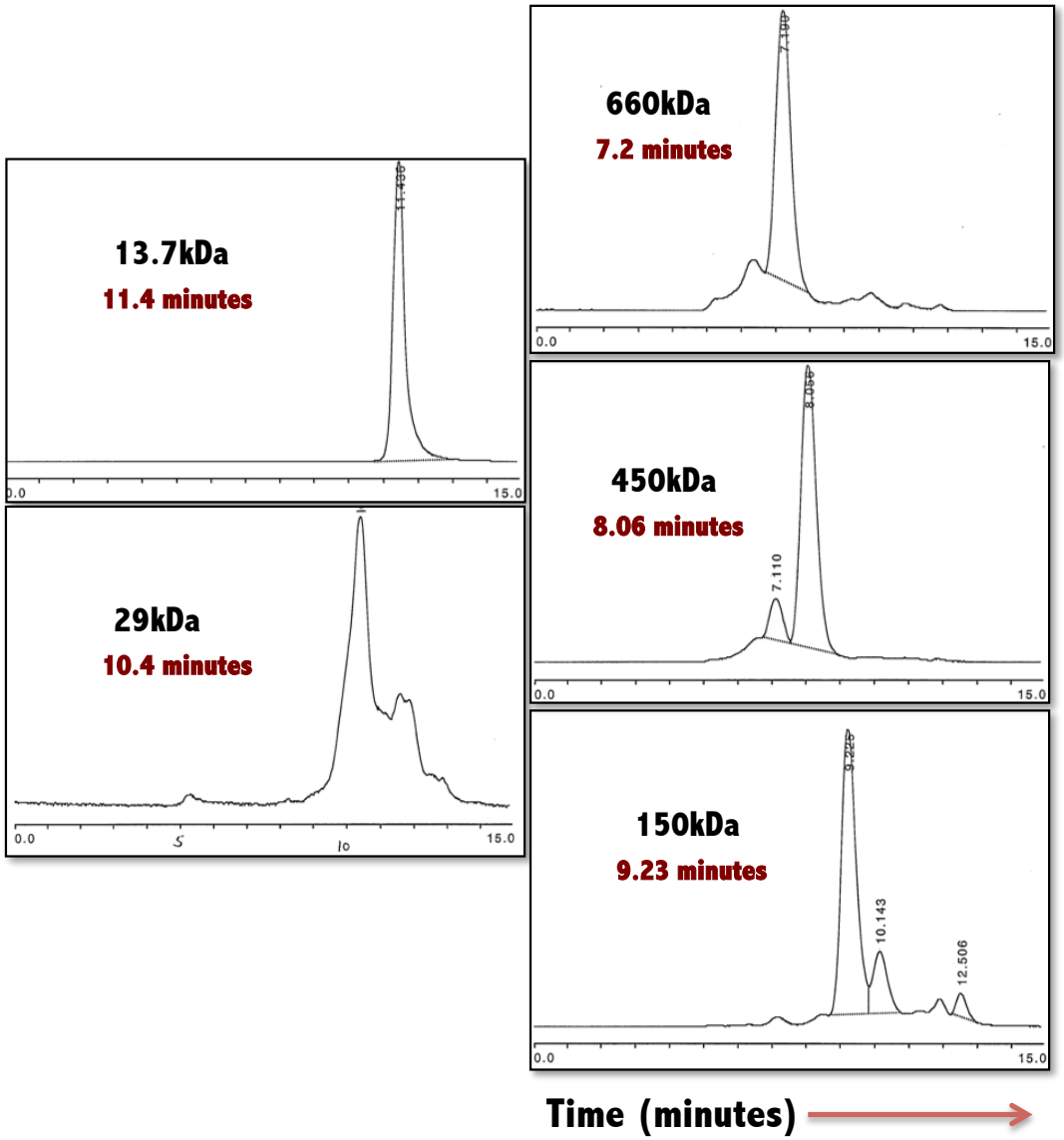

Figure 3.2. HPLC optimisation using different standards of MW ranging from 13.7kDa to 660kDa. The time in red corresponds to the highest peak of each standard. The absorbance readings on the HPLC plots were measured at 280nm.

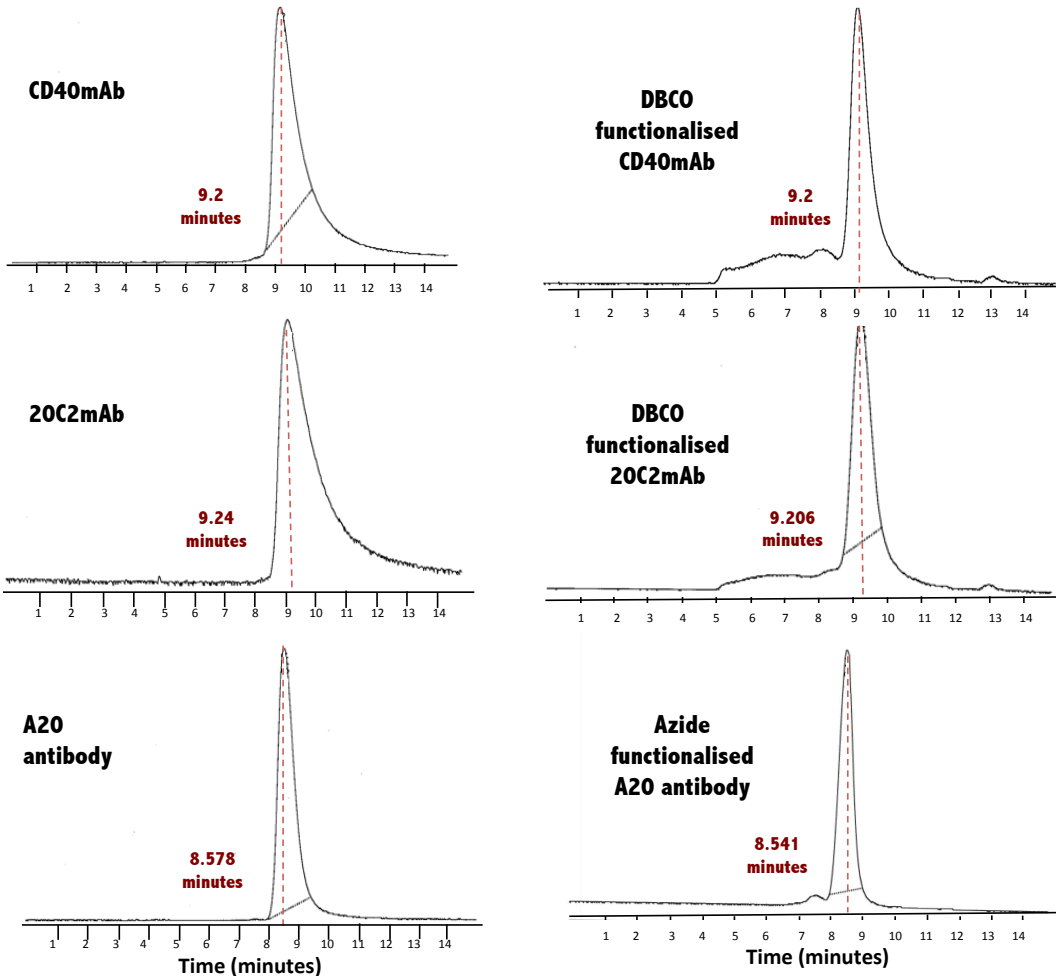

Figure 3.3. HPLC chromatograms of unconjugated antibodies, as well as NHS-PEG4-Azide functionalised A20 and DBCO-NHS functionalised antibodies. The numbers shown in red represent the time taken for the peak of the antibody or the functionalised antibody to emerge on the HPLC chromatogram. The absorbance readings on the HPLC plots were measured at 280nm.

20C2mAb = isotype control mAb

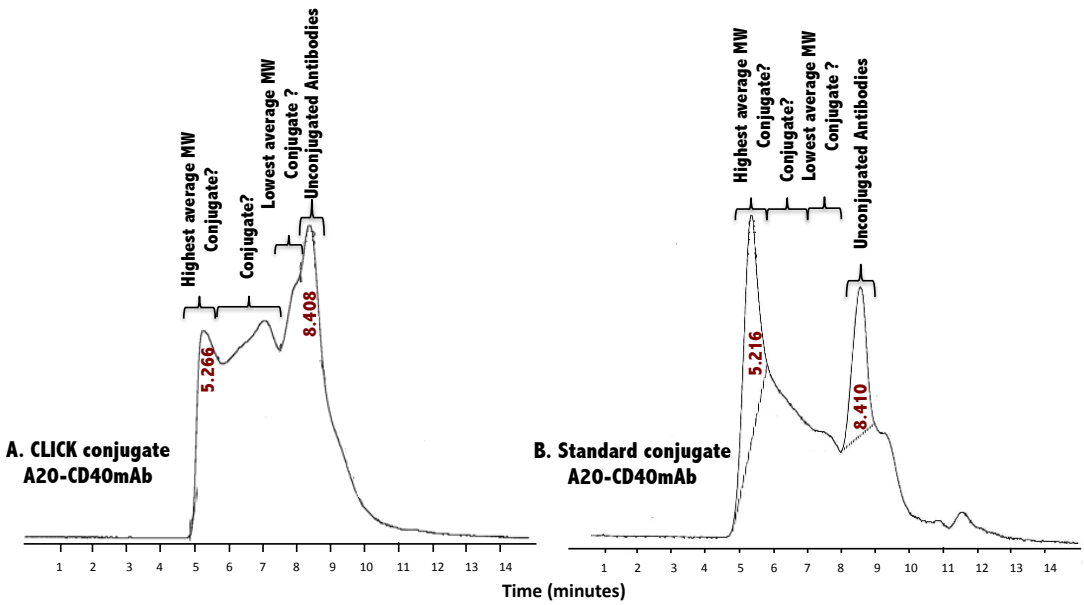

Figure 3.4. Representative HPLC chromatograms of the Standard and CLICK A20-CD40mAb conjugates. The numbers shown in red represent the time taken for the peak of the particular fraction to emerge on the HPLC chromatogram. The absorbance readings on the HPLC plots were measured at 280nm.

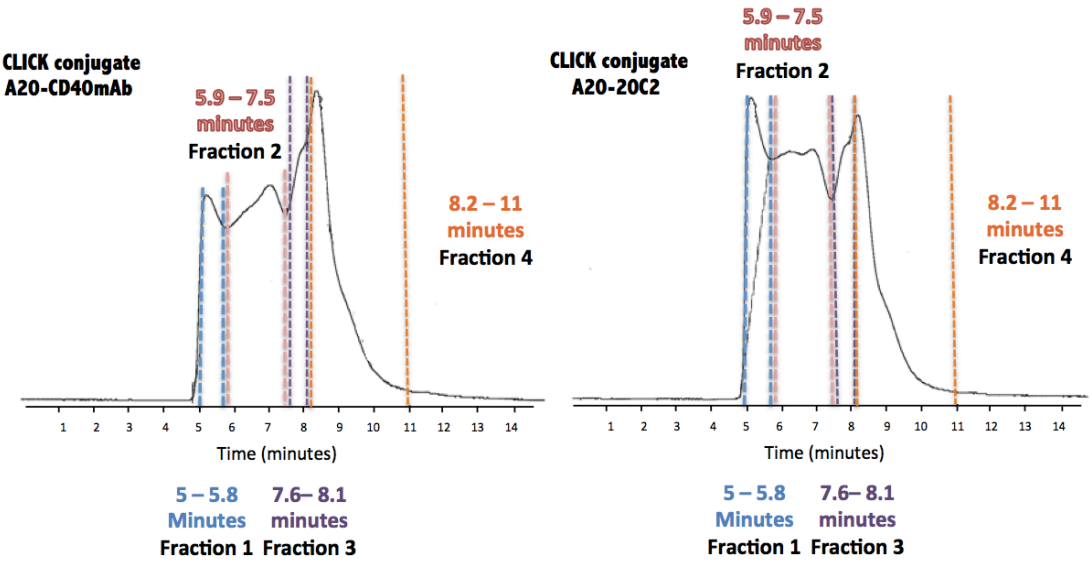

Figure 3.5. Representative HPLC chromatograms of the CLICK A20-mAb conjugates and the different fractions collected. The fractions collected included: Fraction 1 (blue) from 5 minute to 5.8 minutes, Fraction 2 (pink) collected from 5.9 minutes to 7.5 minutes, Fraction 3 (purple) collected from 7.6 minutes to 8.1 minutes and Fraction 4 (orange) collected from 8.2 minutes to 11 minutes. The absorbance readings on the HPLC plots were measured at 280nm. 20C2 = isotype control mAb.

A BCA assay (*see* Section 2.2.3.) was used to quantify the protein concentration of each fraction. The four fractions of the CLICK A20-mAb conjugates were labelled as explained in Table 3.1 and will be referred to as Fraction 1, 2, 3 or 4 (according to decreasing average MW) from this point on.

CLICK A20-mAb conjugate fractions collected
5 - 5.8 minutes (Fraction 1)
5.9 – 7.5 minutes (Fraction 2)
7.6 – 8.1 minutes (Fraction 3)
8.2 - 11 minutes (Fraction 4)

Table 3.1. CLICK A20-mAb conjugate fractions collected by minutes on HPLC

From the four fractions collected, Fraction 1, which contained the highest average MW protein and Fraction 3, which contained the lowest average MW protein, were the fractions of greatest interest to test our hypothesis that CD40mAb conjugates of lowest MW would make better vaccines. Comparative studies with Fraction 2 and Fraction 4 were carried out *in vitro*, but not *in vivo*, for the purpose of characterisation.

3.2.2. Characterisation of unfractionated and fractionated A20-mAb conjugates *in vitro*

3.2.2.1. Characterisation of A20-mAb conjugates using an anti-rat IgG and anti-mouse IgG antibody ELISA

Efficient conjugation of CD40mAb or isotype control 20C2mAb (Rat IgG1) to A20 antibody (Mouse IgG2a) was confirmed by sandwich ELISA. Two types of sandwich ELISAs (Figures 3.6 and 3.7) were used, (i) sandwich ELISA I (rat IgG and mouse IgG specific): used goat anti-rat IgG to capture CD40mAb or isotype control mAb and peroxidase-labelled goat anti-mouse IgG to detect A20 antibody (*see* Section 2.2.4.3.2.) and (ii) sandwich ELISA II (CD40mAb and mouse IgG specific): used a recombinant CD40/Fc chimera to capture CD40mAb and a peroxidase-labelled goat anti-mouse IgG to detect A20 antibody (*see* Section 2.2.4.3.3.).

Due to the specificity of ELISA I only A20 antibody conjugated to CD40mAb or control mAb would be detected whereas unconjugated A20 antibody, CD40mAb and 20C2mAb would be undetected. ELISA I confirmed that A20 antibody was successfully conjugated to CD40mAb and 20C2mAb (Figure 3.6). A closer look at the results demonstrates that unfractionated CLICK A20-mAb conjugates have a greater conjugate purity as a higher OD is observed compared to the Standard A20-mAb conjugates (Figure 3.6A). Fractions 2, 3 and 4 bind to the ELISA I antibodies efficiently down to a concentration of less than 31.3ng/ml. In contrast, Fraction 1 efficient binding to the ELISA I antibodies was only observed down to a concentration of 31.3ng/ml (Figure 3.6B), similar to the Standard A20-mAb conjugates (Figure 3.6A).

When considering the dilution factor (from a starting concentration 1µg/ml) at the specific OD of 0.5, Fraction 2 contains the greatest conjugate purity, followed by Fraction 3 and unfractionated CLICK conjugate. Considering that the functionalised A20 antibody emerged at 8.541 minutes on the HPLC (Figure 3.3), Fraction 4 that was collected from 8.2-11 minutes would contain with high probability free unconjugated A20 antibody, CD40mAb or 20C2mAb. However, some A20-mAb

conjugate is still present in Fraction 4, observed due to the increase in OD compared to the antibody controls (Figure 3.6C). Fraction 1 and whole Standard conjugate bind least efficiently to the ELISA I antibodies, showing least conjugate purity, which could be due to high MW complexes masking the binding sites of the ELISA antibodies.

As ELISA II utilises recombinant CD40/Fc chimera instead of anti-rat IgG as a capturing antibody, limiting its specificity to A20-CD40mAb conjugates, only A20 antibody conjugated to CD40mAb (but not control mAb) have the potential to give a positive signal in this assay, demonstrated by an increase in OD. The unconjugated A20 antibody, CD40mAb and 20C2mAb would also remain undetected. ELISA II not only demonstrates that the A20 antibody is conjugated to CD40mAb but also, that the CD40mAb is still able to bind to CD40 after conjugation.

The unfractionated A20-CD40mAb conjugates, the fraction of highest average MW (Fraction 1) and the fraction of lowest average MW (with possible limited free contaminating antibodies) (Fraction 3) were compared to each other using ELISA II. Fraction 1, Fraction 3 and both unfractionated conjugates contained A20-CD40mAb conjugates (Figure 3.7A), confirmed by the increase in OD compared to the antibody only controls. When observing the relative binding of the conjugates at the specific OD of 1.0, the unfractionated CLICK conjugate consists of highest conjugate purity, whilst the unfractionated Standard conjugate consists of the least conjugate purity (Figure 3.7B).

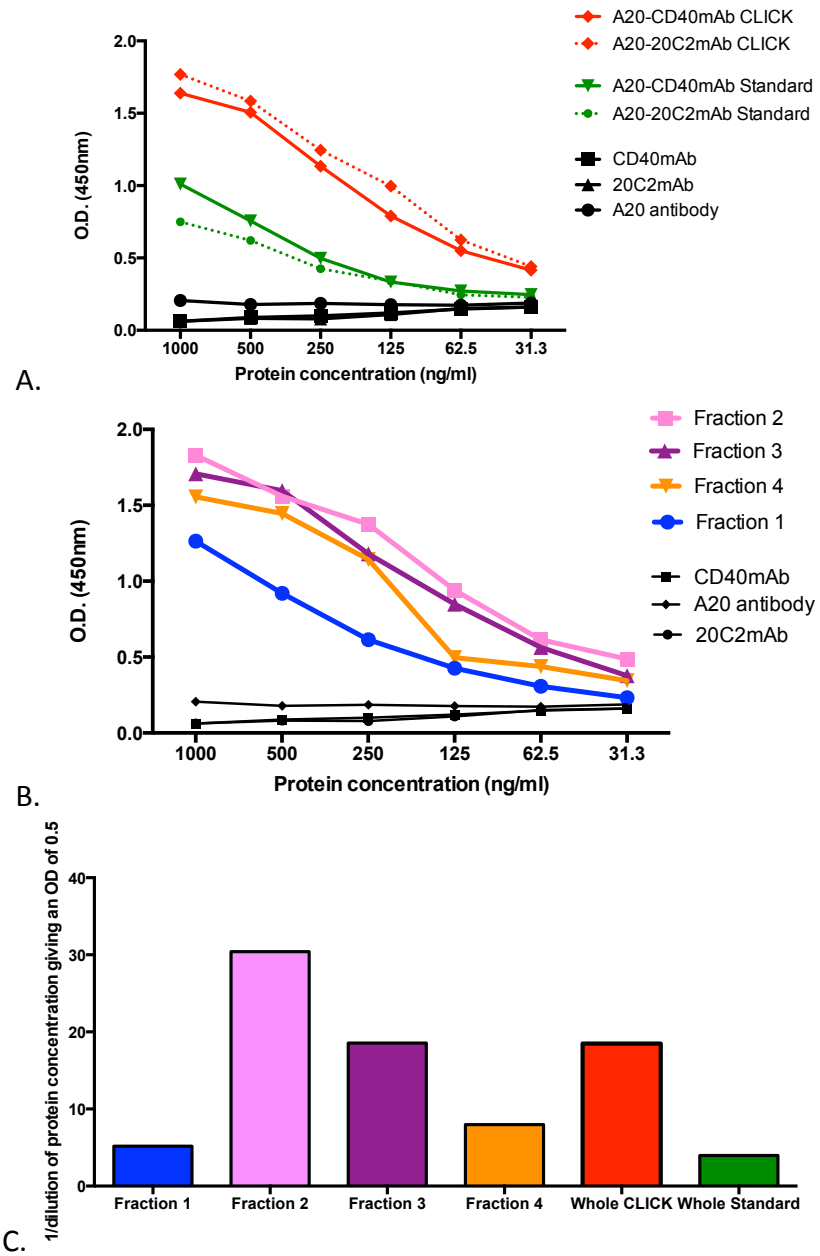

Figure 3.6. Confirmation of CD40mAb (or isotype control mAb) conjugation to A20 antibody by means of sandwich ELISA I. Goat anti-rat IgG antibody was used to capture and peroxidase-conjugated polyclonal anti–mouse Ig antibody was used to detect A20-mAb conjugates. Presence of A20-mAb conjugate is demonstrated by an increase in OD at 450nm. Parental A20 antibody, CD40mAb and 20C2mAb were used as negative controls. A. Relative binding of unfractionated CLICK and Standard A20-mAb conjugates. B. Relative binding of A20-CD40mAb conjugate fractions and unconjugated antibody controls. C. Comparison of the interpolated 1/dilution of the A20-mAb conjugate concentration giving an OD of 0.5. The dilution corresponding to 1/1 is 1000ng/ml (starting concentration). 20C2 = isotype control mAb.

A.

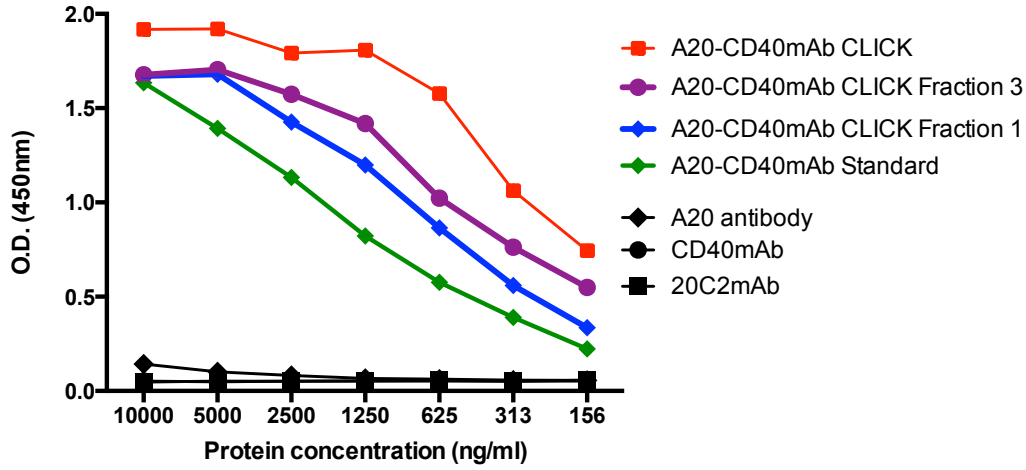

B.

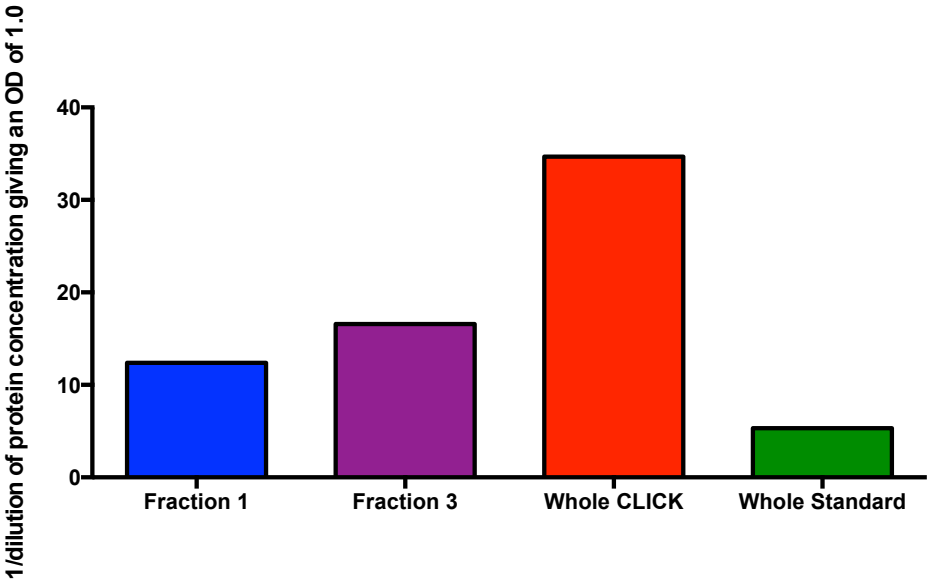

Figure 3.7. Relative binding of the A20-CD40mAb conjugates and fractions via recombinant CD40/anti-mouse Ig hybrid ELISA. Recombinant CD40/Fc chimera was used to capture and peroxidase-conjugated polyclonal anti–mouse Ig antibody was used to detect A20-CD40mAb conjugates. The presence of A20-CD40mAb conjugate is demonstrated by an increase in OD at 450nm. Parental A20 antibody, CD40mAb and 20C2mAb were used as negative controls. A. Relative binding of Fractions 1 and 3, as well as unfractionated CLICK and Standard conjugates. B. Comparison of the interpolated 1/dilution of the A20-CD40mAb conjugate concentration giving an OD of 1.0. The dilution corresponding to 1/1 is 10,000ng/ml (starting concentration). 20C2 = isotype control mAb.

3.2.2.2. Determination of functionality of CD40mAb-containing conjugates using flow cytometry

CD40 transfected fibroblast cells (CD40L929 cells, *see* Section 2.1.6.1) were used to ensure that the CD40mAb was still able to recognise and bind to full-length membrane bound CD40 expressed *in vitro,* following conjugation to A20 antibody.

To verify that A20 antibody is conjugated to CD40mAb, a secondary antibody, namely FITC-labelled anti-mouse IgG, specific to mouse IgG was used (*see* Section 2.2.4.4.1.). Therefore only the A20-CD40mAb conjugates would be detected due to CD40mAb binding to the CD40 expressing CD40L929 cells, demonstrated by an increase in fluorescence. The A20-20C2mAb conjugates served as negative controls in this assay.

CD40L929 cells were incubated with 10µg of each conjugate, conjugate fraction or control. The CD40mAb was able to bind CD40 expressed by CD40L929 cells after conjugation as well as after HPLC fractionation, observed by a shift of the peak to the right indicating increased fluorescence, compared to the isotype control conjugates and fractions (Figure 3.8A,B). Comparison to the respective isoytpe control conjugates and fractions was important to ensure that the increase in fluorescence compared to the unstained cells was not due to non-specific binding. Flow cytometry on CD40L929 cells confirmed that both the unfractionated conjugates and the conjugate fractions contained A20 conjugated to CD40mAb.

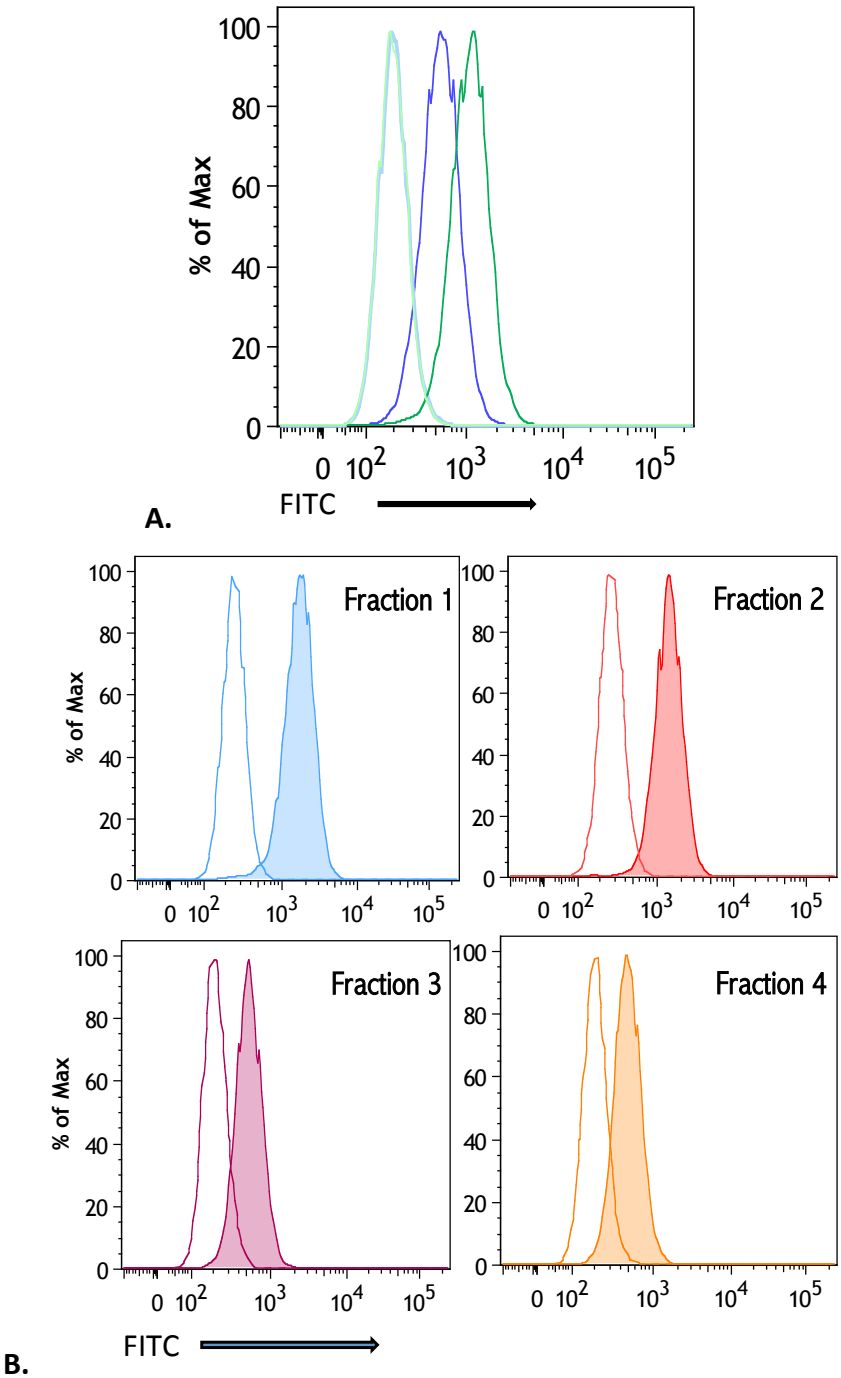

Figure 3.8. Functional capacity of the A20-CD40mAb conjugate to bind to the CD40 receptor of CD40L929 fibroblast cells, detected by a FITC labelled anti-mouse IgG antibody. A. Relative binding of unfractionated Standard and CLICK conjugate (dark blue and dark green outlines respectively) compared to unfractionated Standard and CLICK A20-20C2 conjugate (light blue and light green outlines that appear superimposed) B. Relative binding of the four A20-CD40mAb fractions (solid histograms) compared with their respective A20-20C2mAb fractions (outline histograms). Fraction 1 (blue), Fraction 2 (red), Fraction 3 (purple), Fraction 4 (orange). 20C2 = isotype control mAb.

3.2.2.3. Detection of A20 antibody present in the A20-mAb conjugates by means of Western blotting

HPLC analysis of A20 antibody and CD40mAb showed that A20 antibody is of higher MW than CD40mAb (Figure 3.3). To investigate if free unconjugated A20 antibody was present in Fraction 3, 1µg of the A20-CD40mAb conjugate and fractions were analysed by Western Blot (*see* Section 2.2.4.2.1.), using peroxidase labelled anti-mouse IgG to detect (Figure 3.9). The results showed that A20 antibody was present in all of the A20-mAb conjugate fractions, as well as in unfractionated conjugates (Figure 3.9A). Fractions 1 and 2 contained material of very high average MW and did not separate out into the resolving gel. Furthermore, Fractions 3 and 4 contained material of the lowest average MW. Also, judging from the size of the A20 antibody only control, Fraction 4 contained material of the same apparent MW as unconjugated A20 antibody, a band that was not apparent in Fraction 3. This shows the possibility that Fraction 3 contained none to minimal amounts of unconjugated A20 antibody.

Figure 3.9B demonstrates that non-specific detection of CD40mAb (negative control) demonstrated in Figure 3.9A was due to prolonged exposure time. On this occasion the membrane was visualised using the ChemiDoc™ XRS+ System (Biorad), allowing the MW protein ladder to be merged onto the Western Blotting image. Unconjugated A20 antibody was detected by peroxidase labelled anti-mouse IgG and no non-specific detection of CD40mAb were observed.

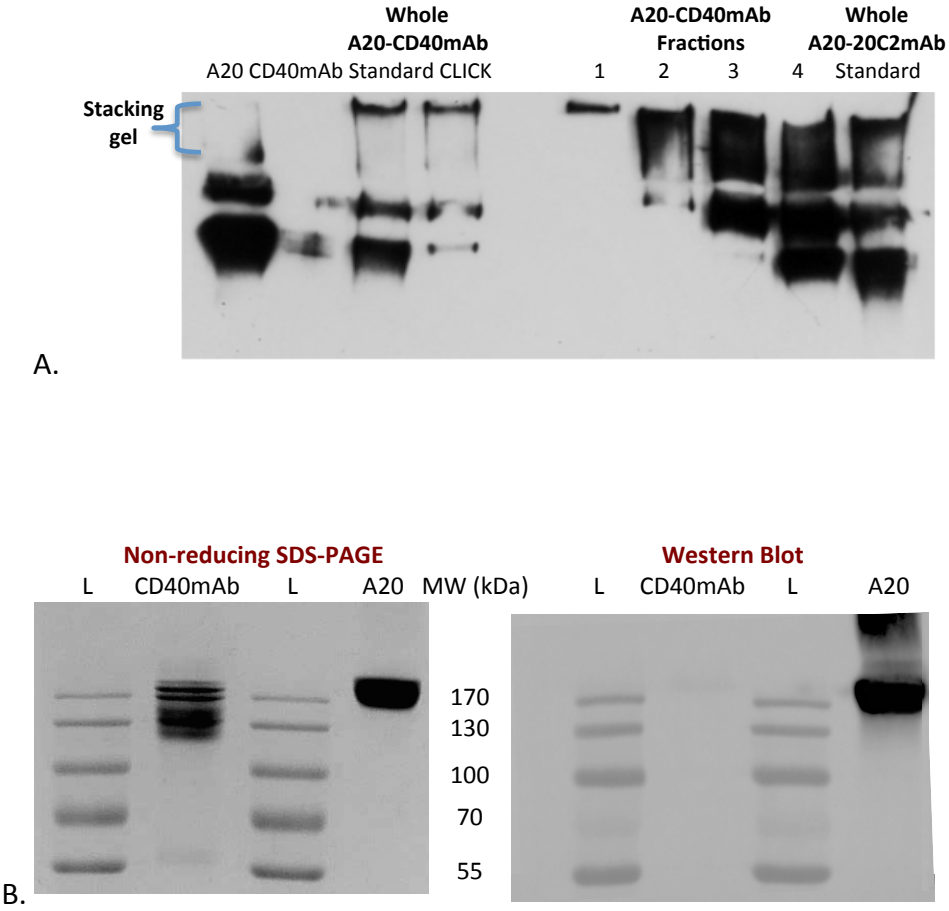

Figure 3.9. Detection of A20 antibody in the conjugate and conjugate fractions by Western Blot, using peroxidase-conjugated polyclonal anti–mouse Ig to detect. A. A20 antibody only (mouse IgG), labelled as A20, was used as a positive control. CD40mAb only (rat IgG) was used a negative control. The fractions shown are the A20-CD40mAb conjugates and fractions. **B.** Coomassie blue stained non-reducing SDS-PAGE gel (left) and respective Western Blot (right) of A20 antibody only (mouse IgG, positive control) and CD40mAb only (rat IgG, negative control).

3.2.3. Comparison of lymphoma antigen and CD40mAb conjugate made by novel and standard techniques in a murine lymphoma model

Comparative immunogenicity and anti-tumour vaccine efficacy of an A20-CD40mAb conjugate made by standard methods and (1) a novel unfractionated conjugate (CLICK unfractionated conjugate), (2) a low average MW conjugate (Fraction 3) or (3) a very high average MW conjugate (Fraction 1) was assessed in an established A20 lymphoma murine model. The prophylactic immunisation schedule used is shown in Figure 3.10 (*see* Section 2.2.7.1.).

Groups of 10 female BALB/c mice were immunised twice (10µg in 50µl volume) with the immunogens subcutaneously in the left flank. After 28 days of first immunisation a lethal dose of 1 x 10^5 A20 cells in 50µl was given subcutaneously on the opposite flank. Immunisation of the mice, performance of tail bleeds, inoculation of A20 cells and monitoring of tumour growth was performed by Ms Amy Lewis in the Department of Infection and Immunity.

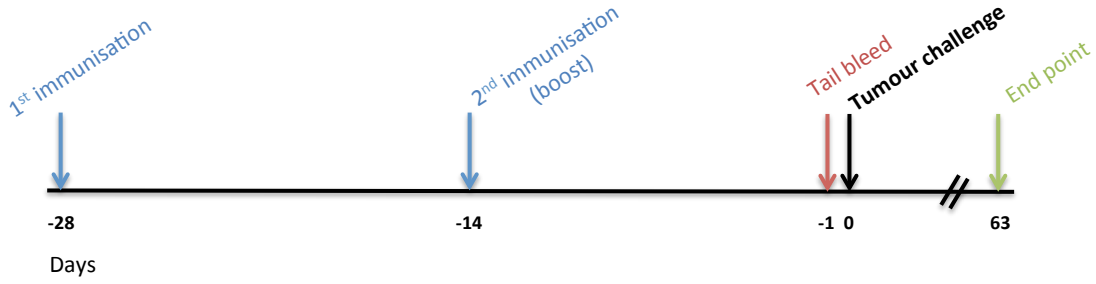

Figure 3.10. Immunisation schedule using the A20-CD40mAb conjugates. BALB/c mice were immunised subcutaneously in the left flank on day -28 and boosted on day -14 (blue). On day -1 mice were bled (red). A subcutaneous lethal dose of 1 x 10^5 A20 cells in 50µl was administered on day 0 (black). Mice were monitored for tumour development until day 63 post-challenge (green).

Serum anti-mouse Ig antibody titres were determined by ELISA using peroxidase-labelled goat anti-mouse IgG to detect (*see* Section 2.2.7.1.1.). Mice immunised with unfractionated Standard A20-CD40mAb conjugate, unfractionated CLICK A20-CD40mAb conjugate, Fraction 1 and Fraction 3 all raised antibodies against A20 antibody compared with the vehicle control PBS (Figure 3.11). The results showed no statistically significant difference between the antibody titres produced by the unfractionated Standard and CLICK A20-CD40mAb immunised groups. However, interestingly, sera from Fraction 3 (low average MW conjugate) immunised mice had significantly higher anti-A20 antibody titres compared to sera from the Standard conjugate immunised group ($p<0.05$, one-way ANOVA, using Dunnett's post-test) (Figure 3.11), whereas Fraction 1 (high average MW conjugate) did not. These results indicated that CD40mAb-adjuvanted vaccines of low average MW are superior to more heterogeneous vaccines.

In order to determine if the anti-tumour efficacy of each of the CLICK A20-CD40mAb conjugates or fractions was better than the Standard conjugate, the mice were challenged with A20 tumour cells. We were interested to see whether prophylactic immunisation with a more defined CD40mAb-adjuvanted conjugate would have the potential to prevent or delay tumour progression, compared to more heterogeneous conjugates. Enhanced median and/or overall survival would indicate the vaccine was more effective.

The overall survival of the Standard A20-CD40mAb immunised group was compared to the PBS group to assess the vaccine efficacy of the Standard conjugation technique. The overall survival of Standard A20-CD40mAb immunised mice was significantly enhanced compared to the control group ($p<0.05$) (Figure 3.12), with the median survival extended by 11 days (33 days for Standard A20-CD40mAb conjugate compared to 22 days for PBS immunised group).

The median survival of the tumour challenged mice immunised with Standard whole conjugate was compared to the mice immunised with CLICK whole conjugate and fractions. Immunisation with unfractionated CLICK conjugates, Fraction 1 and Fraction 3 showed an enhanced median survival by 8.5 days ($p=0.3$), 15 days ($p=0.39$) and more than 33 days ($p=0.07$) respectively compared to immunisation

with unfractionated Standard conjugate. This means that although a strong trend was observed, the difference in the median survival between the groups is not significant. However, the percentage overall survival in the Standard A20-CD40mAb conjugate group (12%) was considerably less than in the CLICK A20-CD40mAb conjugate (40%), Fraction 1 (50%) and especially, Fraction 3 (60%) immunised groups.

The tumour burden or tumour volume in cubic millimetres, calculated by measuring the long and short diameter of the tumour and using the formula: $((\text{short} + \text{long})*0.25)^3*4/3\pi$ (*see* Section 2.2.7.1.), was investigated on day 19 in all groups (Figure 3.13A). Day 19 was chosen because on this day the first mouse immunised with the Standard conjugate had to be culled due to the tumour reaching the maximum permissible tumour diameter (12mm). The PBS group was excluded because the first mouse in this group had already been culled on this date. Interestingly, Fraction 3 and unfractionated CLICK conjugate immunised mice had a significantly lower average tumour burden than the unfractionated Standard conjugate immunised mice (Figure 3.13A, $p<0.05$, One-way ANOVA, using Dunnett's post test). However, there was no significant difference between the tumour burden in groups immunised with Fraction 1 and the unfractionated Standard conjugate. Furthermore, the Fraction 3 immunised group demonstrated the slowest onset of tumour growth. The Fraction 3 immunised group started to develop tumours at day 21, whilst in all other groups tumours were observed on day 17 post-challenge (Figure 3.13B).

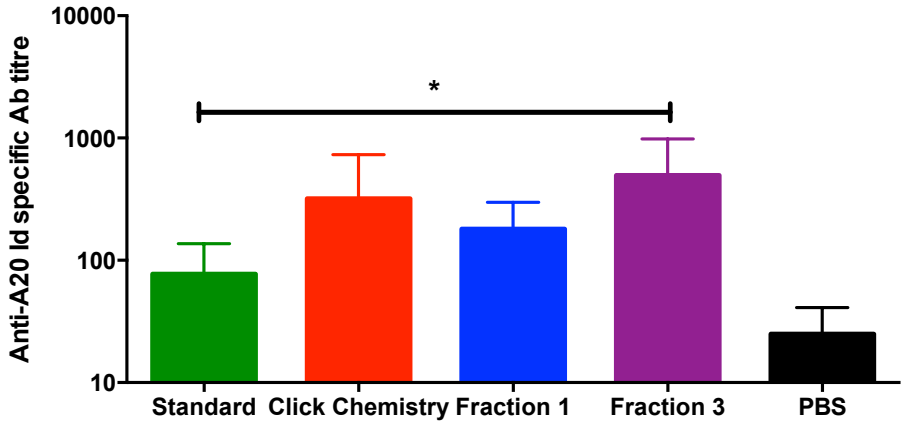

Figure 3.11. Anti-A20 specific antibody end-point titre level after boost (day -1). Anti-A20 antibody levels detected in sera of mice prophylactically immunised with unfractionated Standard conjugate (green), unfractionated CLICK conjugate (red), high average MW conjugate - Fraction 1 (blue), low average MW conjugate - Fraction 3 (purple) and PBS (black) are shown. One-way ANOVA using Dunnett's multiple comparison post-test (mean +/- SD, n = 5-9 mice) was used to determine statistical significance. *p<0.05.

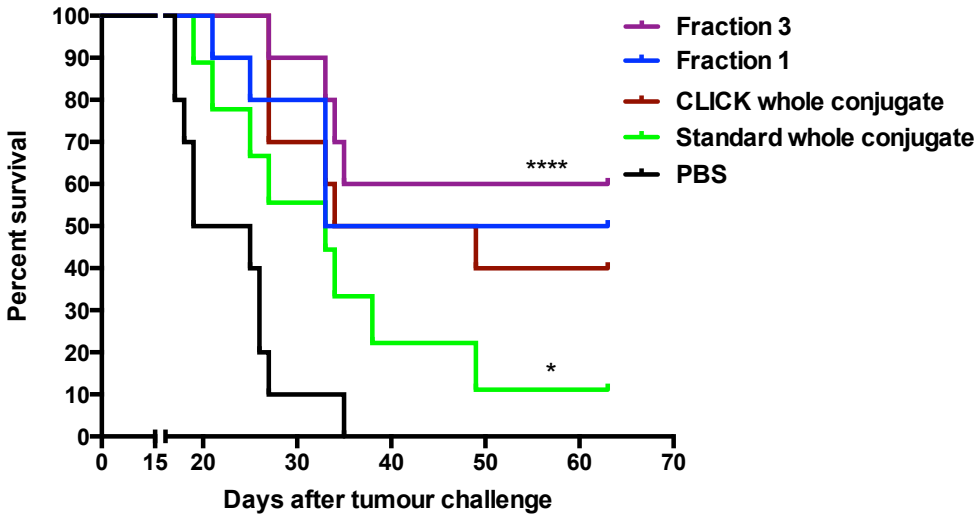

Figure 3.12. The efficacy of the A20-CD40mAb vaccines in the A20 lymphoma mouse model. A Kaplan-Meier survival curve was used to determine the overall survival of A20 tumour challenged mice prophylactically immunised with A20-CD40mAb conjugate made by standard methods and novel methods compared to mice prophylactically immunised with PBS (control group). Statistical significance was determined by means of a log-rank test. *p<0.05. ****p<0.0001. PBS, CLICK whole conjugate, Fraction 1, Fraction 3, n = 10; Standard whole conjugate, n = 9.

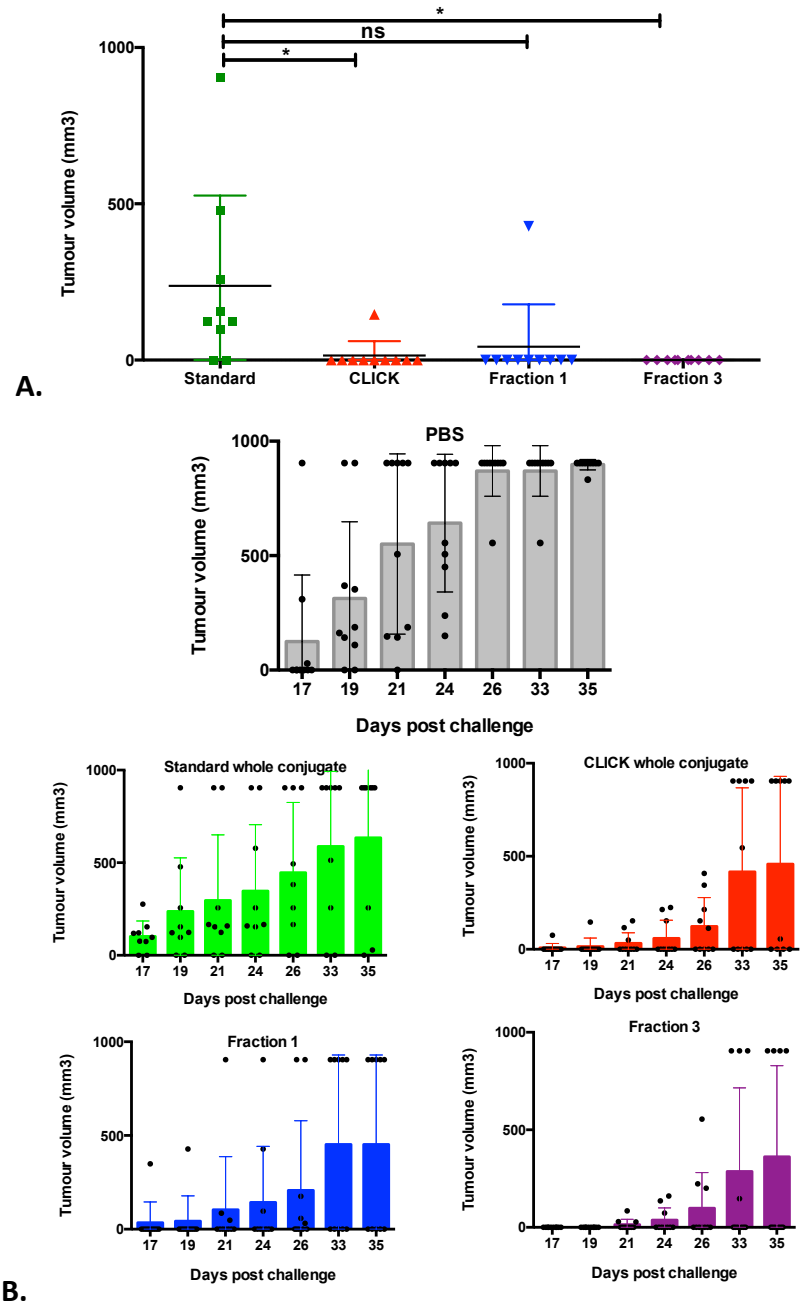

Figure 3.13. Difference in tumour burden between the immunised groups. The tumour burden on day 19 post challenge (A) and speed of tumour growth (B) in mice immunised with Standard A20-CD40mAb conjugate (green) compared to mice immunised with CLICK unfractionated A20-CD40mAb conjugate (red), Fractions 1 (blue) and Fraction 3 (purple). Mice immunized with PBS group are shown in black. Statistical significance was determined by means of One-way ANOVA using Dunnett's multiple comparison test (mean +/- SD) was used to determine statistical significance. *$p<0.05$. ns – non-significant. PBS, CLICK unfractionated conjugate, Fraction 1, Fraction 3, n = 10; Standard conjugate, n = 9. Each dot corresponds to one mouse.

3.3. Comparative immunogenicity of OVA antigen and CD40mAb conjugate made by different conjugation strategies in a murine system

Low average MW A20-CD40mAb conjugates made by click chemistry showed to be superior vaccines to the more heterogeneous vaccines made by standard methods. Following these very encouraging results, OVA-mAb conjugates were made using click chemistry (*see* Section 2.2.1.7.) and standard methods (*see* Section 2.2.1.2.), separated into fractions by HPLC and characterised as described for the A20-mAb conjugates.

OVA antigen has been chosen as a model antigen due to the readily available OVA-specific reagents, that would allow convenient testing of $CD4^+$ and $CD8^+$ T cell responses (studied in the next chapters shown in this thesis). The various OVA-CD40mAb conjugates' ability to induce antibody responses to OVA was assessed *in vivo*. It was of particular interest to determine whether the lowest average MW OVA-CD40mAb conjugate would be the most immunogenic.

3.3.1. Fractionation of OVA-mAb conjugate by HPLC

The fact that the OVA-CD40mAb conjugates are made up of OVA antigen (45 kDa) conjugated to CD40mAb and not A20 antibody (approximately 150 kDa) would affect the time the peaks are observed on the chromatogram after size-exclusion chromatography. Therefore, the time at which the peak of unconjugated and functionalised OVA antigen, CD40mAb and 20C2mAb emerged was again observed. This allowed for a more informed decision on the time the fractions of interest need to be collected, especially the lowest average MW fraction. CD40mAb and 20C2mAb, were observed at 9.24 minutes, whilst OVA antigen which is of lower MW than the antibodies was observed at 9.85 minutes. DBCO-NHS functionalised antibodies and NHS-PEG4-Azide functionalised OVA were observed earlier at 9.2 minutes and 9.8 minutes respectively (Figure 3.14).

A 50µg sample of CLICK OVA-CD40mAb and Standard OVA-CD40mAb were analysed on the HPLC SEC, and the CLICK conjugate fractions of interest were identified (Figure 3.15), by referring to the chromatogram containing various standards (Figure 3.2). The standard of MW 660kDa emerged around 7 minutes therefore we assumed that the peak observed at 5 minutes would be with high probability a conjugate of the highest average MW (Figure 3.15). Considering that CD40mAb peak emerged at 9.2 minutes, the fraction we hypothesized was of lowest average MW with minimal to no contaminating mAb, was collected from 8.1 minutes to 8.7 minutes. A conjugate fraction of lower average MW was not collected because in optimisation experiments conjugate fractions collected closer to 9 minutes seemed to contain unconjugated OVA antigen detected by Western Blot analysis (results not shown). This was surprising because the peak containing NHS-PEG4-Azide-functionalised OVA antigen alone was observed later at 9.8 minutes (Figure 3.14). The four fractions of OVA-mAb collected are illustrated in Figure 3.16.

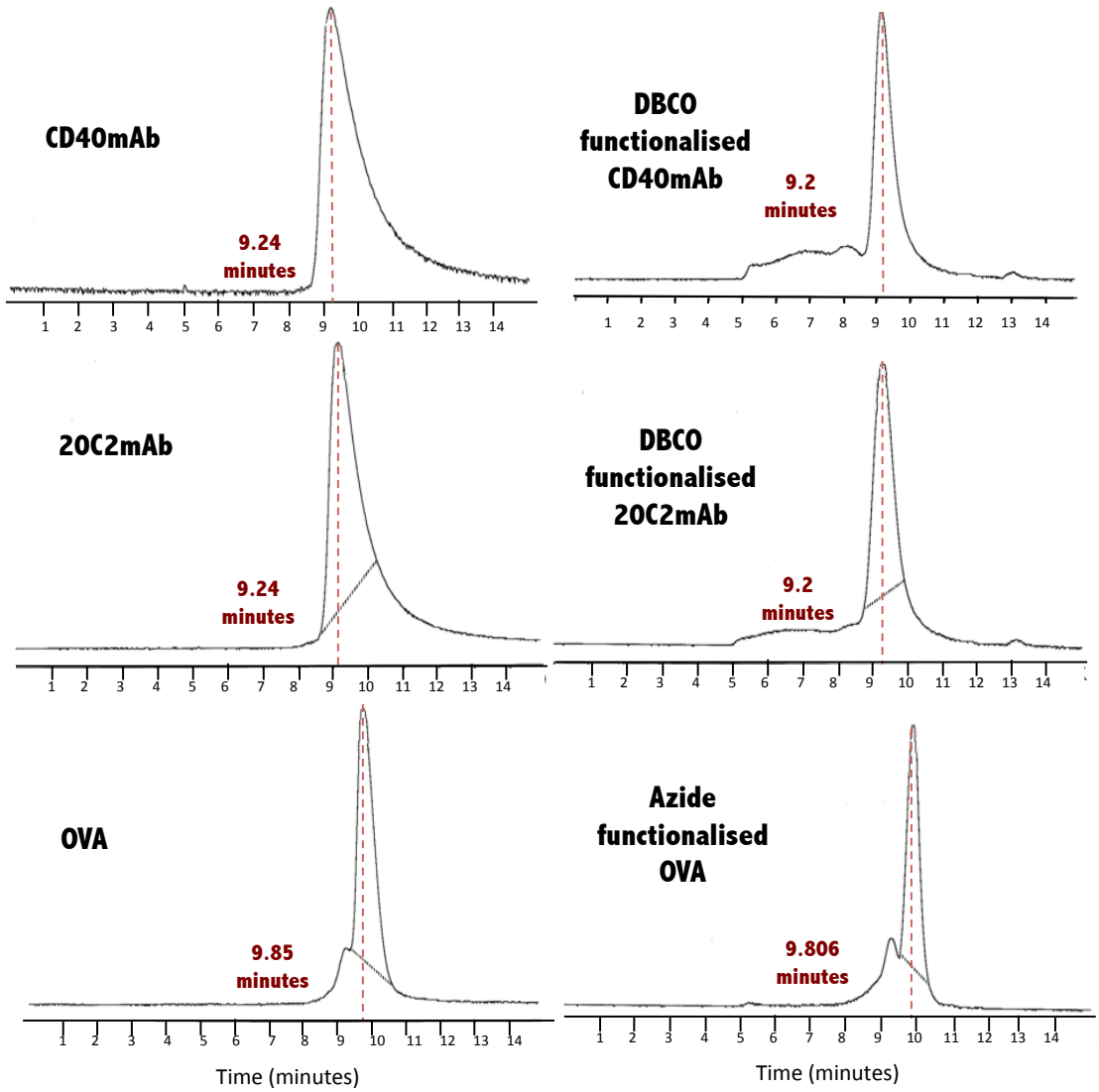

Figure 3.14. HPLC chromatograms showing unconjugated CD40mAb, 20C2mAb and OVA, as well as NHS-PEG4-Azide functionalised OVA and DBCO-NHS functionalised CD40mAb and 20C2mAb. The numbers shown in red represent the time taken for the peak of the non-functionalised and functionalised OVA or antibody to emerge on the HPLC chromatogram. The absorbance readings on the HPLC plots were measured at 280nm. 20C2 = isotype control mAb.

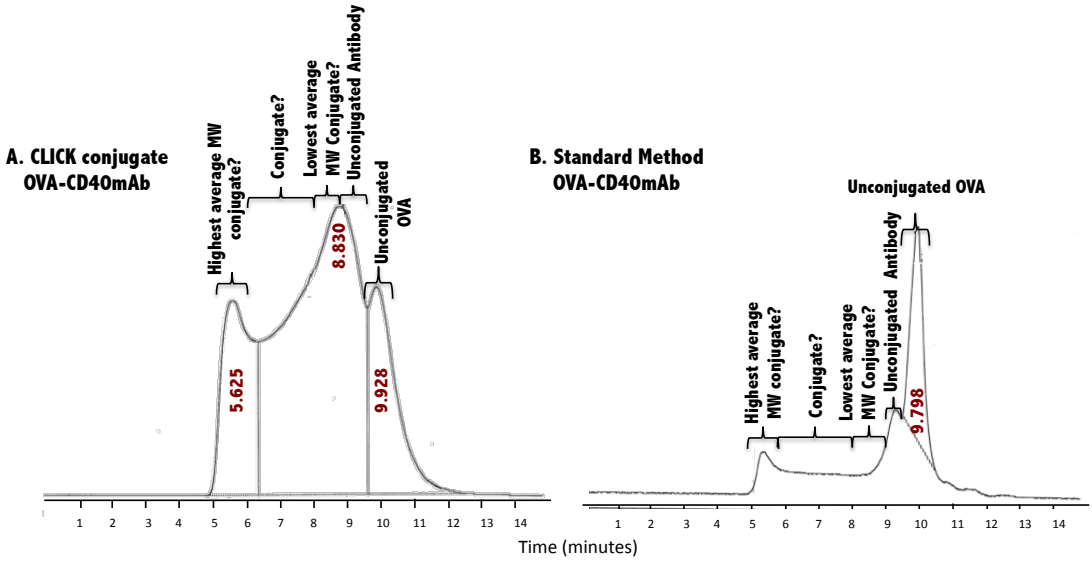

Figure 3.15. Representative HPLC chromatograms of the CLICK and Standard OVA-CD40mAb conjugates. The numbers shown in red represent the time taken for the peak of the particular fraction to emerge on the HPLC chromatogram. The absorbance readings on the HPLC plots were measured at 280nm.

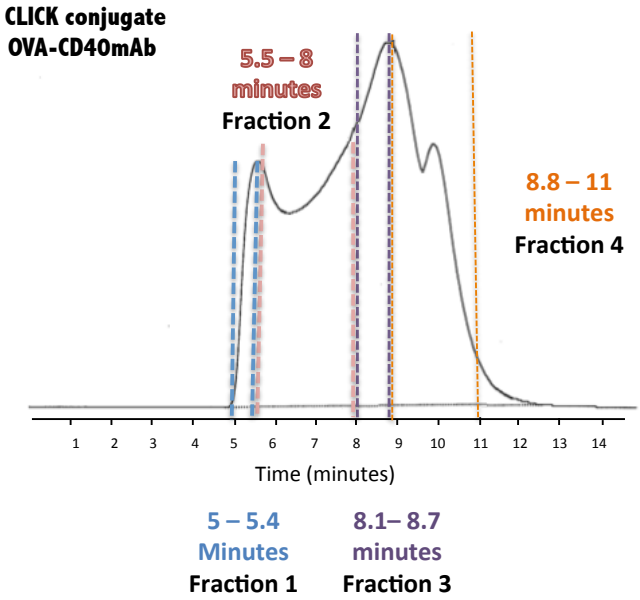

Figure 3.16. Representative HPLC chromatogram of CLICK OVA-CD40mAb conjugate and the different fractions collected. The fractions collected included: Fraction 1 (blue) from 5 minute to 5.4 minutes, Fraction 2 (pink) collected from 5.5 minutes to 8.0 minutes, Fraction 3 (purple) collected from 8.1 minutes to 8.7 minutes and Fraction 4 (orange) collected from 8.8 minutes to 11 minutes. The absorbance readings on the HPLC plots were measured at 280nm.

A BCA assay (*see* Section 2.2.3.) was used to quantify the protein concentration of each fraction. The four fractions of the OVA-mAb conjugates were labelled as explained in Table 3.2 and will be referred to as Fraction 1, 2, 3 or 4 (according to decreasing apparent MW) from this point on. Respective fractions from OVA antigen conjugated to isotype control mAb made by the click chemistry method were also collected (results not shown).

OVA-mAb conjugate fractions collected
5 - 5.4 minutes (Fraction 1)
5.5 – 8 minutes (Fraction 2)
8.1 – 8.7 minutes (Fraction 3)
8.8 - 11 minutes (Fraction 4)

Table 3.2. OVA-mAb conjugate fractions collected by minutes on HPLC.

From the four fractions collected, Fraction 1 and Fraction 3 were the fractions of interest to evaluate the hypothesis that CD40mAb-adjuvanted conjugates of lower average MW and greater CD40mAb accessibility are most immunogenic. Comparative studies with Fraction 2 and Fraction 4 were carried out *in vitro*, but not *in vivo*.

3.3.2. Characterisation of unfractionated and fractionated OVA-mAb conjugates *in vitro*

3.3.2.1. Characterisation using an anti-rat IgG and anti-OVA antibody ELISA

The conjugation of CD40mAb or 20C2mAb (rat IgG1) to OVA antigen was confirmed by sandwich ELISA. Firstly, rat IgG was captured with an anti-rat IgG antibody and the conjugation of rat IgG to OVA was confirmed by simultaneous binding to rabbit (IgG) anti-OVA antibody followed by peroxidase conjugated goat anti-rabbit IgG (*see* Section 2.2.4.3.1.). This was visualised colorimetrically by an increase in OD (Figure 3.17).

The CLICK unfractionated OVA-CD40mAb conjugate and Fractions 2, 3, 4 had the highest conjugate purity and bound the ELISA antibodies to a concentration equal to or greater than 7.8ng/ml, whilst Fraction 1 and Standard unfractionated OVA-CD40mAb conjugate only bind ELISA antibodies to a concentration of 31.3ng/ml (Figure 3.17A,B). When observing the relative binding of the conjugates at the specific OD of 0.5, Fraction 3 consisted of highest conjugate purity. The unfractionated OVA-CD40mAb Standard conjugate and Fraction 1 consisted of least conjugate purity (Figure 3.17C). We hypothesised that the reason for this was because of high MW complexes that could be masking the binding sites of the ELISA antibodies.

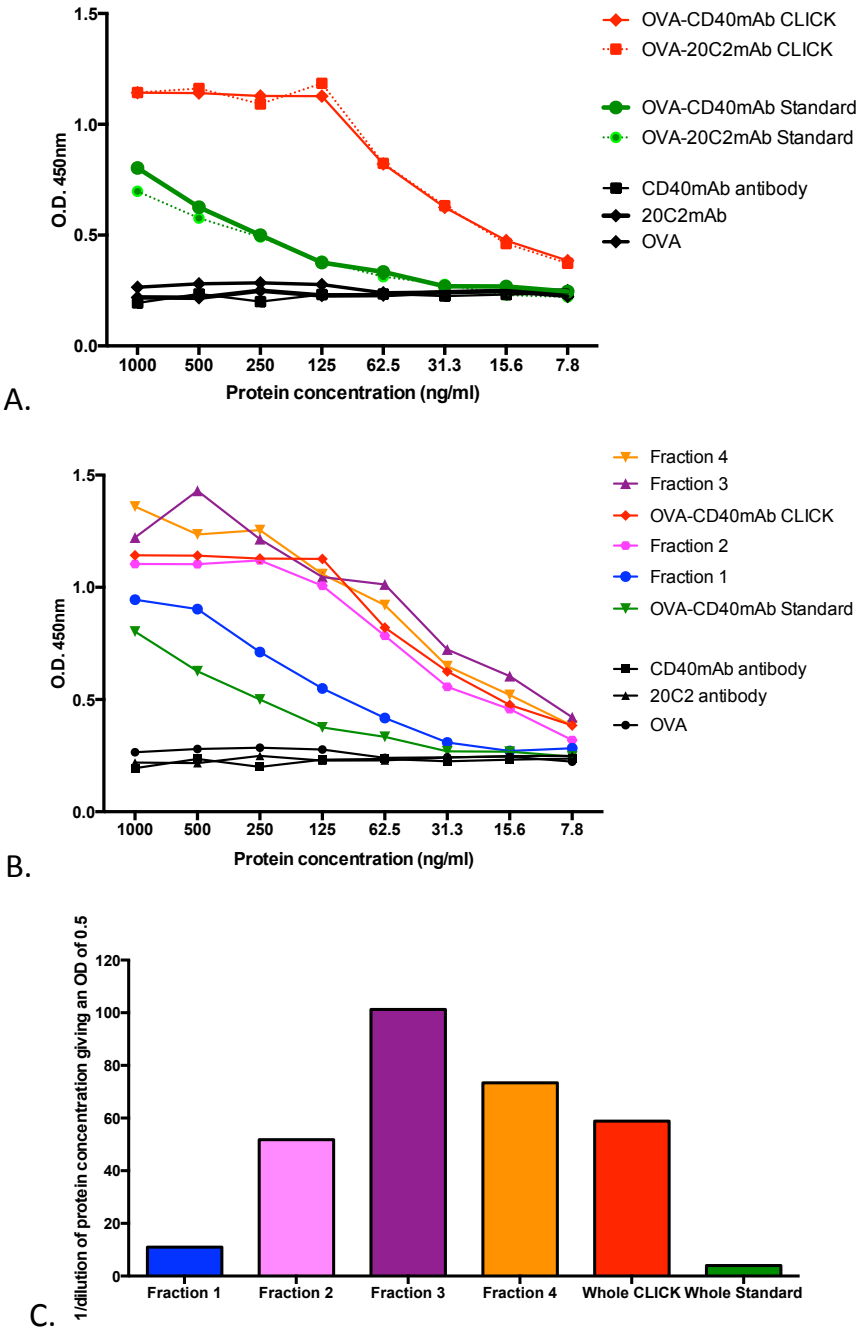

Figure 3.17. Confirmation of OVA to rat IgG conjugation via sandwich ELISA. Goat anti-rat IgG antibody and rabbit (IgG) anti-OVA antibody simultaneously bind to the OVA-mAb conjugates and are detected by peroxidase conjugated anti-rabbit IgG antibody. Presence of OVA-mAb conjugate is demonstrated by an increase in OD at 450nm. Parental A20 antibody, CD40mAb and 20C2mAb were used as negative controls. A. Relative binding of unfractionated CLICK and Standard OVA-mAb conjugates. B. Relative binding of OVA-CD40mAb conjugate fractions and controls. C. Comparison of the interpolated dilution factor of the OVA-CD40mAb conjugate concentration giving an OD of 0.5. The dilution corresponding to 1/1 is 1000ng/ml (starting concentration). 20C2 = isotype control mAb.

3.3.2.2. Characterisation using flow cytometry on CD40 expressing fibroblast cells

CD40L929 fibroblast cells were used to ensure that the CD40mAb was still able to recognise and bind to full-length membrane-bound CD40 expressed *in vitro,* following conjugation to OVA, by flow cytometry (*see* Section 2.2.4.4.1.).

Binding of CD40mAb to CD40L929 cells, and the simultaneous binding of OVA antigen to rabbit (IgG) anti-OVA antibody was detected by a FITC labelled anti-rabbit IgG antibody in the presence of the OVA-CD40mAb. OVA antigen conjugated to 20C2mAb and respective fractions that do not contain CD40mAb served as negative controls. A 10µg sample of each OVA-mAb conjugate and conjugate fraction was analysed on CD40L929 cells per test. Both OVA-CD40mAb unfractionated conjugates (Figure 3.18A) and conjugate fractions (Figure 3.18B) bound to the CD40 expressing cells, which can be observed by an increased fluorescence or a shift to the right in the overlaid histogram compared to their respective isotype control conjugates. Comparison to the isotype control conjugates was important to ensure that the increase in fluorescence observed with the OVA-CD40mAb conjugates was not due to non-specific binding.

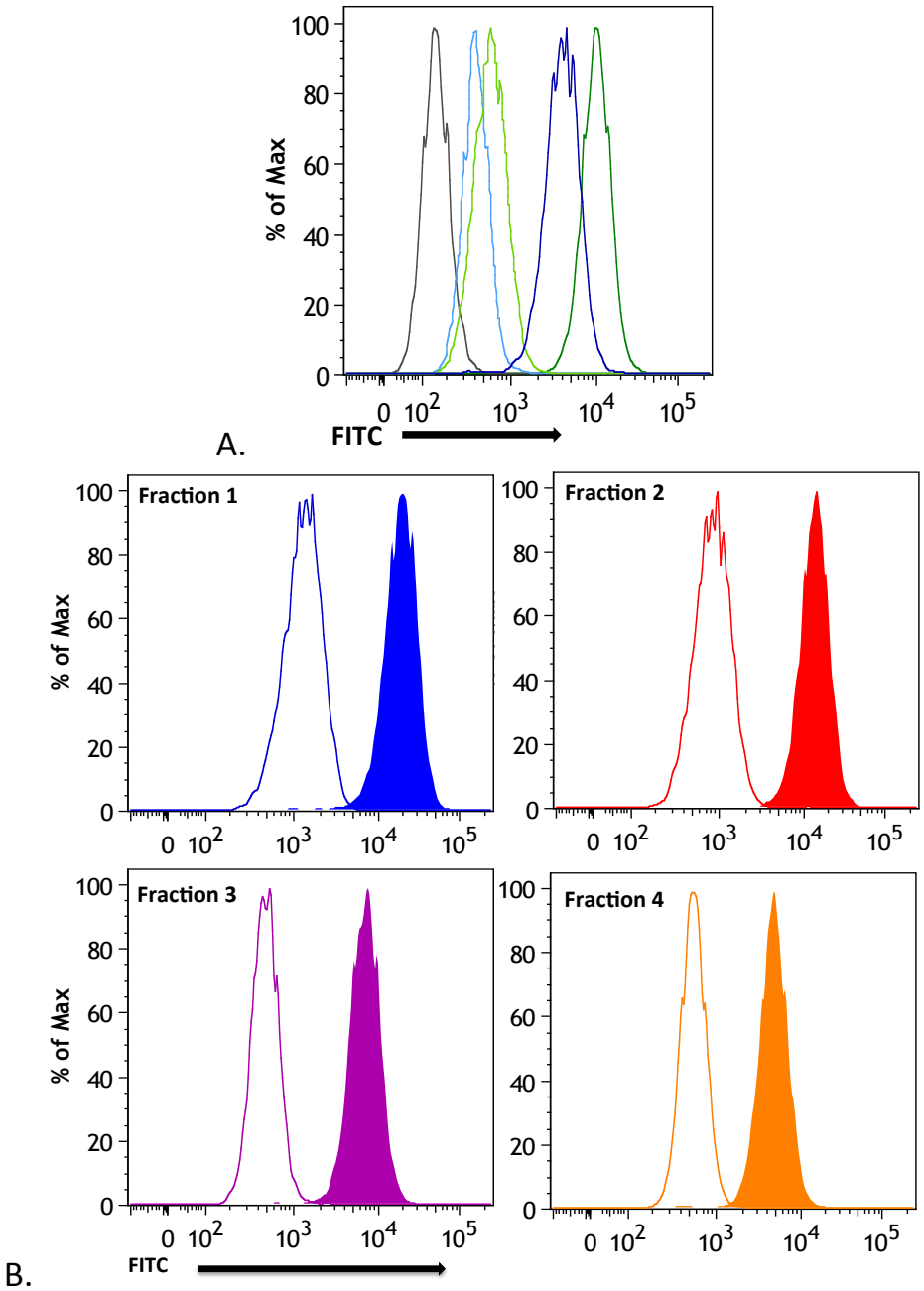

Figure 3.18. Functional capacity of the OVA-CD40mAb conjugate to bind to the CD40 receptor of CD40L929 fibroblast cells. A. Relative binding of unfractionated Standard and CLICK conjugate (dark blue and dark green outlines respectively) compared to unfractionated Standard and CLICK OVA-20C2 conjugate (light blue and light green outlines respectively). The black outline represents the FITC labelled anti-rabbit IgG antibody only control. (B) Relative binding of the four OVA-CD40mAb conjugate fractions (solid histograms) compared with their respective isotype control conjugate fractions (outlines); Fraction 1 (blue), Fraction 2 (red), Fraction 3 (purple), Fraction 4 (orange). 20C2 = isotype control mAb.

3.3.2.3. Detection of OVA antigen and CD40mAb present in the conjugates by means of Western blotting

The purpose of the Western blot analysis was not only to establish the antigenic composition of the conjugate and fractions but it was also important to analyse if unconjugated OVA antigen or CD40mAb were present in Fraction 3. Free unconjugated CD40mAb should be the major contaminating material because of its MW. However, although unconjugated OVA antigen should be of too low a MW to be detected, previous optimisation experiments showed that it sometimes is detected in higher average MW peaks (data not shown), perhaps because it forms dimers in solution. Therefore, 1µg of the different conjugates and fractions was analysed by Western Blotting in two ways (*see* Section 2.2.4.2.). To verify that CD40mAb was present in the conjugate a peroxidase labelled anti-rat IgG antibody was used for detection. The peroxidase labelled anti-rat IgG antibody does not show any non-specific binding to OVA antigen (Figure 3.19). To verify OVA was present in the conjugate a rabbit anti-OVA IgG was used as a primary antibody and a peroxidase-labelled anti-rabbit IgG was used as a secondary antibody to detect OVA. The latter antibodies do not show any non-specific binding to rat IgG. Figure 3.19A shows a non-reducing SDS-PAGE of unconjugated OVA and CD40mAb, and the respective OVA-specific Western Blot. This was visualised using the ChemiDoc™ XRS+ System allowing the MW protein ladder to be merged onto the Western Blotting image. Due to the absence of a marker in Figure 3.19B, the MW protein ladder used in Figure 3.19A was used to estimate the MW.

The results showed that OVA and CD40mAb were present in all of the OVA-CD40mAb conjugate fractions, as well as in unfractionated conjugates (Figure 3.19A). Fraction 1 contained material of very high average MW, which did not migrate into the resolving gel. Fractions 2 and 3 contained material of lower average MW showed better separation in the resolving gel. Both these fractions (particularly Fraction 3) contain some material of the same apparent MW as free unconjugated OVA. Judging from the bands apparent in Fraction 4 and CD40mAb only positive control, Fraction 3 contains minimal amounts of unconjugated CD40mAb. On comparing the unfractionated CLICK to the unfractionated Standard conjugate, the latter seems to have more unconjugated OVA and mAb (consistent with the HPLC plots Figure 3.14).

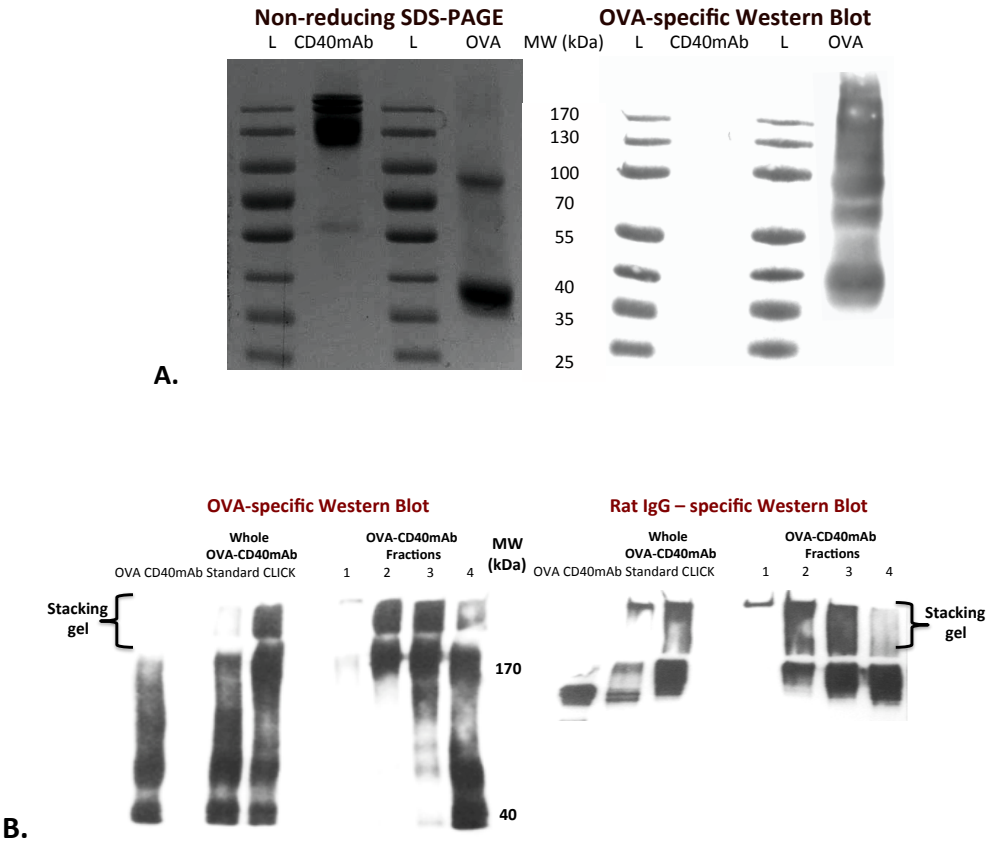

Figure 3.19. Western blot analysis of the OVA-CD40mAb conjugate and fractions.

A. Non-reducing SDS-PAGE showing unconjugated CD40mAb and OVA (left) and the respective Western Blot using peroxidase-labelled goat anti-rabbit IgG to detect OVA antigen bound to the primary antibody rabbit (IgG) anti-OVA (right). B. Peroxidase-labelled goat anti-rabbit IgG was used to detect OVA antigen of the conjugate bound to the primary antibody rabbit (IgG) anti-OVA (left). Peroxidase-labelled anti-rat IgG antibody was used to detect rat IgG (CD40mAb) (right). The MW markers shown are an estimate based on the previous SDS-PAGE gel (shown in A). L refers to the molecular weight ladder shown in kDa.

3.3.3. Evaluation of the anti-OVA response induced by OVA antigen and CD40mAb conjugate made by novel and standard techniques *in vivo*

Comparative immunogenicity of an OVA-CD40mAb conjugate made by standard methods and (1) a novel unfractionated conjugate (CLICK unfractionated conjugate), (2) a defined low average MW conjugate (Fraction 3) or (3) a very high average MW conjugate (Fraction 1) was assessed in a murine system, by investigating anti-OVA specific titres in sera of immunised mice. The prophylactic immunisation schedule used is shown in Figure 3.20 (*see* Section 2.2.7.2.). Sera from immunised mice collected at days 13 and 28 were analysed by ELISA (*see* Section 2.2.7.2.1.).

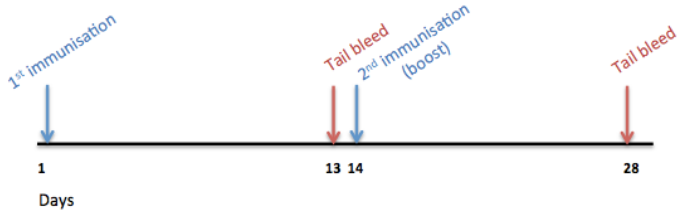

Figure 3.20. Immunisation schedule for OVA-CD40mAb conjugates. BALB/c mice were immunised with 10µg unfractionated CLICK and Standard conjugate, as well as Fraction 1 and Fraction 3 on day 1 and boosted on day 14. Mice were bled on day 13 and day 28. Each immunisation group consisted of 5 mice.

Anti-OVA end-point titres showed that CLICK unfractionated conjugate as well as Fraction 1 and Fraction 3 significantly enhanced antibody responses against OVA antigen when compared to Standard unfractionated conjugate at day 13 (before boost) ($p<0.0001$, One-way ANOVA, using Dunnett's post-test) (Figure 3.21A). However, surprisingly, anti-OVA end-point titres at day 28 (after boost) showed that only Fraction 3 did not significantly enhance antibody responses against OVA antigen Figure 3.21B. However, a trend was observed ($p=0.051$, One-way ANOVA, using Dunnett's post-test). It is worthy to note that after the boost each immunised group (except for PBS group) demonstrated very high OVA end-point titres, including mice immunised with Standard OVA-CD40mAb vaccines. There was a significant difference in the anti-OVA endpoint titres between the sera from Standard conjugate and PBS immunised mice both pre-boost and post-boost.

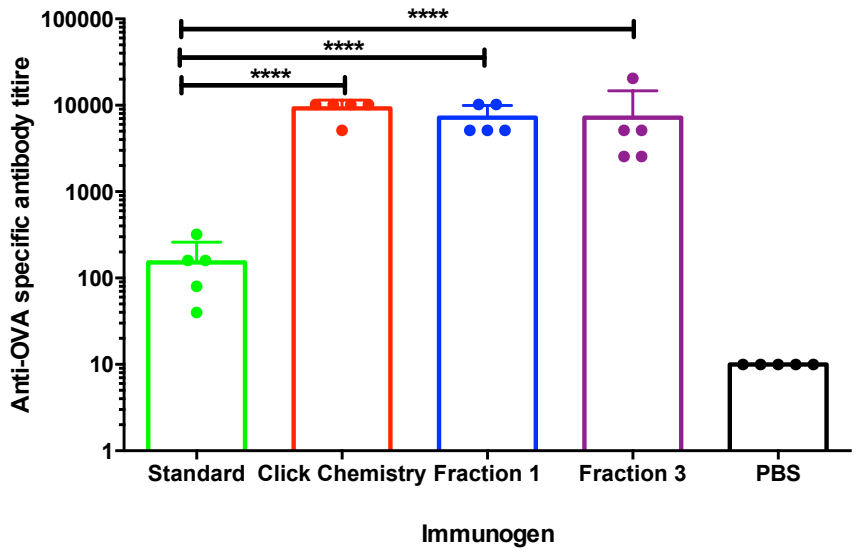

A.

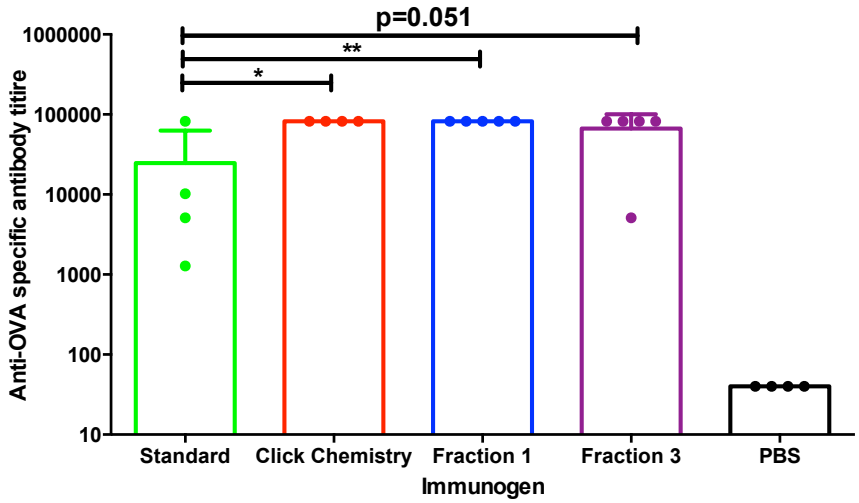

B.

Figure 3.21. Serum anti-OVA antibody end-point titre level at day 13 (A) and day 28 (B) (following boost). Statistical significance was determined by the use of One-way ANOVA using Dunnett's multiple comparison test (mean +/- SD, n = 4 or 5) was used to determine statistical significance. *p<0.05 **p<0.01, ****p<0.0001. Each dot corresponds to one mouse.

Discussion

Vaccines designed for clinical use should be potent and consistent in composition. Conjugation strategies used so far, including the standard method used in our laboratory yield products that are heterogeneous and contain high average MW complexes that may mask the immunogenic epitopes of the vaccine. CD40mAb works best as an adjuvant in a monomeric state (Heath and Laing, 2004). Thus, in order to maximise the potential of CD40mAb as an adjuvant in conjugate vaccines, the novel, highly specific conjugation strategy – click chemistry, was used together with size-exclusion HPLC, in an effort to produce more clearly defined and less heterogeneous conjugates of low average MW.

The reagents used to produce the CLICK and Standard conjugates in this chapter namely, NHS-PEG4-Azide, DBCO-NHS, Sulfo-SMCC and SATA all have an amine-reactive group (NHS ester). OVA antigen contains 20 lysine residues that contain amines for conjugation. Amines are present all over the antibody structure with 21 present on the heavy chain constant region of rat IgG1 and 8 present on the heavy chain constant region of mouse IgG1. Even though there are multiple sites for the formation of an amide bond, the NHS ester reagents are still usually used in excess, as the reaction is not 100% efficient (Adamczyk et al., 1996). This means that most likely more than one NHS ester group could be binding to OVA antigen or antibody (CD40mAb, 20C2mAb or A20 antibody). For example in the case of OVA-CD40mAb conjugates, more than one CD40mAb can bind to one OVA antigen and vice versa. This could lead to the formation of large complexes of conjugate and could be the reason why even though the DBCO-NHS and NHS-PEG4-Azide are very narrowly reactive to each other, conjugates containing more than one antibody conjugated to one antibody/OVA occur. This is the reason why size-exclusion HPLC was utilised to isolate the lowest average MW fraction of the CD40mAb-adjuvanted conjugates.

The HPLC chromatograms of A20-CD40mAb conjugates made by standard and click chemistry methods were analysed first to investigate if there was an apparent difference in protein composition. Both conjugates consisted of products of varying MW (Figure 3.4). HPLC chromatograms of CLICK A20-CD40mAb conjugates showed a distinct peak containing high average MW protein, as well as multiple distinct peaks

containing lower average MW proteins (Figure 3.4A). However the HPLC chromatograms of the Standard conjugate only showed two distinct peaks (Figure 3.4B), a high average MW peak that was observed at 5 minutes that tapered off considerably until the peak at 8.4 minutes emerged. This latter peak possibly contained the unconjugated antibody. The former possibly contained very high average A20-CD40mAb conjugate complexes.

In vitro similarity of the Standard A20-CD40mAb conjugates to Fraction 1 (very high average MW protein) and Fraction 4 (mainly unconjugated antibody) demonstrated by ELISA, was consistent with the fact that the Standard conjugates consisted of predominantly high average MW fractions and unconjugated antibody (Figures 3.6 and Figure 3.7). Both Fraction 1 and Standard conjugate showed a low OD signal in both sandwich ELISAs. This could be due to the extensive cross-linking of the conjugates that possibly mask CD40mAb antigen-binding sites or OVA epitopes important for binding ELISA antibodies. Fractions 2 and 3 (of decreasing average MW) and unfractionated CLICK A20-CD40mAb, all showed high conjugate purity, possibly meaning that binding to ELISA antibodies was not hindered by the presence of aggregates (Figure 3.6 and 3.7). The ability of the CD40mAb in all conjugates, to bind to full-length membrane bound CD40 receptor *in vitro* was confirmed by flow cytometry on CD40L929 cells (Figure 3.8).

The anti-Id response to the A20-CD40mAb conjugates produced by the immunised mice was assessed. All immunised groups of mice produced detectable levels of anti-A20 specific antibodies after boost (Figure 3.11) indicating that all the A20-CD40mAb conjugates were immunogenic. The anti-Id antibody responses to the Standard A20-CD40mAb unfractionated conjugate were comparable to previous studies (Carlring et al., 2012). With great interest to this study, only sera from mice immunised with Fraction 3 (low average MW conjugate vaccine) showed a significantly enhanced anti-A20 antibody titre (Figure 3.11) compared to the unfractionated Standard conjugate, demonstrating that a low MW conjugate enhances vaccine immunogenicity.

A specific anti-Id antibody response was found to be absolutely essential to confer protection against tumour in a B cell leukemia/lymphoma murine model (Cesco-Gaspere et al., 2005), and boosting the anti-Id response *in vivo* positively correlated

with tumour protection (Cesco-Gaspere et al., 2008). Furthermore, a follow-up study 10 years after follicular lymphoma patients were Id-vaccinated showed that the specific anti-Id antibody response also correlated with overall survival. In fact, the overall survival was 90% in patients with anti-Id responses and 69% in patients without anti-id responses (Ai et al., 2009).

The Standard A20-CD40mAb conjugate immunised mice subsequently challenged with A20 tumour cells showed significantly enhanced median and overall survival compared to the control group (Figure 3.12). Intriguingly, amongst the CLICK unfractionated conjugate and fractions, Fraction 3 (low average MW conjugate vaccine) showed the highest median survival of immunised mice compared to the Standard vaccine immunised mice. This trend was however not significant possibly because more than just 10 mice were required to reach statistical significance. However, this is very promising, and does support the hypothesis that the vaccine efficacy of heterogeneous conjugates is inferior compared to more defined conjugates. Moreover, the tumour burden in mice immunised with Fraction 3 and CLICK unfractionated conjugates but not with Fraction 1 was significantly less than that of the Standard conjugate immunised mice (Figure 3.13). The Fraction 3 immunised group also demonstrated the slowest tumour onset. It is noteworthy that Fraction 3 also produced highest anti-Id titres, and in accordance to other studies (Cesco-Gaspere et al., 2005, Cesco-Gaspere et al., 2008, Ai et al., 2009) it was also the vaccine that induced the best tumour protection. This is very interesting as it confirms that conjugation strategy plays an important role in the speed of tumour progression.

Different studies have demonstrated that prophylactic immunisation of mice delays tumour onset and progression, or completely protects against the tumours (Soares et al., 2001, Timmerman et al., 2001, Armstrong et al., 2002). In accordance to our study, different vaccine compositions and formulations containing the same tumour antigen showed different degrees of tumour rejection. For example the use of idiotype-encoding recombinant adenoviral vectors (Armstrong et al., 2002), as opposed to the idiotype-encoding plasmid vaccine encoding the idiotypic gene (King et al., 1998) were found to be more efficient at inducing tumour protection in syngeneic A20 lymphoma murine model. Another study showed that immunisation

with tumour antigen co-administered with either the cytokine GM-CSF or the oil in water emulsion containing QS-21 and MPL prior to tumour challenge did not stop tumour development. In contrast, immunisation with tumour antigen pulsed DCs resulted in 90% tumour rejection (Soares et al., 2001).

A previous study in our laboratory showed that $CD8^+$ T cell depletion but not $CD4^+$ T cell depletion two days prior to tumour challenge significantly reduced median and overall survival of A20-CD40mAb immunised mice (Carlring et al., 2012). While the reduction of vaccine anti-tumour efficacy by CD8 depletion would point towards a role for CTL responses in controlling tumour growth, these were not directly measured in the previous study. To help determine the mode of action of CD40mAb-adjuvanted conjugates (investigated in Chapters 4 and 5) and to simplify assessment of CTL responses (investigated in Chapter 5), we moved to an OVA antigen model. To ensure that the OVA model produced consistent results with the A20-CD40mAb conjugates, the immunogenicity of OVA-CD40mAb conjugates made by the two different conjugation strategies was evaluated. The HPLC chromatogram of CLICK OVA-CD40mAb conjugates protein composition showed the same trend as the CLICK A20-CD40mAb conjugates (Figure 3.15A). Standard OVA-CD40mAb conjugate contained less high average MW protein (Fraction 1) than Standard A20-CD40mAb conjugates, but more unconjugated antibody and unconjugated OVA (Figure 3.15B). *In vitro* analysis of the OVA-CD40mAb conjugates and fractions showed the same trend as A20-CD40mAb conjugates and fractions (Figures 3.16, 3.17, 3.18), and confirmed the presence of OVA-CD40mAb conjugates.

An *in vivo* investigation of the immunogenicity of Standard OVA-CD40mAb, CLICK OVA-CD40mAb, Fraction 3 (low average MW conjugate vaccine) and Fraction 1 (high average MW conjugate vaccine) conjugates in a murine model revealed that anti-OVA specific antibody responses were generated by each of the immunised groups (apart from the control group). The primary responses against OVA produced by unfractionated CLICK conjugate, Fraction 1 and Fraction 3 immunised mice were significantly higher that produced by the unfractionated Standard conjugate immunised mice (Figure 3.21). This shows that the CD40mAb-antigen conjugate vaccines made by click chemistry are superior to the ones made by standard methods. However, it is noteworthy that the anti-OVA antibody end-point titre in

response Standard conjugate immunisation was lower compared to previous studies conducted in our laboratory (Barr et al., 2003).

Conclusion

Click chemistry is a promising conjugation strategy that should be exploited further in the field of vaccine development and design. CD40mAb-antigen conjugates produced by click chemistry were more immunogenic than those made by standard methods.

This technology lead us to the production of a more defined, low average MW conjugate vaccine which was superior to Standard conjugate vaccines in a murine B cell lymphoma setting. This supports our hypothesis that the potential of CD40mAb as an adjuvant in conjugate vaccines is maximised when used in more defined, low average MW conjugates, leading to enhanced vaccine efficacy.

CHAPTER 4

AN INVESTIGATION INTO WHICH APCS ARE INSTRUMENTAL IN THE MODE OF ACTION OF CD40MAB CONJUGATES AS ADJUVANTS LEADING TO $CD4^+$ T CELL RESPONSES

4.1. Introduction

Adjuvants have been classed into (i) immunostimulatory components, which have a direct effect on certain receptors of the innate immune system for example TLRs, (ii) delivery systems, which deliver the antigen of interest leading to enhanced antigen presentation to the immune system for example liposomes or (iii) adjuvant systems that include a combination of both (i) and (ii) (Reed et al., 2013).

Due to its agonistic properties CD40mAb, is thought to work by ligation of the CD40 receptor on APCs, much like the extensively studied CD40-CD154 interaction between APCs and activated T cells (as explained in detail in Chapter 1, *see* Section 1.1.7). Chemical conjugation of antigen to CD40mAb also enhances the likelihood that the antigen will be co-delivered to the very same APC that receive CD40 receptor stimulation. Furthermore, CD40 is expressed on all APCs. Therefore, CD40mAb-adjuvanted vaccines, which contain antigen chemically conjugated to the CD40mAb, have the potential to work as both immunostimulatory components and as delivery systems to B cells, DCs or macrophages. The immunostimulatory and antigen delivery properties of CD40mAb-adjuvanted vaccines to APCs were investigated further to better understand the mode of action of the CD40mAb as an adjuvant.

It has been demonstrated that CD40mAb conjugated to a lymphoma antigen can be taken up by B cells, DCs and macrophages following short term culture with murine splenocytes *in vitro* (Carlring et al., 2012). Significant upregulation of the co-stimulatory molecules on B cells showed that they had become activated, however this was not the case for DCs and macrophages. The percentage of $CD11c^+$ DCs in the spleen is very low (14%) (Duriancik and Hoag, 2009), and consists of a heterogeneous population of DC subsets, specialised for different functions (*see* Section 1.1.2.1.). We therefore wanted to investigate whether a more homogeneous immature population of DCs could become activated in this experimental setting using OVA as a model antigen conjugated to CD40mAb (referred to as OVA-CD40mAb). This is why we optimised a technique to generate immature DCs from murine bone marrow cells. Furthermore, as the spleen contains a diversity of

professional APCs, B cells were purified to allow focussing experiments specifically on a B cell population, without contamination of other APCs.

To investigate the effect of OVA-CD40mAb conjugate on antigen presentation to antigen-specific $CD4^+$ T cells the DO11.10 T hybridoma cell line was used. This hybridoma is ideal as it is OVA-specific and expresses CD4. DO11.10 T hybridoma cells are co-stimulation independent and recognise the immunodominant $CD4^+$ T cell epitope $OVA_{323-339,}$ having the protein sequence ISQAVHAAHAEINEAGR (which will be referred to as ISQ) presented on the MHC class II of the $H\text{-}2^d$ haplotype ($I\text{-}A^d$) (Shimonkevitz et al., 1984). In addition, the activation status of the DO11.10 T hybridoma cells can be measured by their capacity to produce IL-2. An increase in IL-2 levels is an indication of DO11.10 T hybridoma cell activation.

CD40mAb (rat IgG2a) administered alone as an adjuvant enhanced $CD4^+$ T cell response *ex vivo* to its own rat Fc portion (Carlring et al., 2004). SCID mice transferred with $CD4^+$ T cells from CD40 immunised mice and $B220^+$ cells from IgG2a mAb control immunised mice, displayed an enhanced serum anti-IgG2a antibody titre after immunisation with IgG2a. This response that was not observed in SCID mice transferred with $B220^+$ cells from CD40 immunized mice and $CD4^+$ T cells from IgG2a immunised mice (Carlring et al., 2004). The former studies are building blocks to understanding if CD40mAb-adjuvanted conjugates have a role in enhancing $CD4^+$ T cell responses, but only show that CD40mAb administered alone enhances $CD4^+$ T cell proliferation to itself. Therefore other studies were conducted to investigate whether a $CD4^+$ T cell response is required or enhanced as part of vaccine-mediated immunity against the conjugated antigen. CD40mAb conjugated to lymphoma antigen vaccine used in a lymphoma murine model required both $CD4^+$ and $CD8^+$ T cell responses to achieve maximum efficacy *in vivo* (Carlring et al., 2012). Furthermore, CD40mAb conjugated to antigen also enhances lymphocyte proliferation in response to the antigen *ex vivo* (Hatzifoti and Heath, 2007) however, in this study a $CD4^+$ marker was not used and the proliferating cells were assumed to be $CD4^+$ T cells. Therefore, finally, in this chapter the effect of CD40mAb conjugated to antigen on specifically $CD4^+$ T cell responses *ex vivo* was reviewed.

4.2. The effect of OVA-CD40mAb conjugates on antigen-presentation to DO11.10 T hybridoma cells

4.2.1. Isolation and generation of APCs

4.2.1.1. Generation of bone marrow dendritic cells

The technique used to generate DCs from murine C57Bl/6 and BALB/c bone marrow cell populations was based on other studies (Lutz et al., 1999, Lutz et al., 2002, Galea-Lauri et al., 2004). In these studies granulocyte macrophage-colony stimulating factor (GM-CSF) and IL-4 were the growth factors used to drive the bone marrow progenitors to produce immature dendritic cells (BM-DC). IL-4 is particularly important as a growth factor, as it has been shown to prevent or reduce the neutrophil and macrophage contamination (Galea-Lauri et al., 2004).

BM-DCs were analysed for the expression of the phenotypic murine DC marker CD11c as well as Gr-1 expression and F4-80 expression (to exclude neutrophil and macrophage contamination respectively) by flow cytometry (*see* Section 2.2.6.3.2.). Immature DCs were characterised in other studies by high expression of CD11c and low expression of adhesive and co-stimulatory molecules including CD40, CD86 and CD83 (Lutz et al., 1999, Son et al., 2002).

Ten-day old semi-adherent and non-adherent BM-DC generated by this protocol (*see* Section 2.2.6.3.) yielded 2 x 10^7 (+/- 1 x 10^7) cells from a starting cell number of 2 x 10^7 cells (n=5). The BM-DCs demonstrated more than 85% CD11c expression (n=5) (Figure 4.1). This is comparable to the percentage purity obtained in other studies, in which 70% was taken as the acceptable lowest expression level (Lutz et al., 1999, Galea-Lauri et al., 2004, Creusot et al., 2009, Han et al., 2010). The expression levels of F4-80 (macrophage marker) were less than 10% (n=4) (Figure 4.1), and are comparable to BM-DCs generated by other studies (Lutz et al., 1999). The expression levels of Gr-1 (an early myeloid/granulocyte marker) were less than 13% (n=4) (Figure 4.1). These characteristics are also consistent with other studies (Son et al., 2002, Galea-Lauri et al., 2004) suggesting that the BM-DC population generated using this protocol is of myeloid origin, especially since it has been shown that the

depletion of progenitors of T and B cells is not a requirement for the generation of myeloid DCs (Galea-Lauri et al., 2004). Myeloid BM-DCs are ideal especially for the purpose of this chapter as they are better at the generation of antigen-specific T–cell responses compared to lymphoid DCs (Banchereau and Steinman, 1998).

To demonstrate that the cell population generated by this protocol was immature, and thus capable of antigen sampling, the level of CD40 expression on BM-DC before and after LPS-induced maturation was determined (*see* Section 2.2.6.3.1.). As can be observed in Figure 4.2 on day 10, BM-DCs had low CD40 expression (<10%, n=3). This expression increased to 36-44% after 48-hour stimulation with 1µg/ml LPS (n=3) (Figure 4.2), in conformity to other studies (Lutz et al., 1999, Son et al., 2002). This adds to the information that the BM-DCs generated by this protocol were immature and therefore had the best potential for antigen-uptake.

Activation of BM-DCs by LPS stimulation is not only observed via upregulation of adhesion and co-stimulatory molecules of DC but also via morphological changes, including the production of veiled cells (Granucci et al., 1999, Lutz et al., 1999, Verdijk et al., 2004). Brightfield microscopy of DCs at day 12 after 48-hour LPS stimulation and at day 8 (no stimulation) was carried out to observe the contrast in appearance (Figure 4.3). The DCs morphology changes from round cells with limited projections to the characteristic LPS-induced 'large veils' or cytoplasmic sheet-like processes when mature. These cytoplasmic projections are important for DC-T cell interactions and these can be clearly observed under the 40X magnification (Figure 4.3B). This phenotype is consistent with BM-DC cultures that are grown in the presence of IL-4 (Wells et al., 2005).

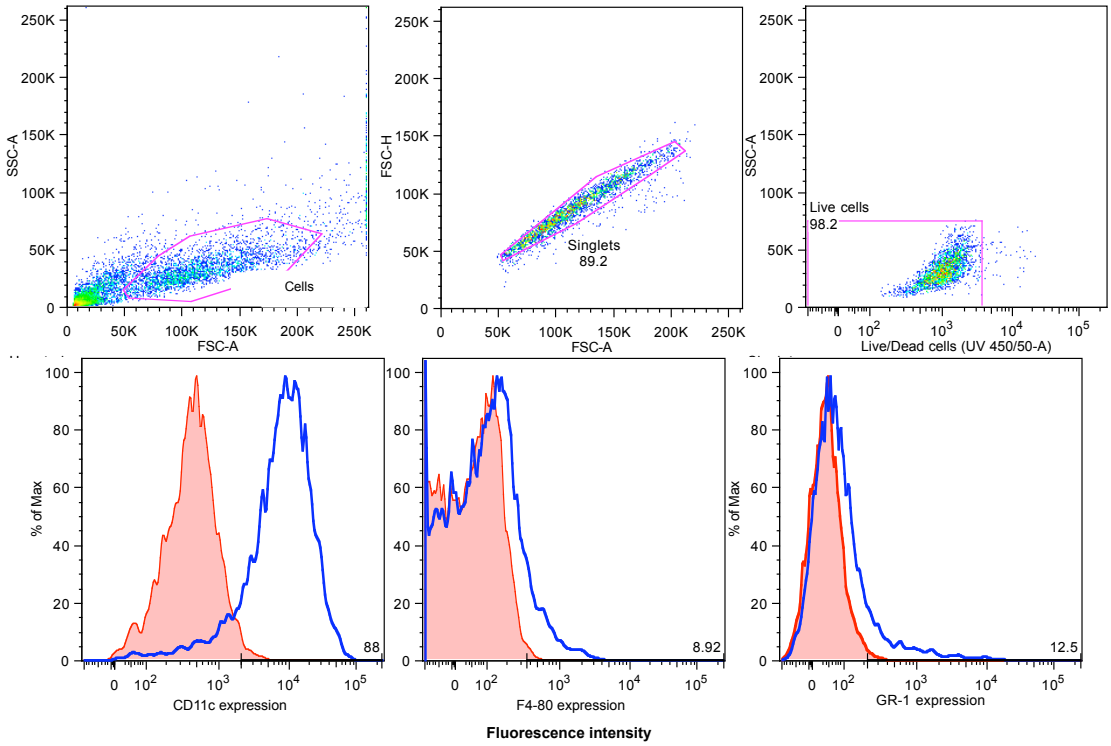

Figure 4.1. Dendritic cell population generated after 10 days in culture from C57Bl/6 bone marrow cells. A. The gating strategy excluded debris and doublets, with subsequent gating on live cells based on UV live/dead staining (UV 450/50). Representative histogram plots of CD11c expression, F4-80 expression and Gr-1 expression (blue peaks), as well as live cells only stained with live/dead discrimination dye (red solid peak) are shown.

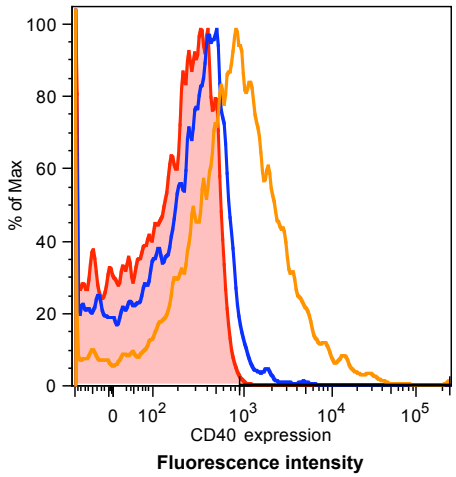

Figure 4.2. CD40 expression as determined by flow cytometry at day 10 of culture and after stimulation with LPS for 48 hours. Histogram plot of CD40 expression on BM-DCs at day 10 of culture (blue peak) and after LPS stimulation (orange peak), as well as live cells only stained with live/dead discrimination dye (red solid peak) are shown.

A.

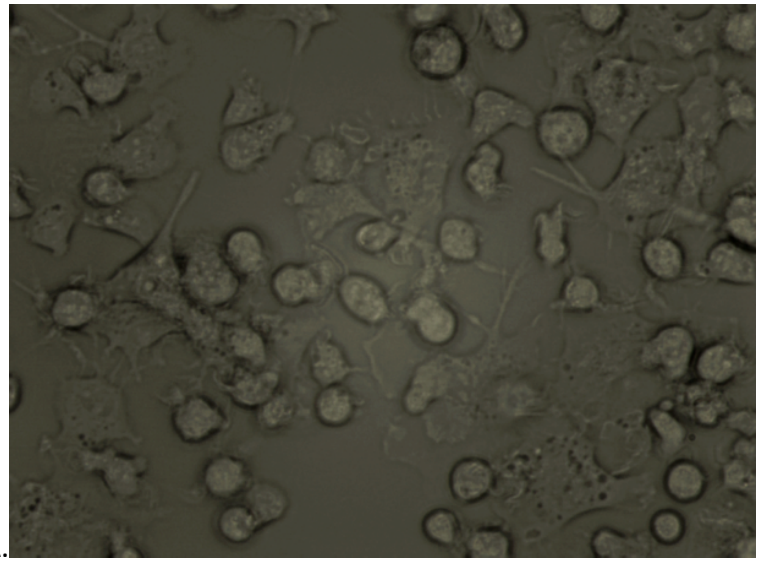

B.

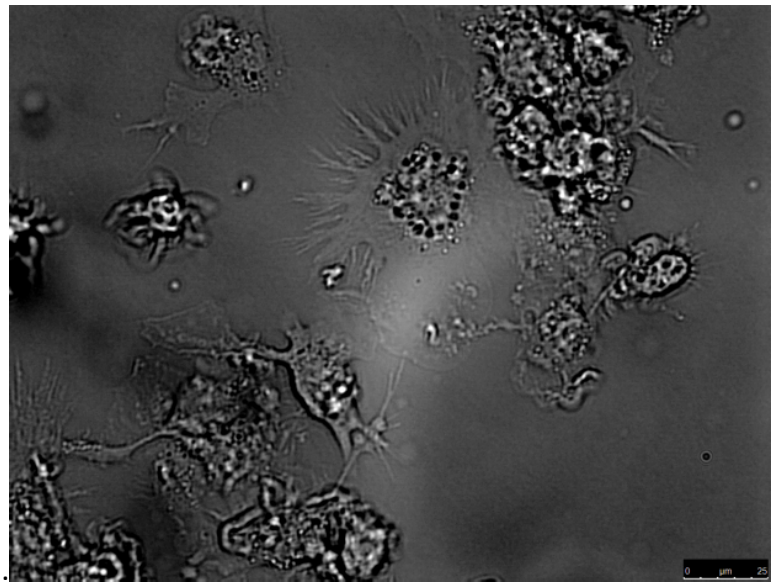

Figure 4.3. Brightfield micrographs illustrating the immature BM-DC phenotype at day 8 (A) and the mature BM-DC phenotype at day 12 after 48 hour LPS stimulation (B). Scale bar = 25µM.

4.2.1.2. Isolation of splenic B cells by positive selection

B cells were isolated from the spleens of C57Bl/6 or BALB/c mice. B cell isolation was performed using magnetic cell sorting, via positive selection (*see* Section 2.2.6.5.1.). This procedure produced a cell yield of 2 x 10^6 (+/- 0.5 x 10^6) CD19-labelled cells from a starting cell number of 2 x 10^7 spleen cells (n=5). CD19 staining before and after sorting was carried out by flow cytometry using PE-labelled CD19 antibody. The percentage $CD19^+$ B cells post-sort was consistently >95% (n=5) (Figure 4.4).

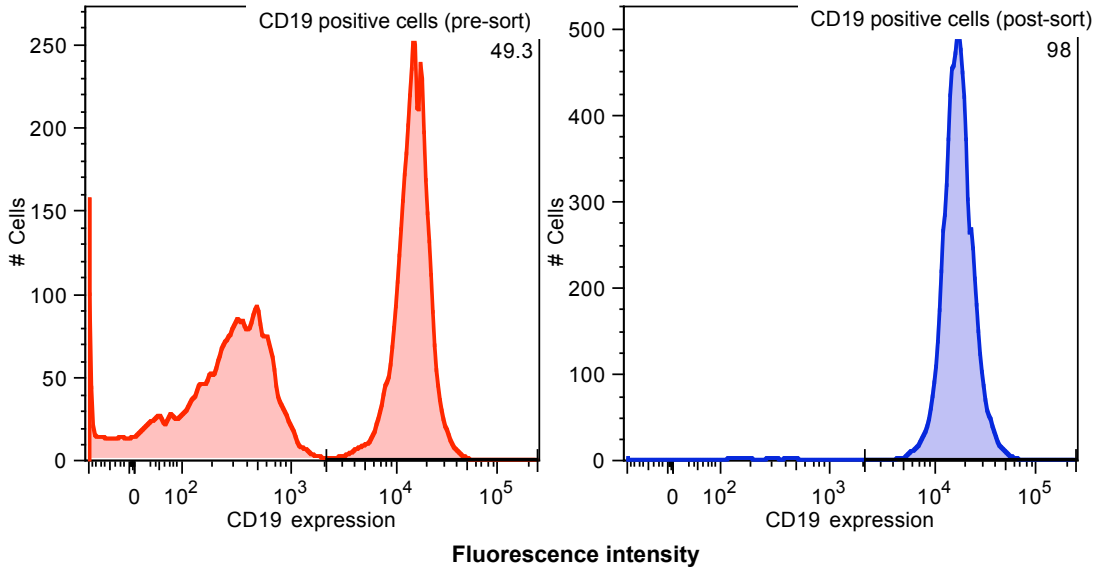

Figure 4.4. B cells labelled with CD19 PE before (red) and after (blue) positive magnetic sorting.

4.2.2. Generation of the DO11.10 T hybridoma cell clone most sensitive to the OVA peptide

It became evident during this study that the DO11.10 hybridoma $CD4^+$ T cell line was unstable and lost sensitivity to the ISQ peptide presented by the APCs with each passage in cell culture. This was concluded from the decreasing IL-2 levels produced by the DO11.10 T hybridoma cells measured by ELISA.

The $CD4^+$ DO11.10 T hybridoma cells were therefore re-cloned by limiting dilution (*see* Section 2.2.6.2.1.) in order to identify the cell clones that were most sensitive to the ISQ peptide. Eleven clones were tested for responsiveness to the ISQ peptide (Figure 4.5) (*see* Section 2.2.5.3.). The concentration of IL-2 secreted into the supernatant by each clone was determined by ELISA (*see* Section 2.2.6.8.1.). Clone G4 produced the highest amount of IL-2 (3000pg/ml) on stimulation with ISQ peptide (Figure 4.5). This level of IL-2 production is comparable to other studies using a similar technique (Son et al., 2002, Cycon et al., 2009).

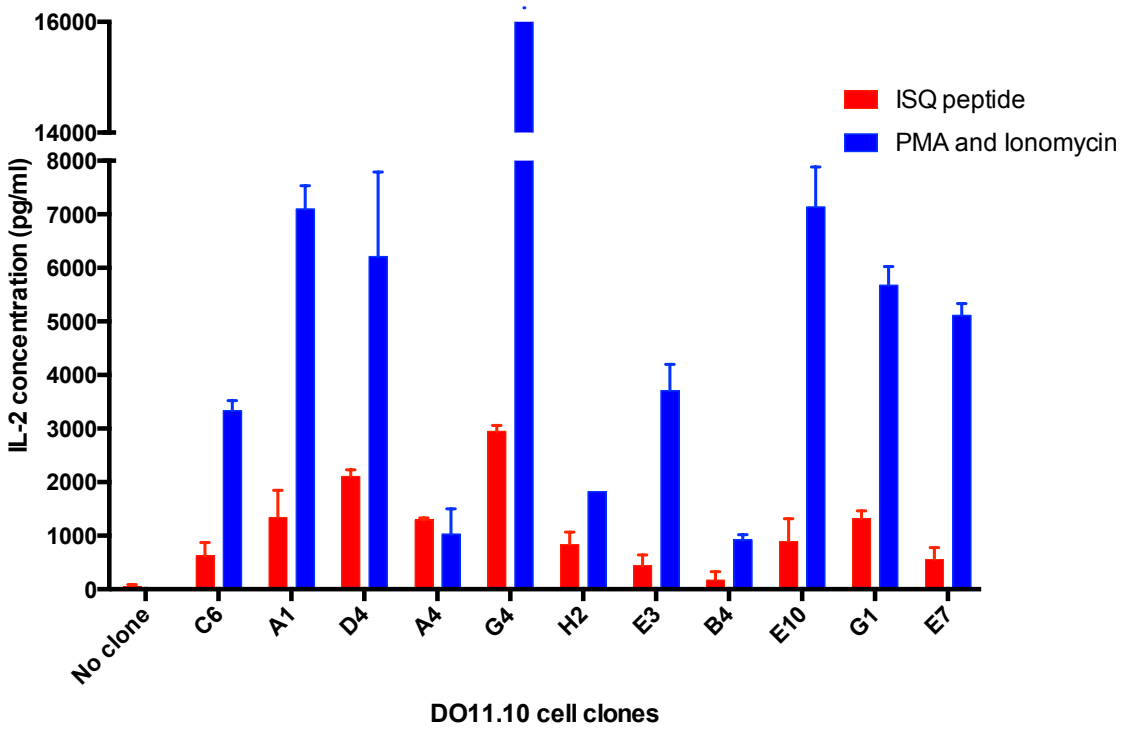

Figure 4.5. Levels of IL-2 secreted into the supernatant by activated DO11.10 T hybridoma cell clones. The DO11.10 T hybridoma cell clones produced by limiting dilution were stimulated specifically via C57Bl/6 splenocytes pulsed with 2µg/ml (1µM) ISQ peptide (red bars) and non-specifically with 50ng/ml PMA (0.1µM) and Ionomycin (1µM) (blue bars) for 48 hours. No clone refers to splenocytes pulsed with ISQ peptide without co-culture with DO11.10 T hybridoma cells, and served as a negative control.

4.2.3. Optimisation of the co-culture of APCs with DO11.10 T hybridoma cells

To determine whether the OVA-CD40mAb conjugate enhances APC antigen presentation to $CD4^+$ T cells compared to the isotype OVA-mAb control conjugate (OVA-20C2mAb), clone G4 was co-cultured with BM-DCs and B cells in the absence or presence of stimuli *in vitro*.

For the purpose of optimisation of this co-culture system only the Standard OVA-mAb conjugates were used. The starting concentration for the Standard OVA-CD40mAb conjugate and Standard OVA-20C2mAb conjugate stimulants was 10µg/ml. B cells or BM-DCs (10^4) were co-cultured with 10^5 DO11.10 T hybridoma cells in a 96 well plate (200µl volume) for 48 hours and IL-2 secreted into supernatant was measured by ELISA (*see* Section 2.2.6.8.1.). Stimulation of BM-DCs and B cells with Standard OVA-CD40mAb conjugates at 10µg/ml did not activate the DO11.10 T hybridoma cells to produce detectable IL-2 levels (Figure 4.6A and B). In fact the IL-2 concentration in the supernatants was not higher than the negative controls. This could be attributed to the fact that too low a concentration of conjugate was used, and not enough ISQ-peptide from the OVA antigen in the conjugate was presented on the APC surface to activate the DO11.10 T hybridoma cells.

The positive controls showed that the DO11.10 T hybridoma cells were responding optimally, and producing detectable IL-2 levels in the supernatant. DO11.10 T hybridoma cells co-cultured with B cells pulsed with ISQ peptide and CD40mAb produced a considerably lower IL-2 concentration in the supernatant (3000pg/ml) after 48 hour culture (Figure 4.6B) compared to co-culture with BM-DC pulsed with the same stimuli (Figure 4.6A) and the positive control (8000pg/ml).

Due to these results, splenocytes and BM-DCs were used for subsequent experiments to focus on identifying primarily which is the lowest concentration of OVA antigen required to activate the DO11.10 T hybridoma cells to produce detectable levels of IL-2 in co-culture with APCs.

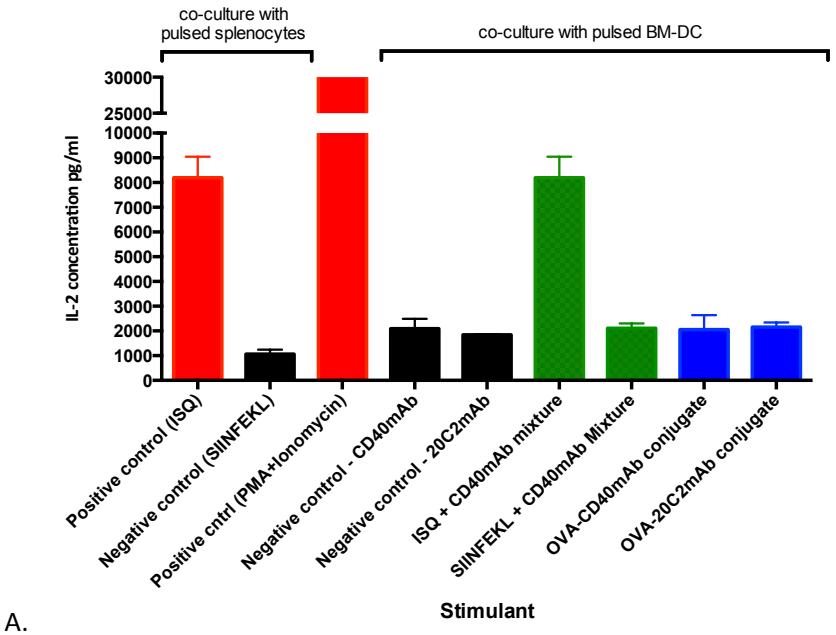

A.

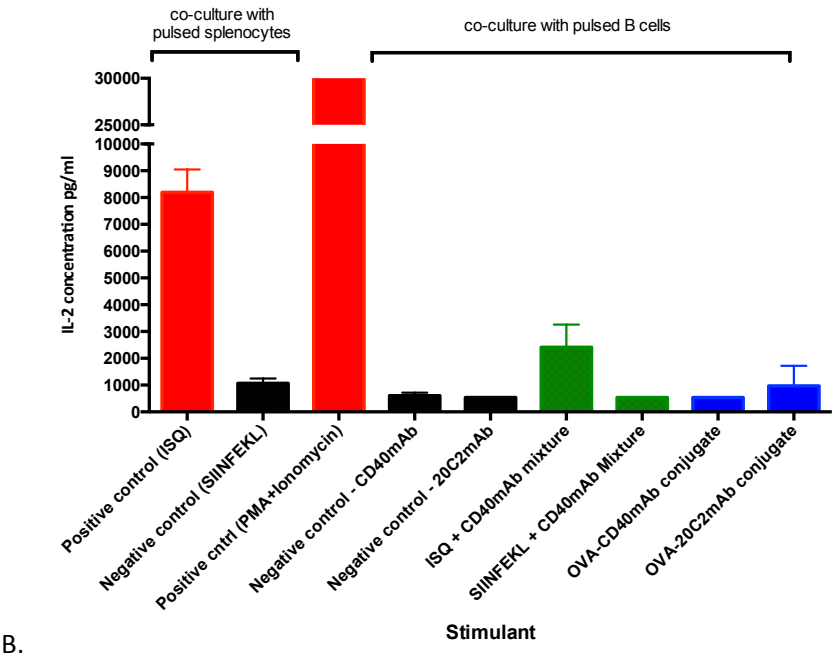

B.

Figure 4.6. Co-culture of BM-DCs (A) or B cells (B) isolated from C57Bl/6 mice with DO11.10 T hybridoma cells. Splenocytes were stimulated with 2µg/ml (1µM) ISQ peptide or 50ng/ml PMA (0.1µM) and Ionomycin (1µM) and the ability of the DO11.10 T hybridoma cells to produce IL-2 on co-culture was shown (red bars - labelled Positive control). Negative controls included stimulation of BM-DC (A) or B cells (B) with 10µg/ml of CD40mAb antibody only, 20C2 isotype control mAb only, as well as 2µg/ml (2µM) of irrelevant (SIINFEKL) peptide (black bars – labelled as Negative control). APCs were stimulated with CD40mAb (10µg/ml) and SIINFEKL or ISQ (2µg/ml) peptide mixture (green bars). APCs were also stimulated with 10µg/ml of Standard OVA-mAb conjugates (blue bars). This figure represents one experiment. Technical replicate = 3.

4.2.3.1. DO11.10 T hybridoma cell response to ISQ peptide on I-A^d versus I-A^b backgrounds

In spite of the fact that the DO11.10 T hybridoma cells were cultured at a concentration of $< 5 \times 10^5$ cells/ml (following the advice given by Professor Philippa Marrack, Kappler Marrack Research Laboratory, Denver) subsequent co-cultures using the DO11.10 T hybridoma clone G4 were unsuccessful as the IL-2 concentration produced by the DO11.10 T hybridoma cell clone when stimulated with splenocytes-pulsed with ISQ peptide was below ELISA baseline levels. A new DO11.10 T hybridoma cell line was obtained (with thanks to Kappler/Marrack Research Laboratory, Denver), and used in subsequent experiments.

The CD4$^+$ DO11.10 T cells were originally generated by immunisation with OVA protein to prime BALB/c mice (Marrack et al., 1983). However, it has been shown that DO11.10 T cells respond to the ISQ peptide from both I-A^d (BALB/c) and I-A^b (C57BL/6) backgrounds (Robertson et al., 2000a). To ensure that the lack of IL-2 production was not due to the MHC class II background, splenocytes obtained from C57Bl/6 and BALB/c mice were pulsed with ISQ peptide and compared to unstimulated controls (Figure 4.7). The results showed that these DO11.10 T hybridoma cells only respond to splenocytes pulsed with ISQ peptide from an I-A^d (BALB/c) background ($p<0.0001$, two-way ANOVA using Sidak's multiple comparisons post-test). Due to these results splenocytes and BM-DCs harvested from BALB/c mice were used in subsequent studies.

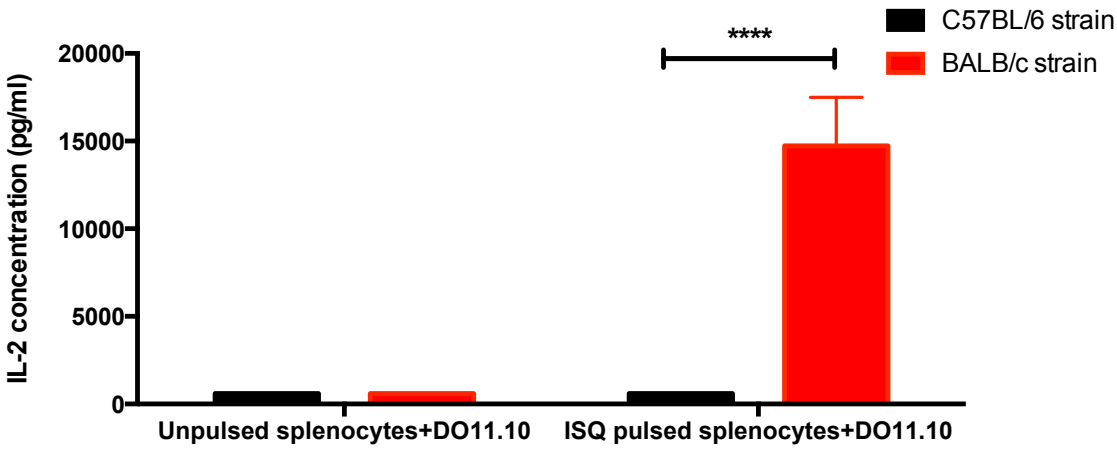

Figure 4.7. New DO11.10 T hybridoma cells tested in co-culture with ISQ-pulsed splenocytes harvested from BALB/c (red bar) and C57Bl/6 mice strains (black bar). Supernatants were collected after 48 hours, and the IL-2 concentration was measured using ELISA. Two-way ANOVA using Sidak's multiple comparisons test (mean +/- SD). ****p<0.0001. This figure represents one experiment. Technical replicate = 3.

4.2.3.2. Dose response of DO11.10 T hybridoma cells to OVA antigen

To identify which concentration of OVA was required to achieve measurable IL-2 levels, splenocytes and DO11.10 T hybridoma cells were co-cultured *in vitro*. The OVA concentrations used in published studies vary, some use OVA concentrations as high as 5000µg/ml, however, 500-1000µg/ml OVA has been used in most similar co-culture systems (Bennett et al., 1992, Mutini et al., 1999, Cycon et al., 2009, Prokopowicz et al., 2010). Based on results from these studies 1000µg/ml of OVA was used as a starting concentration, together with concentrations of 500µg/ml, 250µg/ml, 125µg/ml, 60µg/ml, 30µg/ml and 16µg/ml.

Firstly, the co-culture technique used involved treating 1 x 10^7 BALB/c splenocytes (instead of pure BM-DC or B cells) in 1ml with serial OVA dilutions (starting at 1000µg/ml), or 2µg/ml ISQ peptide for 6 hours in a 24-well plate. Secondly, OVA-pulsed or ISQ-pulsed (used as a positive control) splenocytes (1 x 10^5) were co-cultured with DO11.10 T hybridoma cells (1 x 10^5) in a 96 well plate in a volume of 200µl. Supernatants were collected after 24, 48 and 72 hour incubation, and tested for the presence of IL-2 by ELISA.

Stimulation with ISQ peptide resulted in high levels of IL-2 production by DO11.10 T hybridoma cells at all three time-points (Figure 4.8), indicating that the amount of IL-2 produced in the supernatant is proportional to the time in co-culture. However, no detectable IL-2 levels were produced on co-culture with splenocytes stimulated by OVA concentrations ranging from 1000µg/ml to 16µg/ml (not shown). Similar results were observed when the DO11.10 T hybridoma cells were co-cultured with BM-DC (results not shown). The lack of IL-2 detected could be attributed to the fact that the ELISA used was not sensitive enough i.e. the amount of IL-2 produced by these DO11.10 T hybridoma cell numbers is too low to be detected. The IL-2 ELISA utilised for this work accurately detects concentrations higher than 1000pg/ml.

To address this, the number of cells co-cultured together was increased. T cell:APC cell ratios of 1:6 and 1:10 were used to further improve the sensitivity of the co-culture system. DO11.10 T hybridoma cells were co-cultured with 1 x 10^5 BM-DCs in a cell ratio of 1:6 and 1:10 (respectively), in a volume of 500µl, in a 48 well plate (Figure 4.9). An OVA concentration of 500µg/ml was added directly to the BM-DCs and DO11.10 T hybridoma cells in the 24-well plate. No washing steps were included in this experimental setup. Using higher cell numbers showed a significant increase ($p<0.0001$, Two-way ANOVA using Sidak's multiple comparisons post-test) in the IL-2 concentration compared to the OVA-pulsed BM-DCs only control. Both cell ratios showed significant increase in IL-2 detection in the supernatant. In subsequent experiments, higher cell numbers were used at a cell ratio of 1:6 (DO11.10 T hybridoma cells:BM-DC).

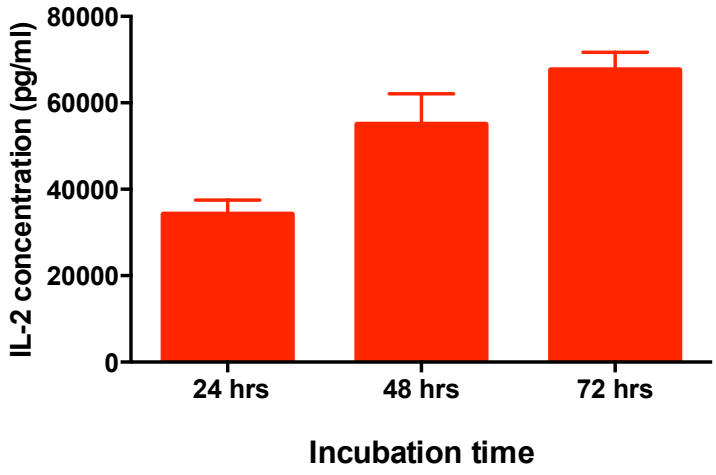

Figure 4.8. Co-culture of DO11.10 T hybridoma cells with ISQ-pulsed splenocytes for 24, 48 and 72 hours. This figure represents one experiment. Technical replicate = 3.

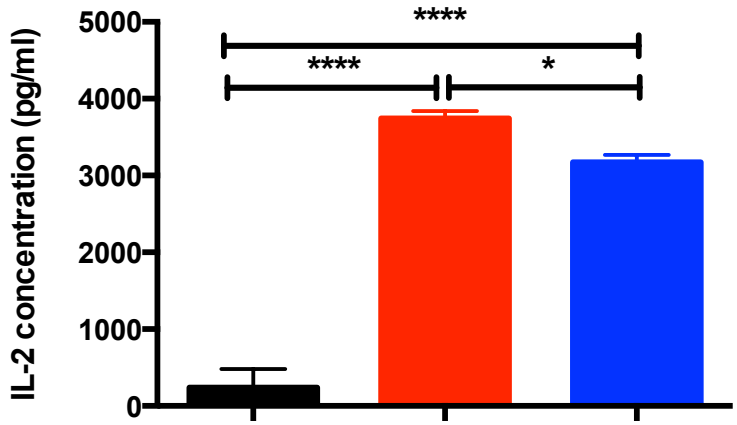

1 x 10^5 BM-DC	+	+	+
OVA antigen (500µg/ml)	+	+	+
6 x 10^5 DO11.10 T cells	-	+	-
1 x 10^6 DO11.10 T cells	-	-	+

Figure 4.9. BM-DCs co-cultured with DO11.10 T hybridoma cells at different cell ratios in a 500µl volume (48-well plate), using 500µg/ml OVA as a stimulant for 48 hours. BM-DCs (10^5) stimulated with 500µg/ml OVA without co-culture with DO11.10 T hybridoma cells (black bar-negative control), co-culture with 6 x 10^5 DO11.10 T hybridoma cells (red bar) and co-culture with 1 x 10^6 DO11.10 T hybridoma cells (blue bar) is shown. Supernatants were collected after 48 hours, and the IL-2 concentration was measured using ELISA. One-way ANOVA using Tukey's multiple comparison test (mean +/- SD) was used to determine statistical significance. *p<0.05, ****p<0.0001. This figure represents one experiment from a total of 2 individual experiments. Technical replicate = 3.

4.2.4. Dose-dependent effect of CD40mAb on the antigen presentation of BM-DCs to DO11.10 T hybridoma cells

To test the effect of the CD40mAb on the BM-DC antigen-presentation to T cells, the co-culture experiment was repeated using BM-DC stimulated with a mixture of OVA and antibody (either CD40mAb or 20C2mAb) in a 1:1 weight ratio. This was performed since Standard OVA-mAb conjugates were conjugated using a 1:1 weight ratio.

A starting concentration of 250µg/ml OVA antigen mixed with 250µg/ml CD40mAb or 20C2mAb was used to stimulate BM-DCs. OVA antigen and CD40mAb or 20C2 isotype antibody mixtures of 100µg/ml (each) and 50µg/ml (each) were also used to see if the use of CD40mAb causes increased antigen-presentation to DO11.10 T hybridoma cells resulting in production of a higher concentration of IL-2 in the supernatant compared to the 20C2mAb or OVA antigen alone.

Detectable levels of IL-2 were only measured when OVA antigen and mAb mixtures were used at a concentration of 250µg/ml (Figure 4.10). The addition of CD40mAb did not enhance antigen presentation of BM-DC to T cells compared to both the OVA antigen alone as well as the 20C2mAb. Due to these results, the OVA-CD40mAb conjugates were not tested in this co-culture system, and experiments focusing on the effect of the CD40mAb-adjuvanted conjugates on the APC co-stimulatory molecule expression *in vitro* and the induction of $CD4^+$ T cell responses *in vivo*, were conducted.

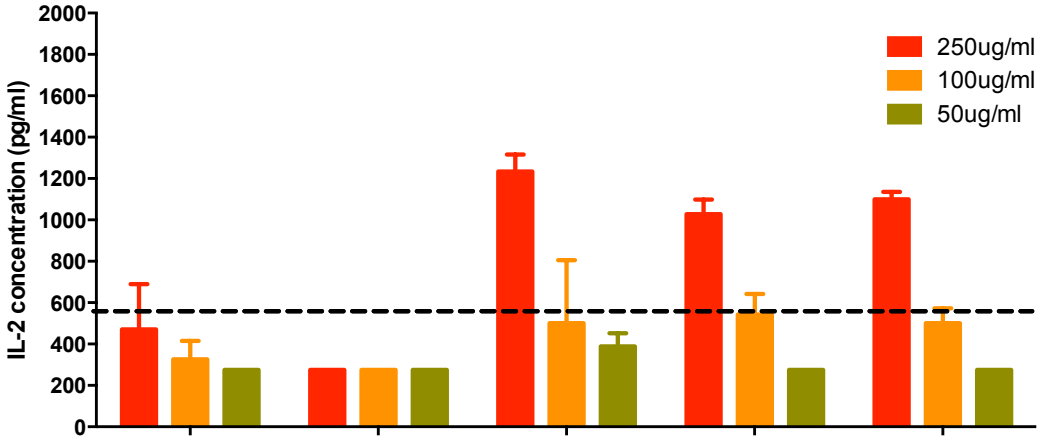

DO11.10	+	-	+	+	+
BM-DC	-	+	+	+	+
OVA	+	+	+	+	+
CD40mAb	-	-	-	+	-
20C2mAb	-	-	-	-	+

Figure 4.10. The effect of CD40mAb on the BM-DC antigen-presentation to DO11.10 T hybridoma cells. 1 x 10^5 BM-DCs were co-cultured with 6 x 10^5 DO11.10 T hybridoma cells in a 500µl volume (48-well plate), using different concentrations of OVA antigen and CD40mAb or 20C2mAb mixtures. Supernatants were collected after 48 hours, and the IL-2 concentration was measured using ELISA. Negative controls included stimulation of either DO11.10 T hybridoma cells or BM-DC only with OVA antigen, as well as the co-culture of DO11.10 T hybridoma cells and BM-DC with no stimulation. This figure represents one experiment. Technical replicate = 3. Dotted line represents lowest detectable ELISA concentration for this experiment.

4.3. Investigation of the adjuvant effect of CD40mAb conjugated to OVA *in vitro* and *in vivo*

4.3.1. Characterisation of the CLICK and Standard OVA-CD40mAb conjugates in vitro

OVA-CD40mAb conjugates made using the standard method gave a lower antibody response against OVA (*see* Section 3.3.3.) compared to a previous study (Barr et al., 2003). The aforementioned study used Imject™ maleimide-activated OVA rather than OVA (Sigma) that had been Sulfo-SMCC treated in the laboratory. To investigate whether anti-OVA antibody responses could be improved upon, CD40mAb (clone 1C10) or isotype control antibody (GL117mAb) were conjugated to OVA antigen by click chemistry (using OVA from Sigma, that will be referred to as sOVA) (*see* Section 2.2.1.7.) or the standard method (using Imject™ maleimide-activated OVA from Thermo Scientific, OVA) (*see* Section 2.2.1.3.). The sOVA antigen was used as a control for immunisation, *ex vivo* proliferation and *in vitro* APC activation experiments.

The conjugation of CD40mAb or GL117mAb (rat IgG2a) to OVA antigen was confirmed by sandwich ELISA (*see* Section 2.2.4.3.1.). Rat IgG was captured with an anti-rat IgG antibody and the conjugation of rat IgG to OVA was confirmed by simultaneous binding to rabbit (IgG) anti-OVA antibody followed by peroxidase conjugated goat anti-rabbit IgG. An increase in optical density (OD) by the OVA-CD40mAb and OVA-GL117mAb conjugates, compared to unconjugated OVA and mAbs (negative controls) confirmed that the OVA antigen was conjugated to the mAb (Figure 4.11A). The CLICK sOVA-mAb conjugates contain higher conjugate purity than the Standard OVA-mAb conjugates. In fact, the CLICK sOVA-CD40mAb conjugate bound the ELISA antibodies at a concentration 5-fold lower than the Standard OVA-CD40mAb conjugate (Figure 4.11B). Flow cytometry analysis using CD40L929 cells (*see* Section 2.2.4.4.1.) showed that CD40mAb of the OVA-mAb conjugates made by both methods, were still able to bind to full-length membrane-bound CD40 expressed *in vitro* after conjugation (results not shown).

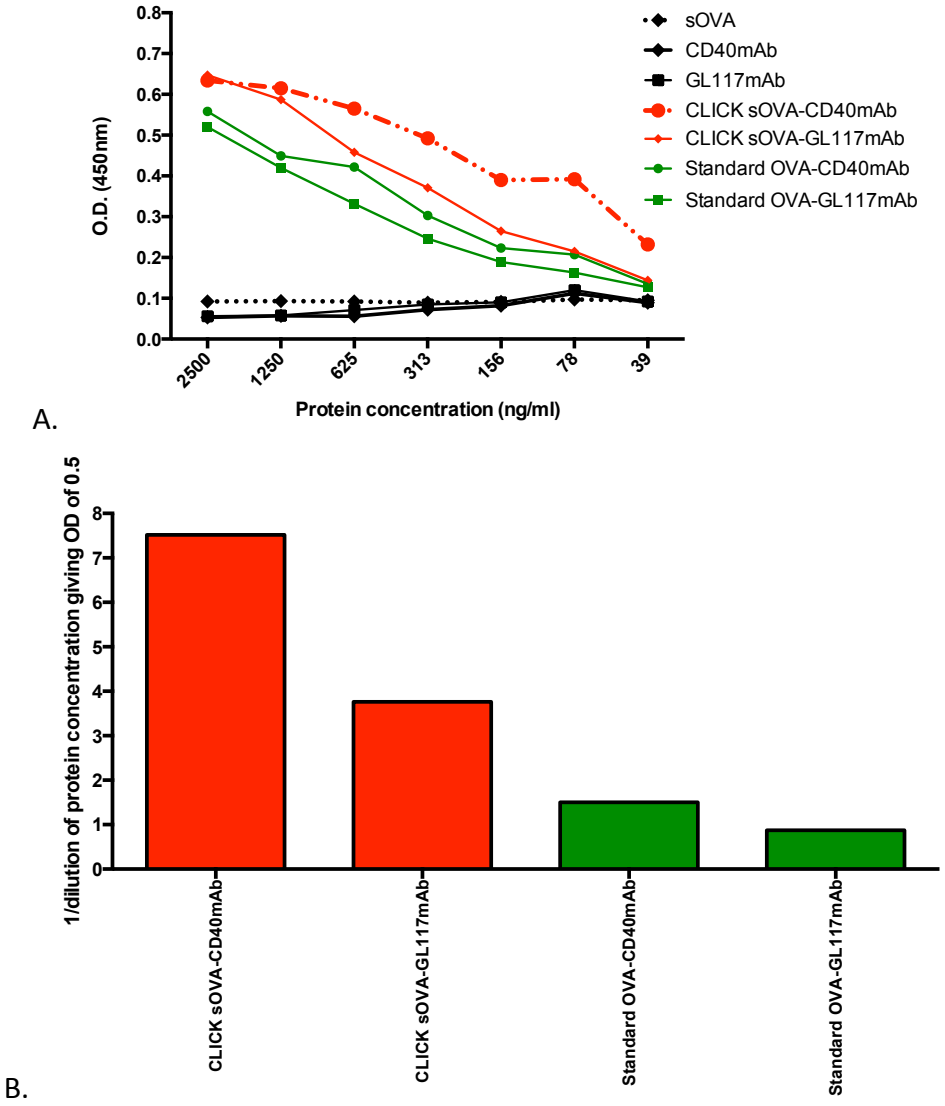

Figure 4.11. Confirmation of OVA to Rat IgG conjugation using sandwich ELISA. The sOVA antigen, CD40mAb and GL117mAb were used as negative controls. (A) Relative binding of CLICK and Standard OVA-mAb conjugates. (B) Comparison of the interpolated 1/dilution of the OVA-mAb conjugate concentration giving an OD of 0.5. The dilution corresponding to 1/1 is 2500ng/ml (starting concentration). **GL117mAb – isotype control antibody*

4.3.2. Effects of OVA-CD40mAb conjugates on APC co-stimulatory molecule expression

The expression of the co-stimulatory molecule CD86 on B cells and splenic $CD11c^+$ DCs was investigated following incubation of splenocytes with 10µg/ml conjugates and sOVA, as well as 200ng/ml LPS (Figure 4.12). The experiment was repeated using BM-DCs to investigate whether the results were consistent upon the use of a more homogenous immature population of DCs (Figure 4.13). Both the Standard and CLICK conjugates were investigated. LPS, a well-characterised PAMP (*see* Section 1.1.1, Table 1.1.) that activates the immune system via TLRs, was used as a positive control. The fold increase in median fluorescence intensity of CD86 expression on $CD19^+$ and $CD11c^+$ cells above the unstimulated control was investigated by flow cytometry (*see* Section 2.2.6.6.).

With regards to splenic B cells (Figure 4.12A), the results were consistent with previous studies (Carlring et al., 2012). CD86 expression levels were significantly enhanced ($p<0.0001$, unpaired, two-tailed Student t test, Figure 4.12B) by both the Standard and CLICK sOVA-CD40mAb conjugates compared to the corresponding OVA-GL117mAb conjugates.

In the case of splenic $CD11c^+$ DCs, both Standard and CLICK OVA-CD40mAb conjugates significantly enhanced upregulation of CD86 expression ($p<0.05$, two-tailed, unpaired Student's t test) (Figure 4.12B).

Interestingly, only the CLICK sOVA-CD40mAb conjugate significantly enhanced the BM-DC CD86 expression compared to the sOVA-GL117mAb conjugate ($p<0.0001$, unpaired, two-tailed Student t test, Figure 4.13). There was no significant difference between the CD86 expression of BM-DC stimulated by the Standard OVA-CD40mAb or Standard OVA-GL117mAb conjugates.

On a closer look at the results, stimulation with sOVA alone increased the CD86, however this was not significantly different to either of the conjugates (unpaired, two-tailed Student t test). LPS did not seem to have an effect on splenic $CD19^+$ and $CD11c^+$ DC CD86 expression (Figure 4.12A and B). However, LPS enhanced co-

stimulatory molecule expression on BM-DCs, demonstrating an immature population (Figure 4.13).

In summary, both Standard and CLICK OVA-CD40mAb conjugates markedly enhance B cell CD86 expression compared to the isotype antibody controls. Experiments carried out using DCs, however, show conflicting results.

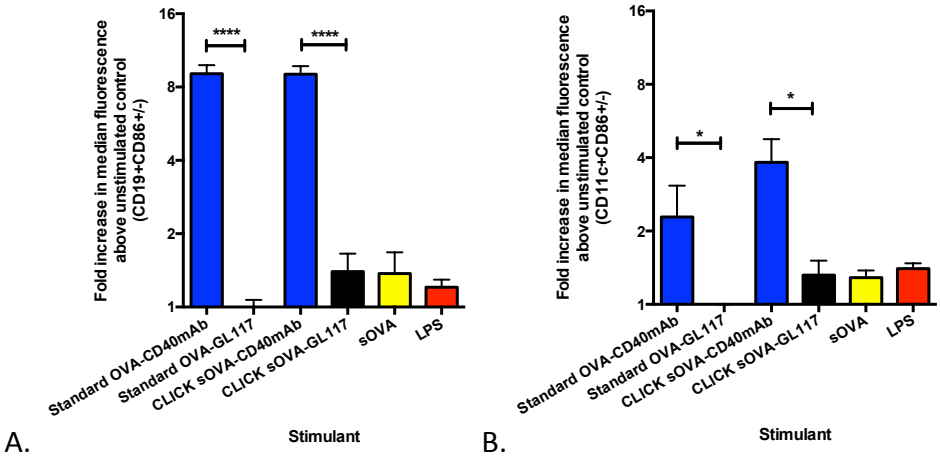

Figure 4.12. The effect of OVA-mAb conjugates on the CD86 expression on splenic B cells and DCs. Splenocytes (1 x 10^6 cells/ml) were incubated in the presence of stimulant; 10µg/ml Standard OVA-mAb conjugates, 10µg/ml CLICK OVA-mAb conjugates, 10µg/ml OVA, 200ng/ml LPS, as well as in the absence of stimulant for 24 hours in a 48-well plate (1ml). The fold increase in median fluorescence intensity above the unstimulated control of CD86 expression on $CD19^+$ cells (A) and $CD11c^+$ cells (B) is shown. A two-tailed, unpaired Student's t-test (mean +/- SD). *p<0.05, ****p<0.0001. This figure represents results from three separate experiments. Technical replicates = 1.

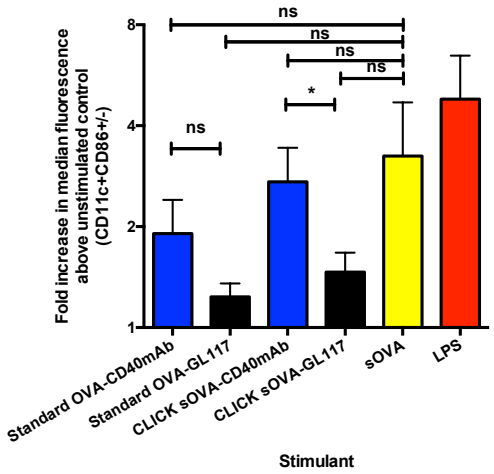

Figure 4.13. The effect of OVA-mAb conjugates on the CD86 expression of BM-DCs. BM-DC (1 x 10^6 cells/ml) were incubated in the presence of stimulant; 10µg/ml Standard OVA-antibody conjugates, 10µg/ml CLICK OVA-antibody conjugates, 10µg/ml sOVA, 200ng/ml LPS, as well as in the absence of stimulant for 24 hours in a 48-well plate (1ml). The fold increase in median fluorescence intensity above the unstimulated control of CD86 expression on BM-DCs is shown. A two-tailed, unpaired Student's t-test (mean +/- SD) was used. *p<0.05. ns = not significant. This figure represents results from three separate experiments. Technical replicate = 1.

4.3.3. Investigation of lymphocyte and antibody responses to OVA-CD40mAb conjugates *in vivo*

Since it has been demonstrated that when CD40mAb is conjugated to antigen, the antigen specific antibody titres are approximately a 1000-fold better than when CD40mAb and antigen are inoculated as a mixture (Barr et al., 2003), the mixture and sOVA controls were important to ensure the quality of the conjugates. Antibody and $CD4^+$ T cell responses were investigated *in vivo*. BALB/c mice were immunised on day 0 and were boosted on day 14 (Figure 4.14), with 10µg immunogen via the intraperitoneal route. Control groups included 5µg sOVA and 5µg CD40mAb (Mixture), 5µg sOVA antigen and PBS.

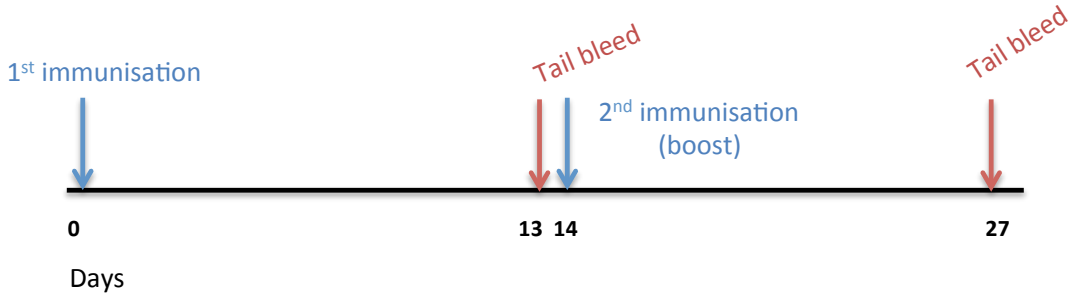

Figure 4.14. Immunisation schedule for OVA-mAb conjugates and controls. BALB/c mice were immunized with CLICK sOVA-CD40mAb conjugate, Standard OVA-CD40mAb and OVA-GL117mAb conjugates, as well as Mixture, sOVA only and PBS. BALB/c mice were boosted on day 14 using the same immunogens. Mice were bled on day 13 and day 27.

4.3.3.1. Investigation of the anti-OVA specific antibody titres in response to immunogen

The anti-OVA specific antibody titre (*see* Section 2.2.7.2.) was assessed alongside the *ex vivo* $CD4^+$ T cell proliferation (*see* Section 2.2.7.3.) experiment. At day 13 (before boost, Figure 4.15A) and day 28 (after boost, Figure 4.15B), the CLICK conjugate, the Mixture and sOVA antigen all induced significantly higher anti-OVA titres, compared to the Standard conjugates ($p<0.0001$, One-way ANOVA using Dunnett's post-test) (Figure 4.15A). However, there was no significant difference between the anti-OVA end-point antibody titres produced by CLICK sOVA-CD40mAb conjugate, the Mixture or the sOVA.

The anti-OVA end-point titres in the sera from Standard OVA-CD40mAb conjugate immunised mice was minimal compared to the titres obtained in previous studies (Barr et al., 2003) as well as the results obtained in Chapter 3, at both before and after boost (Figure 3.21). Furthermore, the anti-OVA antibody titres produced by the Mixture and the sOVA immunised mice were abnormally high. Both results were inconsistent with previous studies (Barr et al., 2003).

In summary, there was no difference between the anti-OVA antibody titres in sera of CLICK OVA-CD40mAb conjugate and the Mixture or sOVA antigen immunised groups. Furthermore, even though the Standard OVA-CD40mAb conjugate was slightly immunogenic after boost, anti-OVA antibody titres are at least 1000-fold lower than shown in published work.

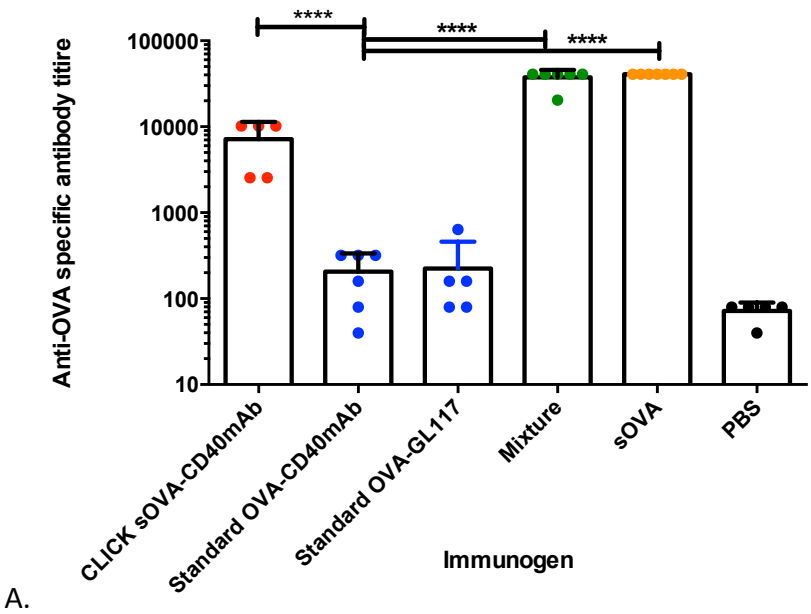

A.

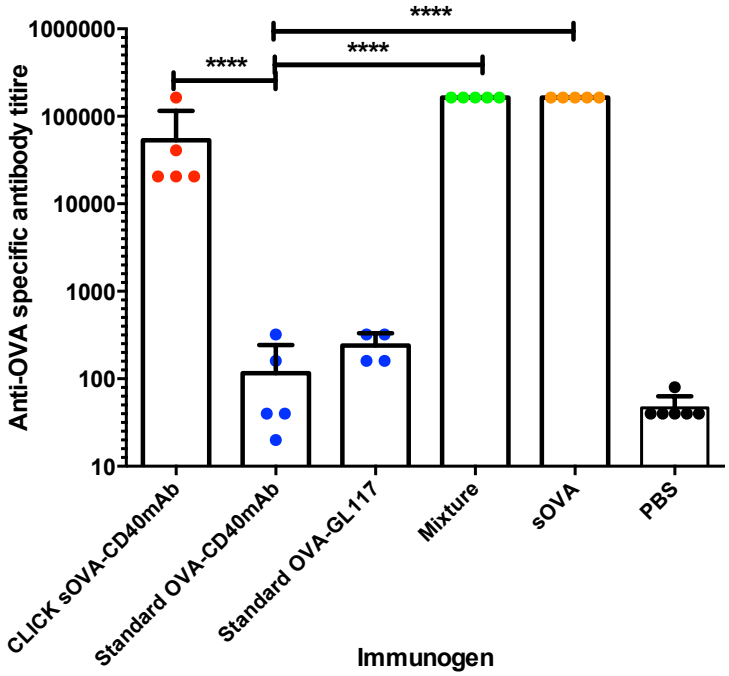

B.

Figure 4.15. Anti-OVA specific antibody end-point titre level at day 13 (before boost) (A) and at day 28 (after boost) (B). Anti-OVA specific antibody levels detected in sera of mice immunised with CLICK conjugate (red), Standard conjugates (blue), Mixture (green), sOVA (orange) and PBS (black). One-way ANOVA with Dunnett's post-test (mean +/- SD) ****p<0.0001. n = ranging from 5 to 7 mice. Each dot represents one mouse.

4.3.3.2. Investigation of lymphocyte proliferation in response to stimulus *ex vivo*

To determine the $CD4^+$ cell proliferation in response to sOVA, splenocytes from each immunised group were labelled with 2µM CFSE (*see* Section 2.2.7.3.3.) and incubated with sOVA antigen or in the absence of antigen for 72 hours. After 72 hours, cells were prepared for flow cytometry. Lymphocytes were stained with PE-Cy7 labelled CD4 antibody to monitor $CD4^+$ T cell proliferation, as well as efluor-450 labelled CD19 antibody to monitor non-specific proliferation. The percentage lymphocytes in the original sample that have divided was recorded.

An optimisation assay was carried out using one BALB/c mice immunised with either Standard OVA-CD40mAb conjugate, Mixture or PBS. Two mice were immunised with sOVA antigen. The five mice were sacrificed at day 13 after immunisation, and the spleens were harvested.

For the purpose of the optimisation assay the concentration of (i) 1000µg/ml and (ii) 500µg/ml of sOVA antigen were used for *ex vivo* stimulation. Surprisingly after 72 hours incubation $CD19^+$ cell proliferation was observed even in mice immunised with PBS (Figure 4.16). This was indicative of non-specific proliferation, which was dose-dependent as there was an increase in proliferation when 1000µg/ml sOVA was used compared to when 500µg/ml sOVA was used.

From the five mice used in this experiment minimal $CD4^+$ T cell proliferation was observed with lymphocytes of one sOVA immunised group, however, no statistical measures could be carried out due to number of mice that were tested, for the purpose of this optimisation assay (Figure 4.17, 4.18). A flow cytometric plot of each sample from each immunisation group is shown in Figure 4.17.

Since B cells from the spleens of the control group (PBS immunised mice) unexpectedly markedly proliferated in response to sOVA antigen, endotoxin contamination was suspected, therefore all the samples were subsequently tested for endotoxin activity.

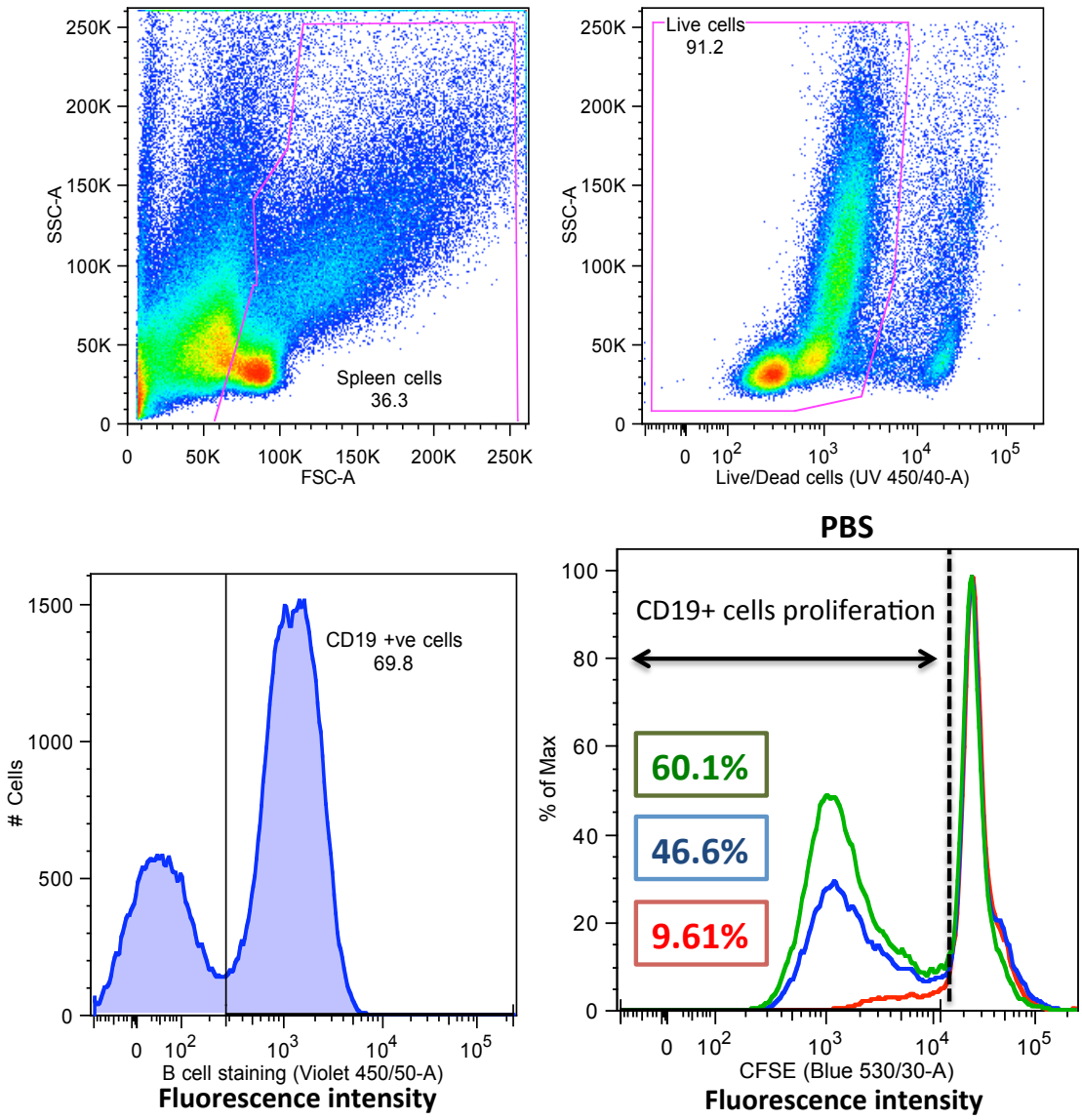

Figure 4.16. The gating strategy used for flow cytometric analysis of B cell proliferation. The gating strategy was designed to exclude debris, include only live cells based on UV live/dead staining (UV 450/50), and gating on cell surface expression marker $CD19^+$ cells. The percentage $CD19^+$cells in the original population of PBS immunised mice that have divided in response to 500µg/ml sOVA (blue) and 1000µg/ml sOVA (green), and in the absence of stimulation (red) is shown as a representative.

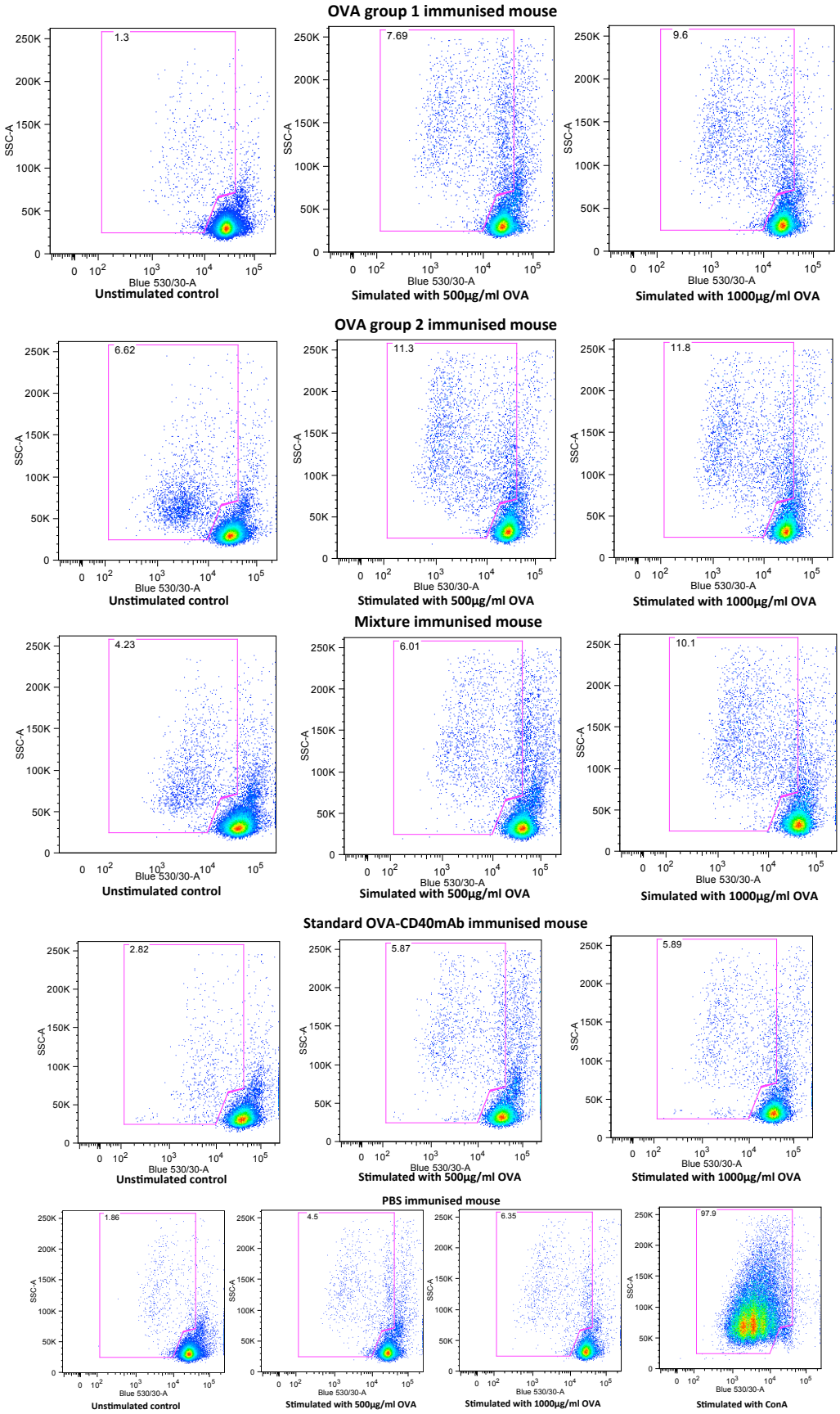

Figure 4.17. The percentage CD4$^+$ cells in the lymphocyte population that have divided in response to no stimulation, 500µg/ml sOVA, 1000µg/ml sOVA or ConA stimulation.

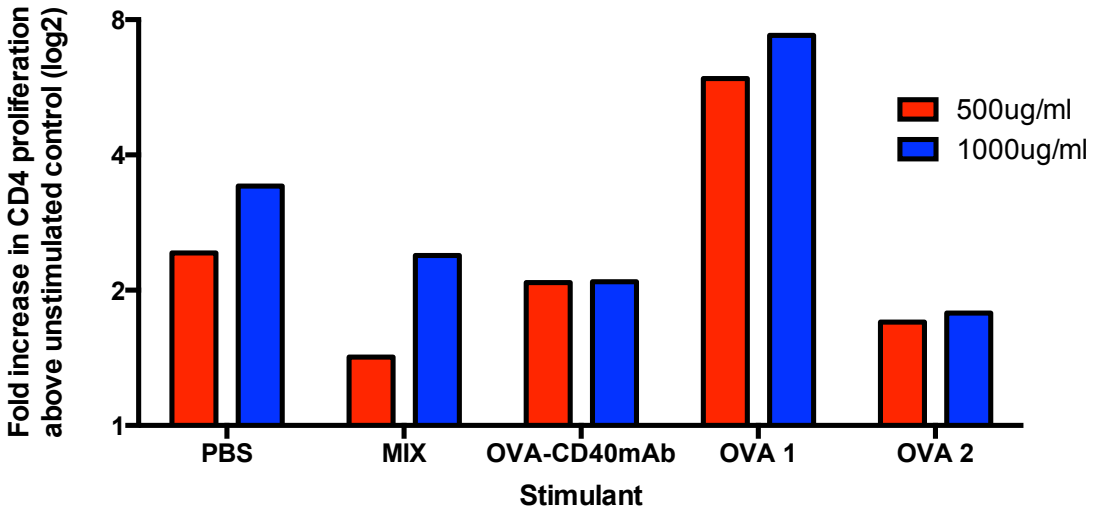

Figure 4.18. CD4$^+$ T cell proliferation on stimulation with 500µg/ml or 1000µg/ml OVA *ex vivo.* Fold percentage increase in CD4 proliferation above the unstimulated control of each group is shown. n= 1 mouse per group.

4.3.4. Determination of endotoxin levels in immunogens

The sOVA used to make CLICK conjugates; (i) enhanced immature BM-DC CD86 molecule expression (Figure 4.13), (ii) induced antibody responses higher than those produced by OVA-CD40mAb conjugates (Figure 4.15) and (iii) induced B cell proliferation *ex vivo* even in PBS immunised groups (Figure 4.16). These results lead us to investigate whether sOVA was contaminated with endotoxin. The levels of endotoxin in the Standard and CLICK conjugates made in Section 4.3.1, together with CD40mAb, GL117mAb and sOVA used for immunisation were quantitated by a Limulus amebocyte lysate assay (QCL-1000^{TM}) (*see* Section 2.8.1). The endotoxin activity present in 1µg of Standard and CLICK conjugates, antibodies and sOVA is shown in Figure 4.19.

Different kinds of LPS are produced by different pathogens, in fact, LPS from different pathogens are capable to generate different forms of immune response *in vivo* (Pulendran et al., 2001). The endotoxin activity measured by the LAL assay varies with the type of LPS standard used, so since the type of endotoxin present in sOVA is unknown, it is very difficult to obtain an accurate measure. A study by Watanabe et al. (2003), found that 3µg/ml commercially available OVA contained 0.5 EU/ml of endotoxic activity. This amount was found enough to fully activate endothelial cells. A very recent study showed that the endotoxin level in four different batches of the same commercial source of OVA used in this study ranged from 7.5ng to 141.5ng per 1µg OVA (Mac Sharry et al., 2014). Studies investigating the immune responses in the presence or absence of LPS (Pulendran et al., 2001, Watanabe et al., 2003, Bal et al., 2011, Abdi et al., 2012), or the mode of action of adjuvants of particularly LPS-based adjuvants (Hartmann et al., 1999, Yoshino et al., 2013) always ensure that controls contain <0.25 EU/ml endotoxin, or are endotoxin-free. All immunogens at a concentration of 50µg/ml, which is the concentration immunised (10µg in 200µl PBS) contained 15-30 EU/ml endotoxin activity, which would be a reason why the high anti-OVA antibody responses and the *ex vivo* non-specific proliferation was observed.

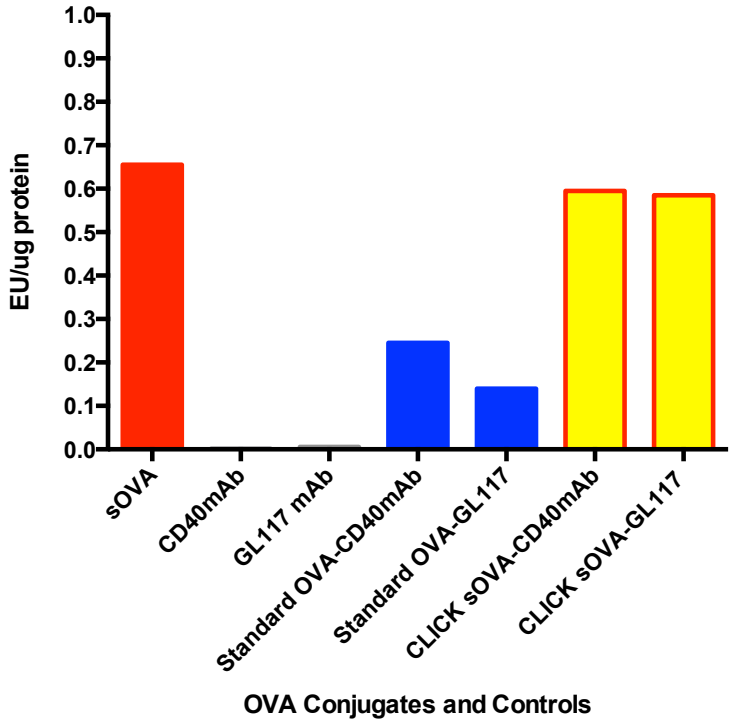

Figure 4.19. Endotoxin activity in 1µg sOVA, unconjugated mAbs and Standard sOVA-mAb conjugates and CLICK sOVA-mAb conjugates.

4.4. Investigation of the effect of ISQC-CD40mAb conjugates *in vitro* and *in vivo*

Due to the disappointing results from the use of OVA conjugates *ex vivo* and *in vivo*, we moved on to using the OVA immunodominant $CD4^+$ T cell epitope $OVA_{323-339}$ or ISQAVHAAHAEINEAGR (ISQ peptide) instead. For the context of this chapter, the use of the $CD4^+$ T cell epitope ISQAVHAAHAEINEAGR would be the ideal way to show what impact the CD40mAb adjuvants have on CD4 T cell responses, as well as B cell and DC activation.

4.4.1. Production and characterisation of ISQC-conjugates *in vitro*

ISQ peptide was synthesised with a cysteine on the C-terminal end (purchased from GeneCust); ISQAVHAAHAEINEAGRC (which will be referred to as ISQC). CD40mAb was treated with Sulfo-SMCC and conjugated to the sulphydryl groups on the cysteine present on the C-terminal end of the peptide (*see* Section 2.2.1.4.).

The peptide was first biotinylated using EZ-Link Sulfo-NHS-Biotin. EZ-Link Sulfo-NHS-Biotin is an NHS-ester that reacts with side-chain of lysines (K) or the amino-terminal (NH_2) group. Since the ISQC peptide does not contain any lysines, biotinylation occurred via the amino-terminal group of the peptide.

Biotinylation was necessary as the conjugation of the ISQC peptide to CD40mAb could not be confirmed by traditional characterisation methods like ELISA or flow cytometry, due to the lack of antibodies that recognise ISQ peptide. The CD40mAb was conjugated to both biotinylated and non-biotinylated ISQC peptide (*see* Section 2.2.1.4.3.). Due to the peptide being biotinylated conjugation of the CD40mAb or GL117mAb to biotinylated ISQC peptide could be confirmed by Western blotting (*see* Section 2.2.4.2.1).

Firstly, peptide biotinylation was confirmed by Western Blotting by the use of horseradish peroxidase (HRP) enzyme conjugated to streptavidin protein. A 15% SDS PAGE gel was run using a 10µg sample of ISQC peptide (1877Da), biotin (443Da) and biotinylated ISQC peptide. Once the streptavidin protein binds to biotin on the peptide, the HRP catalyses the reaction with the substrate that allows for detection

(Figure 4.20). Peptide only and biotin only were also run as controls on the gel, but no band was observed. This could be due to the fact that the Coomassie Blue dye used to stain the gel stains NH_2 groups that are absent on the biotinylation reagent only, and only one is present on the peptide.

After confirming ISQC peptide biotinylation, conjugation of biotinylated ISQC peptide alongside non-biotinylated ISQC peptide to CD40mAb and istoype control mAb was performed.

ISQC peptide has a MW of 1877Da, therefore, since the smallest dialysis membrane available had a pore size of 1000Da, excess biotinylation reagent could not be removed by buffer exchange, without the risk of losing valuable sample. Due to this, precautions had to be taken to ensure that only biotinylated ISQC peptide is conjugated to the mAb and the biotinylation reagent in excess does not. The first precaution was to ensure that the conjugation experiment was performed at least one week after the peptide biotinylation had been performed. The purpose for this was to ensure that the NHS-ester of the biotin reagent is non-reactive and will not also bind to the antibody during biotinylated peptide-antibody conjugation. Another precaution taken included the conjugation of the biotinylation reagent opened and used on the day of peptide biotinylation, to the antibody as a control. Lack of biotin detection by means of HRP-labelled streptavidin on the antibody control confirms that the biotinylation reagent is non-reactive. A quenching buffer was not used to react with all the NHS esters remaining on the surface of the ISQC peptide so that the subsequent conjugation reaction to the mAbs would not be affected.

A reducing 15% SDS page gel was run using a 10µg sample of conjugates and controls. Biotinylated conjugates were detected via Western blot using HRP-labelled Streptavidin (Figure 4.21). Western Blot shows that only the biotinylated ISQC-mAb conjugates were detected by the HRP-labelled streptavidin. No bands were observed in the biotinylated reagent and mAb control. This meant that all the bands observed in lanes 5 and 10 correspond to biotinylated ISQC peptide conjugated to the mAb.

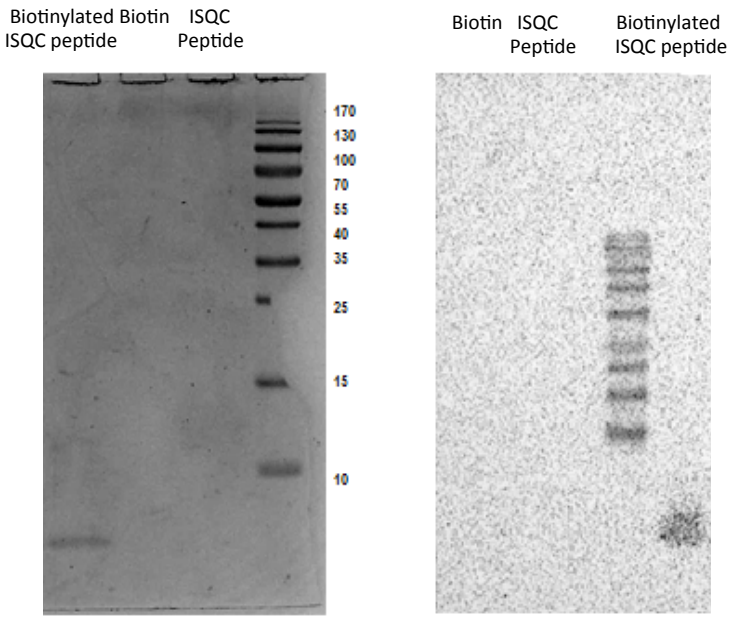

Figure 4.20. Confirmation of biotinylaton of ISQC peptide. 15% SDS page reducing gel is shown on the left. Western Blot using HRP labelled streptavidin to detect is shown on the right.

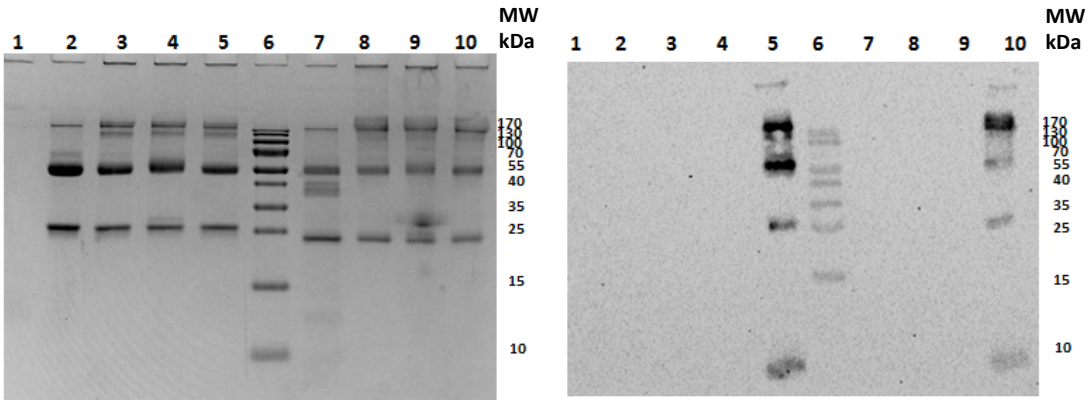

Figure 4.21. Confirmation of conjugation of ISQC peptide to CD40mAb. 15% SDS PAGE reducing gel is shown on the left. Western blot using HRP-labelled streptavidin to detect is shown on the right. Lane 1: ISQC peptide, Lane 2: CD40mAb, Lane 3: CD40mAb treated with biotin reagent control, Lane 4: ISQC-CD40mAb conjugate, Lane 5: Biotinylated ISQC-CD40mAb conjugate, Lane 6: Ladder, Lane 7: GL117mAb, Lane 8: GL117mAb treated with biotin reagent control, Lane 9: ISQC-GL117mAb conjugate, Lane 10: Biotinylated ISQC-GL117mAb conjugate.

Biotinylated ISQC peptide did conjugate to the both CD40mAb and isotype control mAb. Therefore, we assumed that the non-biotinylated ISQC peptide also conjugated to the CD40mAb and isotype control mAb. Only the non-biotinylated ISQC-mAb conjugates were used for the subsequent experiments.

To further ensure that the conjugation was successful 6% and 15% SDS PAGE reducing gels were run at 60V in order to obtain bands of higher definition (Figure 4.22). As observed from the 6% gel, the ISQC-mAb conjugate band running at approximately 150kDa (according to the MW protein standard) is of higher apparent MW than corresponding antibody alone controls (Figure 4.22A). Furthermore, when observing the 15% gel, the bands showing heavy chains and light chains of the antibody of the ISQC-mAb conjugates, are of higher apparent MW than the corresponding antibody controls (Figure 4.22B).

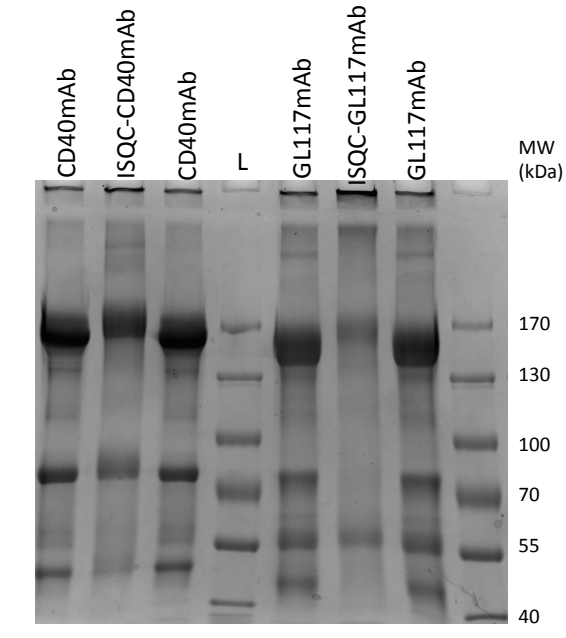

A.

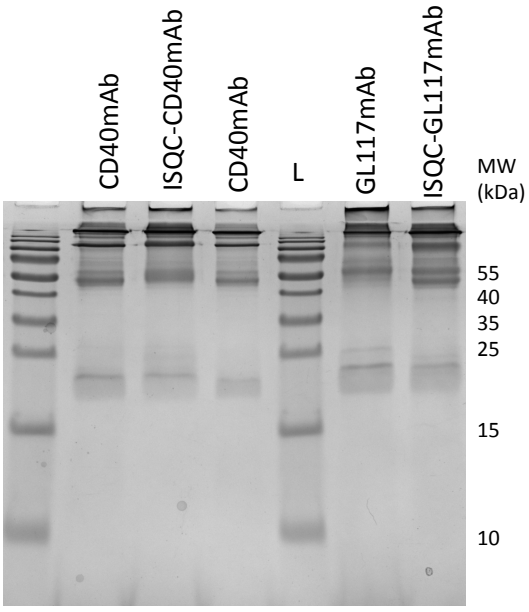

B.

Figure 4.22. Confirmation of conjugation of ISQC peptide to CD40mAb via reducing SDS PAGE. A. 6% SS PAGE reducing gel. B. 15% SDS PAGE reducing gel. L shows the molecular weight protein standard.

4.4.2. Effects of ISQC-CD40mAb conjugates on APC co-stimulatory molecule expression

Splenic B cells, splenic $CD11c^+$ cells as well as BM-DCs were used to evaluate the effect of the ISQC-CD40mAb conjugates on the co-stimulatory molecule expression (*see* Section 2.2.6.6.). The endotoxin activity of these conjugates was tested and found to be <0.01 EU/µg conjugate.

The expression of the co-stimulatory molecules CD80 and CD86 on splenic B cells and $CD11c^+$ DC cells was investigated by incubating with 10µg/ml conjugates, ISQ peptide, which served as a negative control, and 200ng/ml LPS, which served as a positive control (Figure 4.23). The fold increase in median fluorescence intensity above the unstimulated control, of CD80 (Figure 4.23A) and CD86 (Figure 4.23B) expression on $CD19^+$ and $CD11c^+$ cells was determined using flow cytometry. The experiment was repeated using BM-DC to investigate whether the results were consistent upon the use of an immature population of DCs.

Splenic B cell results were consistent with previous studies and the results shown in Section 4.4. Both CD80 and CD86 expression were significantly ($p<0.01$, $p<0.001$, two-tailed, unpaired Student t test) enhanced on stimulation with the ISQC-CD40mAb conjugate compared to the ISQC-GL117mAb conjugate control (Figure 4.23B).

Splenic $CD11c^+$ DC results were also consistent with previous studies, showing that stimulation with ISQC-CD40mAb conjugate did not significantly upregulate CD80 or CD86 expression on splenic DC compared to the controls (Figure 4.23A). Interestingly however, CD80 and CD86 expression were both significantly enhanced ($p<0.05$, $p<0.01$, two-tailed unpaired Student t test) on the immature population of BM-DCs on stimulation with the CD40mAb-adjuvanted conjugate (Figure 4.24). This shows that the CD40mAb-antigen conjugates target and activate both B cells and DCs.

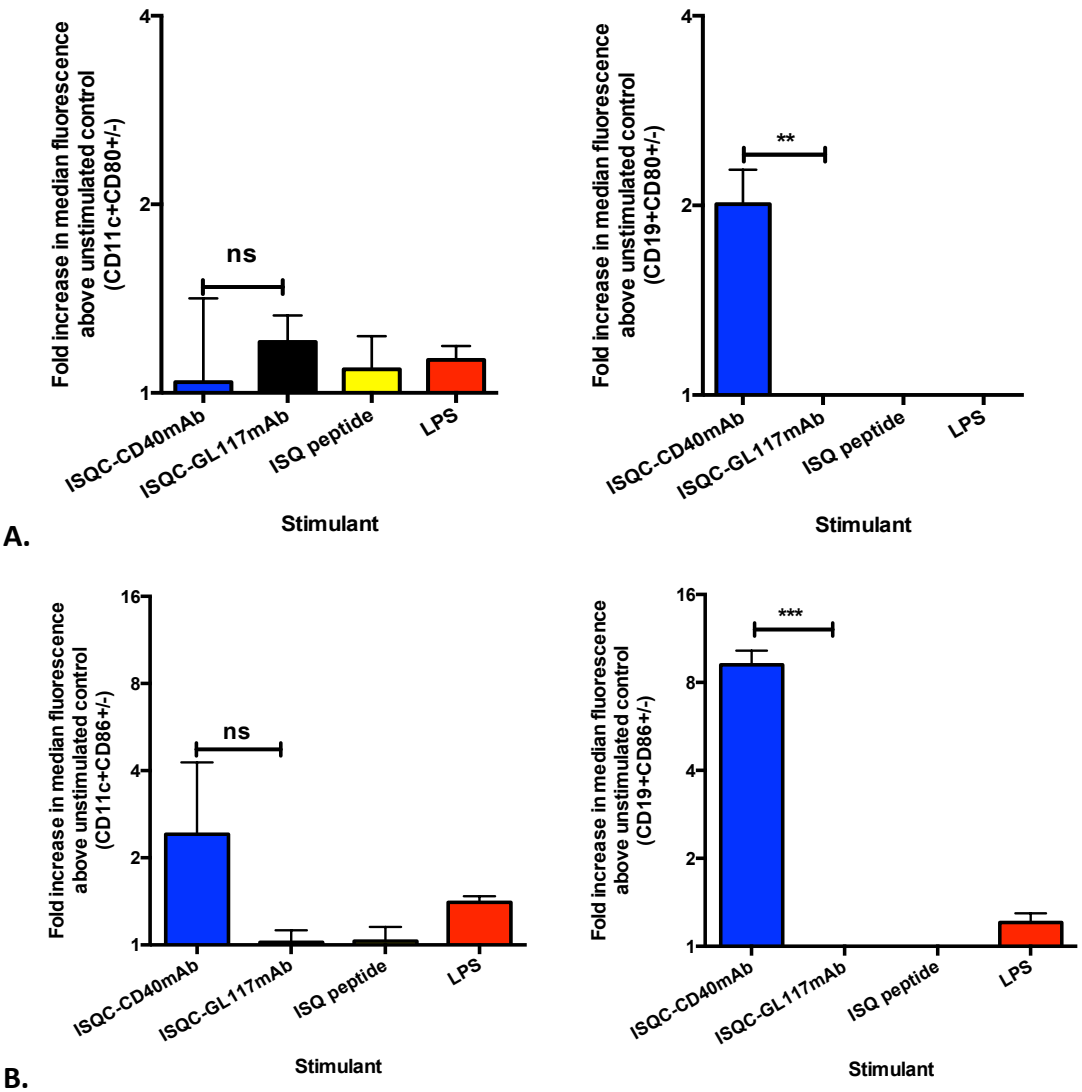

Figure 4.23. The effects of ISQC-antibody conjugates on the CD80 and CD86 expression of splenic B cells and CD11c$^+$ DCs. Splenocytes (1 x 10^6 cells/ml) were incubated in the presence of stimulant; 10µg/ml ISQC-antibody conjugates, 10µg/ml ISQ peptide, 200ng/ml LPS, as well as in the absence of stimulant for 24 hours in a 48-well plate (1ml). A. The fold increase in median fluorescence intensity of the CD80 expression on CD11c$^+$ (left) and CD19$^+$ cells (right), above the unstimulated control of each group is shown. B. The fold increase in median fluorescence intensity of the CD86 expression on CD11c$^+$ (left) and CD19$^+$ cells (right), above the unstimulated control of each group is shown. Two-tailed, unpaired Student's t-test (mean +/- SD) **p<0.01, ***p<0.001, ns = not significant. This figure represents results from three separate experiments. Technical replicate = 1.

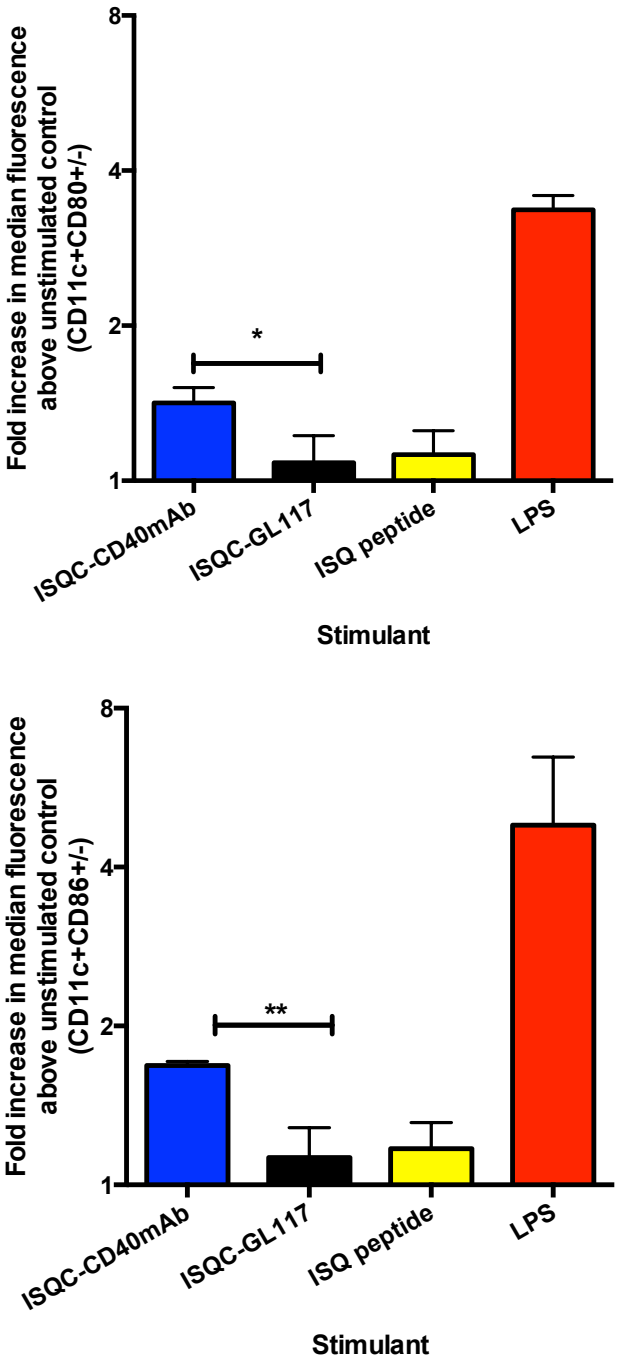

Figure 4.24. The effects of ISQC-antibody conjugates on the CD80 and CD86 expression of BM-DCs. BM-DCs (1 x 10^6 cells/ml) were incubated in the presence of stimulant; 10µg/ml ISQC-antibody conjugates, 10µg/ml ISQ peptide, 200ng/ml LPS, as well as in the absence of stimulant for 24 hours in a 48-well plate (1ml). The fold increase in median fluorescence intensity of CD80 expression (top) and CD86 expression (bottom) on $CD11c^+$ BM-DC, above the unstimulated control of each group is shown. Two-tailed, unpaired Student's t-test (mean +/- SD) *$p<0.05$, **$p<0.01$. This figure represents results from three separate experiments. Technical replicate = 1.

4.4.3. Evaluation of the antibody and lymphocyte responses to ISQC-mAb conjugates *in vivo*

Twenty BALB/c mice were immunised on day 0, and day 15 (Figure 4.25) with 10µg ISQC-CD40mAb conjugate and ISQC-GL117mAb conjugate via the intraperitoneal route. Control groups included; 0.8µg ISQC and 9.2µg CD40mAb (Mixture) and PBS. The Mixture control was used to ensure the quality of the ISQC-CD40mAb vaccine conjugates. Blood was collected and spleens were harvested on day 31 in order to investigate the sera anti-OVA specific antibody titre and $CD4^+$ T cell responses using a lymphocyte proliferation assay (*see* Section 2.2.8).

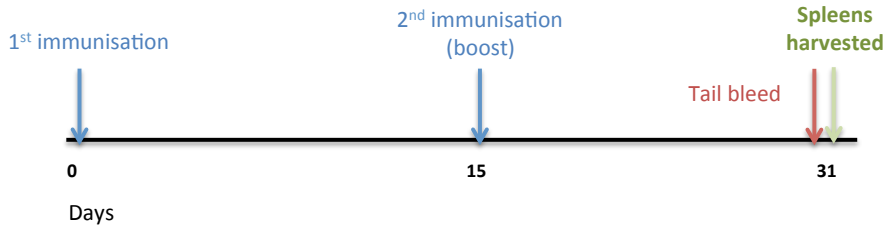

Figure 4.25. Immunisation schedule for ISQC-mAb conjugates. BALB/c mice were immunized with ISQC-CD40mAb conjugate, ISQC-GL117mAb conjugate, Mixture and PBS. BALB/c mice were boosted on day 15 using the same immunogens. Mice were bled on day 31. Spleens were harvested for the *ex vivo* lymphocyte proliferation assay on Day 31.

4.3.3.1. Investigation of the anti-OVA specific antibody titre in response to immunogen

The antibody response against the ISQ peptide was determined by ELISA using OVA protein to coat the plate (*see* Section 2.2.7.3.2.). Mice immunised with ISQC-CD40mAb as well as ISQC-GL117mAb conjugates produced anti-OVA specific antibodies, indicating that they were immunogenic (Figure 4.26). Results showed that mice immunised with ISQC-CD40mAb conjugate produced a significantly higher anti-OVA titre compared to ISQC-GL117mAb, Mixture and PBS immunised groups ($p<0.05$, One-way ANOVA using Sidak's multiple comparisons post-test). This was a very promising result showing conjugation of ISQC peptide to CD40mAb led to a 10-fold and 100-fold enhancement of secondary antibody responses against the peptide relative to the ISQC-GL117mAb conjugate and the Mixture respectively.

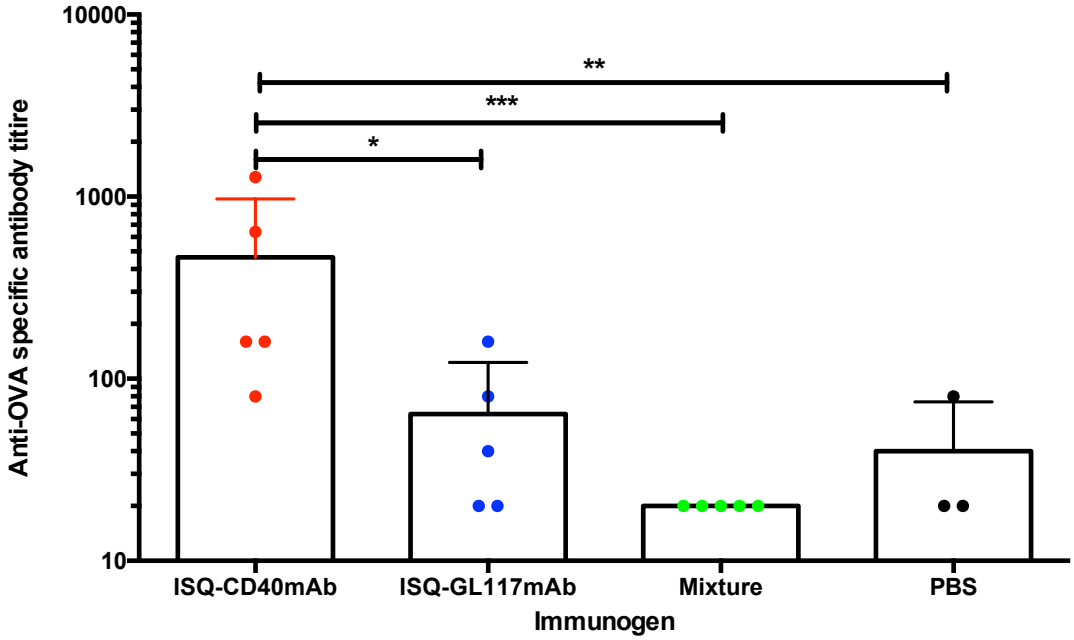

Figure 4.26. Anti-OVA specific antibody end-point titre level at day 31. Anti-OVA specific antibody levels detected in sera of mice immunised with ISQC-CD40mAb conjugate (red), ISQC-GL117 conjugate (blue), Mixture (green) and PBS (black). One-way ANOVA using Sidak's multiple comparisons post-test (mean +/- SD) *p<0.05, **p<0.01, p<0.001. n = 3-5 mice. Each dot represents 1 mouse.

4.3.3.2. Evaluation of lymphocyte proliferation in response to ISQ peptide *ex vivo*

To determine $CD4^+$ cell proliferation in response to ISQ peptide, splenocytes from each immunised group were harvested and labelled with 2µM CFSE (*see* Section 2.2.7.3.3.) and incubated with 1µg/ml ISQ peptide or in the absence of antigen for 72 hours. After 72 hours, each cell group was stained with efluor-450 labelled CD19 antibody and PE-Cy7 labelled CD4 antibody and assessed by flow cytometry (*see* Section 2.2.2.7.4.). The IL-2 concentration in the supernatants was also measured by IL-2 ELISA (see Section 2.2.6.8.1.).

The proliferation of $CD4^+$ cells was investigated by excluding dead cells and debris, gating on $CD4^+$ cells and subsequently the percentage of lymphocytes in the original sample that have divided was recorded (Figure 4.27). $CD19^+$ cell proliferation was assessed to ensure that there was no non-specific proliferation (for the gating strategy of $CD19^+$ cell proliferation *see* Figure 4.16).

There was no $CD4^+$ T cell (Figure 4.29) or $CD19^+$ cell (Figure 4.30) proliferation observed with lymphocytes harvested from ISQC-CD40mAb conjugate, ISQC-GL117mAb conjugate, Mixture or PBS immunised. A representative plot of one sample from each immunisation group is shown in Figure 4.28. Results show that CD4 T cell response is not enhanced by the ISQC-CD40mAb conjugates when using ISQ peptide as a conjugated antigen. This result was further verified by the fact that the supernatants of unstimulated and stimulated samples did not show a difference in IL-2 concentration (results not shown).

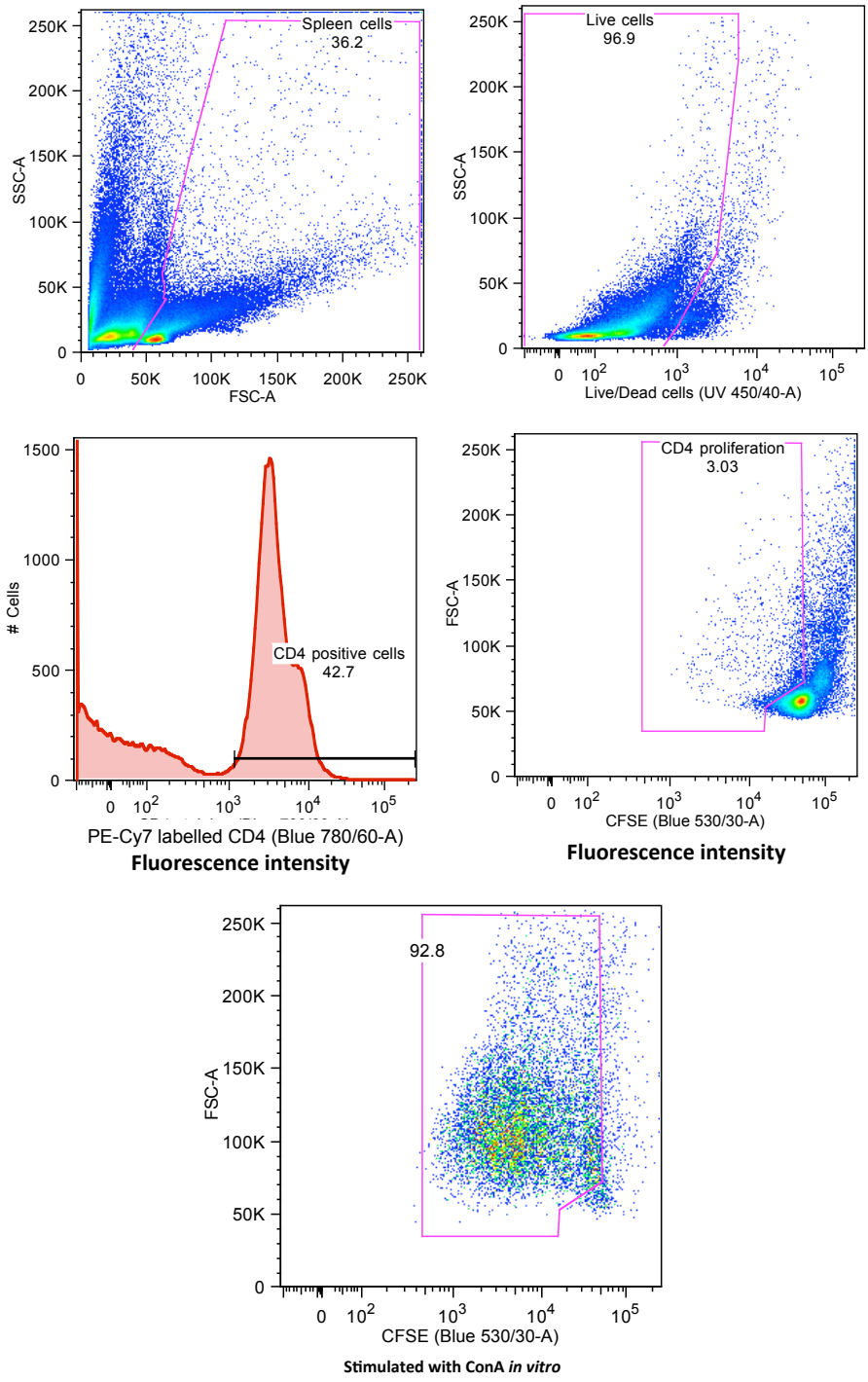

Figure 4.27. The gating strategy used for flow cytometric analysis of CD4$^+$ T cell proliferation. The gating strategy included first gating on the spleen cell population, followed by live cells based on UV live/dead staining (UV 450/50), and subsequently on cell surface expression marker CD4$^+$ cells. The percentage of CD4$^+$ T cells in the original sample that have divided was recorded. A representative plot of one sample stimulated with ConA (positive control) is also shown.

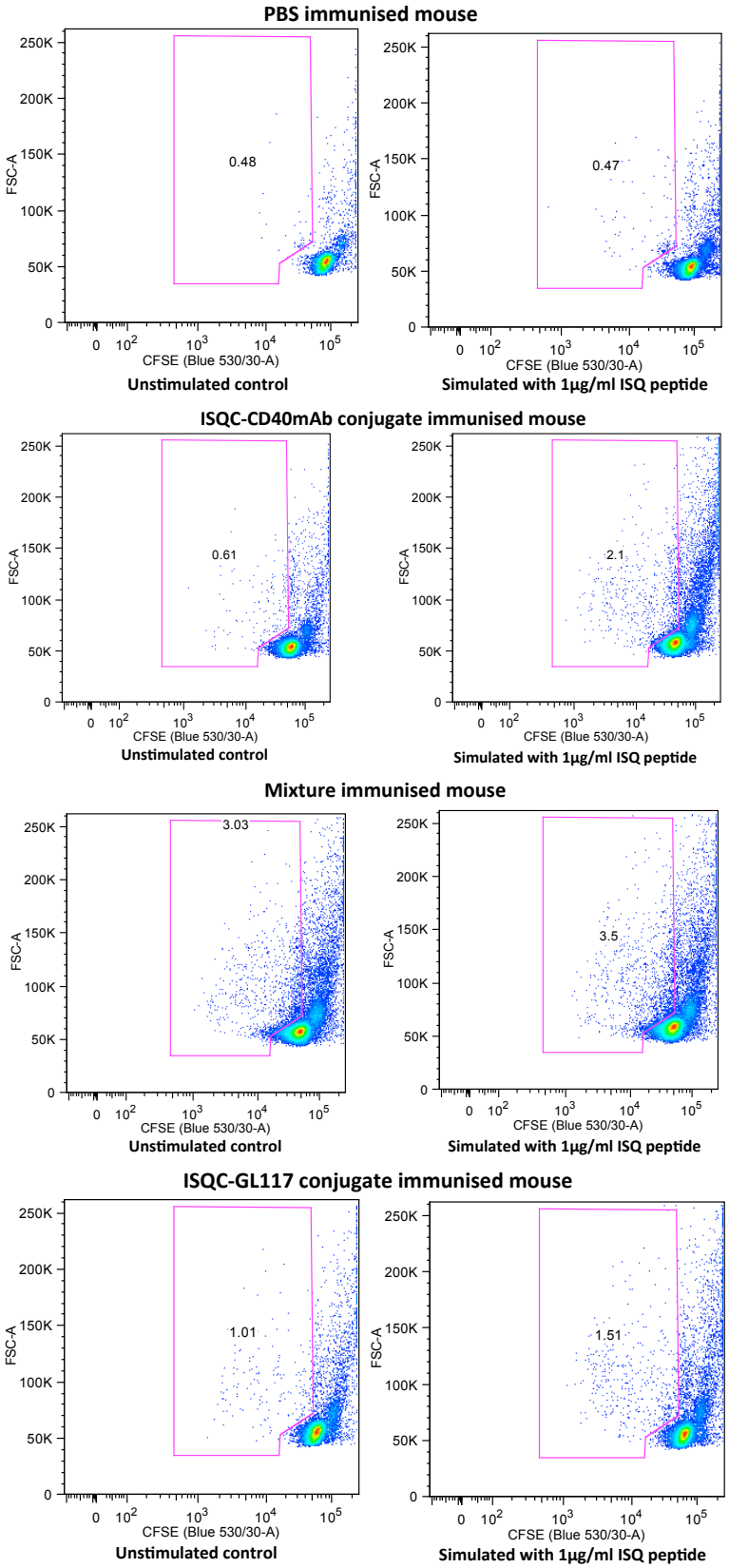

Figure 4.28. Representative plots analysed by FlowJo software for the investigation of CD4$^+$ cell proliferation on stimulation *ex vivo* with 1µg/ml ISQ peptide, or in the absence of stimulation. The percentage CD4$^+$ cells from the original population that have divided are shown.

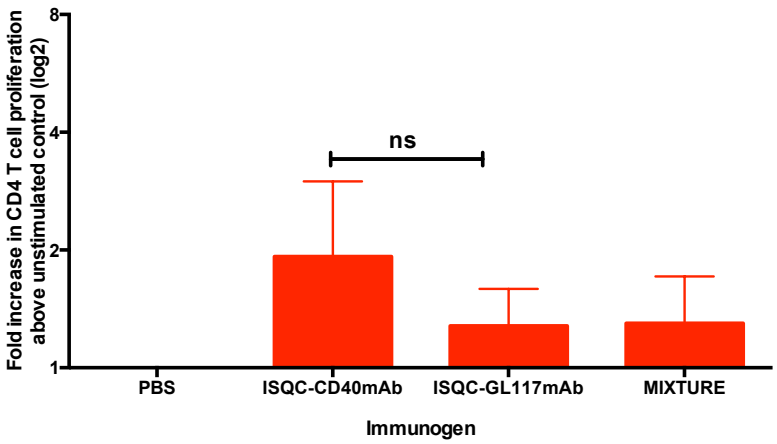

Figure 4.29. CD4$^+$ T cell proliferation on stimulation with 1µg/ml ISQ peptide *ex vivo.* The percentage of CD4$^+$ cells from the original population that have divided were recorded. Fold increase in CD4$^+$ T cell proliferation above unstimulated control of each group is shown. One-way ANOVA with Sidak's multiple comparisons post-test (mean +/- SD). ns = non-significant. n=4/5 per group.

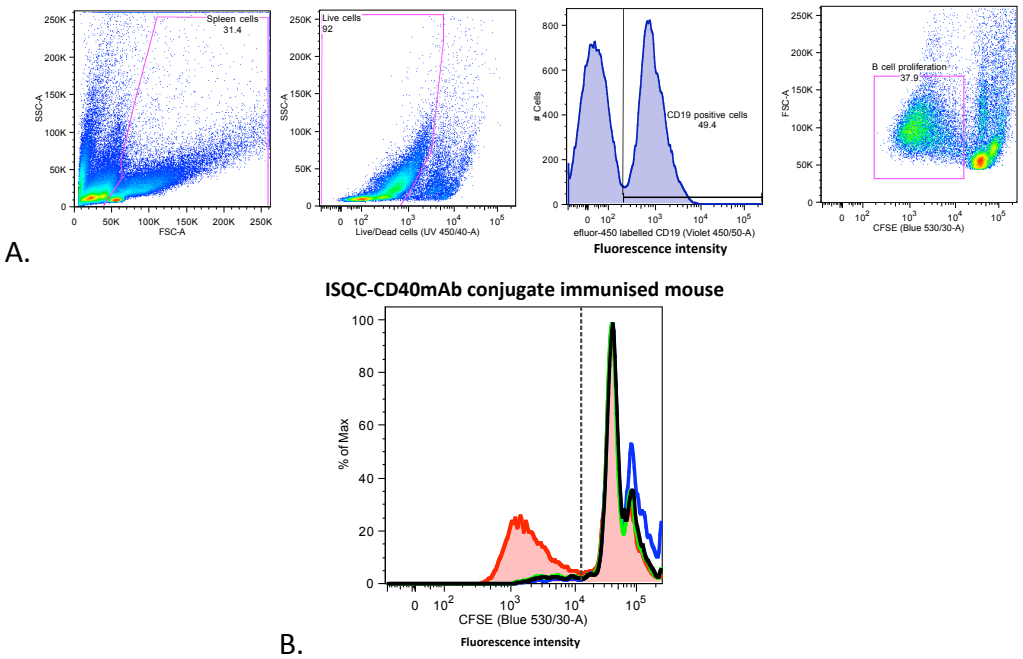

Figure 4.30. CD19$^+$ cell proliferation on stimulation with 1µg/ml ISQ peptide *ex vivo*. A. The gating strategy included first gating on the spleen cell population, followed by live cells based on UV live/dead staining (UV 450/50), and subsequently on cell surface expression marker CD19$^+$ cells. The percentage of CD19$^+$ cells from the original population that have divided when stimulated by LPS is shown. B. Overlaid histogram of a representative plot from a ISQC-CD40mAb immunised mouse. Cells stimulated with LPS (red), 1µg/ml ISQ peptide (blue) and unstimulated (black) are shown. FlowJo software was used for data analysis.

Discussion

The main role of traditional adjuvants made by an empirical approach was to enhance antibody responses against co-inoculated antigen or the removal of infection. These adjuvants were effective for vaccines that are commercially available against bacterial and certain viral diseases, such as diphtheria, tetanus, pertussis (Black et al., 2008) and hepatitis A (Ashur et al., 1999). For the generation of an effective vaccine-mediated immune response against other diseases like cancer, antibody responses only are not enough to confer protection. Induction of T cell responses as well as antibody responses is crucial.

In this chapter we wanted to determine which APC is important for the mechanism of CD40mAb-adjuvanted vaccines with focus on their downstream effect on $CD4^+$ T cell responses. The effect of CD40mAb-adjuvanted vaccines on the (i) antigen-presentation to $CD4^+$ T cells *in vitro*, (ii) APC co-stimulatory molecule expression *in vitro* and (iii) $CD4^+$ T cell responses to vaccine antigen *ex vivo*, was therefore investigated using OVA-CD40mAb conjugates or ISQC-CD40mAb conjugates or both.

OVA is a poorly immunogenic antigen recommended as the standard model weak immunogen (McGee et al., 1994). The vaccine consisting of OVA conjugated to CD40mAb has shown to generate significantly higher titres of anti-OVA antibodies compared to the CD40mAb and OVA mixture (Barr et al., 2003). The use of OVA antigen as a model was beneficial as it allowed testing of the antigen presentation capability of APCs to $CD4^+$ T cells i*n vitro*, by means of the OVA-specific DO11.10 T cell hybridoma cell line. BM-DCs, B cells and splenocytes were used in an effort to investigate the effect of the OVA-CD40mAb conjugates on antigen presentation to DO11.10 T hybridoma cells.

The disheartening fact was that in these experiments, the IL-2 produced in the supernatant during co-culture was not above the minimum detectable limit of the ELISA being used, which made it difficult to formulate a conclusion (Figure 4.6). A trend was only observed when the numbers of BM-DCs and T cells in co-culture were increased. Moreover using the co-culture system with increased BM-DC and DO11.10 T hybridoma cell numbers, CD40mAb did not enhance BM-DC antigen

presentation to T cells compared to the isotype control mAb or the OVA alone control (Figure 4.10). This result was inconsistent with a very recent study that showed that anti-CD40 antibody was more efficient at mediating presentation of conjugated peptides on MHC class II compared to other antibodies against cell surface receptors (for example anti-DEC205) (Chatterjee et al., 2012). Furthermore, in the aforementioned study anti-CD40 conjugated to peptides lead to enhanced $CD4^+$ T cell production of IL-2 and IFN-γ. IFN-γ being the chief cytokine produced by T_H1 differentiated cells. The latter experiments were conducted using a different co-culture system, set-up with human blood isolated DCs and $CD4^+$ T cells

Due to the results obtained using the DO11.10 hybridoma cell line, we did not proceed to investigating the effect of the CD40mAb conjugates in the co-culture system. Different methods in similar co-culture systems have been used to measure DO11.10 T hybridoma cell activation. Published studies utilised a more sensitive ELISA to detect IL-2 in the supernatant (Cycon et al., 2009, Aubin et al., 2010) that was not used in this study due to financial limitations. Other studies utilised the murine IL-2-dependent CTLL-2 cell line that only proliferate in the presence of IL-2 (Bennett et al., 1992, Mutini et al., 1999, Prokopowicz et al., 2010). This cell line was not used due to practical limitations. CTLL-2 proliferation could be measured using an isotope incorporation assay with 3H-thymidine (3H-TdR) that required a scintillation counter that was unavailable and special radiation training. CTLL-2 proliferation could also be detected by means of a colorimetric assay using MTT [3-(4,5-dimethylthiazol-2-yl)-2,5-diphenyltetrazolium bromide], however this assay was found less sensitive than 3H-TdR (Russell and Vindelov, 1998).

DO11.10 T hybridoma cells containing a gene encoding for GFP (DO11-GFP), which is under the control of a nuclear factor of activated T cells regulated promoter have also been used by other studies (Underhill et al., 1999, Sun et al., 2003, Brewer et al., 2004). On activation these cells become fluorescent and can be detected by flow cytometry. Studies have also used $CD4^+$ cells from DO11.10 BALB/c, specific to $H\text{-}2^d$ (Son et al., 2002, Aubin et al., 2010), or OT-II C57Bl/6, specific to $H\text{-}2^b$ (Kool et al., 2011) transgenic mice having an OVA-reactive T cell receptor for antigen presentation assays. Considering the unstable nature of the DO11.10 T hybridoma

cells and the low IL-2 concentration produced by these cells in the supernatants, perhaps the use of different cells in this study would have contributed to a more robust conclusive result.

The identification of the principal APC having a role in the mechanism of action of CD40mAb-adjuvanted vaccines was also investigated. Work carried out in Chapter 3 and a recent study carried out in our laboratory by Carlring et al. (2012), showed that a vaccine consisting of CD40mAb conjugated to a lymphoma idiotype significantly enhanced overall mouse survival as a prophylactic vaccine in a murine lymphoma tumour model (discussed in detail in Chapter 3). The routine treatment for lymphoma is the use of a monoclonal antibody (Rituximab) directed against CD20 antigen present on B cells. This leads to depletion of B cells (Anolik et al., 2007). Therefore understanding whether CD40mAb targets the CD40 receptor of other APCs, for example DCs, would shed some light on whether CD40mAb-Id therapy could be used as an adjunct to therapies such as Rituximab.

The DC has been described as 'nature's adjuvant' because many agents for example MF59, bacterial CpG motifs, MPL, bacterial endotoxin and Freund's adjuvant are able to boost the immune response via direct or indirect activation and maturation of DC (De Smedt et al., 1996, De Becker et al., 2000, Ismaili et al., 2002, Shah et al., 2003, Lambrecht et al., 2009). On activation, the DCs upregulate essential surface co-stimulatory molecules in order to efficiently activate naive T cells, linking the innate and adaptive immune response. CD40mAb-adjuvanted conjugates target professional APCs like B cells, DCs and macrophages, however in these experiments only B cells become activated as shown by an enhanced expression of MHC class II (Carlring et al., 2012). Consistent with the previously mentioned study, B cells were found to be the one of the crucial targets of CD40mAb. Both the OVA-CD40mAb conjugate vaccines as well as a novel epitope-based vaccine, ISQC-CD40mAb significantly enhanced the co-stimulatory molecule expression compared to their respective isotype mAb control conjugates.

The CLICK sOVA-CD40mAb conjugate was better at DC activation compared to the isotype mAb control and the Standard OVA-CD40mAb conjugates (Figure 4.12), however, since (i) the sOVA used to make the OVA-CD40mAb conjugates contained

endotoxin (Figures 4.13, 4.15, 4.16, 4.19) and (ii) the Standard OVA-CD40mAb conjugate was not optimal (due to the very minimal anti-OVA specific antibody titre produced – Figure 4.15), the results were conflicting and difficult to interpret. The CLICK sOVA-CD40mAb conjugate could be enhancing the co-stimulatory molecule expression through CD40 receptor ligation, but it is possible that the effect is due to a synergistic effect of the CD40 receptor binding and the endotoxin contamination of sOVA. Published work has shown that CD40mAb has a synergistic effect with LPS. Immunisation of LPS admixed with CD40mAb enhanced anti-LPS IgG levels compared to immunisation of LPS admixed with the respective isotype mAb control (Barr and Heath, 1999). Moreover, immunisation with a vaccine formulation consisting of CD40mAb conjugated to lymphoma idiotype and MPL (lipid A portion of *Salmonella minnesota* LPS) enhanced tumour rejection compared to CD40mAb conjugated to antigen used alone in a murine lymphoma model (Carlring et al., 2012). This effect could have been the reason why the anti-OVA antibody response against sOVA as well as sOVA admixed with CD40mAb were not significantly different to the CLICK sOVA-CD40mAb conjugates (Figure 4.15). The reason why very low anti-OVA responses were generated from Standard OVA-CD40mAb is not understood, as *in vitro* testing of this conjugate confirmed conjugation.

With regards to the DC co-stimulatory molecule expression, the results using ISQC-antibody conjugates were more straightforward. ISQC-CD40mAb conjugates had no effect on the CD80 or the CD86 expression of splenic $CD11c^+$ DCs compared to the isotype mAb control conjugate (Figure 4.23). Judging from the lack of upregulation of co-stimulatory molecule expression induced by LPS, the splenic DCs used for this work were already mature (fully expressing co-stimulatory molecules). The effect of the ISQC-CD40mAb conjugate on the homogeneous immature BM-DC population optimised for this work showed more straightforward results. Both LPS and sOVA alone but not ISQ peptide alone, had a substantial effect on the upregulation of BM-DC CD80 and CD86 expression. ISQC-CD40mAb conjugates showed a significant increase of both CD80 and CD86 expression of BM-DC compared to isotype mAb control conjugate and controls (Figure 4.24). DC activation by CD40mAb-adjuvanted conjugates is different to other adjuvants like unmethylated CpG motifs on TLRs or

endotoxin because the DCs are not activated by recognition of PAMPs, but via the CD40 receptor.

An investigation into the uptake of CD40mAb-antigen conjugates would shed more light on the interpretation of the mechanism. Although, B cells have been assumed to be the principal target of CD40mAb the fact that DCs are more efficient at antigen-uptake should be kept in mind. Uptake of the CD40mAb-adjuvanted conjugates at the site of inoculation could be by means of receptor-mediated endocytosis, phagocytosis and macropinocytosis (Guermonprez et al., 2002), as well as possibly the CD40 receptor (investigated in Chapter 5).

Mice immunised with ISQC-mAb conjugates produced detectable levels of anti-OVA specific antibodies after boost (Figure 4.25) indicating that they were immunogenic. Furthermore, the fact that mice immunised with ISQC-CD40mAb produced a significantly higher anti-OVA specific response compared to the ISQC admixed with CD40mAb and ISQC-GL117mAb conjugate, shows that the conjugation of CD40mAb to antigen is a step in the right direction to overcoming the lack of immunogenicity of epitope-based vaccines.

The evidence to date shows the role of CD40mAb-adjuvanted vaccines in enhancing antibody responses (Barr et al., 2003, Carlring et al., 2012) and T cell responses (Carlring et al., 2004, Hatzifoti and Heath, 2007) however, the type of T cell ($CD4^+$ versus $CD8^+$) response had not yet been directly investigated. Understanding the type of immune response the adjuvant helps to shape, will allow the use of the adjuvant for the correct application. The final role of CD40mab-adjuvanted conjugates investigated in this chapter was the effect of the CD40mAb-conjugate vaccines on antibody and $CD4^+$ T cell responses to antigen stimulation *ex vivo*. The ISQC-CD40mAb vaccine showed a trend of increased $CD4^+$ T cell responses compared to the isotype antibody control conjugate. This suggests that ISQC-CD40mAb could be inducing $CD4^+$ T cell responses however, more numbers than just four mice are required to reach significance (Figure 4.27).

Multiple adjuvants currently being researched have shown promise in enhancing $CD4^+$ T cell responses including the use of alum compounds. However the immune response induced by alum was found to be largely limited to the induction of T_H2

responses (Grun and Maurer, 1989, Brewer et al., 1996, Brewer et al., 1999). The use of the TLR4 agonist together with aluminium salts, in the AS04 adjuvant, used in two licensed vaccines Cevarix™ (HPV) and Fendrix™ (HBV) also led to enhanced T_H1 responses achieving the desirable effect (Levie et al., 2002, Giannini et al., 2006, Didierlaurent et al., 2009). Induction of a T_H1 response is an unmet requirement for vaccination against many diseases including cancer, as T_H1 cytokines stimulate tumour specific $CD8^+$ CTL responses that are critical for anti-tumour immunity.

Conclusion

In conclusion, epitope-based CD40mAb conjugates are promising models for the investigation of the mechanism of action of CD40mAb adjuvant, better than the previously used OVA model due to their very poor immunogenicity when administered alone. The ISQC-CD40mAb conjugate was more immunogenic than the mixture or the isotype conjugate. The results in this chapter point to the fact that both splenic B cells and immature DCs have a role in the mechanism of CD40mAb-adjuvanted vaccines. However, whether the $CD4^+$ T cells are mediators for CD40mAb conjugate vaccine protection is still subject to further investigation.

CHAPTER 5

AN INVESTIGATION INTO THE IMPACT OF A CD40MAB-ADJUVANTED EPITOPE-BASED VACCINE ON $CD8^+$ T CELL RESPONSES AND THE APCS CONTRIBUTING TO THIS ADJUVANT EFFECT

5.1. Introduction

Robust $CD8^+$ T cell responses are important for protection against cancers and infectious diseases, which together with safety, is where most novel vaccine adjuvants fall short. CD40mAb has been used as immunotherapy in human cancer Phase I clinical trials (Vonderheide et al., 2007, Beatty et al., 2013). The fact that CD40mAb used alone as immunotherapy was well tolerated with only mild to moderate cytokine release syndrome as side-effects that manifest as chills, fever, rigors soon after infusion, shows that the use of CD40mAb as an adjuvant is a step in the right direction.

A study carried out in our laboratory demonstrated that murine CD40mAb-adjuvanted vaccine anti-tumour efficacy was significantly reduced on $CD8^+$ T cell depletion (Carlring et al., 2012), which suggested that $CD8^+$ T cells were the main effectors against B cell lymphoma. However, the cytotoxic T cell response crucial for controlling tumour growth was not directly measured. Therefore, we wanted to investigate the impact of CD40mAb-adjuvanted conjugates on the $CD8^+$ T cell responses, which was assessed by conjugating the immunodominant $CD8^+$ T cell epitope of OVA ($OVA_{257-264}$ or SIINFEKL) to CD40mAb. This was performed in the present study using an *in vivo* killing or cytotoxicity assay.

In Chapter 4, the APCs implicated in the mode of action of CD40mAb-adjuvanted vaccines and their downstream adjuvant effects on $CD4^+$ T cell responses were investigated. In this chapter the hypothesis that both B cells and DCs have an impact on the mechanism of action of CD40mAb-adjuvanted conjugates leading to $CD8^+$ T cell responses were investigated. This was explored in more detail *in vitro* by taking a closer look into antigen-delivery and uptake as well as B cell and DC activation status and antigen-presentation to $CD8^+$ T cells.

The study by Carlring et al. (2012) showed *in vitro* that the conjugate was targeted to the CD40 receptor of splenic B cells, DCs and macrophages (Carlring et al., 2012). However, whether the CD40mAb and the conjugated antigen were co-delivered and internalised by the same APC could not be established as only the antigen was fluorescently labelled. The fluorescently labelled CD40mAb-antigen conjugate

immunised subcutaneously was detected in the harvested draining lymph node cells by confocal microscopy. However, in the *in vivo* experiment, which APCs were taking up the CD40mAb-antigen conjugates was not specified. To investigate this, the SIINFEKL peptide and the CD40mAb were fluorescently labelled with different fluorophores prior to conjugation. Co-localisation and internalisation of co-labelled SIINFEKL-CD40mAb conjugate by B cells and BM-DCs was investigated *in vitro* by epifluorescence microscopy.

The effect of SIINFEKL-CD40mAb conjugates on antigen processing and presentation to $CD8^+$ T cells was demonstrated *in vitro* using the well-characterised B3Z hybridoma CD8+ T cell line. These cells recognise SIINFEKL presented on the MHC class I of the $H\text{-}2K^b$ haplotype (Sanderson and Shastri, 1994), in a quantitative manner. On recognition and binding of the TCR to SIINFEKL/$H\text{-}2K^b$ complex, activated B3Z cells produce IL-2. Therefore, the activation status of the B3Z was measured using IL-2 ELISA. Furthermore, the ability of the APCs to present SIINFEKL was also investigated by flow cytometry by means of a fluorescently labelled anti-SIINFEKL/$H\text{-}2K^b$ complex antibody. Finally, to further investigate the effect of the SIINFEKL-CD40mAb conjugate on APC co-stimulatory molecule expression and presentation, the conjugate was tracked *in vivo*.

5.2. Impact of an epitope-based CD40mAb-adjuvanted conjugate on $CD8^+$ T cell responses *in vivo*

5.2.1. Production and characterisation of SIINFEKLC-mAb conjugates *in vitro*

For the context of this chapter, the $CD8^+$ T cell epitope SIINFEKL was synthesised with a cysteine on the C-terminal end (SIINFEKLC). The CD40mAb and the isotype control mAb (GL117mAb) were treated with Sulfo-SMCC and conjugated to the sulphydryl group on the cysteine present on the C-terminal end of the SIINFEKLC peptide (*see* Section 2.2.1.4.). The endotoxin activity of these conjugates was tested and found to be <0.01 EU/µg conjugate. As explained in Section 4.4.1, using ISQC-mAb conjugates, conjugation of peptide to CD40mAb and respective isotype control mAb could not be confirmed by ELISA or flow cytometry, therefore, CD40mAb was also conjugated to biotinylated SIINFEKLC (*see* Section 2.2.1.4).

SIINFEKLC was biotinylated using EZ-Link Sulfo-NHS-Biotin that reacts with side-chain of lysines (K) or the amino-terminal (NH_2) group. SIINFEKLC peptide has a MW of 1066Da therefore, since the smallest dialysis membrane available has a pore size of 1000Da, excess biotinylation reagent could not be removed by buffer exchange, without the risk of losing valuable sample. The same precautions were taken as explained in detail in Section 4.4.1. Briefly, NHS-biotin used to biotinylate SIINFEKLC was also mixed with SMCC-treated mAb in order to ensure that the NHS-ester was non-reactive and would not also bind to the mAb during biotinylated peptide-mAb conjugation.

A 10µg sample of SIINFEKLC-mAb conjugates and controls were separated on a 15% reducing SDS-PAGE gel. Biotinylated conjugates were detected with HRP-labelled streptavidin by Western blotting (Figure 5.1, *see* Section 2.2.4.2.1.). This showed that only the biotinylated SIINFEKLC-mAb conjugates were detected by the HRP-labelled streptavidin. No bands were observed in the biotinylated reagent and mAb mixture control.

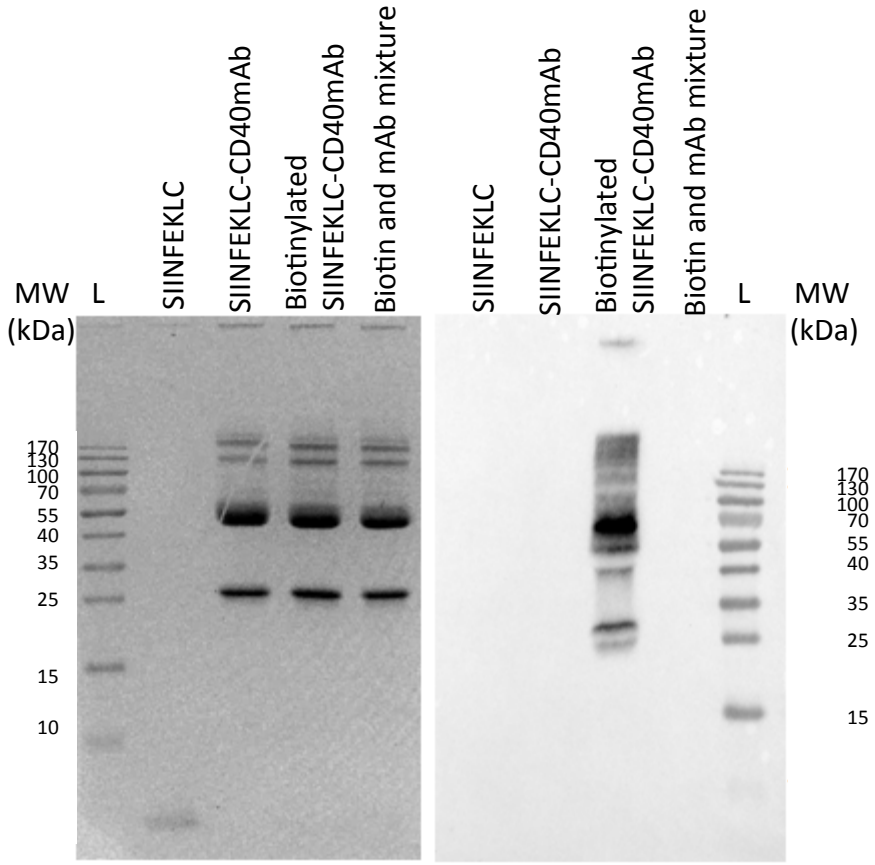

Figure 5.1. Confirmation of conjugation of SIINFEKLC peptide to CD40mAb. 15% SDS PAGE reducing gel is shown on the left. Western blot using HRP-labelled streptavidin to detect biotin is shown on the right. SIINFEKLC-CD40mAb refers to the SIINFEKLC-CD40mAb conjugate. L refers to the molecular weight ladder shown in kDa.

To further ensure that the conjugation was successful 6% and 15% SDS PAGE reducing gels were run at 60V in order to obtain better separation between the bands (Figure 5.2.). The 6% SDS PAGE gel shows that the SIINFEKLC-CD40mAb conjugate bands running at approximately 150kDa and 50kDa are of higher apparent MW than corresponding mAb alone controls (Figure 5.2A). When observing the 15% gel, the bands showing heavy chains of the mAb portion of the SIINFEKLC-mAb conjugates running at approximately 50kDa, are of slightly higher apparent MW than the corresponding mAb controls (Figure 5.2B). The increase in the apparent MW of the antibody heavy chains in the lanes containing the SIINFEKLC-CD40mAb conjugates compared to the mAb only control lanes, suggest that SIINFEKLC peptide is conjugated to the mAb. Since the biotinylated SIINFEKLC peptide did conjugate to the mAb (Figure 5.1), we assumed that the non-biotinylated SIINFEKLC peptide had also conjugated to the mAbs. Only non-biotinylated SIINFEKLC-mAb conjugates were used for the subsequent experiments.

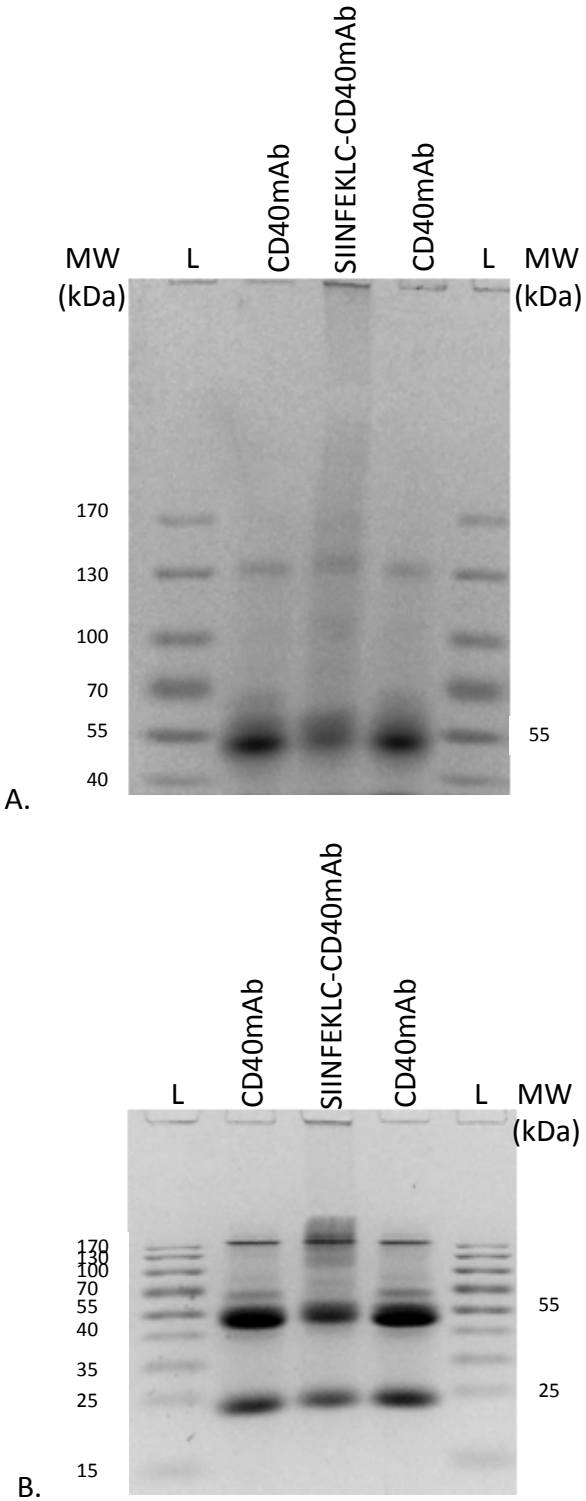

Figure 5.2. Confirmation of conjugation of SIINFEKLC peptide to CD40mAb via reducing SDS PAGE. A. 6% SDS PAGE reducing gel. B. 15% SDS PAGE reducing gel. SIINFEKLC-CD40mAb refers to the SIINFEKLC-CD40mAb conjugate. L refers to the molecular weight ladder shown in kDa.

5.2.2. Investigation of the effect of SIINFEKLC-CD40mAb conjugates on $CD8^+$ T cell responses by means of an *in vivo* cytotoxicity assay

The impact of the SIINFEKLC-CD40mAb conjugates on the $CD8^+$ T cell response was carried out using a cytotoxicity assay in a murine model. The assay involved primarily dividing splenocytes from naive mice into two populations, one of which was pulsed with 2µM SIINFEKL peptide and stained with low concentration CFSE, whilst the other population was left unpulsed and stained with a high concentration of CFSE. The two splenocyte populations were mixed in a 1:1 ratio and injected i.v. into previously SIINFEKLC-CD40mAb immunised mice. After 18 hours, the SIINFEKL-directed cytolytic activity was measured by flow cytometry (*see* Section 2.2.7.5.).

5.2.2.1. Optimisation of the parameters of the *in vivo* cytotoxicity assay

Prior to immunising with SIINFEKLC-CD40mAb conjugates and controls, certain parameters of the assay had to be optimised in order to ensure that:

(1) SIINFEKL-pulsed splenocytes retained the SIINFEKL peptide on their MHC class I even after the series of washing steps involved during staining with CFSE dye

(2) cell death was due to the direct cytotoxic $CD8^+$ T cell response, and not due to the SIINFEKL being toxic to the splenocytes

(3) CFSE concentration used to stain the splenocytes was of sufficient fluorescent intensity for subsequent analysis by flow cytometry

Therefore, as illustrated in Figure 5.3, a spleen from a naive mouse was harvested and a single cell suspension prepared. Splenocytes were divided into two populations; one population was pulsed with 2µM SIINFEKL peptide by incubation with SIINFEKL peptide for 1 hour, whilst the other population was left unpulsed. Subsequently both populations were stained with different concentrations of CFSE. Unpulsed population was stained with 0.2µM CFSE (or $CFSE^{HIGH}$) whilst SIINFEKL-pulsed population was stained with 0.02µM CFSE (or $CFSE^{LOW}$), for this optimisation experiment.

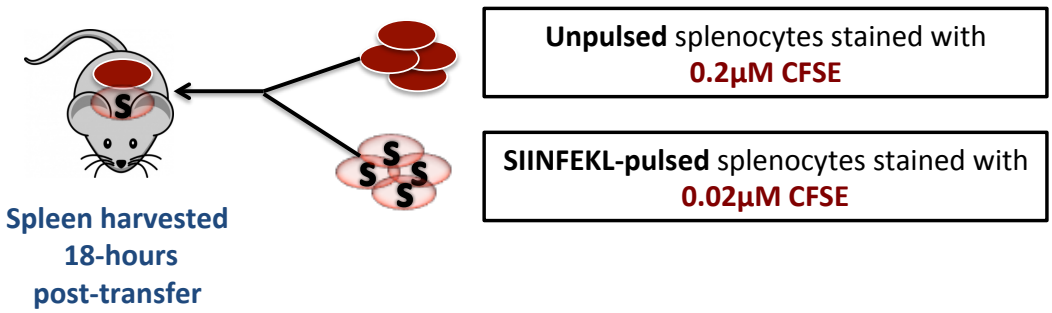

Figure 5.3. A diagrammatic representation of the optimisation of the CFSE-based cytotoxicity assay.

Other studies that performed *in vivo* cytotoxicity assays either pulsed with the relevant peptide prior to CFSE staining (Curtsinger et al., 2003, Byers et al., 2003) or post-CFSE staining (Barber et al., 2003, Yang et al., 2004). In this study, splenocytes were pulsed with SIINFEKL peptide prior to staining. Therefore the 10^5 CFSE-stained SIINFEKL-pulsed splenocytes were co-cultured with 10^5 B3Z cells (in a total volume of 200µl) that recognise SIINFEKL/H-2K^b complex and produce IL-2 on activation, to ensure that the SIINFEKL peptide did not detach from the MHC class I complex (Figure 5.4). The IL-2 concentration in the supernatant after 24-hour co-culture was measured by ELISA (*see* Section 2.2.6.8.1.). Figure 5.4 shows that on co-culture of B3Z with SIINFEKL-pulsed splenocytes, a significant amount of IL-2 was produced in the supernatant compared to the cells only controls ($p<0.0001$, One-way ANOVA using Dunnett's multiple comparisons post-test) demonstrating that SIINFEKL peptide was still present on the splenocyte MHC class I complexes post CFSE staining.

The concentration of CFSE used for staining in cytotoxicity assay between different studies is also variable. Some studies have used concentrations as high as 5µM CFSE (Curtsinger et al., 2003, Yang et al., 2004), whilst others have used concentrations as low as 1nM CFSE (Barber et al., 2003). Based on this information, in the optimisation experiments, SIINFEKL-pulsed splenocyte population was stained with 0.02µM ($CFSE^{LOW}$) whilst the unpulsed population was stained with 0.2µM CFSE ($CFSE^{HIGH}$).

The two different splenocyte populations were mixed in a 1:1 cell ratio, and analysed by flow cytometry, prior to i.v. injection (Figure 5.5A). Since two cell peaks of sufficient intensity were observed a total number of 10^7 splenocytes containing the two populations were injected i.v. into a naive mouse. An *in vitro* control of 10^6 cells of the two populations was incubated overnight in a T25 flask at 37°C, 5% CO_2. After 18 hours, the spleen was harvested and analysed on flow cytometry together with the *in vitro* control (Figure 5.5B, C).

Flow cytometric analysis of the splenocyte populations showed that although prior to the injection the two CFSE-stained populations were of sufficient fluorescence intensity (Figure 5.5A), this was not the case for both the harvested spleen cells (Figure 5.5B) and the *in vitro* control (Figure 5.5C). Results showed that the CFSE concentrations used for staining should be increased. However, on observation of the height of the $CFSE^{HIGH}$ and $CFSE^{LOW}$ peaks, staining with CFSE nor pulsing with the SIINFEKL peptide was toxic to the cells at the concentrations used. However, the CFSE concentrations chosen were not of sufficient fluorescent brightness. Therefore, for the main assay, considering that other studies used concentrations as high as 5µM CFSE (Curtsinger et al., 2003, Yang et al., 2004), CFSE staining was carried out using 2µM ($CFSE^{HIGH}$) and 0.2µM CFSE ($CFSE^{LOW}$).

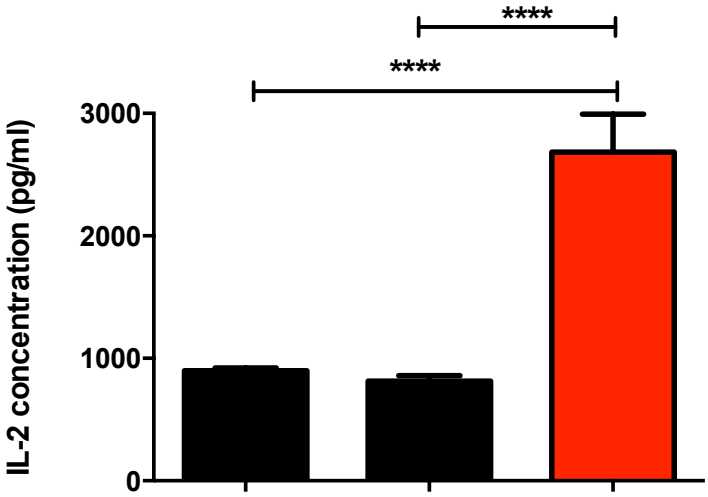

B3Z cells	+	-	+
SIINFEKL-pulsed Splenocytes	-	+	+

Figure 5.4. Co-culture of CFSE-stained splenocytes stimulated with 2µM SIINFEKL peptide and B3Z T cell hybridoma. The ability of B3Z to produce IL-2 in the supernatant after 24-hours co-culture is shown. B3Z alone, and SIINFEKL-pulsed splenocytes alone with no co-culture served as negative controls. This figure represents one experiment. Technical replicates = 3. One-way ANOVA using Dunnett's multiple comparisons test (mean +/- SD) was used to determine statistical significance. ****p<0.0001.

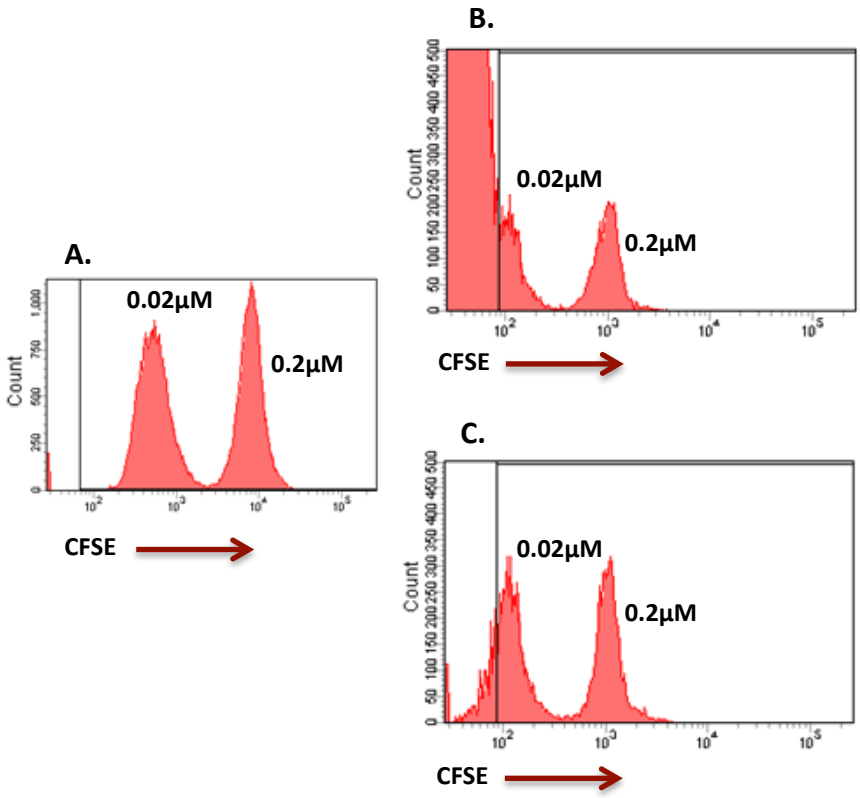

Figure 5.5. Flow cytometric analysis of two splenocyte populations stained with 0.02µM ($CFSE^{LOW}$) and 0.2µM CFSE ($CFSE^{HIGH}$). A. Two mixed populations prior to i.v. injection. B. Two mixed populations 18 hours post i.v. injection. C. Two mixed populations incubated *in vitro* for 18 hours.

5.2.2.2. Targeting of SIINFEKL-pulsed cells by effector $CD8^+$ T cells

To determine whether antigen-specific $CD8^+$ T cells target and kill cells presenting the SIINFEKL peptide, unpulsed (control cells, stained with $CFSE^{HIGH}$), and specific SIINFEKL-pulsed (target cells, stained with $CFSE^{LOW}$) splenocytes were transferred into mice previously immunised with the SIINFEKLC-mAb conjugates and controls (Figure 5.6).

The CFSE-stained transferred splenocyte populations migrate to the secondary lymphoid organs like the spleen but the target cells would only be lysed if peptide-specific $CD8^+$ T cells were generated. The relative decrease of specific SIINFEKL-pulsed target cell numbers to the unpulsed control cell numbers was measured by flow cytometry as a means to identify $CD8^+$ T cell lysis *in vivo.* Target splenocytes were distinguished from control splenocytes based on the intensity of CFSE staining.

Five C57BL/6 mice per group were immunised on day 0 with 40µg SIINFEKLC-CD40mAb conjugate or SIINFEKLC-GL117mAb conjugate i.p. Control groups included 2µg SIINFEKLC and 40µg CD40mAb mixture (or MIX) and PBS (Figure 5.6). A summary of the experimental design of the *in vivo* cytotoxicity assay and immunisation schedule is shown in Figure 5.6.

A.

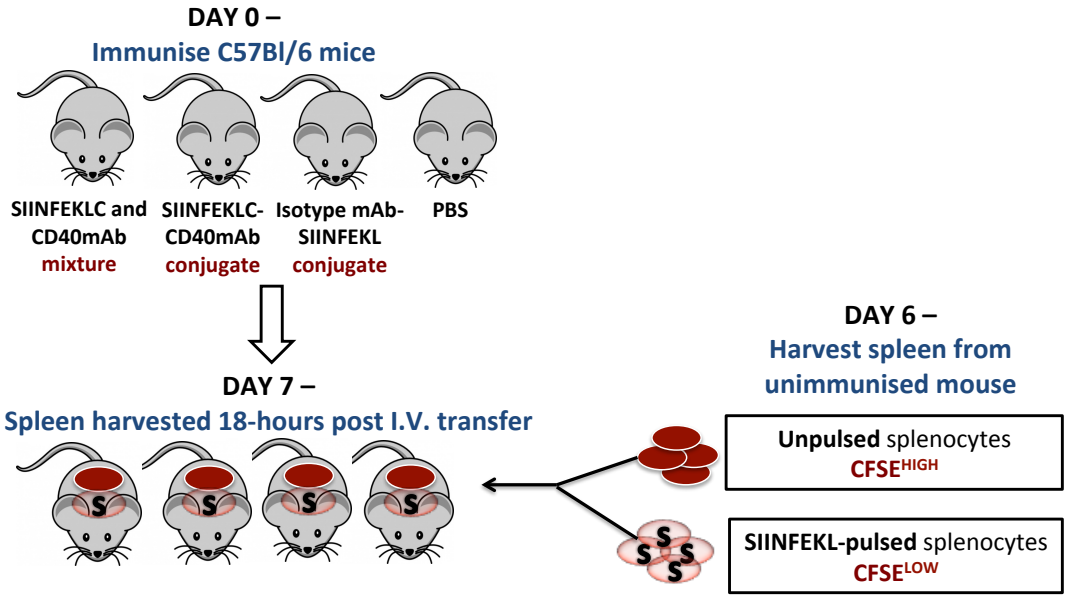

B.

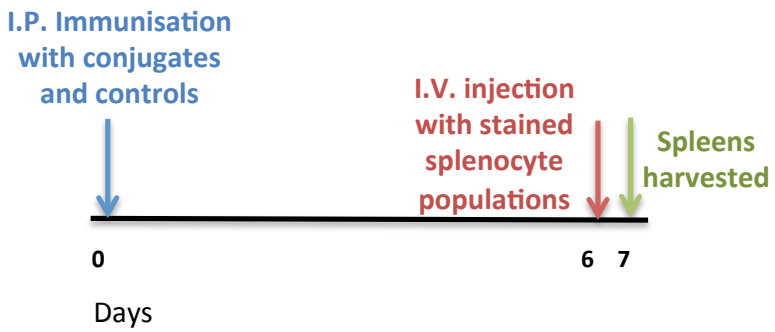

Figure 5.6. The experimental design of the *in vivo* cytotoxicity assay. A. A total of twenty C57Bl/6 mice (5 mice per group) were immunised i.p with SIINFEKLC-CD40mAb conjugate, SIINFEKLC-GL117mAb conjugate, SIINFEKLC and CD40mAb mixture or PBS. On day 6, SIINFEKL-pulsed target cells, harvested from naive mice were stained with $CFSE^{LOW}$ (0.2µM) and unpulsed control cells stained with $CFSE^{HIGH}$ (2µM) and thereafter injected i.v into the immunised mice. The experiment was terminated on day 7 at which point mice were culled and spleens resected. B. Immunisation schedule.

Flow cytometric analysis of splenocytes showed that antigen-specific $CD8^+$ T cells were generated and SIINFEKL-pulsed target cells were lysed only in the CD40mAb-adjuvanted immunised groups (Figure 5.7). The percentage lysis was calculated as explained in Section 2.2.7.5.3. Fifty percent and 51% of the SIINFEKL-pulsed splenocytes were lysed in mice immunised with SIINFEKLC-CD40mAb conjugate and MIX respectively. This was significantly higher than that for the SIINFEKLC-GL117mAb control immunised mice ($p<0.05$, One-way ANOVA using Tukey's multiple comparisons post-test). There was no difference observed between the CD40mAb SIINFEKLC mixture (MIX) and the SIINFEKLC-CD40mAb conjugate.

Cell death was observed at a CFSE concentration of 2µM, assumed because a relative loss of unpulsed control $CFSE^{HIGH}$ stained population compared to $CFSE^{LOW}$ was observed in all groups including PBS (Figure 5.8). As already mentioned, concentrations of CFSE as high as 5µM was used by other studies (Sullivan et al., 2003, Curtsinger et al., 2003, Ahonen et al., 2004, Yang et al., 2004), whilst optimisation experiments have shown that the $CFSE^{LOW}$ population was not bright enough to observe by flow cytometry. This was the reason why the CFSE concentrations of 2µM and 0.2µM were chosen. In spite of this, there was a dramatic loss of $CFSE^{LOW}$ population only in the SIINFEKLC-CD40mAb immunised group (Figure 5.8) and Mixture group (not shown).

Since the CD40mAb adjuvanted conjugates induced killing of SIINFEKL-pulsed target cells *in vivo*, SIINFEKLC-CD40mAb and its respective isotype mAb control conjugate were used for the rest of this chapter as a model to understand further which APCs are instrumental in the mechanism of action of CD40mAb-adjuvanted conjugates as adjuvants upstream of $CD8^+$ T cell responses. This was investigated primarily *in vitro* and subsequently *in vivo*.

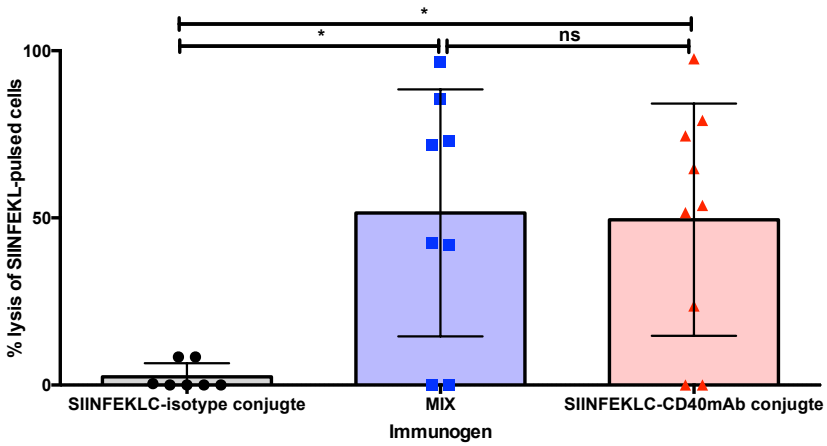

Figure 5.7. Percentage antigen-specific $CD8^+$ T cell lysis of SIINFEKL-pulsed target cells in the spleen. The value shown represents the relative percentage lysis of the SIINFEKLC-CD40mAb, MIX and GL117mAb conjugate immunised groups to the PBS immunised group, using the formula: $(1 - (r^{PBS}/r^{immunised})) \times 100$. The results are representative of two experiments of a total of 8 mice for each group. One-way ANOVA using Tukey's multiple comparisons test (mean +/- SD) was used to determine statistical significance, *p<0.05.
r = number of $CFSE^{HIGH}$ events/number of $CFSE^{LOW}$ events of each mouse spleen.

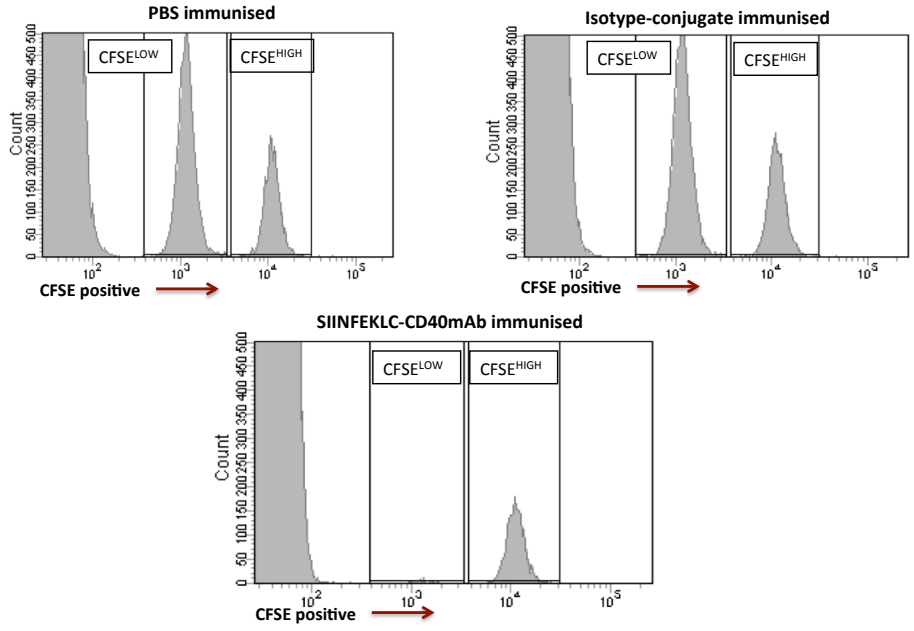

Figure 5.8. Representative results from one spleen harvested from PBS, SIINFEKLC-CD40mAb and SIINFEKLC-GL117mAb conjugate immunised mice. Histograms show numbers of control unpulsed $CFSE^{HIGH}$ stained cells and target SIINFEKL-pulsed $CFSE^{LOW}$ stained cells in the spleens.

5.3. Effects of SIINFEKLC-mAb conjugates on APC co-stimulatory molecule expression *in vitro*

Prior to proceeding to SIINFEKLC-CD40mAb uptake and targeting experiments, we wanted to demonstrate whether this conjugate also enhanced co-stimulatory molecule expression of DCs and B cells. Similar to Section 4.3.2, CD80 and CD86 expression by splenic B cells and splenic $CD11c^+$ DCs was investigated following incubation of splenocytes with 10µg/ml SIINFEKLC-mAb conjugates or SIINFEKLC peptide, as well as 200ng/ml LPS, which served as a positive control (Figure 5.9). SIINFEKLC alone served as a negative control. Flow cytometric analysis of the fold increase in median fluorescence intensity of CD80 and CD86 expression on $CD19^+$ (Figure 5.9A) and $CD11c^+$ (Figure 5.9B) cells above the unstimulated control was performed (*see* Section 2.2.6.6.). The experiment was repeated using BM-DC to investigate whether the results were consistent upon the use of an immature homogeneous population of DCs (Figure 5.10).

Splenic B cell results were consistent with previous studies (Carlring et al., 2012) as well as the results shown in Chapter 4. Both CD80 and CD86 expression were significantly enhanced ($p<0.01$, $p<0.001$, two-tailed, unpaired Student t test) on stimulation with the SIINFEKLC-CD40mAb conjugate compared to the SIINFEKLC-GL117Ab conjugate control (Figure 5.9). Interestingly, SIINFEKLC-CD40mAb conjugate significantly upregulated both splenic $CD11c^+$ (Figure 5.9B) and BM-DC (Figure 5.10) CD80 and CD86 expression compared to controls ($p<0.05$, two-tailed unpaired Student t test).

In summary, SIINFEKLC-CD40mAb conjugates enhanced co-stimulatory molecule expression of both B cells and DCs compared to the SIINFEKLC-GL117mAb conjugate *in vitro*.

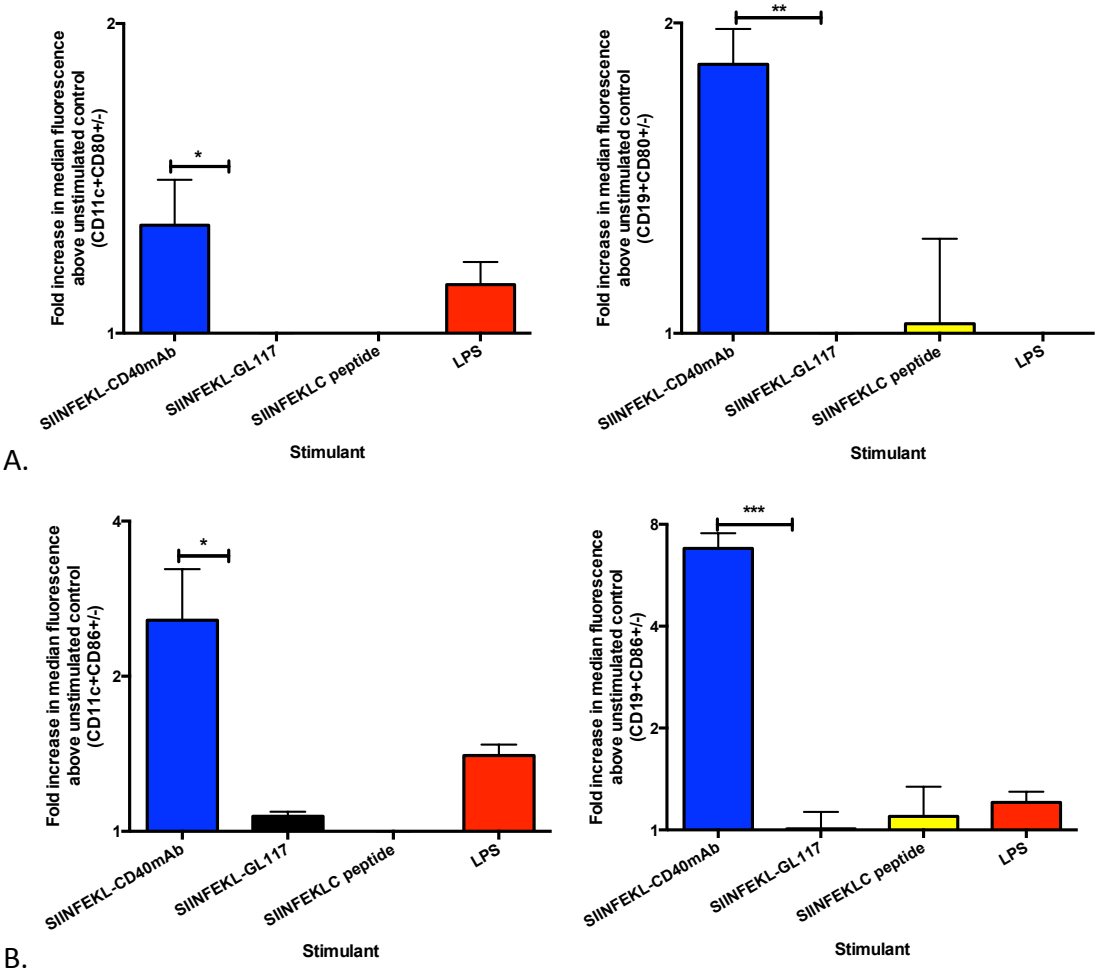

Figure 5.9. CD80 and CD86 expression on splenic B cells and CD11c$^+$ DCs upon incubation with SIINFEKLC-mAb conjugate. Splenocytes (1 x 10^6 cells/ml) were incubated in the presence of stimulant; 10µg/ml SIINFEKL-mAb conjugates, 10µg/ml SIINFEKL peptide, 200ng/ml LPS, or in the absence of stimulant for 24 hours in a 48-well plate (1ml). The fold increase in median fluorescence intensity (MFI) of the (A) CD80 expression or (B) CD86 expression above the unstimulated control on CD11c$^+$ cells (left) (A) and CD19$^+$ cells (right) is shown. Unpaired two-tailed Student's t-test (mean +/- SD) was used to determine statistical significance. *P<0.05, **P<0.01, ***P<0.001. This figure represents results from three separate experiments, each with a technical replicate of 1.

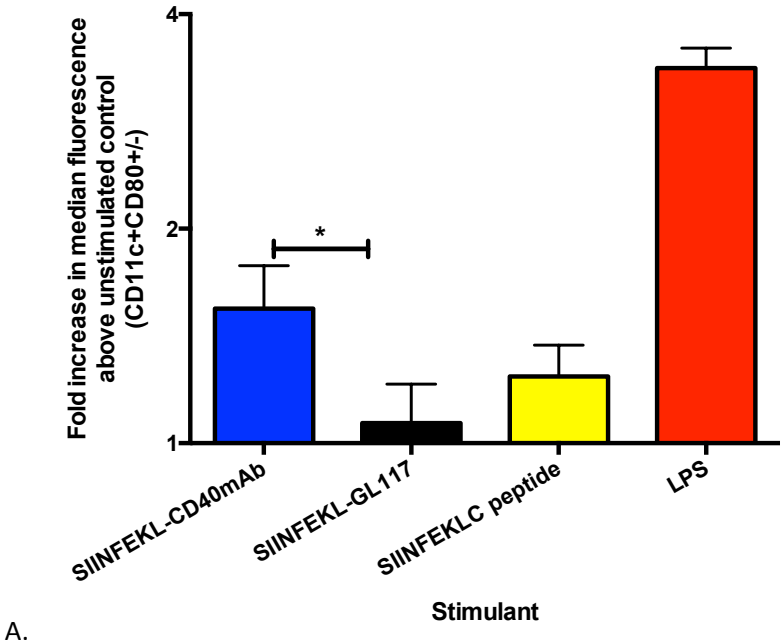

A.

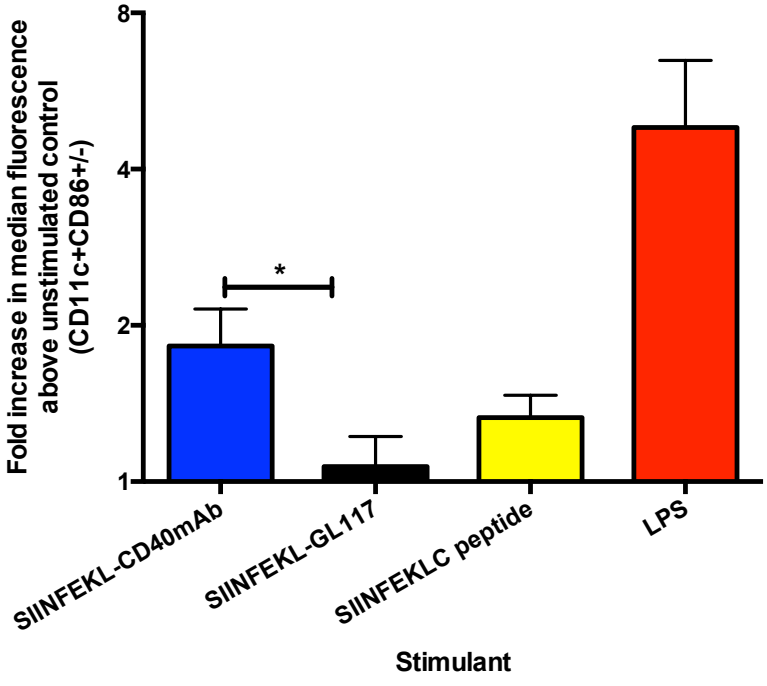

B.

Figure 5.10. CD80 and CD86 expression on BM-DCs upon incubation with SIINFEKLC-mAb conjugate. BM-DCs (1 x 10^6 cells/ml) were incubated in the presence of stimulant; 10µg/ml SIINFEKL-mAb conjugates, 10µg/ml SIINFEKL peptide, 200ng/ml LPS, or in the absence of stimulant for 24 hours in a 48-well plate (1ml). The fold increase in median fluorescence intensity (MFI) of the CD80 (A) or CD86 (B) on $CD11c^+$ BM-DCs expression above the unstimulated control is shown. Unpaired two-tailed Student's t-test (mean +/- SD) was used to determine statistical significance. *$p<0.05$. This figure represents results from three separate experiments, each with a technical replicate of 1.

5.4. Investigation into CD40mAb-adjuvanted conjugate targeting and uptake by B cells and BM-DCs *in vitro*

To investigate whether both the CD40mAb and the conjugated antigen are co-delivered to the same APC and internalised, SIINFEKLC and CD40mAb were fluorescently labelled prior to conjugation. It has been shown that CD40mAb targets B cells, DCs and macrophages and that co-stimulatory molecule expression on B cells is enhanced as a result *in vitro* (Carlring et al., 2012). More information regarding the uptake of CD40mAb-adjuvanted conjugates would shed light on the mechanism of action of the adjuvant.

5.4.1. Production and *in vitro* testing of fluorescently-labelled SIINFEKLC-mAb conjugates

SIINFEKLC (1066Da) was fluorescently labelled with NHS-fluorescein (473.4Da), whilst CD40mAb (approximately 150kDa) was fluorescently labelled with DyLight 650 NHS ester (1066Da) (*see* Section 2.2.1.5.). Both NHS-fluorescein, which will be referred to as FAM and Dylight 650 NHS-ester, which will be referred to as Dylight, were chosen due to (i) their relatively low MW (especially FAM) (ii) amine-reactivity and (iii) emission spectra (which do not overlap).

The MW was taken into consideration, and both FAM and Dylight have low MW relative to SIINFEKLC and CD40mAb respectively. This was performed to minimise any interference of the labelled dye with the conjugation between SIINFEKLC and CD40mAb, and to ensure that the results were representative of the unlabelled CD40mAb-adjuvanted conjugates.

NHS-ester chemistry was used to both label the CD40mAb via side-chains of lysines (K) or the amino-terminal (NH_2) group, and conjugate it to the sulphydryl groups on the cysteine present on the C-terminal end of the SIINFEKLC peptide**.** Due to this Dylight was first conjugated to the CD40mAb or isotype control antibody, GL117mAb, at different molar excess, starting at a molar excess of 7 (as recommended by the manufacturer, *see* Section 2.2.1.5.2.). Labelling at a molar

excess of 3.5, 1.75 and 1 was also performed. This was to ensure that sufficient amino groups were available for treatment with Sulfo-SMCC (another amine-reactive reagent) and subsequent conjugation to SIINFEKLC peptide. Excess dye was removed by means of a 100kDa filter. A filter with such a large pore size was used to ensure the removal of all excess dye, including dye complexes. To investigate the relative brightness, the labelled antibodies were analysed on CD40L929 cells by flow cytometry (Figure 5.11, *see* Section 2.2.4.4.1.).

An increase in fluorescence was observed with all labelled CD40mAb compared to their respective labelled isotype mAb controls (Figure 5.11A). Considering that labelling at the molar excess of 7 was the brightest, and recommended by the manufacturer for best labelling of the CD40mAb, we assumed that not many amino groups would remain available for optimal conjugation to SIINFEKLC. On the contrary, labelling at a molar excess of 1.75 and 0.9 was not of sufficient fluorescent intensity for use (Figure 5.11B). Therefore the CD40mAb labelled with a molar excess of 3.5 was used for subsequent experiments.

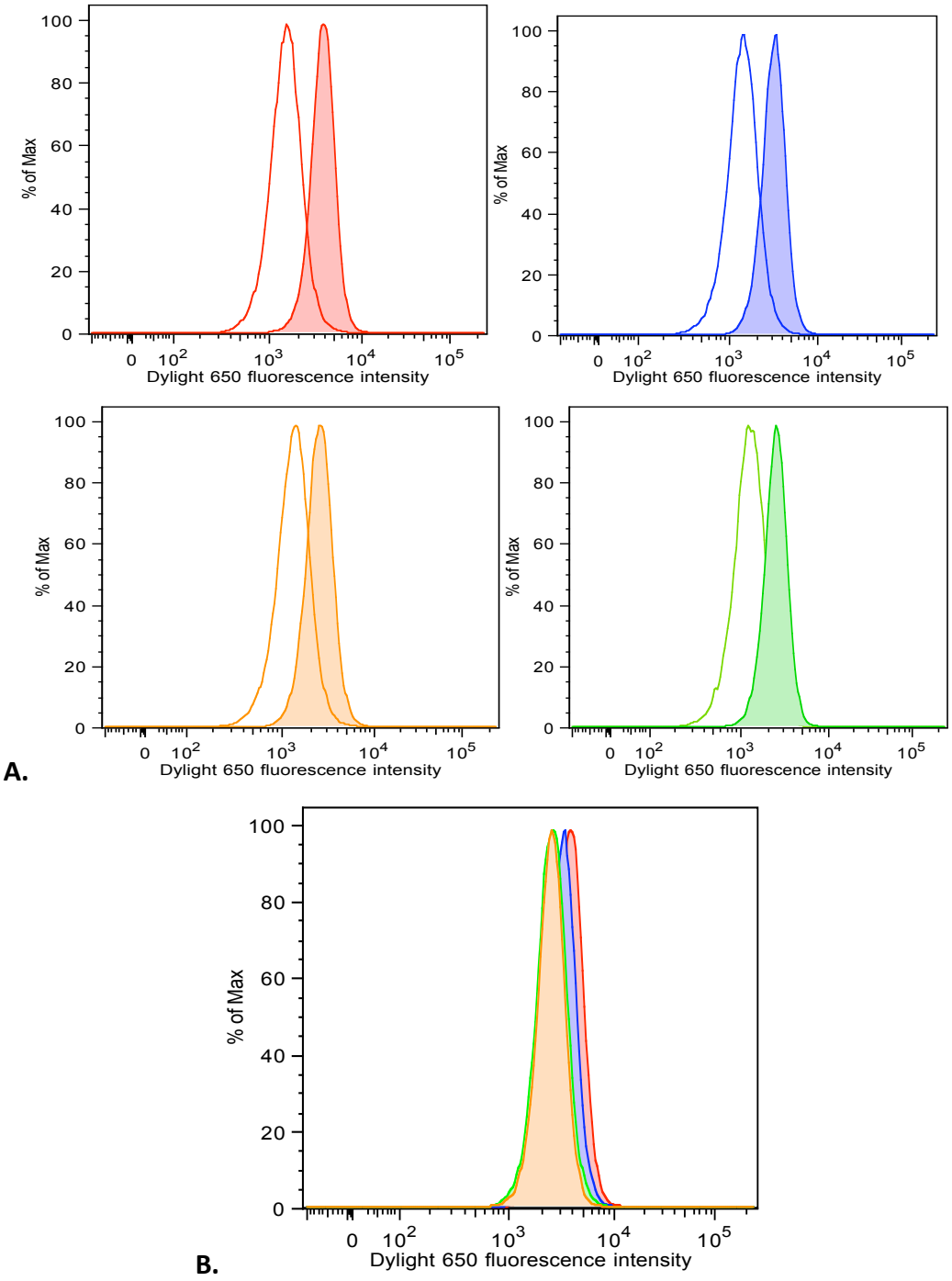

Figure 5.11. Fluorescence intensity of CD40mAb labelled with a range of molar excess of Dylight 650. A. Relative binding of $CD40mAb_{Dylight}$ at a molar excess of 7 (red), 3.5 (blue), 1.75 (orange), 0.9 (green) and their respective labelled isotype controls (outline histograms) to CD40L929 cells. B. Relative binding of all labelled CD40mAb (same colours as A) to CD40L929 cells.

SIINFEKLC was labelled with a 20 molar excess of FAM dye. Once again since no filter with pore size small enough to remove excess FAM dye by buffer exchange without losing valuable sample is available, the same precautions discussed in detail in Section 4.4.1. with biotin labelling were taken (*see* Section 2.2.1.5.3.).

CD40mAb (or respective isotype mAb control) labelled with 3.5 molar excess Dylight ($CD40mAb_{Dylight}$) was subsequently treated with Sulfo-SMCC and conjugated to the sulphydryl groups on the cysteine present on the C-terminal end of the SIINFEKLC labelled with FAM ($SIINFEKLC_{FAM}$). $SIINFEKLC_{FAM}$ was also conjugated to unlabelled CD40mAb for use as a control in the experiments carried out in Section 5.4.2.

FAM used to label SIINFEKLC was also mixed with SMCC-treated mAb in order to ensure that the NHS-ester was non-reactive and would not also bind to the mAb during FAM-labelled peptide-mAb conjugation (*see* Section 2.2.1.5.3.). This will be referred to as FAM+CD40mAb.

Confirmation of conjugation was performed by flow cytometric analysis on CD40L929 fibroblast cells (Figure 5.12). Since the experiments carried out in Section 5.4.2 just involved the addition of $SIINFEKLC_{FAM}$-$CD40mAb_{Dylight}$ conjugate and $SIINFEKLC_{FAM}$-$GL117_{Dylight}$ to the APCs without any washing steps, no washing steps were carried out during staining with CD40L929 cells. This was carried out to ensure that a shift was still observed by $SIINFEKLC_{FAM}$-$CD40mAb_{Dylight}$ conjugate relative to $SIINFEKLC_{FAM}$-$GL117_{Dylight}$ conjugate, when excess unbound conjugate was not removed.

A shift to the right of the $SIINFEKLC_{FAM}$-$CD40mAb_{Dylight}$ and $SIINFEKLC_{FAM}$-CD40mAb conjugate bound to the CD40L929 cells, relative to $SIINFEKLC_{FAM}$-$GL117_{Dylight}$ and $SIINFEKLC_{FAM}$-GL117 (respectively) by both FAM (Figure 5.12A,B) and Dylight (Figure 5.12C) histograms confirm conjugation. A shift to the right of the $SIINFEKLC_{FAM}$-$CD40mAb_{Dylight}$ and $SIINFEKLC_{FAM}$-CD40mAb conjugate was also observed relative to FAM+CD40mAb indicating that FAM did not conjugate to the CD40mAb. The fluorescence intensity of both FAM and Dylight were deemed sufficient for subsequent experiments.

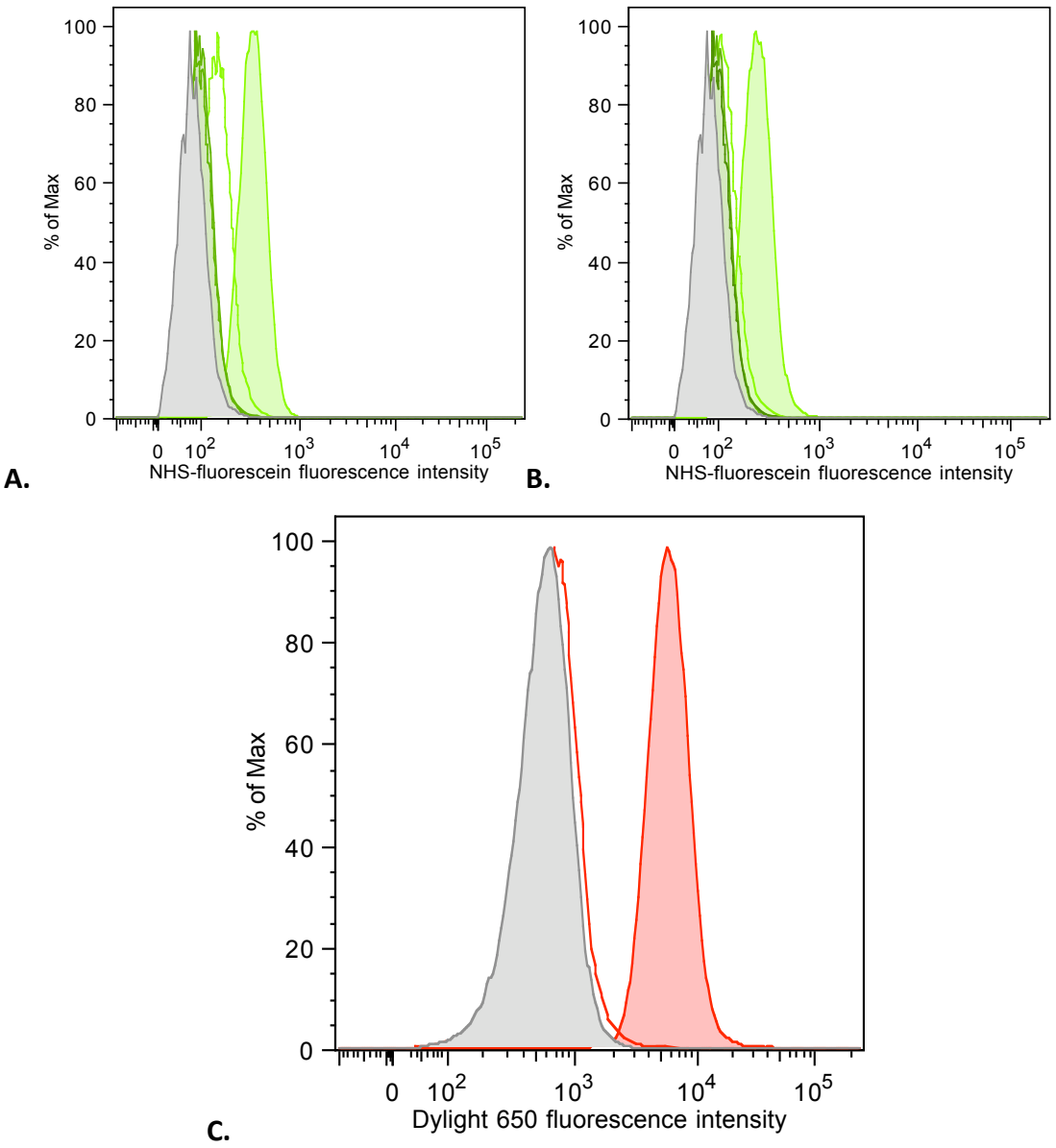

Figure 5.12. Fluorescence intensity of labelled SIINFEKLC-CD40mAb conjugates bound to CD40L929 cells. A. Relative binding of SIINFEKLC$_{FAM}$-CD40mAb (solid, light green), SIINFEKLC$_{FAM}$-GL117mAb (outline, light green) and FAM+CD40mAb (dark green) to CD40L929 cells. B. Relative binding of SIINFEKLC$_{FAM}$-CD40mAb$_{Dylight}$ (solid, light green), SIINFEKLC$_{FAM}$-GL117mAb$_{Dylight}$ (outline, light green) and FAM+CD40mAb (dark green) to CD40L929 cells. C. Relative binding of SIINFEKLC$_{FAM}$-CD40mAb$_{Dylight}$ (solid, red) and SIINFEKLC$_{FAM}$-GL117mAb$_{Dylight}$ (outline, red) to CD40L929 cells. Grey histogram represents UV live/dead stained population only.

5.4.2. Targeting and uptake of fluorescently labelled SIINFEKLC-CD40mAb conjugates by BM-DCs and B cells at different time-points

Fluorescently labelled SIINFEKL$_{FAM}$-CD40mAb$_{Dylight}$ conjugates were used to investigate whether both SIINFEKL$_{FAM}$ and CD40mAb$_{Dylight}$ were co-delivered to the same APC *in vitro using* epifluorescence microscopy (*see* Section 2.2.6.7.). To investigate whether the uptake was time-dependent BM-DCs and splenocytes were cultured *in vitro* in the presence of 10µg/ml of SIINFEKL$_{FAM}$-CD40mAb$_{Dylight}$ or SIINFEKL$_{FAM}$-GL117$_{Dylight}$ (control conjugate) in a 96-well plate (in a total volume of 100µl), for 5 minutes or 60 minutes. SIINFEKL$_{FAM}$-CD40mAb and SIINFEKL$_{FAM}$-GL117mAb as well as CD40mAb$_{Dylight}$ and GL117$_{Dylight}$ were used as single stain control samples to exclude autofluorescence. SIINFEKLC$_{FAM}$ (observed as green dots) and mAb$_{Dylight}$ (observed as red dots) co-localised in or on the cell surface were scored at each time-point.

5.4.2.1. Targeting and uptake of SIINFEKL$_{FAM}$-mAb$_{Dylight}$ conjugates by BM-DCs

Targeting and uptake of co-labelled SIINFEKLC-mAb conjugates by BM-DCs was investigated using normal wide-field fluorescence microscopy. A representative image of one BM-DC stimulated with 10µg/ml of SIINFEKL$_{FAM}$-CD40mAb$_{Dylight}$ or SIINFEKL$_{FAM}$-GL117$_{Dylight}$ at different time-points is shown in Figure 5.12. The co-localised Dylight (red dots) and FAM (green dots) inside the BM-DCs or on the BM-DC surface were scored. The number of co-localised mAb and SIINFEKL were counted on twenty different BM-DCs per field (in a total of six fields)

BM-DCs stimulated with SIINFEKL$_{FAM}$-CD40mAb$_{Dylight}$ for 5 minutes looked different to the BM-DCs stimulated for 60 minutes (Figure 5.12A) in that the FAM dye appeared brighter at 5 minutes than at 60 minutes, whilst the Dylight dye kept the same intensity. This lead to the assumption that the SIINFEKL$_{FAM}$ might be directed to a different cellular compartment of lower pH between 5 and 60 minutes causing the intensity of the dye to be slightly quenched.

There was a morphological difference between stimulation with SIINFEKL$_{FAM}$-CD40mAb$_{Dylight}$ or the SIINFEKL$_{FAM}$-GL117$_{Dylight}$ at both time points (Figure 5.12B). Both stimulated BM-DCs showed co-localised red and green dots, however, the merged image of BM-DCs stimulated at 5 minutes with SIINFEKL$_{FAM}$-GL117$_{Dylight}$ showed brighter dots. This is an indication that the SIINFEKL$_{FAM}$-GL117$_{Dylight}$ conjugate was being internalised by another route and present in a different cellular compartment. In addition, whereas a decrease in FAM brightness was observed after 60 minutes of stimulation with SIINFEKL$_{FAM}$-CD40mAb$_{Dylight}$, this decrease in intensity was not observed by stimulation with SIINFEKL$_{FAM}$-GL117$_{Dylight}$ conjugate. In fact, on closer examination of the SIINFEKL$_{FAM}$-GL117$_{Dylight}$ merged image, although red and green dots were observed next to each other, they are not overlaid like the SIINFEKL$_{FAM}$-CD40mAb$_{Dylight}$ merged image. This could mean that SIINFEKLC and GL117 might not be still bound together.

After 5 minutes of BM-DC stimulation the number of co-localised SIINFEKL$_{FAM}$ and mAb$_{Dylight}$ on the surface or inside 120 BM-DCs was statistically ($p<0.0001$, unpaired Mann-Whitney test) higher when cells were stimulated with SIINFEKL$_{FAM}$-CD40mAb$_{Dylight}$ than with SIINFEKL$_{FAM}$-GL117$_{Dylight}$ conjugate (Figure 5.13A). The result was not dependent on the field of view (Figure 5.13B), as the average number of co-localised dots per cell counted between the different fields of view was similar, and a significant difference ($p<0.01$, unpaired Mann-Whitney test) between SIINFEKL$_{FAM}$-CD40mAb$_{Dylight}$ and SIINFEKL$_{FAM}$-GL117$_{Dylight}$ conjugate was still observed. Moreover, 10 or more co-localised dots were counted in 98% of the BM-DCs stimulated with SIINFEKL$_{FAM}$-CD40mAb$_{Dylight}$ conjugate and in 51% on those stimulated with SIINFEKL$_{FAM}$-GL117$_{Dylight}$ conjugate (Figure 5.14).

A.

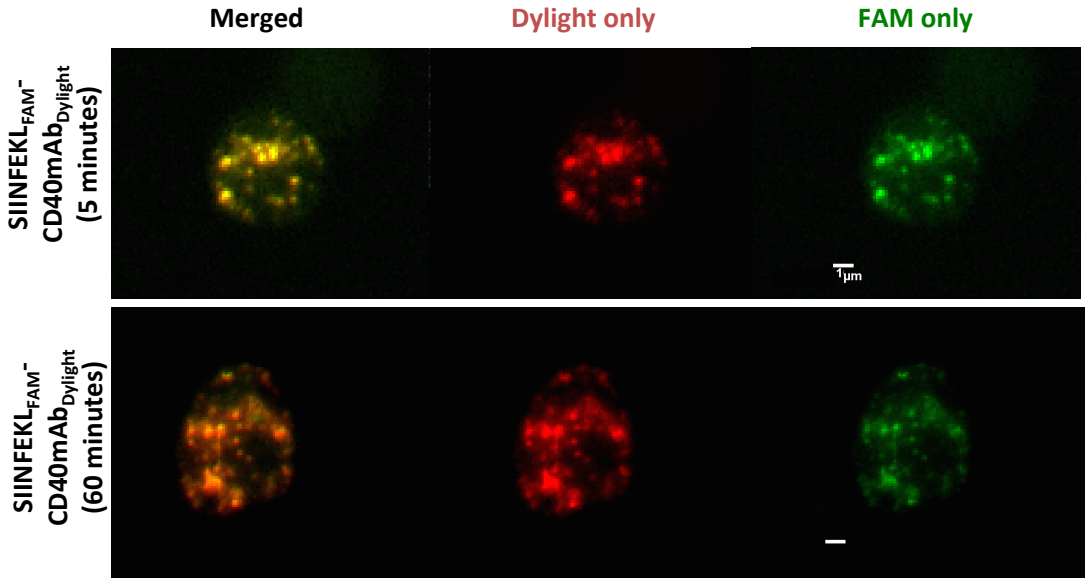

B.

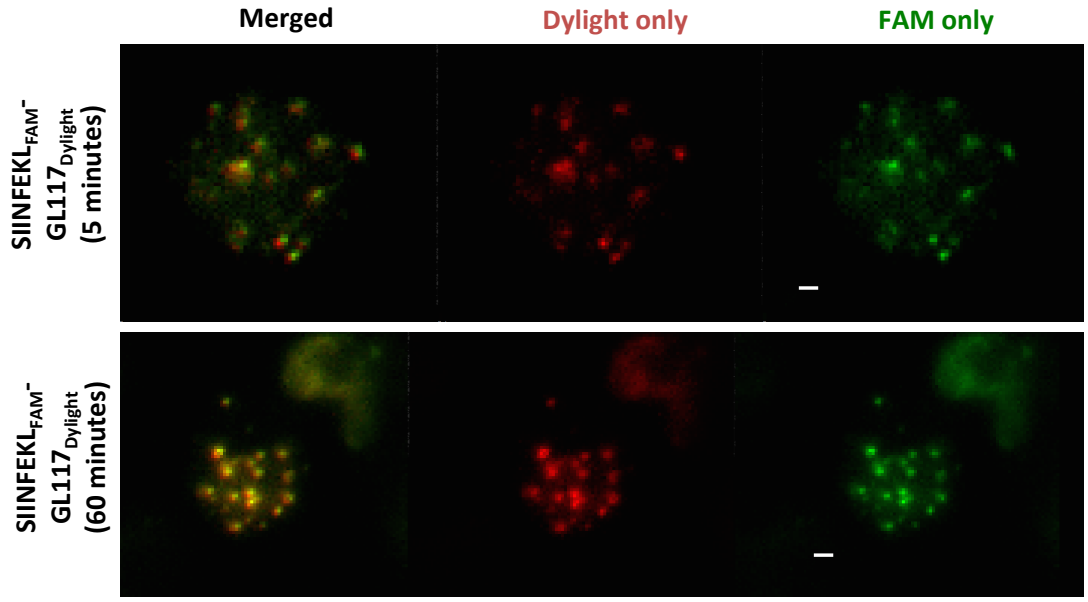

Figure 5.12. Representative images of BM-DCs incubated with SIINFEKL$_{FAM}$-CD40mAb$_{Dylight}$ conjugate (A) and SIINFEKL$_{FAM}$-GL117$_{Dylight}$ conjugate (B) for 5 minutes or 60 minutes. Shown are fluorescence microscopy images of CD40mAb$_{Dylight}$ or GL117$_{Dylight}$ component of conjugate observed as red dots, SIINFEKLC$_{FAM}$ component of conjugate observed as green dots and an overlay or merged image of both (red and green dots). Scale bar - 1µm.

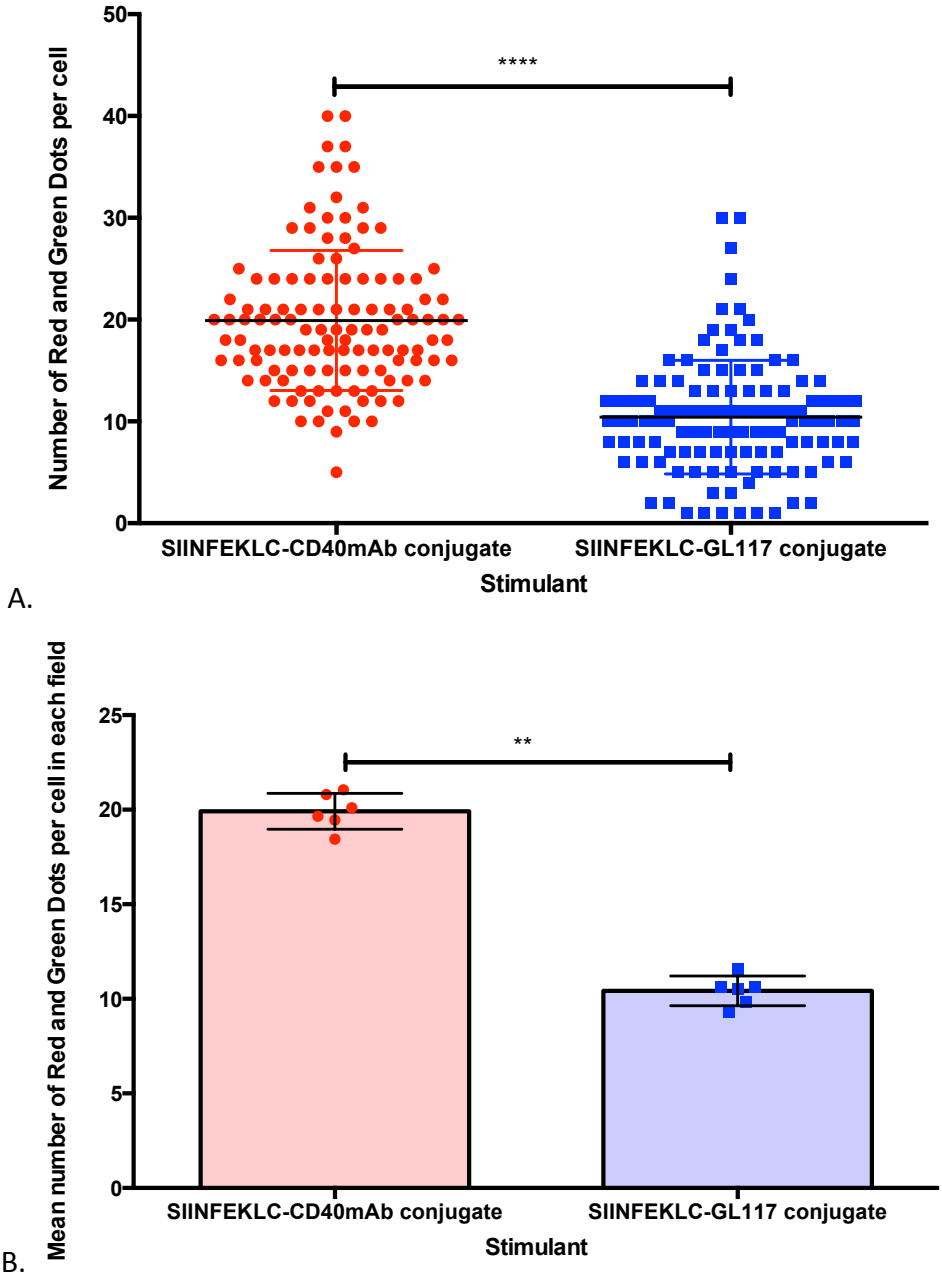

Figure 5.13. Quantification of co-localised SIINFEKLC$_{FAM}$-mAb$_{Dylight}$ conjugates in BM-DCs after 5 minutes of incubation *in vitro*. The number of co-localised mAb and SIINFEKLC internalised or on BM-DC surface were counted on 20 cells per field of view (total of six fields). A. Pooled data of all fields of view (120 cells). B. The mean number of co-localised mAb and SIINFEKLC in each cell in each of the six fields of view. An unpaired Mann-Whitney test was used to determine statistical significance (mean +/- SD). **p<0.01, **** p<0.0001.

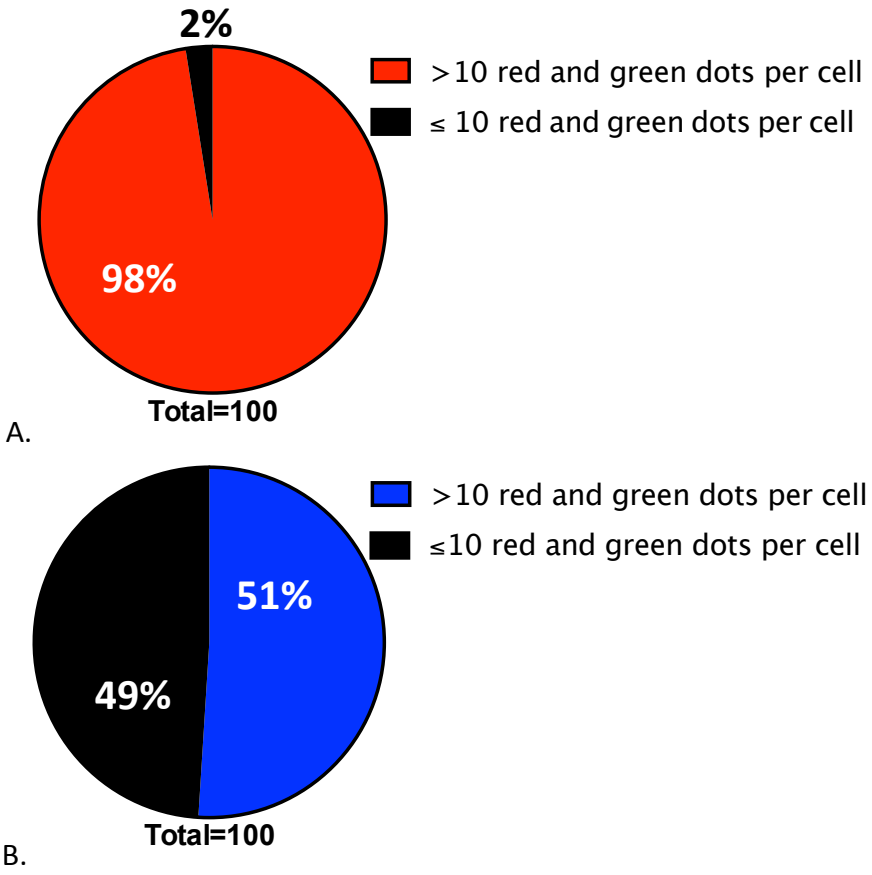

Figure 5.14. Percentage of cells containing co-localised SIINFEKLC and mAb after 5 minutes of incubation. The number of cells containing >10 (red or blue) and ≤10 (black) co-localised mAb and SIINFEKL are shown as a percentage of all the cells counted in the six fields of view. A. $SIINFEKL_{FAM}$-$CD40mAb_{Dylight}$. B. $SIINFEKL_{FAM}$-$GL117_{Dylight}$.

After 60 minutes stimulation of BM-DCs with fluorescently labelled conjugates, results were similar to the results observed after 5 minutes of stimulation. The number of co-localised $SIINFEKL_{FAM}$ and $mAb_{Dylight}$ targeting and internalised by 120 BM-DCs was statistically higher ($p<0.0001$, unpaired Mann-Whitney test) when cells were stimulated with $SIINFEKL_{FAM}$-$CD40mAb_{Dylight}$ than with $SIINFEKL_{FAM}$-$GL117_{Dylight}$ conjugate (Figure 5.15A). The result was not dependent on the field of view (Figure 5.15B, $p<0.01$, unpaired Mann-Whitney test). The number of co-localised dots counted in BM-DCs stimulated with $SIINFEKL_{FAM}$-$GL117_{Dylight}$ conjugate did not increase after 60 minute incubation and was still observed in 52% of all cells (Figure 5.16). Uptake of $SIINFEKL_{FAM}$-$CD40mAb_{Dylight}$ conjugate was time-dependent ($p<0.01$, two-tailed, unpaired Mann-Whitney test) (Figure 5.17). Even though the results showed that targeting and uptake occurs very quickly (after 5 minutes), after 60 minute stimulation cells internalise an increased amount of conjugate, in fact 10% contain >35 co-localised dots, compared to the 2.5% of those stimulated for 5 minutes.

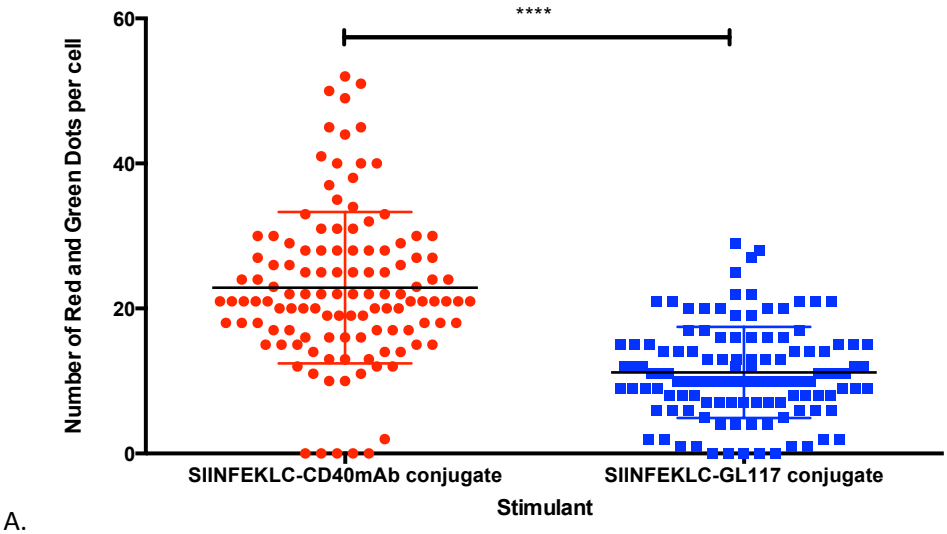

A.

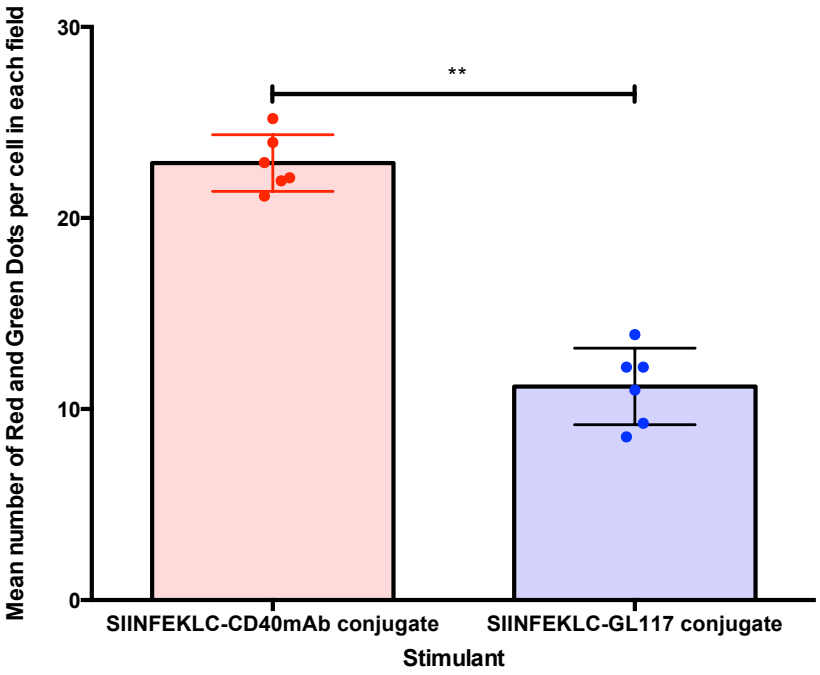

B.

Figure 5.15. Quantification of co-localised SIINFEKLC$_{FAM}$-mAb$_{Dylight}$ conjugates in BM-DCs after a 60 minute incubation *in vitro*. The number of co-localised mAb and SIINFEKL internalised or on BM-DC surface were counted on 20 cells in six fields of view (a total of 120 cells). A. Pooled data of all fields of view. B. The mean number of co-localised mAb and SIINFEKL in each cell in each of the six fields of view. An unpaired Mann-Whitney test was used to determine statistical significance (mean +/- SD). **p<0.01, **** p<0.0001.

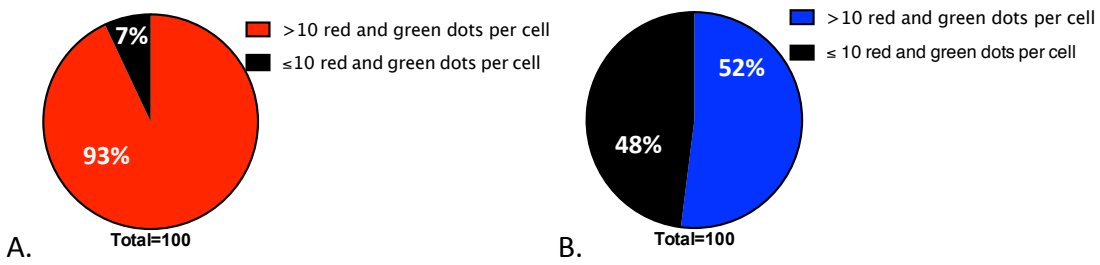

Figure 5.16. Percentage of cells containing co-localised SIINFEKLC and mAb after 60 minute incubation. The number of cells containing > 10 (red or blue) and ≤ 10 (black) co-localised mAb and SIINFEKL are shown as a percentage number of all the cells counted in the six fields of view. A. $SIINFEKL_{FAM}$-$CD40mAb_{Dylight}$. B. $SIINFEKL_{FAM}$-$GL117_{Dylight}$.

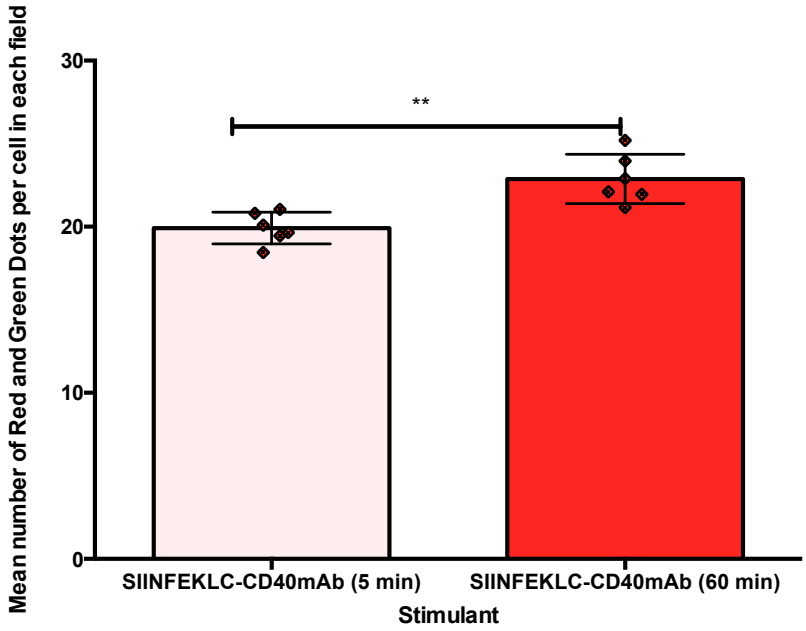

Figure 5.17. Time dependent uptake by BM-DC stimulated with $SIINFEKL_{FAM}$-$CD40mAb_{Dylight}$ conjugate. The number of co-localised mAb and SIINFEKL internalised or on BM-DC surface were counted on 20 cells in six fields of view. The mean number of co-localised mAb and SIINFEKL in each cell in each field of view, after 5 minutes (pale red) and 60 minutes (red) incubation is shown. An unpaired Mann-Whitney test was used to determine statistical significance (mean +/- SD). **p<0.01

5.4.2.2. Targeting and uptake of SIINFEKL$_{FAM}$-mAb$_{Dylight}$ conjugates by B cells

The study was expanded to investigate targeting and uptake of co-labelled SIINFEKLC-mAb conjugates by B cells. A representative image of one B cell stimulated with 10µg/ml of SIINFEKL$_{FAM}$-CD40mAb$_{Dylight}$ or SIINFEKL$_{FAM}$-GL117$_{Dylight}$ at different time-points is shown in Figure 5.18. As splenocytes were used in this experimental setup, a CD19^{+} marker was used to identify the B cells (visualised in blue). The co-localised Dylight (red) and FAM (green) dots within the CD19^{+} B cell stimulated with SIINFEKL$_{FAM}$-CD40mAb$_{Dylight}$ or SIINFEKL$_{FAM}$-GL117$_{Dylight}$ for 5 and 60 minutes were scored (*see* Section 2.2.6.7.2.). Co-localised red and green dots observed inside or on the surface of B cells when stimulated with SIINFEKL$_{FAM}$-CD40mAb$_{Dylight}$ for 5 minutes were dimmer than after 60 minute stimulation (Figure 5.18A), possibly indicating that the conjugates were only internalised after 5 minutes of incubation. Interestingly, the opposite occurred in B cells stimulated with SIINFEKL$_{FAM}$-GL117$_{Dylight}$ (Figure 5.18B). This could be due to the isotype-control conjugate being internalised by another mechanism (not via the CD40 receptor), and therefore processed differently.

Fewer cells were observed in each field of view compared to the BM-DC experiments because the magnification used was higher. Therefore the maximum number of cells per field (in a total of six fields) were scored. This resulted in a total of 112 cells counted for SIINFEKL$_{FAM}$-CD40mAb$_{Dylight}$ conjugate group and a total of 76 cells for the SIINFEKL$_{FAM}$-GL117$_{Dylight}$ conjugate group (Figure 5.19). The number of B cell surface or internalised co-localised SIINFEKL$_{FAM}$ and mAb$_{Dylight}$ was not significantly different when cells were stimulated for 5 minutes with SIINFEKL$_{FAM}$-CD40mAb$_{Dylight}$ than with SIINFEKL$_{FAM}$-GL117$_{Dylight}$ conjugate (Figure 5.19A). Figure 5.19B shows that the number of co-localised dots varies between the different fields of view ranging from an average of 1.5 per field to 6.5 per field. In addition, there was no difference in the percentage of co-localised dots observed with SIINFEKL$_{FAM}$-CD40mAb$_{Dylight}$ conjugate or SIINFEKL$_{FAM}$-GL117$_{Dylight}$ conjugate after 5 minute stimulation (Figure 5.20).

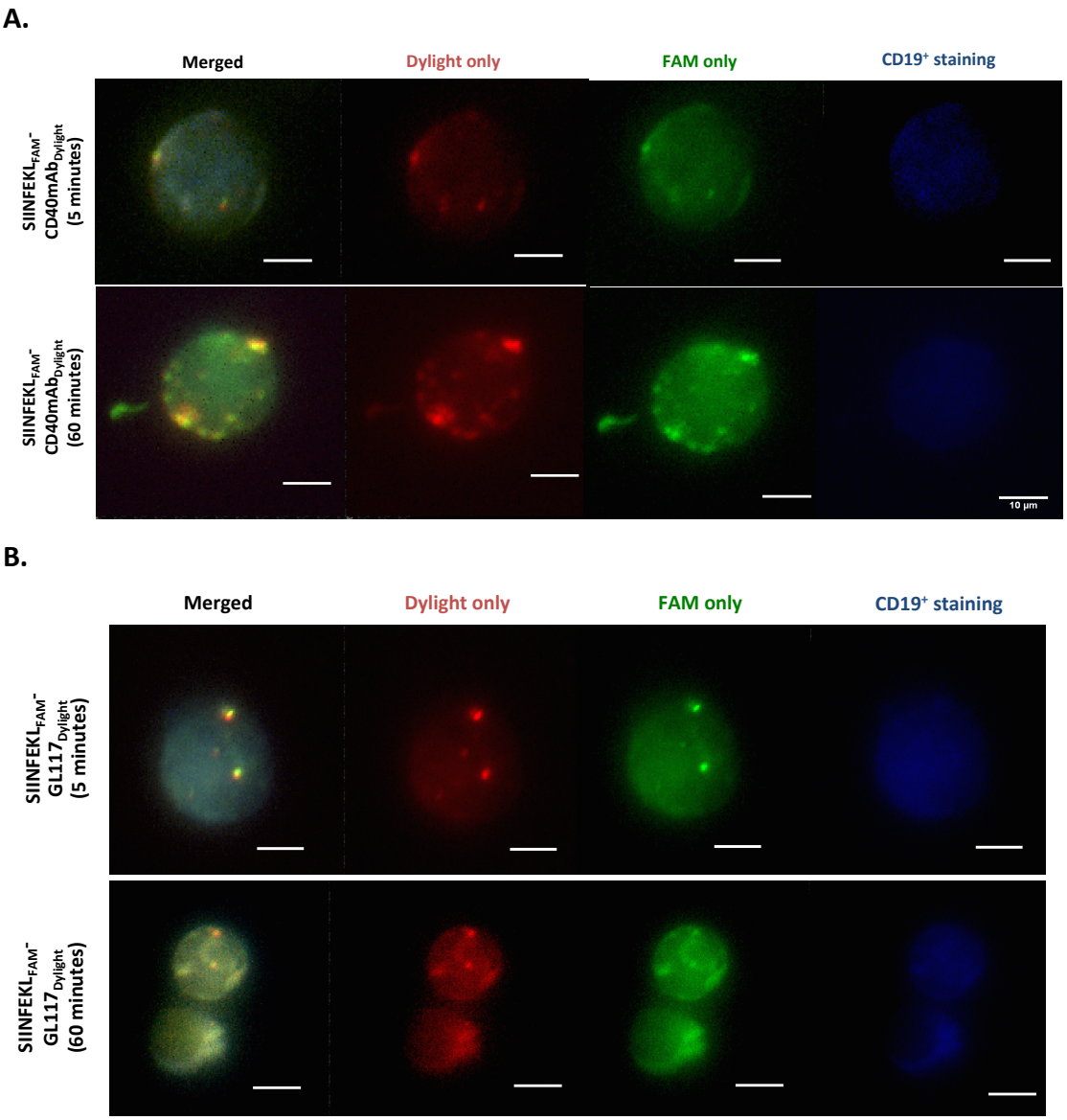

Figure 5.18. Representative images of B cells incubated with SIINFEKL$_{FAM}$-CD40mAb$_{Dylight}$ conjugate (A) and SIINFEKL$_{FAM}$-GL117$_{Dylight}$ conjugate (B) for 5 minutes and 60 minutes at a magnification of X40. Shown are fluorescence microscopy images of CD40mAb$_{Dylight}$ or GL117$_{Dylight}$ component of conjugate observed as red dots, SIINFEKLC$_{FAM}$ component of conjugate observed as green dots, CD19^{+} B cells observed in blue and an overlay or merged image of all (red and green dots on a blue background). Scale bar - 10µm.

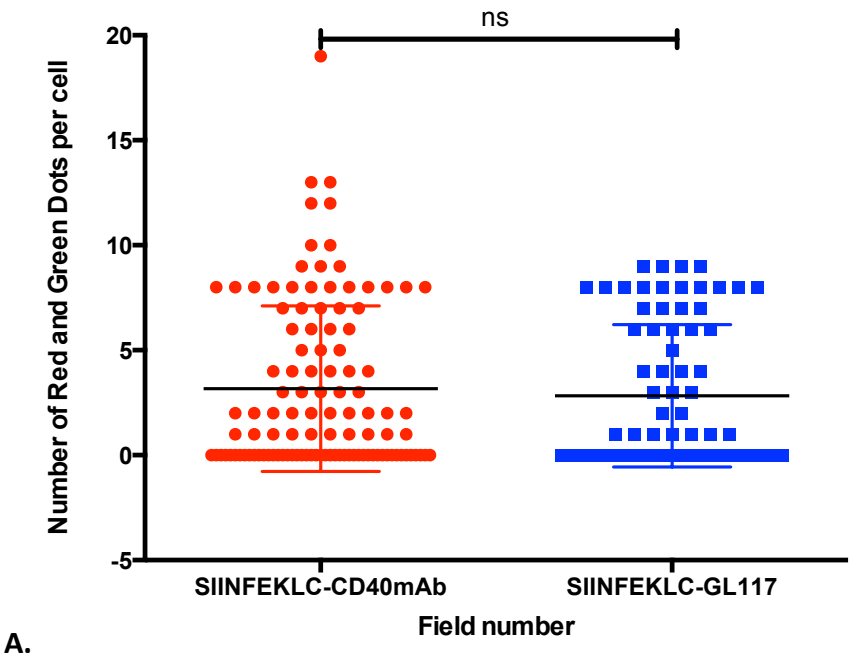

A.

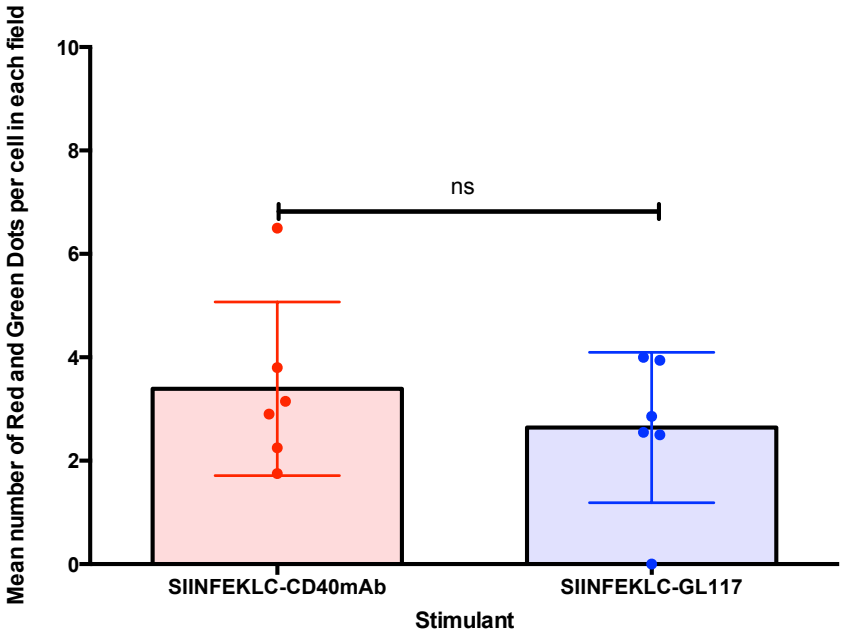

B.

Figure 5.19. Quantification of co-localised SIINFEKLC$_{FAM}$-mAb$_{Dylight}$ conjugates in B cells after a 5 minute incubation *in vitro*. The number of co-localised mAb and SIINFEKL internalised or on B cell surface were counted on 10-20 CD19^{+} cells per field of view in a total of six fields of view. A. Pooled data of all fields of view. B. The mean number of co-localised mAb and SIINFEKL in each cell in each field of view. An unpaired Mann-Whitney test was used to determine statistical significance (mean +/- SD). ns = not significant.

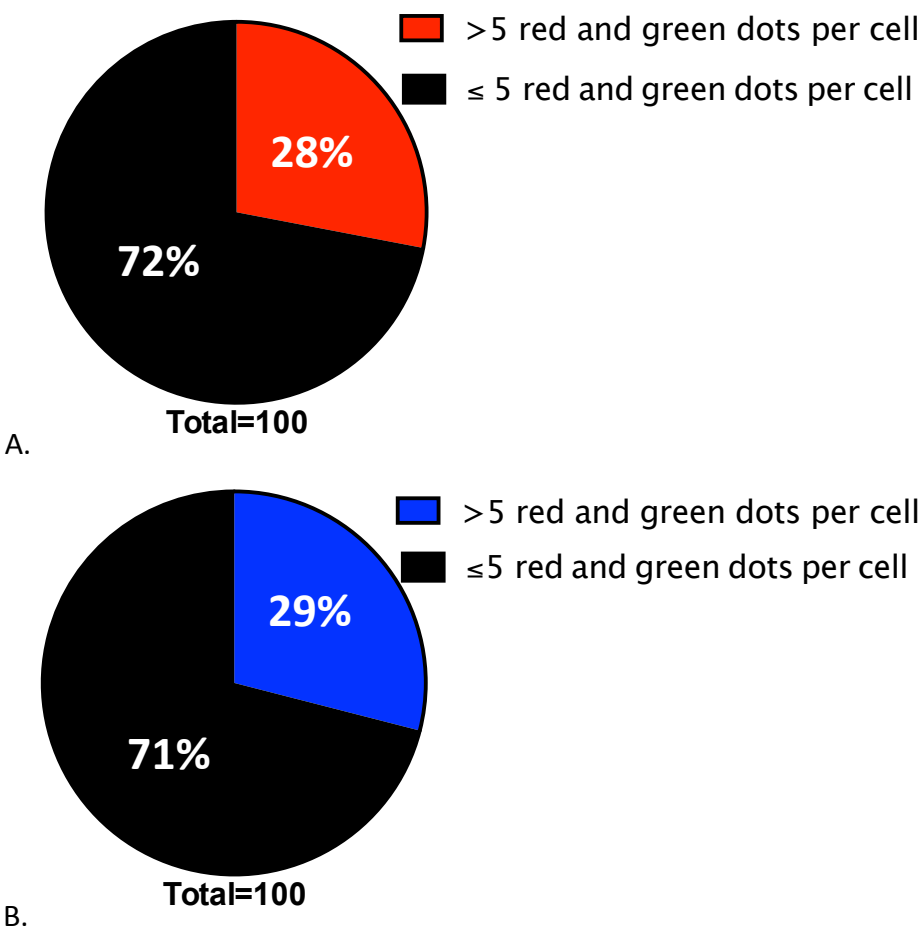

Figure 5.20. Percentage of cells containing co-localised SIINFEKLC and mAb after 5 minutes of incubation. The number of cells containing >5 and ≤5 co-localised mAb and SIINFEKL are shown as a percentage number of all the cells counted in the six fields of view. A. $SIINFEKL_{FAM}$-$CD40mAb_{Dylight}$ percentage uptake. B. $SIINFEKL_{FAM}$-$GL117_{Dylight}$ percentage uptake.

After 60 minutes of stimulation $CD19^+$ B cells showed significantly increased ($p<0.01$, unpaired Mann-Whitney test) co-localised red and green dots with $SIINFEKL_{FAM}$-$CD40mAb_{Dylight}$ conjugate compared to $SIINFEKL_{FAM}$-$GL117_{Dylight}$ conjugate (Figure 5.21A). The mean number of co-localised dots per cell (Figure 5.21B) in each field is less variable compared to results observed after 5 minutes of incubation (Figure 5.19). However, interestingly, this difference was not due to increased uptake of $SIINFEKL_{FAM}$-$CD40mAb_{Dylight}$. In fact the mean number of co-localised dots did not increase. The difference was due to the fact that the co-localised dots on B cells stimulated with $SIINFEKL_{FAM}$-$GL117_{Dylight}$ conjugate decreased after 60 minutes of incubation (Figure 5.22). The number of cells stimulated with $SIINFEKL_{FAM}$-$GL117_{Dylight}$ containing >5 dots decreased to 12% from 29% observed after 5 minutes of incubation. Targeting and uptake at 5 minutes and at 60 minutes only varied slightly on stimulation with the $SIINFEKL_{FAM}$-$CD40mAb_{Dylight}$ conjugate (Figure 5.23), possibly because the B cells were already saturated with $SIINFEKL_{FAM}$-$CD40mAb_{Dylight}$ conjugate after 5 minutes. However, a significant difference was observed between stimulation with $SIINFEKL_{FAM}$-$CD40mAb_{Dylight}$ conjugate and $SIINFEKL_{FAM}$-$GL117_{Dylight}$ conjugate at 60 minutes ($p<0.01$, unpaired Dunn's multiple comparison test), showing two routes of internalisation for the two conjugates.

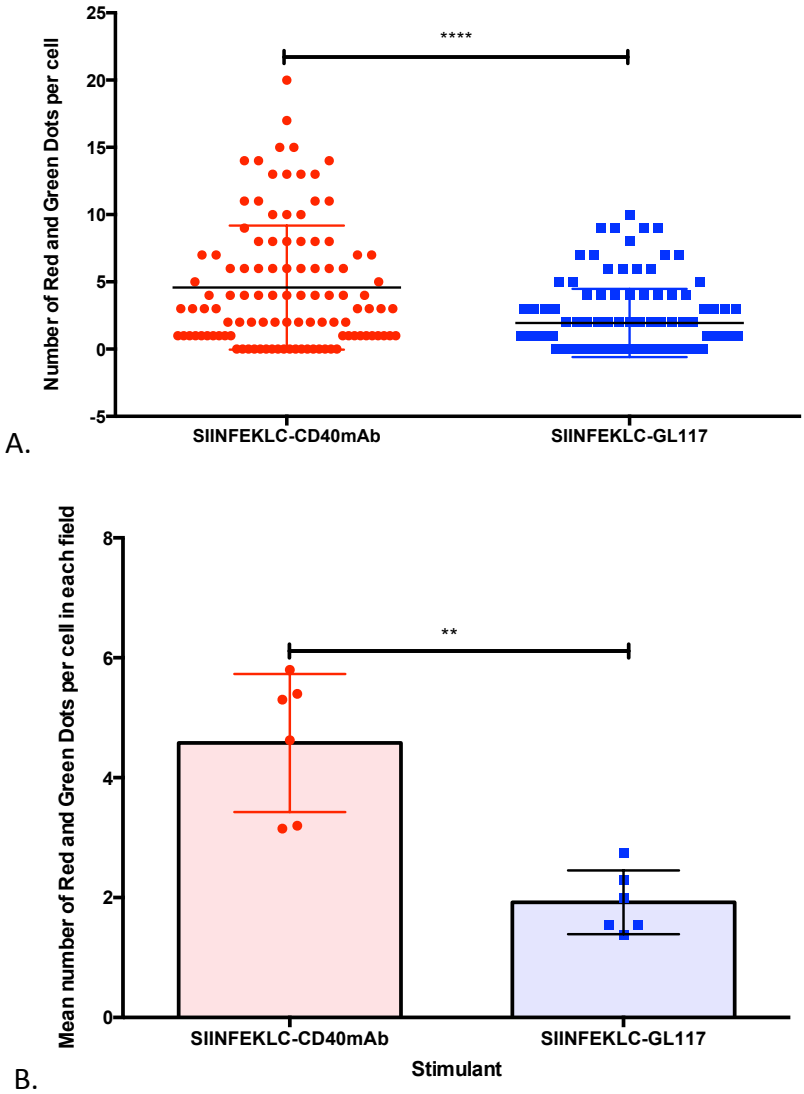

Figure 5.21. Quantification of co-localised SIINFEKLC$_{FAM}$-mAb$_{Dylight}$ conjugates in B cells after a 60 minute incubation *in vitro.* The number of co-localised mAb and SIINFEKL internalised or on B cell surface were counted on 10-20, CD19^{+} cells in six fields of view. A. Pooled data of all fields of view. B. The mean number of co-localised mAb and SIINFEKL in each cell in each field of view. An unpaired Mann-Whitney test was used to determine statistical significance (mean +/- SD). **p<0.01, **** p<0.0001.

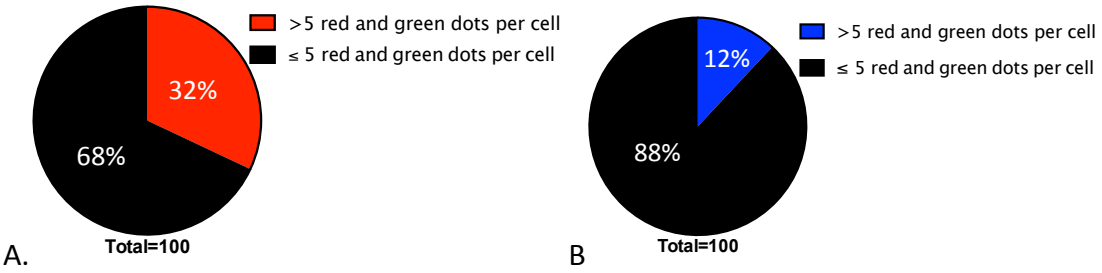

Figure 5.22. Percentage of cells containing co-localised SIINFEKLC and mAb after 60 minute incubation. The number of cells containing >5 and ≤5 co-localised antibody and SIINFEKL are shown as a percentage of all the cells counted in the six fields of view. A. $SIINFEKL_{FAM}$-$CD40mAb_{Dylight}$ percentage uptake. B. $SIINFEKL_{FAM}$-$GL117_{Dylight}$ percentage uptake.

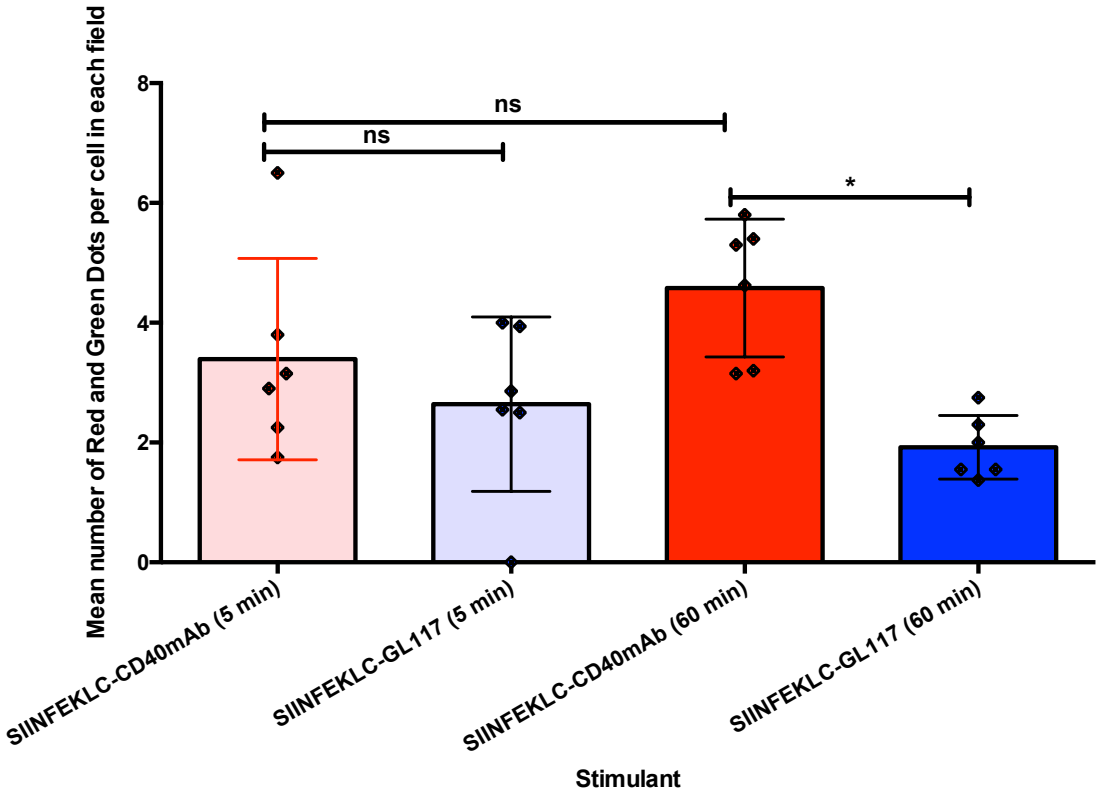

Figure 5.23. Time dependent uptake by B cells stimulated with $SIINFEKL_{FAM}$-$mAb_{Dylight}$ conjugate. The number of co-localised mAb and SIINFEKLC internalised or on B cell surface were counted in six fields of view. The mean number of co-localised antibody and SIINFEKL in each cell in each field of view, after 5 minutes (pale red and pale blue) and 60 minutes (dark red and dark blue) incubation is shown. $SIINFEKL_{FAM}$-$CD40mAb_{Dylight}$ is shown in red. $SIINFEKL_{FAM}$-$GL117_{Dylight}$ is shown in blue. An unpaired Dunn's (non-parametric) multiple comparison test was used to determine statistical significance (mean +/- SD). *p<0.05.

5.5. Effect of CD40mAb on B cell and DC antigen presentation to B3Z T hybridoma cells

The effect that SIINFEKLC-mAb conjugates, SIINFEKL peptide and CD40mAb mixtures had on B cell and BM-DC antigen-presentation to T cells *in vitro* was investigated, as was the ability of DCs or B cells to cross-present SIINFEKL to the OVA-specific B3Z T hybridoma cells (*see* Section 2.2.6.8.). Splenocytes were primarily used in co-culture with B3Z cells to establish the optimal concentration at which the SIINFEKLC-CD40mAb conjugate or mixture to be used *in vitro*.

Firstly, 10^5 splenocytes were stimulated with a mixture of CD40mAb (or GL117mAb) and SIINFEKL at a starting concentration of 20µg/ml and 2µg/ml respectively, and secondly SIINFEKLC-CD40mAb and SIINFEKLC-GL117 conjugates starting at a concentration of 20µg/ml. Two fold dilutions were then made to a concentration of 1.25µg/ml (mAb or SIINFEKL-mAb conjugate) and 0.125µg/ml (SIINFEKL).

Splenocytes were stimulated for 2 hours (Figure 5.24), 18 hours (results not shown) and 24 hours (results not shown) prior to addition of B3Z hybridoma cells. After the stimulation period, 10^5 B3Z cells were added, and co-cultured with the splenocytes in a total volume of 200µl for 24 hours. Figure 5.24A shows that CD40mAb with SIINFEKL peptide as a mixture significantly enhanced antigen presentation to B3Z cells compared to the isotype antibody control mixture. This difference was observed down-to a concentration of 2.5µg/ml CD40mAb and 0.125µg/ml SIINFEKL peptide mixture ($p<0.05$, unpaired two-tailed Student t test). This difference was observed at all stimulation time points. Interestingly, SIINFEKLC-CD40mAb conjugate did not enhance antigen presentation to B3Z cells compared to SIINFEKLC-GL117 conjugates (ns, unpaired two-tailed Student t test).

To ensure that the latter result was not due to low splenocyte viability, SIINFEKL peptide was also added to the SIINFEKLC-mAb conjugates to observe if CD40mAb enhanced antigen-presentation (Figure 5.25). Therefore, 10^5 splenocytes were stimulated with 20µg/ml, 10µg/ml, 5µg/ml, 2.5µg/ml or 1.25µg/ml SIINFEKLC-CD40mAb or SIINFEKLC-GL117 conjugates as well as 2µg/ml, 1µg/ml, 0.5µg/ml, 0.25µg/ml or 0.125µg/ml SIINFEKL peptide (respectively). Again, splenocytes were

stimulated for 2 hours (Figure 5.25), 18 hours (results not shown) and 24 hours (results not shown) prior to addition of B3Z hybridoma cells. After the stimulation period, 10^5 B3Z cells were added, and co-cultured in a total volume of 200µl for 24 hours. The addition of SIINFEKL peptide showed that the SIINFEKL-mAb conjugates were not having a detrimental effect on the splenocytes (Figure 5.25). Once SIINFEKL peptide was included a difference in the antigen-presentation between the SIINFEKLC-CD40mAb and SIINFEKLC-GL117 conjugates was observed down to the concentration of 1.25µg/ml ($p<0.01$, unpaired two-tailed Student t test). This was observed after 2 hour (results shown), 18 hour and 24 hour incubation.

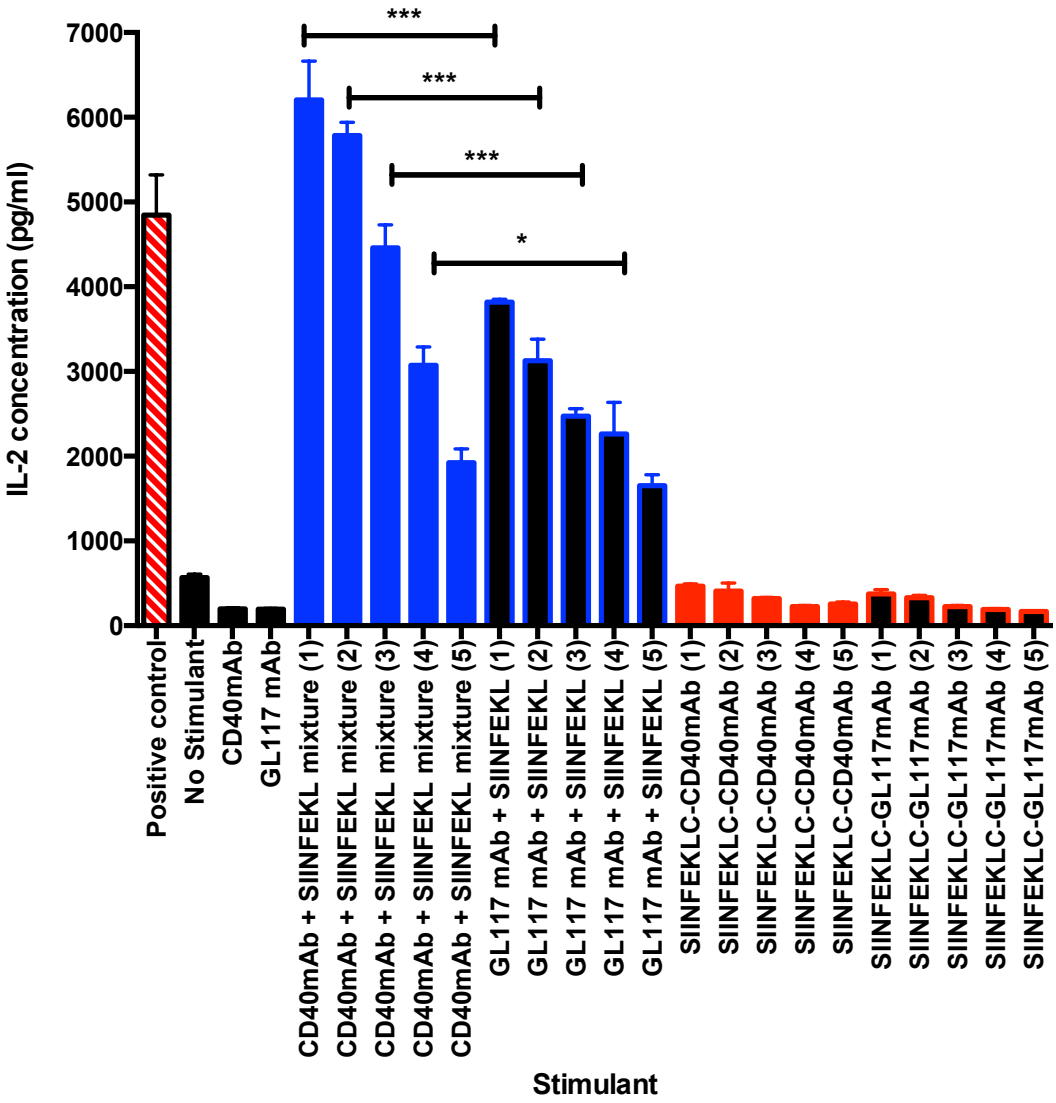

Figure 5.24. Co-culture of splenocytes stimulated with SIINFEKLC-mAb conjugate or SIINFEKL and mAb mixtures, and B3Z T cell hybridomas. The concentration of IL-2 produced by B3Z after 24 hour co-culture is shown. Splenocytes stimulated with 2µg/ml (2µM) SIINFEKL peptide (dashed red) served as a positive control. No stimulation or stimulation of splenocytes with 20µg/ml of CD40mAb only or GL117mAb only (black bars) served as negative controls. Splenocytes were stimulated with four series of two-fold dilutions starting at 20µg/ml CD40mAb and 2µg/ml SIINFEKL peptide mixture (blue) or GL117mAb and SIINFEKL peptide mixture (black with blue background). Splenocytes stimulated with 20µg/ml (1), 10µg/ml (2), 5µg/ml (3), 2.5µg/ml (4) or 1.25µg/ml (5) of SIINFEKLC-CD40mAb (red) and SIINFEKLC-GL117 (black with red background) conjugates are shown. Splenocytes were stimulated with all stimulants for 2 hours prior to co-culture with B3Z. Unpaired two-tailed Student's t-test was used to determine statistical significance (mean +/- SD). ***p<0.0001 *p<0.05. This figure represents one experiment. Technical replicates = 3.

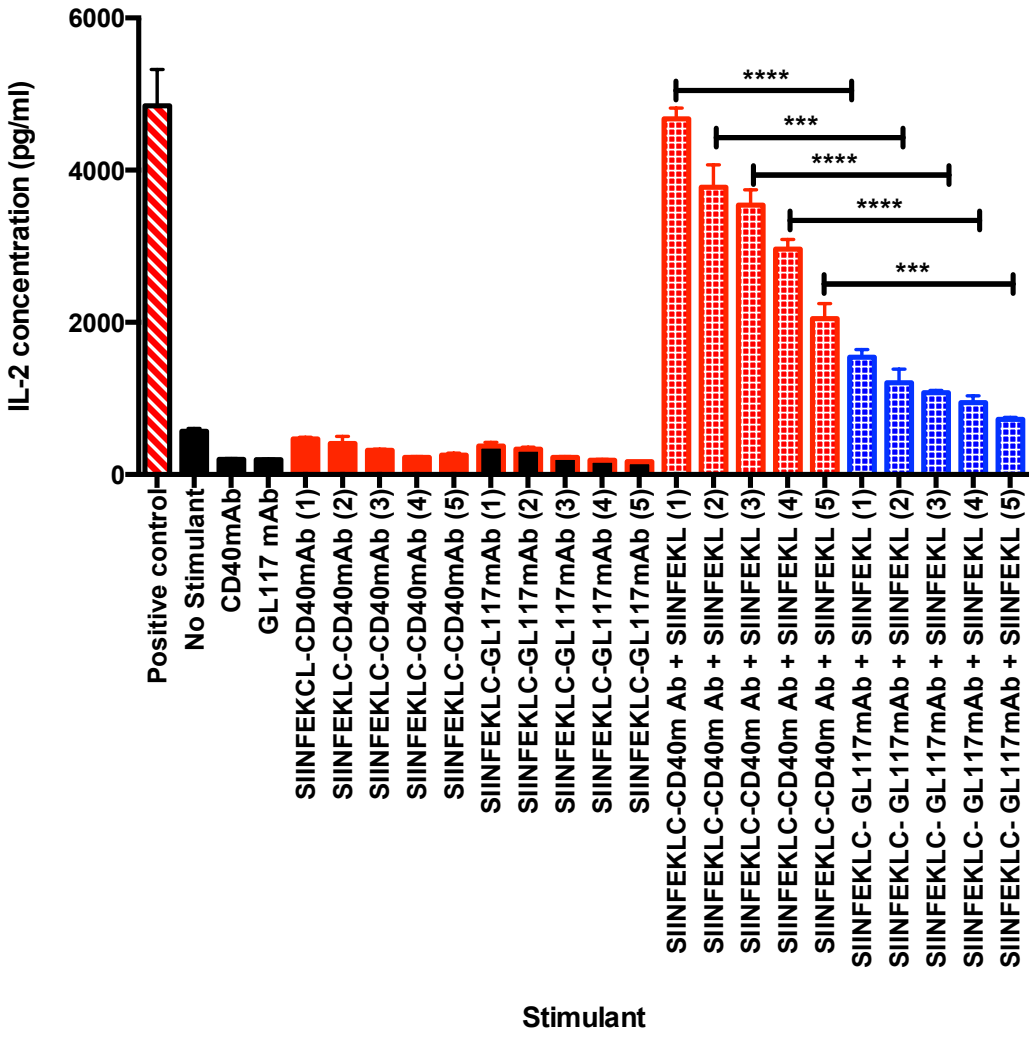

Figure 5.25. Co-culture of splenocytes stimulated with different concentrations of SIINFEKLC-mAb conjugate in the absence or presence of SIINFEKL peptide, with B3Z T cell hybridomas. The ability of B3Z to produce IL-2 after 24 hour co-culture is shown. Splenocytes stimulated with 2µg/ml (2µM) SIINFEKL peptide (dashed red) served as a positive control. No stimulation or stimulation of splenocytes with 20µg/ml of CD40mAb only or GL117 mAb only (black bars) served as negative controls. Splenocytes stimulated with 20µg/ml (1), 10µg/ml (2), 5µg/ml (3), 2.5µg/ml (4) or 1.25µg/ml (5) of SIINFEKLC-CD40mAb (red) and SIINFEKLC-GL117mAb (black with red background) conjugates are shown. Splenocytes stimulated with the same concentrations of SIINFEKLC-CD40mAb (red dotted) and SIINFEKLC-GL117mAb (blue dotted) conjugates each with the addition of 2µg/ml, 1µg/ml, 0.5µg/ml, 0.25µg/ml or 0.125µg/ml SIINFEKL peptide is shown. Splenocytes were stimulated for 2 hours prior to the addition of B3Z. Unpaired two-tailed Student's t-test was used to determine statistical significance (mean +/- SD). **** $p<0.0001$, ***$p<0.001$. This figure represents one experiment. Technical replicates = 3.

As the CD40mAb and SIINFEKL mixtures, but not the SIINFEKLC-CD40mAb conjugates, enhanced antigen presentation to B3Z, the co-culture experiment was repeated and the SIINFEKL presentation on MHC class I was analysed by flow cytometry (*see* Section 2.2.6.8.2.). The highest concentrations of 20µg/ml SIINFEKLC-mAb conjugates, or 2µg/ml SIINFEKL and 20µg/ml mAb mixture were used. In this experiment the APCs relevant for this chapter were investigated by gating on $CD19^+$ $CD86^+$ cells (Figure 5.29A) and $CD11c^+$ $CD86^+$ cells (Figure 5.29B), presenting SIINFEKL bound to MHC class I (*see* gating strategy in Section 2.2.6.8.2). The supernatants of the co-cultures used for the flow cytometry experiment were analysed for IL-2 measured by ELISA. The results were consistent with the previous results (not shown).

Consistent with results shown by IL-2 ELISA (Figure 5.24), activated splenic B cells (Figure 5.26A) and DCs (Figure 5.26B) stimulated with SIINFEKL and CD40mAb mixture presented significantly more (**$p<0.01$, unpaired, two-tailed Student's t-test) SIINFEKL on their MHC class I than isotype control mAb mixture. Interestingly however, in contrast with the results shown by IL-2 ELISA (Figure 5.24), activated splenic B cells and DCs stimulated with SIINFEKLC-CD40mAb conjugate presented significantly more (**$p<0.01$, unpaired, two-tailed Student's t-test) SIINFEKL on their MHC class I compared to the SIINFEKLC-GL117mAb conjugate. Due to this development, we considered the fact that the IL-2 ELISA used was not sensitive enough to detect accurately low concentrations of IL-2 produced by B3Z cells. Therefore, splenocytes, BM-DCs and positively-selected B cells stimulated with SIINFEKLC-CD40mAb conjugate concentrations as high as 100µg/ml were co-cultured with B3Z (results not shown). Still, however there was no difference in the IL-2 concentration in the supernatants of SIINFEKLC-CD40mAb conjugate-stimulated and the SIINFEKLC-GL117 conjugate-stimulated cells.

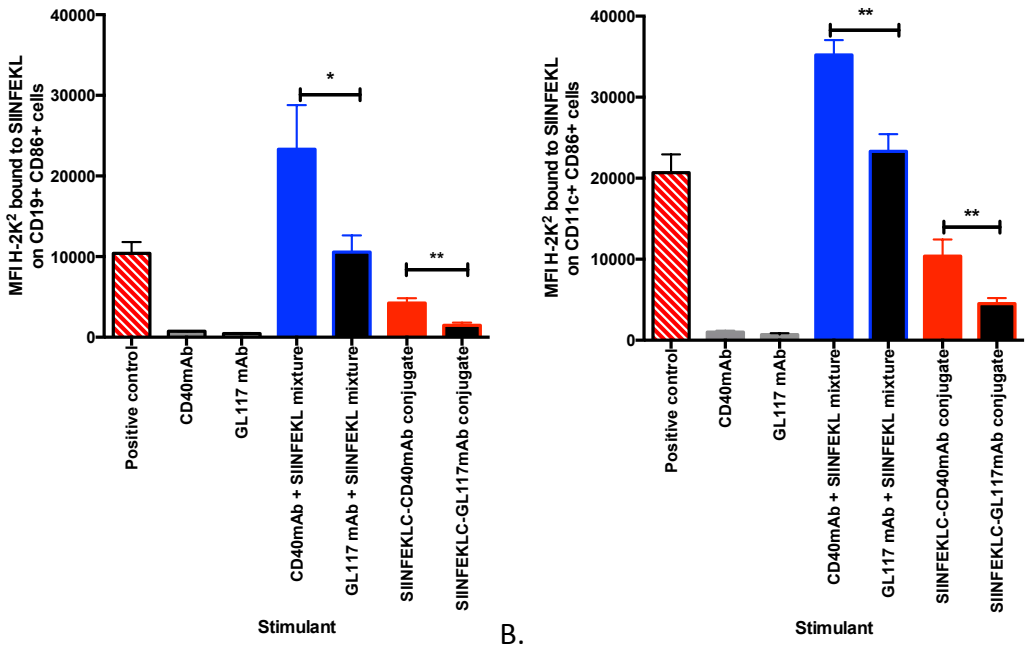

Figure 5.26. Flow cytometry analysis demonstrating the effect CD40mAb had on the antigen-presenting capacity of splenic CD19$^+$ and CD11c$^+$ cells. Splenocytes stimulated with 2µg/ml (2µM) SIINFEKL peptide (dashed red) served as a positive control. Stimulation of splenocytes with 20µg/ml of CD40mAb or GL117mAb only (grey bars) served as negative controls. Splenocytes stimulated with 2µg/ml SIINFEKL and 20µg/ml CD40mAb (blue) or GL117mAb (black with blue background) mixture are shown. Splenocytes stimulated with 20µg/ml SIINFEKL-CD40mAb (red) and SIINFEKL-GL117mAb (black with red background) conjugates are shown. Splenocytes were stimulated for 4 hours. MFI of H-2K^b/SIINFEKL expression on CD86$^+$ CD19$^+$ cells (A) and the MFI of H-2K^b/SIINFEKL expression on CD86$^+$ CD11c$^+$ cells are shown. Unpaired two-tailed Student's t-test was used to determine statistical significance (mean +/- SD). ** $p<0.01$. This figure represents three experiments. Technical replicates = 1.

5.6. Investigation into CD40mAb-adjuvanted conjugate uptake and activation of B cells and BM-DCs *in vivo*

The *in vitro* work conducted in this chapter supported the hypothesis that both B cells and DCs can potentially play a role in the adjuvant effect of antigen-CD40mAb-conjugates. We therefore moved on to test the hypothesis *in vivo* by investigating the effect SIINFEKLC-CD40mAb had on the capacity of DCs to take up antigen and, after activation, migrate to the draining lymph nodes. In addition, we investigated whether lymph node-resident B cells also become activated after subcutaneous injection with the SIINFEKLC-CD40mAb conjugate. This was investigated by subcutaneously immunising C57Bl/6 or BALB/c mice with 10µg SIINFEKLC-CD40mAb conjugate on the right flank and 10µg SIINFEKLC-GL117mAb conjugate on the left flank (Figure 5.27, *see* Section 2.2.7.6.1.). The draining inguinal lymph nodes were harvested after 24 hours and the levels of the co-stimulatory molecule CD86 on B cells and DCs was analysed by flow cytometry (see Section 2.2.7.6.2.). The presence of SIINFEKLC bound to H-2K^{b} on non-activated CD19^{+} and CD11c^{+} cells or on CD19^{+} and CD11c^{+} cells with enhanced co-stimulatory molecule expression in the draining lymph node was analysed with an anti-mouse H-2K^{b} bound to SIINFEKL antibody (Figure 5.28). Results showed that there was no difference in SIINFEKLC presentation on MHC class I of activated or non-activated B cells or DCs between the draining lymph nodes of right (SIINFEKLC-CD40mAb conjugate immunised) or left flank (SIINFEKLC-GL117mAb conjugate immunised). Interestingly however, SIINFEKLC-CD40mAb conjugate significantly upregulated CD86 expression on B cells in the draining lymph node compared to the SIINFEKLC-GL117 control (Figure 5.29A). This effect was not observed with CD11c^{+} DCs (Figure 5.29B).

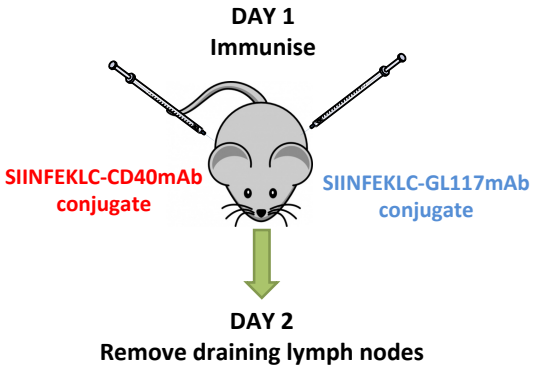

Figure 5.27. A diagrammatic representation of the experimental design.

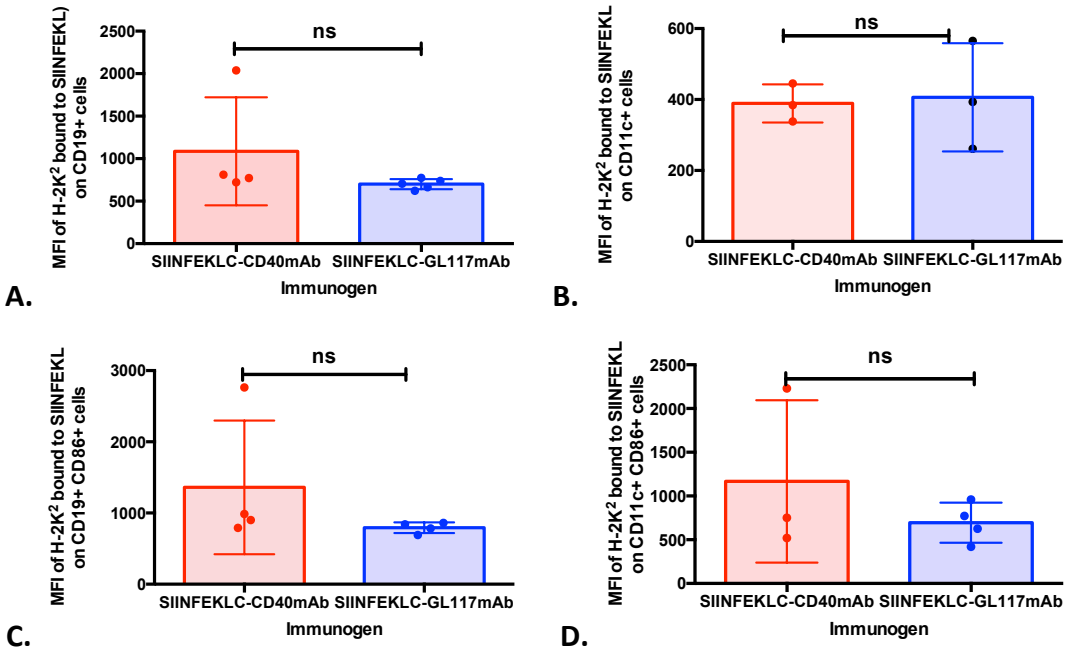

Figure 5.28. The ability of SIINFEKL-mAb conjugates to modulate antigen-presentation of B cells and DCs. C57Bl/6 mice were subcutaneously immunised with 10µg SIINFEKLC-CD40mAb conjugate on the right flank and SIINFEKLC-GL117 conjugate on the left flank. The effect of SIINFEKLC-CD40mAb (red) or SIINFEKLC-GL117 (blue) on lymph node: A. B cell SIINFEKL presentation, B. DC SIINFEKL presentation, C. Activated B cell SIINFEKL presentation and D. Activated DC SIINFEKL presentation, are shown. A paired two-tailed student's t-test was used to determine statistical significance (mean +/- SD). ns=non-significant. This figure represents results from two separate experiments, and a total of 5 mice. Each dot represents 1 mouse.

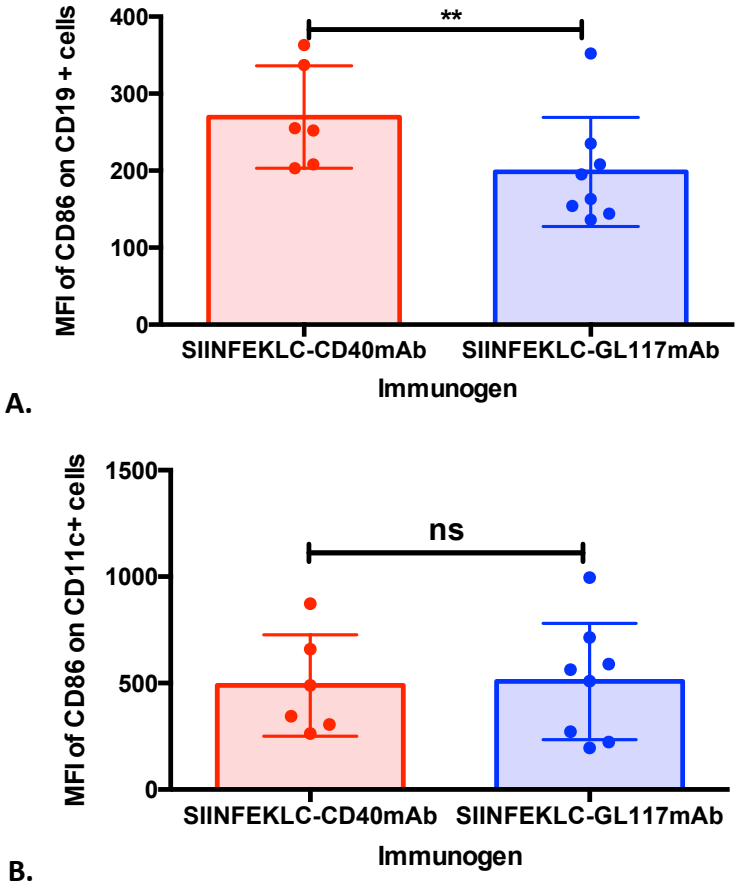

Figure 5.29. Effect of the SIINFEKL-mAb conjugates on the activation status of B cells and DCs. C57Bl/6 or BALB/c mice were subcutaneously immunised with 10µg SIINFEKLC-CD40mAb conjugate on the right flank and SIINFEKLC-GL117mAb conjugate on the left flank. The effect of SIINFEKLC-CD40mAb (red) or SIINFEKLC-GL117mAb (blue) on lymph node: A. Activation status of B cells and B. Activation status of DCs are shown. A paired two-tailed Student's t-test was used to determine statistical significance (mean +/- SD). **p<0.01. ns=non-significant. This figure represents results from three separate experiments, and a total of 8 mice per group. Each dot represents 1 mouse.

Discussion

The induction of a robust cytotoxic $CD8^+$ T cell response is critical for protective and long-lasting immunity against intracellular infections and cancers. This is the unmet requirement of cancer vaccines under development. For the CD40mAb-adjuvanted vaccines to induce a $CD8^+$ T cell response, conjugated antigen has to be internalised by phagocytosis or endocytosis and cross-presented onto MHC class I. Other integral qualities for an effective vaccine is the ability to co-deliver antigens to professional APCs with consequent APC activation and antigen presentation to T cells leading to the initiation of an antigen-specific immune response. In this chapter, these qualities were investigated in the context of CD40mAb-adjuvanted vaccines incorporating the use of an OVA $CD8^+$ T cell epitope-based vaccine, SIINFEKLC-CD40mAb as a model.

Epitope-based vaccines are considered as an ideal choice as a vaccine because they allow the delivery of antigens to $CD4^+$ or $CD8^+$ T cells in the right immune context, which results in a specific immune response. In fact, vaccines based on $CD8^+$ T cell epitopes have induced both viral-specific and tumour-specific protective cytotoxic immunity (Feltkamp et al., 1993, Aichele et al., 1995). However, immunisation of exogenous or synthetic peptides admixed with an adjuvant to enhance immunogenicity is suboptimal and inefficient, as the peptide and the adjuvant are not directed to the same APC. This leads to the production of a mixed population of APCs that are just activated or just antigen presenting with only a few being both. Activated peptide-loaded APCs are necessary for an efficient immune response (Aichele et al., 1995, De Vries et al., 2003a, De Vries et al., 2003b, Heit et al., 2008), whereas peptide-loaded APCs that are not activated promote tolerance (Diehl et al., 1999). To ensure that peptide-loaded APCs in this study were activated the peptide and the CD40mAb (acting as the adjuvant) were chemically conjugated.

Naive $CD8^+$ T cells are not able to directly kill infected cells or tumour cells. However, on antigen-encounter the naive $CD8^+$ T cells proliferate and differentiate into antigen-specific effector $CD8^+$ T cells. The effector $CD8^+$ T cells target and kill the cells presenting the antigen (Barber et al., 2003). $CD8^+$ T cells were implicated as the major effector cells in the immune response generated due to immunisation with

CD40mAb conjugated to a lymphoma antigen in a murine tumour model (Carlring et al., 2012). However, the $CD8^+$ T cell response was never directly assessed. This study was the first that directly showed that CD40mAb conjugated to antigen vaccine stimulated effector $CD8^+$ cytotoxic T cell responses against the conjugated antigen. Immunisation with the SIINFEKLC-CD40mAb conjugate induced the production of effector $CD8^+$ T cells that directly targeted and killed 51% of the SIINFEKL-loaded cells (Figure 5.7). In contrast, immunisation with the control conjugate induced negligible killing of SIINFEKL-loaded cells (Figure 5.7). This result was the impetus for the work carried out in this chapter.

The mice were also immunised with SIINFEKLC and CD40mAb as a mixture in the *in vivo* cytotoxicity experiment. The CD40mAb in the mixture also induced an antigen-specific effector $CD8^+$ T cell response against the SIINFEKLC peptide. This was consistent with other studies that also demonstrated that triggering of CD40 receptor by CD40mAb significantly enhances epitope- or peptide-based anti-tumour vaccine efficacy due to priming of $CD8^+$ T cells (Diehl et al., 1999, Ito et al., 2000a, Ito et al., 2000b, Ninomiya et al., 2002). However, in these studies, various important differences to ours were noted, namely (i) high doses of peptides (100µg) were co-administered with CD40mAb per mouse, (ii) peptides were encapsulated in liposomes which also induce cytotoxic $CD8^+$ T cell responses, (iii) peptides were admixed with other adjuvants like Freund's adjuvant and/or (iv) CD40mAb was used in doses as high as 250µg per mouse. Therefore, considering the mentioned studies, effector $CD8^+$ T cell directed killing of SIINFEKL-loaded cells induced by the CD40mAb and SIINFEKLC mixture in our experiment was expected. What was surprising was the fact that the CD40mAb-SIINFEKLC conjugate did not induce significantly better effector $CD8^+$ T cell responses against SIINFEKLC peptide than the CD40mAb and SIINFEKLC mixture (Figure 5.7). A similar response between the two vaccines could be attributed to the relatively high dose administered. Each mouse in this work was immunised with 40µg CD40mAb and 2µg peptide. Early studies with CD40mAb-adjuvanted conjugates showed that immunising with doses as low as 1µg significantly enhanced antigen-specific antibody responses compared to CD40mAb admixed with antigen, which also resulted in reduced side-effects (Barr et al., 2003).

This means that 10µg or less peptide-CD40mAb conjugates should be used for subsequent *in vivo* studies.

Prior to proceeding to the targeting and uptake experiments, the SIINFEKLC-CD40mAb conjugates were also used to test their effect on the activation status of DCs and B cells. Consistent with results in chapter 4, SIINFEKL-CD40mAb conjugates, significantly enhanced co-stimulatory molecule expression of both B cells (Figure 5.9) and DCs (Figure 5.9, 5.10) *in vitro* compared to the SIINFEKLC-GL117mAb control conjugate.

Conjugation of labelled peptide ($SIINFEKL_{FAM}$) to labelled antibody ($mAb_{Dylight}$) allowed testing of the hypothesis that conjugation enables co-delivery of the CD40mAb and the antigen to the same APC, by means of fluorescence microscopy. The number of conjugates targeting B cells (Figure 5.12) and DCs (Figure 5.18) varied according to the APC type.

DCs are very efficient at internalising numerous different antigens and presenting them in a highly immunogenic format (Romani et al., 1989, Inaba et al., 1993, Caux et al., 1994). The aforementioned properties including their ability to traffic antigens from the periphery to the secondary lymphoid organs which are T cell rich, is why DCs are so prominently investigated and targeted in adjuvant research. Different DC receptors for example DEC205, and CD40 have been targeted in vaccine development (Bonifaz et al., 2004). When antigens bind to these receptors, they are internalised by means of clathrin-coated domains and both enhance presentation by MHC class I and MHC class II (Bonifaz et al., 2004). A study targeting the DEC205 and CD40 receptors on human DC subtypes using corresponding antibodies showed that the antibodies were both internalised. However, anti-DEC205 antibodies localised in the late endosome, whilst anti-CD40 antibodies localised mainly in the early endosomes and only minimally in late endosomes after 6 hours of *in vitro* stimulation (Chatterjee et al., 2012). Anti-DEC205 antibodies were internalised to a greater extent than anti-CD40 antibodies but CD40 receptor targeting was more efficient for cross presentation (Chatterjee et al., 2012). In this study $SIINFEKLC_{FAM}$-$CD40mAb_{Dylight}$ and $SIINFEKLC_{FAM}$-$GL117mAb_{Dylight}$ (Figure 5.13, 5.15) were incubated with DCs for up to an hour, and high numbers of both SIINFEKLC-mAb conjugates

targeted BM-DCs even after 5 minutes. This suggested that the different conjugates were targeting different receptors and being internalised by separate mechanisms at later time points. However, significantly more co-localised SIINFEKLC$_{FAM}$ and CD40mAb$_{Dylight}$ was observed at the 60 minute time-point, which is a possible consequence of CD40 ligation. The latter phenomenon could be shown by the fact that the pH sensitive FAM (green) dye of the SIINFEKLC$_{FAM}$-CD40mAb$_{Dylight}$ conjugate decreased in brightness between 5 and 60 minutes. The decrease in brightness could be attributed to the peptide being trafficked into an endosomal compartment of lower pH, and is a marker of internalisation. Fluorescein-derived dyes have been in fact used as an indicator of the pH of endosomes (Murphy et al., 1984).

DCs can internalise antigens by three mechanisms namely clathrin-mediated endocytosis, phagocytosis and macropinocytosis (Blum et al., 2013). In contrast to DCs, B cells are less efficient at taking up antigen non-specifically, and are more focused on antigen-specific uptake (Lanzavecchia, 1985), which could be clearly observed by the low numbers of co-localised SIINFEKL$_{FAM}$ and CD40mAb$_{Dylight}$ present after 5 and 60 minutes compared to DC (Figure 5.21). B cells are most efficient at internalising antigens through their BCR (Lanzavecchia, 1985), and are better APCs when the antigen load is limited (Malynn et al., 1985, Bouaziz et al., 2007). At 5 minutes both SIINFEKL$_{FAM}$-CD40mAb$_{Dylight}$ and SIINFEKLC$_{FAM}$-GL117mAb$_{Dylight}$ conjugates might be just localising on the B cell surface. However, at 60 minutes, there is a significant difference between the two conjugates, probably because of internalisation. Chatterjee and colleagues (2012) explain that once internalised CD40-targeted antigens are more stable than antigens targeting other receptors, showing that antigens internalised into other compartments were degraded at a higher rate. Although the latter study was conducted in DCs, this could be a reason why less co-localised SIINFEKLC$_{FAM}$-GL117mAb$_{Dylight}$ was observed after 60 minutes whilst the SIINFEKL$_{FAM}$-CD40mAb$_{Dylight}$ persists.

Further to APC targeting and uptake, the ability of APCs to cross-present the CD40mAb-adjuvanted vaccines to CD8^{+} T cells was investigated *in vitro*. Even though DCs are considered specialised at cross-presenting exogenous antigens to MHC class I (Maurer et al., 2002), B cells have also shown to have the capacity to do this

(Shirota et al., 2002, Heit et al., 2004). Whether CD40mAb enhances B cell or BM-DC cross-presentation of SIINFEKL to B3Z hybridoma T cells in co-culture was investigated by the use of both the CD40mAb admixed with SIINFEKL peptide as well as by SIINFEKLC-CD40mAb conjugates. The unconjugated CD40mAb enhanced antigen presentation by BM-DCs and B cells to B3Z compared to their respective isotype antibodies (Figure 5.24). This was concluded due to increased IL-2 production, indicative of B3Z activation. However, the stimulation of APCs with SIINFEKLC-CD40mAb conjugates did not lead to B3Z activation. This might have been due to the fact that the SIINFEKL peptide in the mixture with CD40mAb was just loading onto the MHC class I of the APC, and not being processed, or the B3Z hybridoma T cells were not producing detectable levels of IL-2. The original study using B3Z hybridoma T cells to research antigen presentation demonstrated that the optimal activity of the B3Z cells depended upon the presentation of the exact analogue of the naturally processed octamer, SIINFEKL (Shastri and Gonzalez, 1993). Another study showed that an extra residue at the N-terminal or C-terminal or both termini of SIINFEKL reduces B3Z activity by 30-, 1000-, and 30,000-fold respectively (Serwold and Shastri, 1999). They also subsequently showed that the lack of B3Z activity was due to the poor recognition by the TCR rather than the failure of the peptides to bind to the MHC class I. This is consistent with our study because the addition of a cysteine to the octamer terminal resulted in no detectable B3Z activity, whilst SIINFEKL peptide (with no terminal cysteine) used admixed with CD40mAb demonstrated detectable B3Z activation.

Published work showed that CD40mAb enhanced cross-presentation of the conjugated peptide (Chatterjee et al., 2012). However, in the aforementioned study, human DC subtypes isolated from the blood and $CD8^+$ T cells isolated from lymphocytes were utilised, different to the murine BM-DCs and the B3Z $CD8^+$ hybridoma T cells utilised in our study. To further investigate cross-presentation, the SIINFEKL/Kb complex presented by APCs was tested by flow cytometry using an anti-SIINFEKL/Kb complex antibody. Flow cytometry showed that significantly more SIINFEKL was presented by both SIINFEKLC-CD40mAb conjugate as well as CD40mAb and SIINFEKL mixture stimulated cells, compared to the respective GL117mAb

controls. This was observed on both activated splenic $CD19^+$ and $CD11c^+$ cells, showing that CD40mAb adjuvant works and targets both these cell types and enhances cross-presentation of SIINFEKLC to the MHC class I.

An earlier study carried out in our laboratory showed that a fluorescently labelled CD40mAb-antigen conjugate immunised subcutaneously, was detected inside cells in the draining inguinal lymph node (Carlring et al., 2012). We wanted to take this experiment a step further in this study to investigate which APCs are taking up the CD40mAb-antigen conjugate and whether they become activated in the process. Different adjuvants have different effects at the site of injection, which lead to antigen transport to the lymph nodes by a number of different cell types. For example, whilst alum adjuvants seem to act mainly on monocytes and macrophages (Seubert et al., 2008), MF59 adjuvant largely acts on granulocytes, in fact neutrophils are the first cell type recruited to the injection site, followed by monocytes, eosinophils, DCs and a very small numbers of B cells and T cells (Calabro et al., 2011). However, both adjuvants have an impact on the differentiation of monocytes to DCs (Rimaniol et al., 2004, Seubert et al., 2008). Even though the draining lymph nodes harvested from mice injected intramuscularly with alum or MF59 admixed with antigen both contained antigen-containing DCs and B cells after 24 hours, alum unlike MF59 only demonstrated slight enhanced numbers of antigen-containing APCs. Furthermore, draining lymph nodes of mice injected intramuscularly with MF59 admixed with antigen showed antigen-containing neutrophils after just 7 hours of injection, which were not detected after alum injection. This indicates that neutrophils could also traffic antigens to secondary lymphoid organs (Calabro et al., 2011).

Other adjuvants, like TLR-agonists for example MPL (Ismaili et al., 2002, Didierlaurent et al., 2009, Didierlaurent et al., 2014) directly activate DCs *in vitro* and *in vivo*. A DC-activating adjuvant is a necessary component for an effective cancer vaccine. Intramuscular injection with TLR-agonist MPL also lead to increased DC and monocyte numbers compared to injection with alum adjuvant, at both 24 and 72 hours. However, whilst lymph node DCs expressed higher levels of CD40 and CD86, only CD40 was enhanced on lymph node monocytes (Didierlaurent et al., 2009). In

our study the DCs present in the inguinal draining lymph nodes 24 hours after a subcutaneous injection did not present SIINFEKL and were not activated (Figure 5.28). This was surprising as *in vitro* work showed that the CD40mAb-antigen conjugate enhanced DC activation as well as SIINFEKL presentation by DCs. In contrast, although activated and non-activated B cells in the draining lymph node did not present SIINFEKL, B cell activation status was enhanced in mice immunised with SIINFEKLC-CD40mAb compared to those immunised with SIINFEKLC-GL117mAb conjugate. B cells have recently been found to take up antigen from the surface of follicular DCs and macrophages *in vivo* (Suzuki et al., 2009), however this still does not explain why SIINFEKL is not presented on the B cell surface. One reason could be that flow cytometry might not be sensitive enough to detect the presented SIINFEKL. However, B cells might also be taking up CD40mAb from cell surface, which would be an explanation of why they are activated. Studies have demonstrated that soluble antigens smaller than 70kDa gain direct access to the lymph nodes via fibroblastic reticular cell conduits (Pape et al., 2007, Roozendaal et al., 2009). However, the SIINFEKLC-mAb conjugates are of higher MW, so it is unlikely that they gain access to the lymph nodes directly.

Further experiments have to be performed to verify and reach conclusions over the fate of CD40mAb-antigen conjugates *in vivo*. The use of a fluorescently labelled conjugate would give more detailed information on the APCs important at the site of immunisation as well as the APCs migrating in high numbers to the draining lymph nodes to present the conjugated antigen. A detail to be taken in consideration for subsequent experiments is the differentiation between migratory DCs and resident DCs in the lymph nodes. Other cell types such as for example neutrophils, monocytes and macrophages, which have found to be play a role in trafficking of antigens from the periphery to the secondary lymphoid organs (Abadie et al., 2005, Bonneau et al., 2006, Calabro et al., 2011), were they deliver antigens to professional APCs should also be considered and studied as potential targets of CD40mAb-adjuvanted vaccines.

Conclusions

Our results support the hypothesis that CD40mAb-adjuvanted vaccines induce effector $CD8^+$ T cell responses *in vivo*. CD40mAb co-delivers conjugated antigen to both B cells and DCs *in vitro.* In addition, even though further testing is required *in vivo*, both B cells and DCs become activated on stimulation with the CD40mAb-adjuvanted vaccines, and play a role in enhancing CD40mAb-antigen vaccine antigen cross-presentation to $CD8^+$ T cells *in vitro*.

CHAPTER 6

FINAL DISCUSSION

6.1. Overview

Our group has been investigating CD40mAb as an adjuvant for more than a decade. Experimental progress so far has shown that immunisation with CD40mAb at high doses (500µg) can enhance antibody responses against co-inoculated TI-1 and TI-2 antigens (Dullforce et al., 1998, Barr and Heath, 1999). This adjuvant effect can also be achieved when using 50-fold lower doses when chemically conjugated to antigen (Barr et al., 2003), which also resulted in less side-effects. Immunisation with CD40mAb conjugated to antigen at low doses enhanced antigen-specific antibody titres up to a 1000-fold compared to immunisation with CD40mAb admixed with antigen (Barr et al., 2003). Moreover, a more rapid antigen-specific immune response was observed in mice immunised with the CD40mAb-antigen conjugate compared to the licensed adjuvants, like MPL or alum, admixed with antigen (Bhagawati-Prasad et al., 2010). Early studies also demonstrated that CD40mAb administered alone enhanced *ex vivo* lymphocyte responses to itself (Carlring et al., 2004). In addition, CD40mAb conjugated to antigen enhanced lymphocyte proliferation in response to the antigen *ex vivo* compared to the isotype mAb control conjugate (Hatzifoti and Heath, 2007). However, in the quoted study the proliferating lymphocytes were only assumed to be $CD4^+$ T cells.

The most recent study by our group demonstrated that CD40mAb conjugated to the A20 murine B cell lymphoma Id (A20-CD40mAb) showed synergy with MPL in the murine A20 lymphoma model, resulting in enhanced overall and median survival, and also delayed tumour progression in response to A20 tumour challenge compared to control groups. Furthermore, effector $CD8^+$ T cells were highlighted as the major mediators for tumour rejection by means of *in vivo* depletion studies, although $CD8^+$ CTL responses were not directly measured. It is noteworthy that immunisation with A20-CD40mAb conjugate vaccine did not result in any tumour protection when both $CD4^+$ and $CD8^+$ T cells were depleted prior to tumour challenge, highlighting the importance of both cell types (Carlring et al., 2012).

Considerable progress has been made regarding the roles of CD40mAb as an adjuvant but the mode of action is still unclear. Studies carried out to investigate the

CD40-CD154 interaction have shown CD40 expressing B cells (Hasbold et al., 1994, Heath et al., 1994, Vallé et al., 1989) and DCs (Caux et al., 1994, Cella et al., 1996, Björck et al., 1997, Mutini et al., 1999) are both candidates crucial in the immunogenicity of CD40mAb as an adjuvant. A recent study showed that the co-engagement of both the inhibitory FcγRIIB receptor through the CD40mAb Fc region and the CD40 receptor is essential for CD40mAb to work as a T cell adjuvant through APCs (Li and Ravetch, 2011). In addition, Li and Ravetch (2011) also showed that modulating the CD40mAb Fc domain to bind to FcγRIIB at a higher affinity, leads to enhanced antigen-specific $CD8^+$ T cell responses. This is an example showing that a better understanding of how CD40mAb works will lead to improving the efficacy of the current immunotherapies and its use as an adjuvant.

The main findings of this PhD work have already been discussed. The current chapter aims to reconcile the results together and address their application in a clinical context. In addition the limitations of certain methodologies are also discussed together with possible future work. The first aim of this work was to refine the conjugation strategy currently used in our laboratory to maximise the potential of CD40mAb-adjuvanted conjugates (Chapter 3). The second aim was to bridge the gaps in understanding certain roles of CD40mAb-antigen conjugates and determine which APC is crucial to the mechanism of action of CD40mAb conjugated to vaccine antigen as a T cell adjuvant (Chapters 4 and 5). For the purpose of the work in this thesis, research was focused on B cells and DCs.

6.2. Development of more refined CD40mAb-adjuvanted conjugate vaccines

In vitro cross-linking of the CD40 receptor on B cells by multimeric CD40mAb positively correlates with B cell proliferation (Banchereau et al., 1991). In contrast*, in vivo* CD40mAb as an adjuvant works best at a low MW (Heath and Laing, 2004). The previously mentioned observation was the impetus behind the hypothesis that a low average MW CD40mAb-antigen conjugate would maximise the potential of CD40mAb as an adjuvant, leading to improved vaccines (Chapter 3). The hypothesis

was investigated using click chemistry together with size-exclusion HPLC. These two techniques allowed us to refine the method by which the CD40mAb-antigen conjugates were made.

The important property of click chemistry is that it involves specific reagent components that have unique functional groups that are narrowly reactive towards each other, and no side-reactions occur (Kolb et al., 2001). This property allows better control than the technique currently used in our laboratory, over the formation of large complexes of CD40mAb-antigen conjugate, resulting in the development of vaccines with more consistent composition. The size-exclusion HPLC used together with copper free click chemistry allowed the isolation of the low average MW conjugate containing minimal to no contaminating unconjugated protein and the high average MW conjugate.

Our hypothesis was tested using CD40mAb conjugated to the A20 murine lymphoma Id as a prophylactic vaccine in the murine A20 lymphoma model. The immunogenicity and anti-tumour effects of low average MW, high average MW and heterogeneous A20-CD40mAb conjugates made by click chemistry were compared to the Standard A20-CD40mAb conjugate (made by sulphydryl-maleimide coupling). Only immunisation with the CLICK A20-CD40mAb conjugate of low average MW significantly enhanced specific anti-Id responses compared to the Standard A20-CD40mAb conjugate. In addition, the low average MW conjugate administered prophylactically prior to A20 tumour challenge, demonstrated the longest median survival and best tumour rejection compared to the other CLICK and Standard conjugates. These results were consistent with our hypothesis, showing that increased CD40mAb accessibility leads to superior vaccines.

The increase in median and overall survival observed in tumour challenged mice immunised with the low average MW conjugate compared to immunisation with the Standard A20-CD40mAb conjugate was not statistically significant, but a strong trend was observed. The lack of significance could be attributed to a low number of mice included in the study. Future work should involve repetition of the experiment using larger numbers of mice making the results more robust.

The effectiveness of conjugates made by click chemistry versus standard conjugation strategy was also assessed using OVA as a model antigen conjugated to CD40mAb. Low average MW, high average MW and heterogeneous CLICK OVA-CD40mAb conjugate immunised mice all showed significantly enhanced primary antibody responses against OVA compared to the Standard OVA-CD40mAb immunised mice. However, it is important to note that the Standard OVA-CD40mAb conjugate was less immunogenic compared to previous studies (Barr et al., 2003). HPLC chromatograms showed that the Standard OVA-CD40mAb conjugate was composed of largely high average MW protein together with unconjugated OVA or CD40mAb. *In vitro* ELISA and flow cytometry investigations confirmed that a proportion of the high average MW protein was OVA-CD40mAb conjugate. The presence of high average MW complexes formed due to unspecific interactions could have reduced CD40mAb accessibility. This could have been a reason why Standard OVA-CD40mAb conjugate used for this study was found to be less immunogenic.

Click chemistry has shown success in other studies since its discovery slightly more than a decade ago. One example is, that click chemistry allowed the controlled coupling of different numbers of MUC1 glycopeptides to TLR2 lipopeptide ligands forming oligovalent glycopeptide-lipopeptide conjugates (Cai et al., 2011). MUC1 glycoprotein is one of the most characterized tumour antigens, and vaccines previously made by this group involved the conjugation of MUC1 to the protein carrier BSA, which led to non-specific immune responses towards the BSA *in vivo*. MUC1 complex conjugates produced by click chemistry were immunogenic producing IgG1 and IgG2a-type antibodies. Furthermore, the vaccine containing four MUC1 glycopeptides conjugated to TLR2 lipopeptides produced IgG2a-type antibodies which bound to and initiated killing of MCF-7 breast tumor cells *in vitro* (Cai et al., 2014). Cai and colleagues (2014) stated that the response by the more defined synthetic vaccines was stronger than that elicited by previously used vaccines of MUC1 conjugated to BSA.

In conclusion, the results from our work demonstrated that the development of more refined, low average MW conjugates maximises the potential of CD40mAb as an adjuvant and enhances vaccine efficacy satisfying our hypothesis. Further

investigation of OVA-CD40mAb conjugates made by click chemistry and the standard method in Chapter 4 showed that OVA was contaminated with endotoxin. Due to this development, further studies in Chapters 4 and 5 were carried out using OVA-immunodominant epitopes conjugated to CD40mAb vaccines instead of OVA. The OVA-peptides were synthesised with a cysteine terminal on their carboxyl-end. This allowed efficient conjugation of maleimide-activated mAbs to the OVA-peptides. Sulphydryl-maleimide coupling was the conjugation of choice for two reasons; (i) only one sulphydryl-containing cysteine group was present on the peptide therefore cross-linking was minimised and (ii) the amino-terminal of the peptide was free for labelling with fluorescent compounds or biotin.

6.3. Mode of action of CD40mAb-adjuvanted conjugate vaccines

The choice of adjuvant in modern vaccine development must be justified and must fulfill an unmet requirement of the vaccine. A better understanding of the mode of action of adjuvants will lead to vaccine formulations that directly influence the immune effectors crucial for vaccine-mediated protection. CD40mAb-adjuvanted conjugates in the presented work were shown in the clinical context of B cell lymphoma (Chapter 3). The most suitable candidates for the application of Id-based vaccines are patients affected with follicular lymphoma, a type of non-Hodgkin's lymphoma, in first remission (Bendandi, 2009). The current standard treatment for B cell non-Hodgkin's lymphoma includes the use of the monoclonal antibody anti-CD20 (Rituxan^{TM} or rituximab; Genentech) (Marcus et al., 2005, Schulz et al., 2007). The addition of rituximab together with chemotherapy, was found to improve overall survival, disease control and response rates in patients with follicular lymphoma (Schulz et al., 2007). However, advanced stage follicular lymphoma is still considered incurable, this is why novel therapeutic strategies are crucial for the elimination of the residual disease after chemotherapy and immunotherapy.

Therapeutic Id-based vaccines aim to improve passive immunotherapies, like rituximab, by inducing long-lasting antibody, $CD4^+$ and $CD8^+$ T cell responses against

the tumour. Furthermore, vaccine-mediated immune responses tend to be directed towards different tumour epitopes creating immunological memory, diminishing the risk of the tumour escaping the immune system (Park and Neelapu, 2008). Id-based vaccine-mediated immune responses are assumed to have better outcomes when the tumour burden is minimal (Park and Neelapu, 2008), therefore chemotherapy with or without rituximab is usually administered. In fact, the most recent phase III clinical trial using Id-based vaccines showed clinical benefit against follicular lymphoma patients because the treatment was restricted only to patients who achieved complete response after first-line chemotherapy (Schuster et al., 2011, Melero et al., 2014).

It is noteworthy that chemotherapy also affects normal tissues and targets dividing lymphocytes, which are required for the immune response, whilst treatment with rituximab leads to depletion of both malignant and normal B cells (Maloney et al., 1994, Anolik et al., 2007). As a consequence, some time for immunological recovery has to be allowed prior to administration of the Id-based vaccine. In fact, timing of post-treatment vaccination is critical, and possibly a reason why two from three substantial phase III clinical trials in which lymphoma Id-based vaccines were used were unsuccessful (Levy et al., 2008, Freedman et al., 2009, Schuster et al., 2009). Better study design and understanding of treatment would lead to better outcomes (Bendandi, 2009).

Vaccination used as an adjunct to or after rituximab therapy needs to be able to activate APCs other than B cells to be successful. Otherwise some time for B cell recovery needs to be allowed. Ascertaining which APC plays a crucial role in the adjuvant effect of the CD40mAb-adjuvanted conjugates will give valuable information regarding whether their use will be successful after treatment with immunotherapies. The work presented in this thesis (Chapters 4 and 5) was heavily focused on determining which APCs play a crucial role in the adjuvant effect of CD40mAb conjugated to antigen, and their roles leading to $CD4^+$ or $CD8^+$ T cell responses. This information would be valuable for the optimal timing of CD40mAb-Id therapy relative to other therapies such as rituximab.

The CD4 and CD8 OVA immunodominant epitopes, ISQAVHAAHAEINAGR and SIINFEKL (respectively) conjugated to CD40mAb were used to investigate whether CD40mAb-adjuvanted conjugates work via B cells, DCs or both. The work shown in this thesis demonstrates that both aforementioned conjugates upregulated CD80 and CD86 co-stimulatory molecules on splenic B cells and immature BM-DCs indicating that both cell types were activated *in vitro*. Surprisingly *in vivo*, B cells but not DCs in the draining inguinal lymph node had up-regulated their surface co-stimulatory molecules after subcutaneous immunisation with the SIINFEKLC-CD40mAb vaccine compared to the isotype control mAb conjugate. However, the activated B cells were not presenting SIINFEKL on MHC class I. The SIINFEKLC-CD40mAb conjugate could have gained access to the lymph node indirectly by means of other APCs like peripheral monocytes, macrophages or follicular DCs. We have assumed that the B cells have taken-up antigen from the surface of the mentioned cell types, but the work in this thesis did not extend to investigate this.

A very recent study monitored the distribution of labelled QS-21 and antigen with different fluorochromes at the site of injection (muscle) and tracked these conjugates to the draining lymph nodes (Didierlaurent et al., 2014). Results showed that both QS-21 and antigen were detected in the lymph node within just 30 minutes of injection, showing that they had drained directly to the lymph node. It was interesting to note that within 24 hours, the QS-21 and the antigen could be observed in different areas of the lymph node. Another study used fluorescent OVA to show that OVA-loaded DCs and monocytes migrate to the draining lymph nodes in higher numbers and enhance their co-stimulatory molecule expression on intramuscular co-injection with MPL but not alum (Didierlaurent et al., 2009). The use of fluorescently-labelled conjugates would therefore possibly enable better tracking of the conjugates *in vivo* in order to verify our results and reach conclusions regarding the effects of CD40mAb-antigen conjugates on B cells, DCs as well as monocytes or macrophages.

CD40mAb fluorescently labelled with $Dylight_{650}$ conjugated to SIINFEKL fluorescently labelled with FAM, allowed the investigation of whether CD40mAb-adjuvanted conjugates co-deliver the antigen and CD40mAb signal to the same APC. The results

showed that CD40mAb co-delivered antigen to both B cells and BM-DCs *in vitro*. The difference observed between the two APCs was that BM-DCs uptake more SIINFEKLC-CD40mAb conjugates and at a much quicker rate than B cells compared to the respective isotype mAb control conjugates. This was attributed to the fact that immature DCs are more efficient at the uptake of antigen by different mechanisms (Romani et al., 1989, Inaba et al., 1993, Caux et al., 1994), whilst B cells focus on antigen-specific uptake (Lanzavecchia, 1985).

B cells and BM-DCs targeted by the CD40mAb-SIINFEKLC conjugates also enhanced cross-presentation of SIINFEKL on MHC class I compared to the isotype mAb control conjugate *in vitro*. Due to limitations in the technique used, it could not be concluded whether CD40mAb-antigen conjugates enhances B cell or BM-DC antigen presentation on MHC class II. As discussed in Chapter 4, alternative cells should be utilized instead of DO11.10 hybridoma T cells in order to achieve a more conclusive result in future experiments. Examples of such alternatives include $CD4^+$ cells from DO11.10 BALB/c, specific to $H\text{-}2^d$ (Son et al., 2002, Aubin et al., 2010), or OT-II C57Bl/6, specific to $H\text{-}2^b$ (Kool et al., 2011) transgenic mice having an OVA-reactive T cell receptor.

Generally, it is still unclear whether an Id-specific humoral or cell-mediated immune response is the main mechanism by which tumour protection is achieved. A specific anti-Id response was found crucial in protection against tumours (Cesco-Gaspere et al., 2005, Inogès et al., 2006, Cesco-Gaspere et al., 2008) in murine models and clinically correlated with overall survival (Ai et al., 2009). However, T cell responses were also associated with pre-clinical benefit experimentally in murine models (Biragyn et al., 1999, Carlring et al., 2012) and in humans (Bendandi et al., 1999, Inogès et al., 2006). Both humoral and cell-mediated responses contribute to the therapeutic effects of the Id-vaccines, however their relative effect has not yet been fully confirmed. Until a better understanding of the mechanism leading to tumour protection is better ascertained, Bendandi (2009) suggests that Id-based vaccines should aim to induce both humoral and cell-mediated immune responses.

Results from the work discussed in Section 6.2, show that CD40mAb-Id conjugates are able to induce specific anti-Id antibody responses in the A20 murine B cell

lymphoma model. SIINFEKLC and ISQAVHAAHAEINAGRC (referred to as ISQC in this work) peptides conjugated to CD40mAb were used in this work as models to investigate the impact of CD40mAb-adjuvanted epitope-based vaccine on $CD8^+$ and $CD4^+$ T cell responses respectively. Disappointingly, in my hands using ISQC-CD40mAb conjugates, whether $CD4^+$ T cell responses are enhanced after *ex vivo* stimulation could not be fully ascertained. However, our work showed the novel discovery that CD40mAb conjugated to SIINFEKLC peptide induced a peptide-targeted CD8 cytotoxic response. This is a valuable finding because the induction of a robust effective CD8 T cell response is one of the shortcomings of most novel adjuvants. Some adjuvants have shown the ability to induce strong CD8 T cell responses like TLR-agonists, but most TLR-agonists except for the licensed MPL are not safe for use in humans. The fact that CD40mAb currently tested in phase I clinical trials as immunotherapy is well tolerated and safe for use in humans (Vonderheide et al., 2007, Johnson et al., 2010, Vonderheide and Glennie, 2013, Beatty et al., 2013, Fanale et al., 2014), shows that the use of CD40mAb as an adjuvant is a step in the right direction towards better and safer prophylactic and therapeutic cancer vaccines.

Conclusion

The main novel finding in this work is the fact that epitope-based CD40mAb conjugate vaccine induced an antigen-specific CD8 T cell response, consolidating the potential of CD40mAb as an adjuvant in cancer vaccines. Furthermore, the use of low average MW CD40mAb-adjuvanted conjugate vaccines maximised the adjuvant properties of CD40mAb, and showed to be superior to heterogeneous vaccines.

The experimental progress on CD40mAb-adjuvanted conjugates presented in this work is summarised in Figure 6.1, which bridges some of the gaps in the understanding of the mechanism of the vaccines. However, some questions still remain unanswered, for example the role of DCs contributing to the adjuvant effect of the conjugate still needs to be fully ascertained *in vivo*. Another example is whether $CD4^+$ T cell responses are enhanced and if so whether T_H1 or T_H2 responses

are predominant. Information regarding $CD4^+$ T cell responses will allow justify the application of CD40mAb-adjuvanted vaccines either alone or in combination with other adjuvants in clinical contexts not exclusive to B cell lymphoma for example other types of cancer or viral diseases.

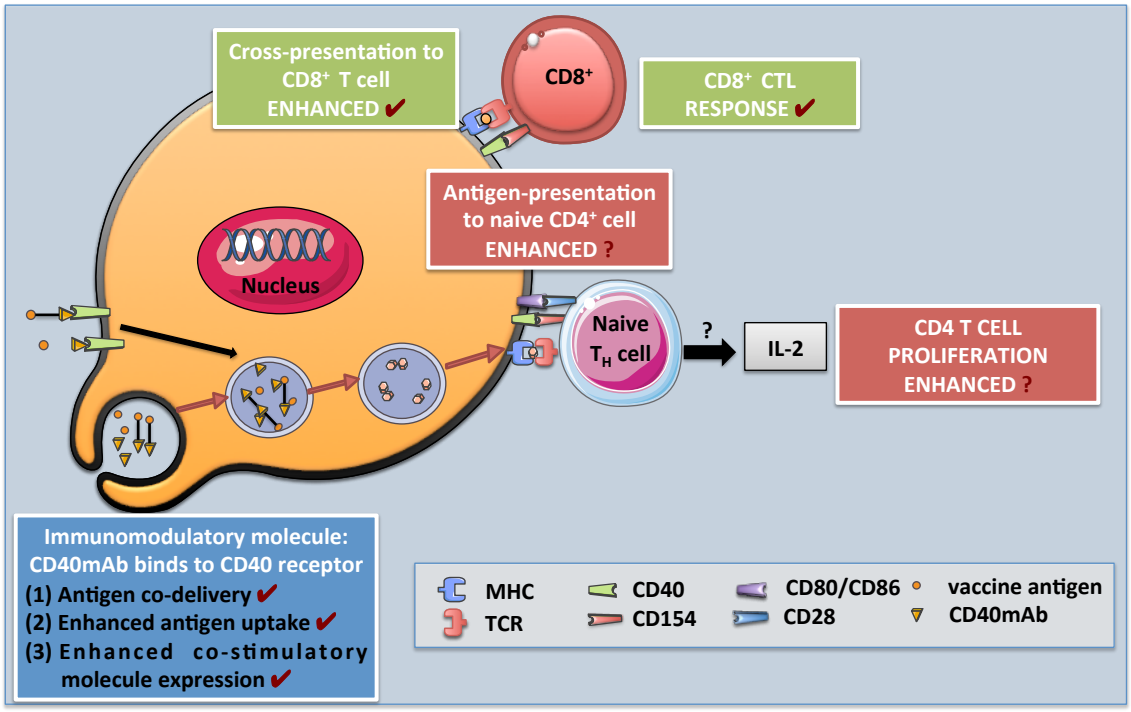

Figure 6.1. Some of the answered questions regarding the mechanism of action of CD40mAb-adjuvanted conjugate. Vaccine antigen and CD40mAb are co-delivered to the same B cell or DC. CD40mAb stimulation leads to B cell or DC activation by means of upregulation of surface co-stimulatory molecules CD80 and CD86. CD40mAb conjugated to antigen enhances B cell or DC antigen-presentation to $CD8^+$ T cells leading to a CTL response against vaccine antigen. Whether CD40mAb conjugated to antigen enhances presentation to $CD4^+$ T cells and leads to either T_H1 or T_H2 (or both) response still needs to be ascertained. All results with CD40mAb-antigen conjugates were compared to their respective isotype mAb control conjugates.

REFERENCES

AALTONEN, L. M., WAHLSTRÖM, T., RIHKANEN, H. & VAHERI, A. 1998. A novel method to culture laryngeal human papillomavirus-positive epithelial cells produces papilloma-type cytology on collagen rafts. *Eur J Cancer,* 34**,** 1111-6.

ABADIE, V., BADELL, E., DOUILLARD, P., ENSERGUEIX, D., LEENEN, P. J., TANGUY, M., FIETTE, L., SAELAND, S., GICQUEL, B. & WINTER, N. 2005. Neutrophils rapidly migrate via lymphatics after Mycobacterium bovis BCG intradermal vaccination and shuttle live bacilli to the draining lymph nodes. *Blood,* 106**,** 1843-50.

ABDI, K., SINGH, N. J. & MATZINGER, P. 2012. Lipopolysaccharide-activated dendritic cells: "exhausted" or alert and waiting? *J Immunol,* 188**,** 5981-9.

ABDOLLAHI-ROODSAZ, S., JOOSTEN, L. A., KOENDERS, M. I., DEVESA, I., ROELOFS, M. F., RADSTAKE, T. R., HEUVELMANS-JACOBS, M., AKIRA, S., NICKLIN, M. J., RIBEIRO-DIAS, F. & VAN DEN BERG, W. B. 2008. Stimulation of TLR2 and TLR4 differentially skews the balance of T cells in a mouse model of arthritis. *J Clin Invest,* 118**,** 205-16.

ACKERMAN, A. L., KYRITSIS, C., TAMPÉ, R. & CRESSWELL, P. 2003. Early phagosomes in dendritic cells form a cellular compartment sufficient for cross presentation of exogenous antigens. *Proc Natl Acad Sci U S A,* 100**,** 12889-94.

ADAMCZYK, M., GEBLER, J. C. & MATTINGLY, P. G. 1996. Characterization of protein-hapten conjugates. 2. Electrospray mass spectrometry of bovine serum albumin-hapten conjugates. *Bioconjug Chem,* 7**,** 475-81.

AGNANDJI, S. T., LELL, B., FERNANDES, J. F., ABOSSOLO, B. P., METHOGO, B. G., KABWENDE, A. L., ADEGNIKA, A. A., MORDMÜLLER, B., ISSIFOU, S., KREMSNER, P. G., SACARLAL, J., AIDE, P., LANASPA, M., APONTE, J. J., MACHEVO, S., ACACIO, S., BULO, H., SIGAUQUE, B., MACETE, E., ALONSO, P., ABDULLA, S., SALIM, N., MINJA, R., MPINA, M., AHMED, S., ALI, A. M., MTORO, A. T., HAMAD, A. S., MUTANI, P., TANNER, M., TINTO, H., D'ALESSANDRO, U., SORGHO, H., VALEA, I., BIHOUN, B., GUIRAUD, I., KABORÉ, B., SOMBIÉ, O., GUIGUEMDÉ, R. T., OUÉDRAOGO, J. B., HAMEL, M. J., KARIUKI, S., ONEKO, M., ODERO, C., OTIENO, K., AWINO, N., MCMORROW, M., MUTURI-KIOI, V., LASERSON, K. F., SLUTSKER, L., OTIENO, W., OTIENO, L., OTSYULA, N., GONDI, S., OTIENO, A., OWIRA, V., OGUK, E., ODONGO, G., WOODS, J. B., OGUTU, B., NJUGUNA, P., CHILENGI, R., AKOO, P., KERUBO, C., MAINGI, C., LANG, T., OLOTU, A., BEJON, P., MARSH, K., MWAMBINGU, G., OWUSU-AGYEI, S., ASANTE, K. P., OSEI-KWAKYE, K., BOAHEN, O., DOSOO, D., ASANTE, I., ADJEI, G., KWARA, E., CHANDRAMOHAN, D., GREENWOOD, B., LUSINGU, J., GESASE, S., MALABEJA, A., ABDUL, O., MAHENDE, C., LIHELUKA, E., MALLE, L., LEMNGE, M., THEANDER, T. G., DRAKELEY, C., ANSONG, D., AGBENYEGA, T., ADJEI, S., BOATENG, H. O., RETTIG, T., BAWA, J., SYLVERKEN, J., SAMBIAN, D., SARFO, A., AGYEKUM, A., et al. 2012. A phase 3 trial of RTS,S/AS01 malaria vaccine in African infants. *N Engl J Med,* 367**,** 2284-95.

AGNANDJI, S. T., LELL, B., SOULANOUDJINGAR, S. S., FERNANDES, J. F., ABOSSOLO, B. P., CONZELMANN, C., METHOGO, B. G., DOUCKA, Y., FLAMEN, A., MORDMÜLLER, B., ISSIFOU, S., KREMSNER, P. G., SACARLAL, J., AIDE, P., LANASPA, M., APONTE, J. J., NHAMUAVE, A., QUELHAS, D., BASSAT, Q., MANDJATE, S., MACETE, E., ALONSO, P., ABDULLA, S., SALIM, N., JUMA, O., SHOMARI, M., SHUBIS, K., MACHERA, F., HAMAD, A. S., MINJA, R., MTORO, A., SYKES, A., AHMED, S., URASSA, A. M., ALI, A. M., MWANGOKA, G., TANNER, M., TINTO, H., D'ALESSANDRO, U., SORGHO, H., VALEA, I., TAHITA, M. C., KABORÉ, W., OUÉDRAOGO, S., SANDRINE, Y., GUIGUEMDÉ, R. T., OUÉDRAOGO, J. B., HAMEL, M. J., KARIUKI, S., ODERO, C., ONEKO, M., OTIENO, K., AWINO, N., OMOTO, J., WILLIAMSON, J., MUTURI-KIOI, V., LASERSON, K. F., SLUTSKER,

L., OTIENO, W., OTIENO, L., NEKOYE, O., GONDI, S., OTIENO, A., OGUTU, B., WASUNA, R., OWIRA, V., JONES, D., ONYANGO, A. A., NJUGUNA, P., CHILENGI, R., AKOO, P., KERUBO, C., GITAKA, J., MAINGI, C., LANG, T., OLOTU, A., TSOFA, B., BEJON, P., PESHU, N., MARSH, K., OWUSU-AGYEI, S., ASANTE, K. P., OSEI-KWAKYE, K., BOAHEN, O., AYAMBA, S., KAYAN, K., OWUSU-OFORI, R., DOSOO, D., ASANTE, I., ADJEI, G., CHANDRAMOHAN, D., GREENWOOD, B., LUSINGU, J., GESASE, S., MALABEJA, A., ABDUL, O., KILAVO, H., MAHENDE, C., LIHELUKA, E., LEMNGE, M., et al. 2011. First results of phase 3 trial of RTS,S/AS01 malaria vaccine in African children. *N Engl J Med,* 365**,** 1863-75.

AHONEN, C. L., DOXSEE, C. L., MCGURRAN, S. M., RITER, T. R., WADE, W. F., BARTH, R. J., VASILAKOS, J. P., NOELLE, R. J. & KEDL, R. M. 2004. Combined TLR and CD40 triggering induces potent CD8+ T cell expansion with variable dependence on type I IFN. *J Exp Med,* 199**,** 775-84.

AI, W. Z., TIBSHIRANI, R., TAIDI, B., CZERWINSKI, D. & LEVY, R. 2009. Anti-idiotype antibody response after vaccination correlates with better overall survival in follicular lymphoma. *Blood,* 113**,** 5743-6.

AICHELE, P., BRDUSCHA-RIEM, K., ZINKERNAGEL, R. M., HENGARTNER, H. & PIRCHER, H. 1995. T cell priming versus T cell tolerance induced by synthetic peptides. *J Exp Med,* 182**,** 261-6.

AMZEL, L. M. & POLJAK, R. J. 1979. Three-dimensional structure of immunoglobulins. *Annu Rev Biochem,* 48**,** 961-97.

ANDERSON, P. 1983. Antibody responses to Haemophilus influenzae type b and diphtheria toxin induced by conjugates of oligosaccharides of the type b capsule with the nontoxic protein CRM197. *Infect Immun,* 39**,** 233-8.

ANDREWS, N., STOWE, J., AL-SHAHI SALMAN, R. & MILLER, E. 2011. Guillain-Barré syndrome and H1N1 (2009) pandemic influenza vaccination using an AS03 adjuvanted vaccine in the United Kingdom: self-controlled case series. *Vaccine,* 29**,** 7878-82.

ANOLIK, J. H., FRIEDBERG, J. W., ZHENG, B., BARNARD, J., OWEN, T., CUSHING, E., KELLY, J., MILNER, E. C., FISHER, R. I. & SANZ, I. 2007. B cell reconstitution after rituximab treatment of lymphoma recapitulates B cell ontogeny. *Clin Immunol,* 122**,** 139-45.

ARMITAGE, R. J., FANSLOW, W. C., STROCKBINE, L., SATO, T. A., CLIFFORD, K. N., MACDUFF, B. M., ANDERSON, D. M., GIMPEL, S. D., DAVIS-SMITH, T. & MALISZEWSKI, C. R. 1992. Molecular and biological characterization of a murine ligand for CD40. *Nature,* 357**,** 80-2.

ARMITAGE, R. J., MACDUFF, B. M., SPRIGGS, M. K. & FANSLOW, W. C. 1993. Human B cell proliferation and Ig secretion induced by recombinant CD40 ligand are modulated by soluble cytokines. *J Immunol,* 150**,** 3671-80.

ARMSTRONG, A. C., DERMIME, S., ALLINSON, C. G., BHATTACHARYYA, T., MULRYAN, K., GONZALEZ, K. R., STERN, P. L. & HAWKINS, R. E. 2002. Immunization with a recombinant adenovirus encoding a lymphoma idiotype: induction of tumor-protective immunity and identification of an idiotype-specific T cell epitope. *J Immunol,* 168**,** 3983-91.

ARPIN, C., DÉCHANET, J., VAN KOOTEN, C., MERVILLE, P., GROUARD, G., BRIÈRE, F., BANCHEREAU, J. & LIU, Y. J. 1995. Generation of memory B cells and plasma cells in vitro. *Science,* 268**,** 720-2.

ASHUR, Y., ADLER, R., ROWE, M. & SHOUVAL, D. 1999. Comparison of immunogenicity of two hepatitis A vaccines--VAQTA and HAVRIX--in young adults. *Vaccine,* 17**,** 2290-6.

AUBIN, E., LEMIEUX, R. & BAZIN, R. 2010. Indirect inhibition of in vivo and in vitro T-cell responses by intravenous immunoglobulins due to impaired antigen presentation. *Blood,* 115**,** 1727-34.

AUJLA, S. J., CHAN, Y. R., ZHENG, M., FEI, M., ASKEW, D. J., POCIASK, D. A., REINHART, T. A., MCALLISTER, F., EDEAL, J., GAUS, K., HUSAIN, S., KREINDLER, J. L., DUBIN, P. J., PILEWSKI, J. M., MYERBURG, M. M., MASON, C. A., IWAKURA, Y. & KOLLS, J. K. 2008. IL-22 mediates mucosal host defense against Gram-negative bacterial pneumonia. *Nat Med,* 14**,** 275-81.

AVALOS, A. M. & PLOEGH, H. L. 2014. Early BCR Events and Antigen Capture, Processing, and Loading on MHC Class II on B Cells. *Front Immunol,* 5**,** 92.

BAL, S. M., SLÜTTER, B., JISKOOT, W. & BOUWSTRA, J. A. 2011. Small is beautiful: N-trimethyl chitosan-ovalbumin conjugates for microneedle-based transcutaneous immunisation. *Vaccine,* 29**,** 4025-32.

BALDRICK, P., RICHARDSON, D., WORONIECKI, S. R. & LEES, B. 2007. Pollinex Quattro Ragweed: safety evaluation of a new allergy vaccine adjuvanted with monophosphoryl lipid A (MPL) for the treatment of ragweed pollen allergy. *J Appl Toxicol,* 27**,** 399-409.

BANCHEREAU, J., DE PAOLI, P., VALLÉ, A., GARCIA, E. & ROUSSET, F. 1991. Long-term human B cell lines dependent on interleukin-4 and antibody to CD40. *Science,* 251**,** 70-2.

BANCHEREAU, J. & STEINMAN, R. M. 1998. Dendritic cells and the control of immunity. *Nature,* 392**,** 245-52.

BARBER, D. L., WHERRY, E. J. & AHMED, R. 2003. Cutting edge: rapid in vivo killing by memory CD8 T cells. *J Immunol,* 171**,** 27-31.

BARR, T. A., CARLRING, J. & HEATH, A. W. 2005. CD40 antibody as a potent immunological adjuvant: CD40 antibody provides the CD40 signal to B cells, but does not substitute for T cell help in responses to TD antigens. *Vaccine,* 23**,** 3477-82.

BARR, T. A., CARLRING, J. & HEATH, A. W. 2006. Co-stimulatory agonists as immunological adjuvants. *Vaccine,* 24**,** 3399-407.

BARR, T. A. & HEATH, A. W. 1999. Enhanced in vivo immune responses to bacterial lipopolysaccharide by exogenous CD40 stimulation. *Infect Immun,* 67**,** 3637-40.

BARR, T. A. & HEATH, A. W. 2001. Functional activity of CD40 antibodies correlates to the position of binding relative to CD154. *Immunology,* 102**,** 39-43.

BARR, T. A., MCCORMICK, A. L., CARLRING, J. & HEATH, A. W. 2003. A potent adjuvant effect of CD40 antibody attached to antigen. *Immunology,* 109**,** 87-92.

BEATTY, G. L., TORIGIAN, D. A., CHIOREAN, E. G., SABOURY, B., BROTHERS, A., ALAVI, A., TROXEL, A. B., SUN, W., TEITELBAUM, U. R., VONDERHEIDE, R. H. & O'DWYER, P. J. 2013. A phase I study of an agonist CD40 monoclonal antibody (CP-870,893) in combination with gemcitabine in patients with advanced pancreatic ductal adenocarcinoma. *Clin Cancer Res,* 19**,** 6286-95.

BEAUDETTE, T. T., BACHELDER, E. M., COHEN, J. A., OBERMEYER, A. C., BROADERS, K. E., FRÉCHET, J. M., KANG, E. S., MENDE, I., TSENG, W. W., DAVIDSON, M. G. & ENGLEMAN, E. G. 2009. In vivo studies on the effect of co-encapsulation of CpG DNA and antigen in acid-degradable microparticle vaccines. *Mol Pharm,* 6**,** 1160-9.

BEDOUI, S., WHITNEY, P. G., WAITHMAN, J., EIDSMO, L., WAKIM, L., CAMINSCHI, I., ALLAN, R. S., WOJTASIAK, M., SHORTMAN, K., CARBONE, F. R., BROOKS, A. G. & HEATH, W. R. 2009. Cross-presentation of viral and self antigens by skin-derived CD103+ dendritic cells. *Nat Immunol,* 10**,** 488-95.

BENDANDI, M. 2009. Idiotype vaccines for lymphoma: proof-of-principles and clinical trial failures. *Nat Rev Cancer,* 9**,** 675-81.

BENDANDI, M., GOCKE, C. D., KOBRIN, C. B., BENKO, F. A., STERNAS, L. A., PENNINGTON, R., WATSON, T. M., REYNOLDS, C. W., GAUSE, B. L., DUFFEY, P. L., JAFFE, E. S., CREEKMORE, S. P., LONGO, D. L. & KWAK, L. W. 1999. Complete molecular remissions induced by patient-specific vaccination plus granulocyte-monocyte colony-stimulating factor against lymphoma. *Nat Med,* 5**,** 1171-7.

BENNETT, K., LEVINE, T., ELLIS, J. S., PEANASKY, R. J., SAMLOFF, I. M., KAY, J. & CHAIN, B. M. 1992. Antigen processing for presentation by class II major histocompatibility complex requires cleavage by cathepsin E. *Eur J Immunol,* 22**,** 1519-24.

BENNETT, S. R., CARBONE, F. R., KARAMALIS, F., FLAVELL, R. A., MILLER, J. F. & HEATH, W. R. 1998. Help for cytotoxic-T-cell responses is mediated by CD40 signalling. *Nature,* 393**,** 478-80.

BERGTOLD, A., DESAI, D. D., GAVHANE, A. & CLYNES, R. 2005. Cell surface recycling of internalized antigen permits dendritic cell priming of B cells. *Immunity,* 23**,** 503-14.

BETTELLI, E., CARRIER, Y., GAO, W., KORN, T., STROM, T. B., OUKKA, M., WEINER, H. L. & KUCHROO, V. K. 2006. Reciprocal developmental pathways for the generation of pathogenic effector TH17 and regulatory T cells. *Nature,* 441**,** 235-8.

BETTING, D. J., KAFI, K., ABDOLLAHI-FARD, A., HURVITZ, S. A. & TIMMERMAN, J. M. 2008. Sulfhydryl-based tumor antigen-carrier protein conjugates stimulate superior antitumor immunity against B cell lymphomas. *J Immunol,* 181**,** 4131-40.

BHAGAWATI-PRASAD, V. N., DE LEENHEER, E., KEEFE, N. P., RYAN, L. A., CARLRING, J. & HEATH, A. W. 2010. CD40mAb adjuvant induces a rapid antibody response that may be beneficial in post-exposure prophylaxis. *J Immune Based Ther Vaccines,* 8**,** 1.

BIRAGYN, A., TANI, K., GRIMM, M. C., WEEKS, S. & KWAK, L. W. 1999. Genetic fusion of chemokines to a self tumor antigen induces protective, T-cell dependent antitumor immunity. *Nat Biotechnol,* 17**,** 253-8.

BJORKMAN, P. J., SAPER, M. A., SAMRAOUI, B., BENNETT, W. S., STROMINGER, J. L. & WILEY, D. C. 1987. Structure of the human class I histocompatibility antigen, HLA-A2. *Nature,* 329**,** 506-12.

BJÖRCK, P., BANCHEREAU, J. & FLORES-ROMO, L. 1997. CD40 ligation counteracts Fas-induced apoptosis of human dendritic cells. *Int Immunol,* 9**,** 365-72.

BLACK, S., FRIEDLAND, L. R., ENSOR, K., WESTON, W. M., HOWE, B. & KLEIN, N. P. 2008. Diphtheria-tetanus-acellular pertussis and inactivated poliovirus vaccines given separately or combined for booster dosing at 4-6 years of age. *Pediatr Infect Dis J,* 27**,** 341-6.

BLASIUS, A. L., GIURISATO, E., CELLA, M., SCHREIBER, R. D., SHAW, A. S. & COLONNA, M. 2006. Bone marrow stromal cell antigen 2 is a specific marker of type I IFN-producing cells in the naive mouse, but a promiscuous cell surface antigen following IFN stimulation. *J Immunol,* 177**,** 3260-5.

BLUM, J. S., WEARSCH, P. A. & CRESSWELL, P. 2013. Pathways of antigen processing. *Annu Rev Immunol,* 31**,** 443-73.

BONIFAZ, L. C., BONNYAY, D. P., CHARALAMBOUS, A., DARGUSTE, D. I., FUJII, S., SOARES, H., BRIMNES, M. K., MOLTEDO, B., MORAN, T. M. & STEINMAN, R. M. 2004. In vivo targeting of antigens to maturing dendritic cells via the DEC-205 receptor improves T cell vaccination. *J Exp Med,* 199**,** 815-24.

BONNEAU, M., EPARDAUD, M., PAYOT, F., NIBORSKI, V., THOULOUZE, M. I., BERNEX, F., CHARLEY, B., RIFFAULT, S., GUILLOTEAU, L. A. & SCHWARTZ-CORNIL, I. 2006. Migratory monocytes and granulocytes are major lymphatic carriers of Salmonella from tissue to draining lymph node. *J Leukoc Biol,* 79**,** 268-76.

BOUAZIZ, J. D., YANABA, K., VENTURI, G. M., WANG, Y., TISCH, R. M., POE, J. C. & TEDDER, T. F. 2007. Therapeutic B cell depletion impairs adaptive and autoreactive CD4+ T cell activation in mice. *Proc Natl Acad Sci U S A,* 104**,** 20878-83.

BOVIER, P. A. 2008. Epaxal: a virosomal vaccine to prevent hepatitis A infection. *Expert Rev Vaccines,* 7**,** 1141-50.

BREMAN, J. G. & ARITA, I. 1980. The confirmation and maintenance of smallpox eradication. *N Engl J Med,* 303**,** 1263-73.

BREWER, J. M., CONACHER, M., HUNTER, C. A., MOHRS, M., BROMBACHER, F. & ALEXANDER, J. 1999. Aluminium hydroxide adjuvant initiates strong antigen-specific Th2 responses in the absence of IL-4- or IL-13-mediated signaling. *J Immunol,* 163**,** 6448-54.

BREWER, J. M., CONACHER, M., SATOSKAR, A., BLUETHMANN, H. & ALEXANDER, J. 1996. In interleukin-4-deficient mice, alum not only generates T helper 1 responses equivalent to freund's complete adjuvant, but continues to induce T helper 2 cytokine production. *Eur J Immunol,* 26**,** 2062-6.

BREWER, J. M., POLLOCK, K. G., TETLEY, L. & RUSSELL, D. G. 2004. Vesicle size influences the trafficking, processing, and presentation of antigens in lipid vesicles. *J Immunol,* 173**,** 6143-50.

BRUSA, D., GARETTO, S., CHIORINO, G., SCATOLINI, M., MIGLIORE, E., CAMUSSI, G. & MATERA, L. 2008. Post-apoptotic tumors are more palatable to dendritic cells and enhance their antigen cross-presentation activity. *Vaccine,* 26**,** 6422-32.

BUNGENER, L., SERRE, K., BIJL, L., LESERMAN, L., WILSCHUT, J., DAEMEN, T. & MACHY, P. 2002. Virosome-mediated delivery of protein antigens to dendritic cells. *Vaccine,* 20**,** 2287-95.

BUONAGURO, L., AURISICCHIO, L., BUONAGURO, F. M. & CILIBERTO, G. 2013. New developments in cancer vaccines. *Expert Rev Vaccines,* 12**,** 1109-10.

BYERS, A. M., KEMBALL, C. C., MOSER, J. M. & LUKACHER, A. E. 2003. Cutting edge: rapid in vivo CTL activity by polyoma virus-specific effector and memory CD8+ T cells. *J Immunol,* 171**,** 17-21.

CAI, H., HUANG, Z. H., SHI, L., ZHAO, Y. F., KUNZ, H. & LI, Y. M. 2011. Towards a fully synthetic MUC1-based anticancer vaccine: efficient conjugation of glycopeptides with mono-, di-, and tetravalent lipopeptides using click chemistry. *Chemistry,* 17**,** 6396-406.

CAI, H., SUN, Z. Y., CHEN, M. S., ZHAO, Y. F., KUNZ, H. & LI, Y. M. 2014. Synthetic multivalent glycopeptide-lipopeptide antitumor vaccines: impact of the cluster effect on the killing of tumor cells. *Angew Chem Int Ed Engl,* 53**,** 1699-703.

CALABRO, S., TORTOLI, M., BAUDNER, B. C., PACITTO, A., CORTESE, M., O'HAGAN, D. T., DE GREGORIO, E., SEUBERT, A. & WACK, A. 2011. Vaccine adjuvants alum and MF59 induce rapid recruitment of neutrophils and monocytes that participate in antigen transport to draining lymph nodes. *Vaccine,* 29**,** 1812-23.

CALL, M. E., PYRDOL, J., WIEDMANN, M. & WUCHERPFENNIG, K. W. 2002. The organizing principle in the formation of the T cell receptor-CD3 complex. *Cell,* 111**,** 967-79.

CALLARD, R. E., ARMITAGE, R. J., FANSLOW, W. C. & SPRIGGS, M. K. 1993. CD40 ligand and its role in X-linked hyper-IgM syndrome. *Immunology Today,* 14**,** 559-64.

CALMETTE, A. 1931. Preventive Vaccination Against Tuberculosis with BCG. *Proc R Soc Med,* 24**,** 1481-90.

CAMPBELL, M. J., CARROLL, W., KON, S., THIELEMANS, K., ROTHBARD, J. B., LEVY, S. & LEVY, R. 1987. Idiotype vaccination against murine B cell lymphoma. Humoral and cellular responses elicited by tumor-derived immunoglobulin M and its molecular subunits. *J Immunol,* 139**,** 2825-33.

CAMPBELL, M. J., ESSERMAN, L. & LEVY, R. 1988. Immunotherapy of established murine B cell lymphoma. Combination of idiotype immunization and cyclophosphamide. *J Immunol,* 141**,** 3227-33.

CARLRING, J., BARR, T. A., MCCORMICK, A. L. & HEATH, A. W. 2004. CD40 antibody as an adjuvant induces enhanced T cell responses. *Vaccine,* 22**,** 3323-8.

CARLRING, J., SZABO, M. J., DICKINSON, R., DE LEENHEER, E. & HEATH, A. W. 2012. Conjugation of lymphoma idiotype to CD40 antibody enhances lymphoma vaccine immunogenicity and antitumor effects in mice. *Blood,* 119**,** 2056-65.

CASAMAYOR-PALLEJA, M., KHAN, M. & MACLENNAN, I. C. 1995. A subset of CD4+ memory T cells contains preformed CD40 ligand that is rapidly but transiently expressed on their surface after activation through the T cell receptor complex. *J Exp Med,* 181**,** 1293-301.

CASTIGLI, E., ALT, F. W., DAVIDSON, L., BOTTARO, A., MIZOGUCHI, E., BHAN, A. K. & GEHA, R. S. 1994. CD40-deficient mice generated by recombination-activating gene-2-deficient blastocyst complementation. *Proc Natl Acad Sci U S A,* 91**,** 12135-9.

CAUX, C., MASSACRIER, C., VANBERVLIET, B., DUBOIS, B., VAN KOOTEN, C., DURAND, I. & BANCHEREAU, J. 1994. Activation of human dendritic cells through CD40 cross-linking. *J Exp Med,* 180**,** 1263-72.

CELLA, M., JARROSSAY, D., FACCHETTI, F., ALEBARDI, O., NAKAJIMA, H., LANZAVECCHIA, A. & COLONNA, M. 1999. Plasmacytoid monocytes migrate to inflamed lymph nodes and produce large amounts of type I interferon. *Nat Med,* 5**,** 919-23.

CELLA, M., SALLUSTO, F. & LANZAVECCHIA, A. 1997. Origin, maturation and antigen presenting function of dendritic cells. *Curr Opin Immunol,* 9**,** 10-6.

CELLA, M., SCHEIDEGGER, D., PALMER-LEHMANN, K., LANE, P., LANZAVECCHIA, A. & ALBER, G. 1996. Ligation of CD40 on dendritic cells triggers production of high levels of interleukin-12 and enhances T cell stimulatory capacity: T-T help via APC activation. *J Exp Med,* 184**,** 747-52.

CESCO-GASPERE, M., BENVENUTI, F. & BURRONE, O. R. 2005. BCL1 lymphoma protection induced by idiotype DNA vaccination is entirely dependent on anti-idiotypic antibodies. *Cancer Immunol Immunother,* 54**,** 351-8.

CESCO-GASPERE, M., ZENTILIN, L., GIACCA, M. & BURRONE, O. R. 2008. Boosting anti-idiotype immune response with recombinant AAV enhances tumour protection induced by gene gun vaccination. *Scand J Immunol,* 68**,** 58-66.

CHATTERJEE, B., SMED-SÖRENSEN, A., COHN, L., CHALOUNI, C., VANDLEN, R., LEE, B. C., WIDGER, J., KELER, T., DELAMARRE, L. & MELLMAN, I. 2012. Internalization and endosomal degradation of receptor-bound antigens regulate the efficiency of cross presentation by human dendritic cells. *Blood,* 120**,** 2011-20.

CHICZ, R. M., URBAN, R. G., LANE, W. S., GORGA, J. C., STERN, L. J., VIGNALI, D. A. & STROMINGER, J. L. 1992. Predominant naturally processed peptides bound to HLA-DR1 are derived from MHC-related molecules and are heterogeneous in size. *Nature,* 358**,** 764-8.

CHO, H. J., TAKABAYASHI, K., CHENG, P. M., NGUYEN, M. D., CORR, M., TUCK, S. & RAZ, E. 2000. Immunostimulatory DNA-based vaccines induce cytotoxic lymphocyte activity by a T-helper cell-independent mechanism. *Nat Biotechnol,* 18**,** 509-14.

CHONG, C. S., CAO, M., WONG, W. W., FISCHER, K. P., ADDISON, W. R., KWON, G. S., TYRRELL, D. L. & SAMUEL, J. 2005. Enhancement of T helper type 1 immune responses against hepatitis B virus core antigen by PLGA nanoparticle vaccine delivery. *J Control Release,* 102**,** 85-99.

CHOWDHURY, D. & LIEBERMAN, J. 2008. Death by a thousand cuts: granzyme pathways of programmed cell death. *Annu Rev Immunol,* 26**,** 389-420.

CLARK, E. A. & LEDBETTER, J. A. 1986. Activation of human B cells mediated through two distinct cell surface differentiation antigens, Bp35 and Bp50. *Proc Natl Acad Sci U S A,* 83**,** 4494-8.

COFFMAN, R. L., OHARA, J., BOND, M. W., CARTY, J., ZLOTNIK, A. & PAUL, W. E. 1986. B cell stimulatory factor-1 enhances the IgE response of lipopolysaccharide-activated B cells. *J Immunol,* 136**,** 4538-41.

COFFMAN, R. L., SHER, A. & SEDER, R. A. 2010. Vaccine adjuvants: putting innate immunity to work. *Immunity,* 33**,** 492-503.

COLLINS, P. D., MARLEAU, S., GRIFFITHS-JOHNSON, D. A., JOSE, P. J. & WILLIAMS, T. J. 1995. Cooperation between interleukin-5 and the chemokine eotaxin to induce eosinophil accumulation in vivo. *J Exp Med,* 182**,** 1169-74.

CONSTANT, S., PFEIFFER, C., WOODARD, A., PASQUALINI, T. & BOTTOMLY, K. 1995. Extent of T cell receptor ligation can determine the functional differentiation of naive CD4+ T cells. *J Exp Med,* 182**,** 1591-6.

CREUSOT, R. J., YAGHOUBI, S. S., CHANG, P., CHIA, J., CONTAG, C. H., GAMBHIR, S. S. & FATHMAN, C. G. 2009. Lymphoid-tissue-specific homing of bone-marrow-derived dendritic cells. *Blood,* 113**,** 6638-47.

CROTTI, S., ZHAI, H., ZHOU, J., ALLAN, M., PROIETTI, D., PANSEGRAU, W., HU, Q. Y., BERTI, F. & ADAMO, R. 2014. Defined conjugation of glycans to the lysines of CRM197 guided by their reactivity mapping. *Chembiochem,* 15**,** 836-43.

CRUCELL. http://www.crucell.com. [Accessed October 2014.

CURTSINGER, J. M., LINS, D. C. & MESCHER, M. F. 2003. Signal 3 determines tolerance versus full activation of naive CD8 T cells: dissociating proliferation and development of effector function. *J Exp Med,* 197**,** 1141-51.

CYCON, K. A., CLEMENTS, J. L., HOLTZ, R., FUJI, H. & MURPHY, S. P. 2009. The immunogenicity of L1210 lymphoma clones correlates with their ability to function as antigen-presenting cells. *Immunology,* 128**,** e641-51.

DAVIDSON, H. W., WEST, M. A. & WATTS, C. 1990. Endocytosis, intracellular trafficking, and processing of membrane IgG and monovalent antigen/membrane IgG complexes in B lymphocytes. *J Immunol,* 144**,** 4101-9.

DE BECKER, G., MOULIN, V., PAJAK, B., BRUCK, C., FRANCOTTE, M., THIRIART, C., URBAIN, J. & MOSER, M. 2000. The adjuvant monophosphoryl lipid A increases the function of antigen-presenting cells. *Int Immunol,* 12**,** 807-15.

DE SMEDT, T., PAJAK, B., MURAILLE, E., LESPAGNARD, L., HEINEN, E., DE BAETSELIER, P., URBAIN, J., LEO, O. & MOSER, M. 1996. Regulation of dendritic cell numbers and maturation by lipopolysaccharide in vivo. *J Exp Med,* 184**,** 1413-24.

DE VRIES, I. J., KROOSHOOP, D. J., SCHARENBORG, N. M., LESTERHUIS, W. J., DIEPSTRA, J. H., VAN MUIJEN, G. N., STRIJK, S. P., RUERS, T. J., BOERMAN, O. C., OYEN, W. J., ADEMA, G. J., PUNT, C. J. & FIGDOR, C. G. 2003a. Effective migration of antigen-pulsed dendritic cells to lymph nodes in melanoma patients is determined by their maturation state. *Cancer Res,* 63**,** 12-7.

DE VRIES, I. J., LESTERHUIS, W. J., SCHARENBORG, N. M., ENGELEN, L. P., RUITER, D. J., GERRITSEN, M. J., CROOCKEWIT, S., BRITTEN, C. M., TORENSMA, R., ADEMA, G. J., FIGDOR, C. G. & PUNT, C. J. 2003b. Maturation of dendritic cells is a prerequisite for inducing immune responses in advanced melanoma patients. *Clin Cancer Res,* 9**,** 5091-100.

DECKER, M. D., EDWARDS, K. M., BRADLEY, R. & PALMER, P. 1992. Comparative trial in infants of four conjugate Haemophilus influenzae type b vaccines. *J Pediatr,* 120**,** 184-9.

DEMENTO, S. L., SIEFERT, A. L., BANDYOPADHYAY, A., SHARP, F. A. & FAHMY, T. M. 2011. Pathogen-associated molecular patterns on biomaterials: a paradigm for engineering new vaccines. *Trends Biotechnol,* 29**,** 294-306.

DEN HAAN, J. M., LEHAR, S. M. & BEVAN, M. J. 2000. CD8(+) but not CD8(-) dendritic cells cross-prime cytotoxic T cells in vivo. *J Exp Med,* 192**,** 1685-96.

DIDIERLAURENT, A. M., COLLIGNON, C., BOURGUIGNON, P., WOUTERS, S., FIERENS, K., FOCHESATO, M., DENDOUGA, N., LANGLET, C., MALISSEN, B., LAMBRECHT, B. N., GARÇON, N., VAN MECHELEN, M. & MOREL, S. 2014. Enhancement of adaptive immunity by the human vaccine adjuvant AS01 depends on activated dendritic cells. *J Immunol,* 193**,** 1920-30.

DIDIERLAURENT, A. M., MOREL, S., LOCKMAN, L., GIANNINI, S. L., BISTEAU, M., CARLSEN, H., KIELLAND, A., VOSTERS, O., VANDERHEYDE, N., SCHIAVETTI, F., LAROCQUE, D., VAN MECHELEN, M. & GARÇON, N. 2009. AS04, an aluminum salt- and TLR4 agonist-based adjuvant system, induces a transient localized innate immune response leading to enhanced adaptive immunity. *J Immunol,* 183**,** 6186-97.

DIEHL, L., DEN BOER, A. T., SCHOENBERGER, S. P., VAN DER VOORT, E. I., SCHUMACHER, T. N., MELIEF, C. J., OFFRINGA, R. & TOES, R. E. 1999. CD40 activation in vivo overcomes peptide-induced peripheral cytotoxic T-lymphocyte tolerance and augments anti-tumor vaccine efficacy. *Nat Med,* 5**,** 774-9.

DIETRICH, J., ANDREASEN, L. V., ANDERSEN, P. & AGGER, E. M. 2014. Inducing dose sparing with inactivated polio virus formulated in adjuvant CAF01. *PLoS One,* 9**,** e100879.

DINTZIS, R. Z., MIDDLETON, M. H. & DINTZIS, H. M. 1983. Studies on the immunogenicity and tolerogenicity of T-independent antigens. *J Immunol,* 131**,** 2196-203.

DONG, H., STROME, S. E., SALOMAO, D. R., TAMURA, H., HIRANO, F., FLIES, D. B., ROCHE, P. C., LU, J., ZHU, G., TAMADA, K., LENNON, V. A., CELIS, E. & CHEN, L. 2002. Tumor-associated B7-H1 promotes T-cell apoptosis: a potential mechanism of immune evasion. *Nat Med,* 8**,** 793-800.

DUDZIAK, D., KAMPHORST, A. O., HEIDKAMP, G. F., BUCHHOLZ, V. R., TRUMPFHELLER, C., YAMAZAKI, S., CHEONG, C., LIU, K., LEE, H. W., PARK, C. G., STEINMAN, R. M. & NUSSENZWEIG, M. C. 2007. Differential antigen processing by dendritic cell subsets in vivo. *Science,* 315**,** 107-11.

DULLFORCE, P., SUTTON, D. C. & HEATH, A. W. 1998. Enhancement of T cell-independent immune responses in vivo by CD40 antibodies. *Nat Med,* 4**,** 88-91.

DUPONT, J., ALTCLAS, J., LEPETIC, A., LOMBARDO, M., VÁZQUEZ, V., SALGUEIRA, C., SEIGELCHIFER, M., ARNDTZ, N., ANTUNEZ, E., VON ESCHEN, K. & JANOWICZ, Z. 2006. A controlled clinical trial comparing the safety and immunogenicity of a new adjuvanted hepatitis B vaccine with a standard hepatitis B vaccine. *Vaccine,* 24**,** 7167-74.

DUPUIS, M., MURPHY, T. J., HIGGINS, D., UGOZZOLI, M., VAN NEST, G., OTT, G. & MCDONALD, D. M. 1998. Dendritic cells internalize vaccine adjuvant after intramuscular injection. *Cell Immunol,* 186**,** 18-27.

DURIANCIK, D. M. & HOAG, K. A. 2009. The identification and enumeration of dendritic cell populations from individual mouse spleen and Peyer's patches using flow cytometric analysis. *Cytometry A,* 75**,** 951-9.

DUSTIN, M. L. & SPRINGER, T. A. 1989. T-cell receptor cross-linking transiently stimulates adhesiveness through LFA-1. *Nature,* 341**,** 619-24.

DZIONEK, A., SOHMA, Y., NAGAFUNE, J., CELLA, M., COLONNA, M., FACCHETTI, F., GÜNTHER, G., JOHNSTON, I., LANZAVECCHIA, A., NAGASAKA, T., OKADA, T., VERMI, W., WINKELS, G., YAMAMOTO, T., ZYSK, M., YAMAGUCHI, Y. & SCHMITZ, J. 2001. BDCA-2, a novel plasmacytoid dendritic cell-specific type II C-type lectin, mediates antigen capture and is a potent inhibitor of interferon alpha/beta induction. *J Exp Med,* 194**,** 1823-34.

ELGUETA, R., BENSON, M. J., DE VRIES, V. C., WASIUK, A., GUO, Y. & NOELLE, R. J. 2009. Molecular mechanism and function of CD40/CD40L engagement in the immune system. *Immunol Rev,* 229**,** 152-72.

ELLOUZ, F., ADAM, A., CIORBARU, R. & LEDERER, E. 1974. Minimal Structural Requirements for Adjuvant Activity of Bacterial Peptidoglycan Derivatives. *Biochemical and Biophysical Research Communications,* 59**,** 1317-1325.

ENG, N. F., BHARDWAJ, N., MULLIGAN, R. & DIAZ-MITOMA, F. 2013. The potential of 1018 ISS adjuvant in hepatitis B vaccines: HEPLISAV™ review. *Hum Vaccin Immunother,* 9**,** 1661-72.

FALK, K., RÖTZSCHKE, O., STEVANOVIĆ, S., JUNG, G. & RAMMENSEE, H. G. 1991. Allele-specific motifs revealed by sequencing of self-peptides eluted from MHC molecules. *Nature,* 351**,** 290-6.

FANALE, M., ASSOULINE, S., KURUVILLA, J., SOLAL-CÉLIGNY, P., HEO, D. S., VERHOEF, G., CORRADINI, P., ABRAMSON, J. S., OFFNER, F., ENGERT, A., DYER, M. J., CARREON, D., EWALD, B., BAECK, J., YOUNES, A. & FREEDMAN, A. S. 2014. Phase IA/II, multicentre, open-label study of the CD40 antagonistic monoclonal antibody lucatumumab in adult patients with advanced non-Hodgkin or Hodgkin lymphoma. *Br J Haematol,* 164**,** 258-65.

FELTKAMP, M. C., SMITS, H. L., VIERBOOM, M. P., MINNAAR, R. P., DE JONGH, B. M., DRIJFHOUT, J. W., TER SCHEGGET, J., MELIEF, C. J. & KAST, W. M. 1993. Vaccination with cytotoxic T lymphocyte epitope-containing peptide protects against a tumor induced by human papillomavirus type 16-transformed cells. *Eur J Immunol,* 23**,** 2242-9.

FENNER, F., HENDERSON, D., ARITA, I., JEZEK, Z. & LADNYI, I. 1988. Smallpox and its eradication. Geneva, Switzerland: World Health Organisation.

FLACH, T. L., NG, G., HARI, A., DESROSIERS, M. D., ZHANG, P., WARD, S. M., SEAMONE, M. E., VILAYSANE, A., MUCSI, A. D., FONG, Y., PRENNER, E., LING, C. C., TSCHOPP, J., MURUVE, D. A., AMREIN, M. W. & SHI, Y. 2011. Alum interaction with dendritic cell membrane lipids is essential for its adjuvanticity. *Nat Med,* 17**,** 479-87.

FOY, T. M., LAMAN, J. D., LEDBETTER, J. A., ARUFFO, A., CLAASSEN, E. & NOELLE, R. J. 1994. gp39-CD40 interactions are essential for germinal center formation and the development of B cell memory. *J Exp Med,* 180**,** 157-63.

FRANCHI, L. & NÚÑEZ, G. 2008. The Nlrp3 inflammasome is critical for aluminium hydroxide-mediated IL-1beta secretion but dispensable for adjuvant activity. *Eur J Immunol,* 38**,** 2085-9.

FREEDMAN, A., NEELAPU, S. S., NICHOLS, C., ROBERTSON, M. J., DJULBEGOVIC, B., WINTER, J. N., BENDER, J. F., GOLD, D. P., GHALIE, R. G., STEWART, M. E., ESQUIBEL, V. & HAMLIN, P. 2009. Placebo-controlled phase III trial of patient-specific immunotherapy with mitumprotimut-T and granulocyte-macrophage colony-stimulating factor after rituximab in patients with follicular lymphoma. *J Clin Oncol,* 27**,** 3036-43.

FREMONT, D. H., MATSUMURA, M., STURA, E. A., PETERSON, P. A. & WILSON, I. A. 1992. Crystal structures of two viral peptides in complex with murine MHC class I H-2Kb. *Science,* 257**,** 919-27.

FRENCH, R. R., CHAN, H. T., TUTT, A. L. & GLENNIE, M. J. 1999. CD40 antibody evokes a cytotoxic T-cell response that eradicates lymphoma and bypasses T-cell help. *Nat Med,* 5**,** 548-53.

FREUND, J. 1956. The mode of action of immunologic adjuvants. *Bibl Tuberc***,** 130-48.

GALANOS, C., LÜDERITZ, O., RIETSCHEL, E. T., WESTPHAL, O., BRADE, H., BRADE, L., FREUDENBERG, M., SCHADE, U., IMOTO, M. & YOSHIMURA, H. 1985. Synthetic and natural Escherichia coli free lipid A express identical endotoxic activities. *Eur J Biochem,* 148**,** 1-5.

GALEA-LAURI, J., WELLS, J. W., DARLING, D., HARRISON, P. & FARZANEH, F. 2004. Strategies for antigen choice and priming of dendritic cells influence the polarization and efficacy of antitumor T-cell responses in dendritic cell-based cancer vaccination. *Cancer Immunol Immunother,* 53**,** 963-77.

GALEN, J. E., WANG, J. Y., CHINCHILLA, M., VINDURAMPULLE, C., VOGEL, J. E., LEVY, H., BLACKWELDER, W. C., PASETTI, M. F. & LEVINE, M. M. 2010. A new generation of stable, nonantibiotic, low-copy-number plasmids improves immune responses to foreign antigens in Salmonella enterica serovar Typhi live vectors. *Infect Immun,* 78**,** 337-47.

GAO, J., MA, X., GU, W., FU, M., AN, J., XING, Y., GAO, T., LI, W. & LIU, Y. 2012. Novel functions of murine B1 cells: active phagocytic and microbicidal abilities. *Eur J Immunol,* 42**,** 982-92.

GARBOCZI, D. N., GHOSH, P., UTZ, U., FAN, Q. R., BIDDISON, W. E. & WILEY, D. C. 1996. Structure of the complex between human T-cell receptor, viral peptide and HLA-A2. *Nature,* 384**,** 134-41.

GARCIA DE VINUESA, C., MACLENNAN, I. C., HOLMAN, M. & KLAUS, G. G. 1999. Anti-CD40 antibody enhances responses to polysaccharide without mimicking T cell help. *European journal of immunology,* 29**,** 3216-24.

GARRONE, P., NEIDHARDT, E. M., GARCIA, E., GALIBERT, L., VAN KOOTEN, C. & BANCHEREAU, J. 1995. Fas ligation induces apoptosis of CD40-activated human B lymphocytes. *J Exp Med,* 182**,** 1265-73.

GAUCHAT, J. F., AUBRY, J. P., MAZZEI, G., LIFE, P., JOMOTTE, T., ELSON, G. & BONNEFOY, J. Y. 1993. Human CD40-ligand: molecular cloning, cellular distribution and regulation of expression by factors controlling IgE production. *FEBS Lett,* 315**,** 259-66.

GAVIN, A. L., HOEBE, K., DUONG, B., OTA, T., MARTIN, C., BEUTLER, B. & NEMAZEE, D. 2006. Adjuvant-enhanced antibody responses in the absence of toll-like receptor signaling. *Science,* 314**,** 1936-8.

GEISBERGER, R., LAMERS, M. & ACHATZ, G. 2006. The riddle of the dual expression of IgM and IgD. *Immunology,* 118**,** 429-37.

GEISSMANN, F., JUNG, S. & LITTMAN, D. R. 2003. Blood monocytes consist of two principal subsets with distinct migratory properties. *Immunity,* 19**,** 71-82.

GHIMIRE, T. R., BENSON, R. A., GARSIDE, P. & BREWER, J. M. 2012. Alum increases antigen uptake, reduces antigen degradation and sustains antigen presentation by DCs in vitro. *Immunol Lett,* 147**,** 55-62.

GIANNINI, S. L., HANON, E., MORIS, P., VAN MECHELEN, M., MOREL, S., DESSY, F., FOURNEAU, M. A., COLAU, B., SUZICH, J., LOSONKSY, G., MARTIN, M. T., DUBIN, G. & WETTENDORFF, M. A. 2006. Enhanced humoral and memory B cellular immunity using HPV16/18 L1 VLP vaccine formulated with the MPL/aluminium salt combination (AS04) compared to aluminium salt only. *Vaccine,* 24**,** 5937-49.

GINHOUX, F., LIU, K., HELFT, J., BOGUNOVIC, M., GRETER, M., HASHIMOTO, D., PRICE, J., YIN, N., BROMBERG, J., LIRA, S. A., STANLEY, E. R., NUSSENZWEIG, M. & MERAD, M. 2009. The origin and development of nonlymphoid tissue CD103+ DCs. *J Exp Med,* 206**,** 3115-30.

GLAXOSMITHKLINE 2011. Cervarix®. Prescribing information.

GLAXOSMITHKLINE 2012. Engerix-B®. Prescribing information.

GLENNY, A. T., ALLEN, K. & HOPKINS, B. E. 1923. Testing the antigenic value of diphtheria toxin-antitoxin mixtures. *British Journal of Experimental Pathology,* 4**,** 19-27.

GLENNY, A. T. & POPE, C. G. 1925. The antigenic effect of intravenous injection of diphtheria toxin. *The Journal of Pathology and Bacteriology,* 28**,** 273-278.

GRAF, D., MULLER, S., KORTHAUER, U., VAN KOOTEN, C., WEISE, C. & KROCZEK, R. A. 1995. A soluble form of TRAP (CD40 ligand) is rapidly released after T cell activation. *Eur J Immunol,* 25**,** 1749-54.

GRANUCCI, F., FERRERO, E., FOTI, M., AGGUJARO, D., VETTORETTO, K. & RICCIARDI-CASTAGNOLI, P. 1999. Early events in dendritic cell maturation induced by LPS. *Microbes Infect,* 1**,** 1079-84.

GROMMÉ, M. & NEEFJES, J. 2002. Antigen degradation or presentation by MHC class I molecules via classical and non-classical pathways. *Mol Immunol,* 39**,** 181-202.

GRUN, J. L. & MAURER, P. H. 1989. Different T helper cell subsets elicited in mice utilizing two different adjuvant vehicles: the role of endogenous interleukin 1 in proliferative responses. *Cell Immunol,* 121**,** 134-45.

GUERMONPREZ, P., VALLADEAU, J., ZITVOGEL, L., THÉRY, C. & AMIGORENA, S. 2002. Antigen presentation and T cell stimulation by dendritic cells. *Annu Rev Immunol,* 20**,** 621-67.

GUILLOT, S., OTELEA, D., DELPEYROUX, F. & CRAINIC, R. 1994. Point mutations involved in the attenuation/neurovirulence alternation in type 1 and 2 oral polio vaccine strains detected by site-specific polymerase chain reaction. *Vaccine,* 12**,** 503-7.

HAN, R., ZHU, J., YANG, X. & XU, H. 2010. Surface modification of poly(D,L-lactic-co-glycolic acid) nanoparticles with protamine enhanced cross-presentation of encapsulated ovalbumin by bone marrow-derived dendritic cells. *J Biomed Mater Res A*.

HARDING, C. V. 1995. Intracellular organelles involved in antigen processing and the binding of peptides to class II MHC molecules. *Semin Immunol,* 7**,** 355-60.

HARDING, C. V. & GEUZE, H. J. 1992. Class II MHC molecules are present in macrophage lysosomes and phagolysosomes that function in the phagocytic processing of Listeria monocytogenes for presentation to T cells. *J Cell Biol,* 119**,** 531-42.

HARDING, C. V., UNANUE, E. R., SLOT, J. W., SCHWARTZ, A. L. & GEUZE, H. J. 1990. Functional and ultrastructural evidence for intracellular formation of major histocompatibility complex class II-peptide complexes during antigen processing. *Proc Natl Acad Sci U S A,* 87**,** 5553-7.

HARRIS, J. R. & MARKL, J. 1999. Keyhole limpet hemocyanin (KLH): a biomedical review. *Micron,* 30**,** 597-623.

HARTMANN, G., WEINER, G. J. & KRIEG, A. M. 1999. CpG DNA: a potent signal for growth, activation, and maturation of human dendritic cells. *Proc Natl Acad Sci U S A,* 96**,** 9305-10.

HASBOLD, J., JOHNSON-LÉGER, C., ATKINS, C. J., CLARK, E. A. & KLAUS, G. G. 1994. Properties of mouse CD40: cellular distribution of CD40 and B cell activation by monoclonal anti-mouse CD40 antibodies. *Eur J Immunol,* 24**,** 1835-42.

HATZIFOTI, C., BACON, A., MARRIOTT, H., LAING, P. & HEATH, A. W. 2008. Liposomal co-entrapment of CD40mAb induces enhanced IgG responses against bacterial polysaccharide and protein. *PLoS One,* 3**,** e2368.

HATZIFOTI, C. & HEATH, A. W. 2007. CD40-mediated enhancement of immune responses against three forms of influenza vaccine. *Immunology,* 122**,** 98-106.

HAYAKAWA, Y., KELLY, J. M., WESTWOOD, J. A., DARCY, P. K., DIEFENBACH, A., RAULET, D. & SMYTH, M. J. 2002. Cutting edge: tumor rejection mediated by NKG2D receptor-ligand interaction is dependent upon perforin. *J Immunol,* 169**,** 5377-81.

HEATH, A. & LAING, P. 2004. *Vaccine Comprising An Antigen Conjugated To Low Valency Anti-cd40 Or Anti-cd28 Antibodies*. 03789540.6.

HEATH, A. W., WU, W. W. & HOWARD, M. C. 1994. Monoclonal antibodies to murine CD40 define two distinct functional epitopes. *Eur J Immunol,* 24**,** 1828-34.

HEIT, A., BUSCH, D. H., WAGNER, H. & SCHMITZ, F. 2008. Vaccine protocols for enhanced immunogenicity of exogenous antigens. *Int J Med Microbiol,* 298**,** 27-32.

HEIT, A., HUSTER, K. M., SCHMITZ, F., SCHIEMANN, M., BUSCH, D. H. & WAGNER, H. 2004. CpG-DNA aided cross-priming by cross-presenting B cells. *J Immunol,* 172**,** 1501-7.

HENRI, S., VREMEC, D., KAMATH, A., WAITHMAN, J., WILLIAMS, S., BENOIST, C., BURNHAM, K., SAELAND, S., HANDMAN, E. & SHORTMAN, K. 2001. The dendritic cell populations of mouse lymph nodes. *J Immunol,* 167**,** 741-8.

HERNÁNDEZ-SANTOS, N., HUPPLER, A. R., PETERSON, A. C., KHADER, S. A., MCKENNA, K. C. & GAFFEN, S. L. 2013. Th17 cells confer long-term adaptive immunity to oral mucosal Candida albicans infections. *Mucosal Immunol,* 6**,** 900-10.

HERZOG, C., HARTMANN, K., KÜNZI, V., KÜRSTEINER, O., MISCHLER, R., LAZAR, H. & GLÜCK, R. 2009. Eleven years of Inflexal V-a virosomal adjuvanted influenza vaccine. *Vaccine,* 27**,** 4381-7.

HEWLETT, L. J., PRESCOTT, A. R. & WATTS, C. 1994. The coated pit and macropinocytic pathways serve distinct endosome populations. *J Cell Biol,* 124**,** 689-703.

HIGANO, C. S., SCHELLHAMMER, P. F., SMALL, E. J., BURCH, P. A., NEMUNAITIS, J., YUH, L., PROVOST, N. & FROHLICH, M. W. 2009. Integrated data from 2 randomized, double-blind, placebo-controlled, phase 3 trials of active cellular immunotherapy with sipuleucel-T in advanced prostate cancer. *Cancer,* 115**,** 3670-9.

HILLEMAN, M. R., BUYNAK, E. B., WEIBEL, R. E. & STOKES, J. 1968. Live, attenuated mumps-virus vaccine. *N Engl J Med,* 278**,** 227-32.

HUET, S., BOUMSELL, L., RAYNAL, B., DEGOS, L., DAUSSET, J. & BERNARD, A. 1987. Role in T-cell activation for HLA class I molecules from accessory cells: further distinction between activation signals delivered to T cells via CD2 and CD3 molecules. *Proc Natl Acad Sci U S A,* 84**,** 7222-6.

HUNT, D. F., MICHEL, H., DICKINSON, T. A., SHABANOWITZ, J., COX, A. L., SAKAGUCHI, K., APPELLA, E., GREY, H. M. & SETTE, A. 1992. Peptides presented to the immune system by the murine class II major histocompatibility complex molecule I-Ad. *Science,* 256**,** 1817-20.

HUTCHISON, S., BENSON, R. A., GIBSON, V. B., POLLOCK, A. H., GARSIDE, P. & BREWER, J. M. 2012. Antigen depot is not required for alum adjuvanticity. *FASEB J,* 26**,** 1272-9.

IBRAHIM, N. K., MURRAY, J. L., ZHOU, D., MITTENDORF, E. A., SAMPLE, D., TAUTCHIN, M. & MILES, D. 2013. Survival Advantage in Patients with Metastatic Breast Cancer Receiving Endocrine Therapy plus Sialyl Tn-KLH Vaccine: Post Hoc Analysis of a Large Randomized Trial. *J Cancer,* 4**,** 577-84.

IINO, S., FUJIYAMA, S., HORIUCHI, K., JYO, K., KUWABARA, Y., SATO, S., SAIKA, S., MORITA, M., ODOH, K. & KUZUHARA, S. 1992. Clinical trial of a lyophilized inactivated hepatitis A candidate vaccine in healthy adult volunteers. *Vaccine,* 10**,** 323-8.

INABA, K., INABA, M., NAITO, M. & STEINMAN, R. M. 1993. Dendritic cell progenitors phagocytose particulates, including bacillus Calmette-Guerin organisms, and sensitize mice to mycobacterial antigens in vivo. *J Exp Med,* 178**,** 479-88.

INOGÈS, S., RODRÌGUEZ-CALVILLO, M., ZABALEGUI, N., LÒPEZ-DÌAZ DE CERIO, A., VILLANUEVA, H., SORIA, E., SUÁREZ, L., RODRÍGUEZ-CABALLERO, A., PASTOR, F., GARCÍA-MUÑÓZ, R., PANIZO, C., PÈREZ-CALVO, J., MELERO, I., ROCHA, E., ORFAO, A., BENDANDI, M., GROUP, G. E. D. L. T. A. D. M. O. S. & GROUP, P. P. E. E. Y. T. D. H. M. S. 2006. Clinical benefit associated with idiotypic vaccination in patients with follicular lymphoma. *J Natl Cancer Inst,* 98**,** 1292-301.

ISMAILI, J., RENNESSON, J., AKSOY, E., VEKEMANS, J., VINCART, B., AMRAOUI, Z., VAN LAETHEM, F., GOLDMAN, M. & DUBOIS, P. M. 2002. Monophosphoryl lipid A activates both human dendritic cells and T cells. *J Immunol,* 168**,** 926-32.

ITO, D., OGASAWARA, K., IWABUCHI, K., INUYAMA, Y. & ONOÉ, K. 2000a. Induction of CTL responses by simultaneous administration of liposomal peptide vaccine with anti-CD40 and anti-CTLA-4 mAb. *J Immunol,* 164**,** 1230-5.

ITO, D., OGASAWARA, K., MATSUSHITA, K., MOROHASHI, T., NAMBA, K., MATSUKI, N., KITAICHI, N., INUYAMA, Y., HOSOKAWA, M., NAKAYAMA, E., IWABUCHI, K. & ONOÉ, K. 2000b. Effective priming of cytotoxic T lymphocyte precursors by subcutaneous administration of peptide antigens in liposomes accompanied by anti-CD40 and anti-CTLA-4 antibodies. *Immunobiology,* 201**,** 527-40.

IWAI, Y., ISHIDA, M., TANAKA, Y., OKAZAKI, T., HONJO, T. & MINATO, N. 2002. Involvement of PD-L1 on tumor cells in the escape from host immune system and tumor immunotherapy by PD-L1 blockade. *Proc Natl Acad Sci U S A,* 99**,** 12293-7.

JACKSON, D. C., LAU, Y. F., LE, T., SUHRBIER, A., DELIYANNIS, G., CHEERS, C., SMITH, C., ZENG, W. & BROWN, L. E. 2004. A totally synthetic vaccine of generic structure that targets

Toll-like receptor 2 on dendritic cells and promotes antibody or cytotoxic T cell responses. *Proc Natl Acad Sci U S A,* 101**,** 15440-5.

JACOB, J., KASSIR, R. & KELSOE, G. 1991. In situ studies of the primary immune response to (4-hydroxy-3-nitrophenyl)acetyl. I. The architecture and dynamics of responding cell populations. *J Exp Med,* 173**,** 1165-75.

JACOB, J. & KELSOE, G. 1992. In situ studies of the primary immune response to (4-hydroxy-3-nitrophenyl)acetyl. II. A common clonal origin for periarteriolar lymphoid sheath-associated foci and germinal centers. *J Exp Med,* 176**,** 679-87.

JAKUBZICK, C., BOGUNOVIC, M., BONITO, A. J., KUAN, E. L., MERAD, M. & RANDOLPH, G. J. 2008. Lymph-migrating, tissue-derived dendritic cells are minor constituents within steady-state lymph nodes. *J Exp Med,* 205**,** 2839-50.

JANEWAY, C. 1989a. Immunogenicity Signals 1,2,3 ... And 0. *Immunology Today,* 10**,** 283-286.

JANEWAY, C. A. 1989b. Approaching the asymptote? Evolution and revolution in immunology. *Cold Spring Harb Symp Quant Biol,* 54 Pt 1**,** 1-13.

JENNER, E. 1798. *An Inquiry into the Causes and Effects of Variolae Vaccinae, a Disease Discovered in Some Western Counties of England.,* London, Samson Law.

JIANG, W., SWIGGARD, W. J., HEUFLER, C., PENG, M., MIRZA, A., STEINMAN, R. M. & NUSSENZWEIG, M. C. 1995. The receptor DEC-205 expressed by dendritic cells and thymic epithelial cells is involved in antigen processing. *Nature,* 375**,** 151-5.

JOHANSEN, K., SCHRÖDER, U. & SVENSSON, L. 2003. Immunogenicity and protective efficacy of a formalin-inactivated rotavirus vaccine combined with lipid adjuvants. *Vaccine,* 21**,** 368-75.

JOHNSON, A. G., GAINES, S. & LANDY, M. 1956. Studies on the O antigen of Salmonella typhosa. V. Enhancement of antibody response to protein antigens by the purified lipopolysaccharide. *J Exp Med,* 103**,** 225-46.

JOHNSON, P. W., STEVEN, N. M., CHOWDHURY, F., DOBBYN, J., HALL, E., ASHTON-KEY, M., HODGES, E., OTTENSMEIER, C. H., WILLIAMS, A. & GLENNIE, M. 2010. A Cancer Research UK phase I study evaluating safety, tolerability, and biological effects of chimeric anti-CD40 monoclonal antibody (MAb), Chi Lob 7/4. *Journal of Clinical Oncology* [Online], 28.

JONULEIT, H., SCHMITT, E., SCHULER, G., KNOP, J. & ENK, A. H. 2000. Induction of interleukin 10-producing, nonproliferating CD4(+) T cells with regulatory properties by repetitive stimulation with allogeneic immature human dendritic cells. *J Exp Med,* 192**,** 1213-22.

JUNT, T., MOSEMAN, E. A., IANNACONE, M., MASSBERG, S., LANG, P. A., BOES, M., FINK, K., HENRICKSON, S. E., SHAYAKHMETOV, D. M., DI PAOLO, N. C., VAN ROOIJEN, N., MEMPEL, T. R., WHELAN, S. P. & VON ANDRIAN, U. H. 2007. Subcapsular sinus macrophages in lymph nodes clear lymph-borne viruses and present them to antiviral B cells. *Nature,* 450**,** 110-4.

KAFI, K., BETTING, D. J., YAMADA, R. E., BACICA, M., STEWARD, K. K. & TIMMERMAN, J. M. 2009. Maleimide conjugation markedly enhances the immunogenicity of both human and murine idiotype-KLH vaccines. *Mol Immunol,* 46**,** 448-56.

KAMINSKI, M. S., KITAMURA, K., MALONEY, D. G. & LEVY, R. 1987. Idiotype vaccination against murine B cell lymphoma. Inhibition of tumor immunity by free idiotype protein. *J Immunol,* 138**,** 1289-96.

KAPLAN, M. H., SCHINDLER, U., SMILEY, S. T. & GRUSBY, M. J. 1996. Stat6 is required for mediating responses to IL-4 and for development of Th2 cells. *Immunity,* 4**,** 313-9.

KASTENMÜLLER, W., KASTENMÜLLER, K., KURTS, C. & SEDER, R. A. 2014. Dendritic cell-targeted vaccines - hope or hype? *Nat Rev Immunol,* 14**,** 705-11.

KASTURI, S. P., SKOUNTZOU, I., ALBRECHT, R. A., KOUTSONANOS, D., HUA, T., NAKAYA, H. I., RAVINDRAN, R., STEWART, S., ALAM, M., KWISSA, M., VILLINGER, F., MURTHY, N., STEEL, J., JACOB, J., HOGAN, R. J., GARCÍA-SASTRE, A., COMPANS, R. & PULENDRAN, B.

2011. Programming the magnitude and persistence of antibody responses with innate immunity. *Nature,* 470**,** 543-7.

KAWABE, T., NAKA, T., YOSHIDA, K., TANAKA, T., FUJIWARA, H., SUEMATSU, S., YOSHIDA, N., KISHIMOTO, T. & KIKUTANI, H. 1994. The immune responses in CD40-deficient mice: impaired immunoglobulin class switching and germinal center formation. *Immunity,* 1**,** 167-78.

KHUBCHANDANI, S., CZUCZMAN, M. S. & HERNANDEZ-ILIZALITURRI, F. J. 2009. Dacetuzumab, a humanized mAb against CD40 for the treatment of hematological malignancies. *Curr Opin Investig Drugs,* 10**,** 579-87.

KIM, K. J., KANELLOPOULOS-LANGEVIN, C., MERWIN, R. M., SACHS, D. H. & ASOFSKY, R. 1979. Establishment and characterization of BALB/c lymphoma lines with B cell properties. *J Immunol,* 122**,** 549-54.

KING, C. A., SPELLERBERG, M. B., ZHU, D., RICE, J., SAHOTA, S. S., THOMPSETT, A. R., HAMBLIN, T. J., RADL, J. & STEVENSON, F. K. 1998. DNA vaccines with single-chain Fv fused to fragment C of tetanus toxin induce protective immunity against lymphoma and myeloma. *Nat Med,* 4**,** 1281-6.

KING, I. L., KROENKE, M. A. & SEGAL, B. M. 2010. GM-CSF-dependent, CD103+ dermal dendritic cells play a critical role in Th effector cell differentiation after subcutaneous immunization. *J Exp Med,* 207**,** 953-61.

KOLB, H. C., FINN, M. G. & SHARPLESS, K. B. 2001. Click Chemistry: Diverse Chemical Function from a Few Good Reactions. *Angew Chem Int Ed Engl,* 40**,** 2004-2021.

KOLLE, W. 1896. *Die aktive Immunisierung der Menschen gegen Cholera: nach Haffkine's Verfahren in Indien ausgeführt*.

KOOL, M., GEURTSVANKESSEL, C., MUSKENS, F., MADEIRA, F. B., VAN NIMWEGEN, M., KUIPERS, H., THIELEMANS, K., HOOGSTEDEN, H. C., HAMMAD, H. & LAMBRECHT, B. N. 2011. Facilitated antigen uptake and timed exposure to TLR ligands dictate the antigen-presenting potential of plasmacytoid DCs. *J Leukoc Biol,* 90**,** 1177-90.

KOOL, M., PÉTRILLI, V., DE SMEDT, T., ROLAZ, A., HAMMAD, H., VAN NIMWEGEN, M., BERGEN, I. M., CASTILLO, R., LAMBRECHT, B. N. & TSCHOPP, J. 2008. Cutting edge: alum adjuvant stimulates inflammatory dendritic cells through activation of the NALP3 inflammasome. *J Immunol,* 181**,** 3755-9.

KRISHNASWAMY, J. K., CHU, T. & EISENBARTH, S. C. 2013. Beyond pattern recognition: NOD-like receptors in dendritic cells. *Trends Immunol,* 34**,** 224-33.

KRUMMEN, M., BALKOW, S., SHEN, L., HEINZ, S., LOQUAI, C., PROBST, H. C. & GRABBE, S. 2010. Release of IL-12 by dendritic cells activated by TLR ligation is dependent on MyD88 signaling, whereas TRIF signaling is indispensable for TLR synergy. *J Leukoc Biol,* 88**,** 189-99.

KUNDI, M. 2007. New hepatitis B vaccine formulated with an improved adjuvant system. *Expert Rev Vaccines,* 6**,** 133-40.

KURTS, C., HEATH, W. R., CARBONE, F. R., ALLISON, J., MILLER, J. F. & KOSAKA, H. 1996. Constitutive class I-restricted exogenous presentation of self antigens in vivo. *J Exp Med,* 184**,** 923-30.

KWAK, L. W., CAMPBELL, M. J., CZERWINSKI, D. K., HART, S., MILLER, R. A. & LEVY, R. 1992. Induction of immune responses in patients with B-cell lymphoma against the surface-immunoglobulin idiotype expressed by their tumors. *N Engl J Med,* 327**,** 1209-15.

LAMBRECHT, B. N., KOOL, M., WILLART, M. A. & HAMMAD, H. 2009. Mechanism of action of clinically approved adjuvants. *Curr Opin Immunol,* 21**,** 23-9.

LANZAVECCHIA, A. 1985. Antigen-specific interaction between T and B cells. *Nature,* 314**,** 537-9.

LATCHMAN, Y., WOOD, C. R., CHERNOVA, T., CHAUDHARY, D., BORDE, M., CHERNOVA, I., IWAI, Y., LONG, A. J., BROWN, J. A., NUNES, R., GREENFIELD, E. A., BOURQUE, K.,

BOUSSIOTIS, V. A., CARTER, L. L., CARRENO, B. M., MALENKOVICH, N., NISHIMURA, H., OKAZAKI, T., HONJO, T., SHARPE, A. H. & FREEMAN, G. J. 2001. PD-L2 is a second ligand for PD-1 and inhibits T cell activation. *Nat Immunol,* 2**,** 261-8.

LEE, S. M., KOK, K. H., JAUME, M., CHEUNG, T. K., YIP, T. F., LAI, J. C., GUAN, Y., WEBSTER, R. G., JIN, D. Y. & PEIRIS, J. S. 2014. Toll-like receptor 10 is involved in induction of innate immune responses to influenza virus infection. *Proc Natl Acad Sci U S A,* 111**,** 3793-8.

LENSCHOW, D. J., WALUNAS, T. L. & BLUESTONE, J. A. 1996. CD28/B7 system of T cell costimulation. *Annu Rev Immunol,* 14**,** 233-58.

LEROUX-ROELS, G. 2010. Unmet needs in modern vaccinology: adjuvants to improve the immune response. *Vaccine,* 28 Suppl 3**,** C25-36.

LESTERHUIS, W. J., DE VRIES, I. J., SCHREIBELT, G., LAMBECK, A. J., AARNTZEN, E. H., JACOBS, J. F., SCHARENBORG, N. M., VAN DE RAKT, M. W., DE BOER, A. J., CROOCKEWIT, S., VAN ROSSUM, M. M., MUS, R., OYEN, W. J., BOERMAN, O. C., LUCAS, S., ADEMA, G. J., PUNT, C. J. & FIGDOR, C. G. 2011. Route of administration modulates the induction of dendritic cell vaccine-induced antigen-specific T cells in advanced melanoma patients. *Clin Cancer Res,* 17**,** 5725-35.

LEVIE, K., GJORUP, I., SKINHØJ, P. & STOFFEL, M. 2002. A 2-dose regimen of a recombinant hepatitis B vaccine with the immune stimulant AS04 compared with the standard 3-dose regimen of Engerix-B in healthy young adults. *Scand J Infect Dis,* 34**,** 610-4.

LEVY, R., ROBERTSON, M., LEONARD, J., VOSE, J. & DENNEY, D. 2008. Results of a phase 3 trial evaluating safety and efficacy of specific immunotherapy, recombinant idiotype (ID) conjugated to KLh (ID-KLH) with GM-CSF, compared to non-specific immunotherapy, KLH with GM-CSF, in patients with follicular non-Hodgkins lymphoma (FNHL). *Annals of Oncology,* 19**,** 101-101.

LEÓN, B., LÓPEZ-BRAVO, M. & ARDAVÍN, C. 2007. Monocyte-derived dendritic cells formed at the infection site control the induction of protective T helper 1 responses against Leishmania. *Immunity,* 26**,** 519-31.

LI, F. & RAVETCH, J. V. 2011. Inhibitory Fcγ receptor engagement drives adjuvant and anti-tumor activities of agonistic CD40 antibodies. *Science,* 333**,** 1030-4.

LIM, S. G., MOHAMMED, R., YUEN, M. F. & KAO, J. H. 2009. Prevention of hepatocellular carcinoma in hepatitis B virus infection. *J Gastroenterol Hepatol,* 24**,** 1352-7.

LINSLEY, P. S., BRADY, W., GROSMAIRE, L., ARUFFO, A., DAMLE, N. K. & LEDBETTER, J. A. 1991a. Binding of the B cell activation antigen B7 to CD28 costimulates T cell proliferation and interleukin 2 mRNA accumulation. *J Exp Med,* 173**,** 721-30.

LINSLEY, P. S., BRADY, W., URNES, M., GROSMAIRE, L. S., DAMLE, N. K. & LEDBETTER, J. A. 1991b. CTLA-4 is a second receptor for the B cell activation antigen B7. *J Exp Med,* 174**,** 561-9.

LIPINSKI, T., FITIEH, A., ST PIERRE, J., OSTERGAARD, H. L., BUNDLE, D. R. & TOURET, N. 2013. Enhanced immunogenicity of a tricomponent mannan tetanus toxoid conjugate vaccine targeted to dendritic cells via Dectin-1 by incorporating β-glucan. *J Immunol,* 190**,** 4116-28.

LIPINSKI, T., LUU, T., KITOV, P. I., SZPACENKO, A. & BUNDLE, D. R. 2011. A structurally diversified linker enhances the immune response to a small carbohydrate hapten. *Glycoconj J,* 28**,** 149-64.

LIU, K., VICTORA, G. D., SCHWICKERT, T. A., GUERMONPREZ, P., MEREDITH, M. M., YAO, K., CHU, F. F., RANDOLPH, G. J., RUDENSKY, A. Y. & NUSSENZWEIG, M. 2009. In vivo analysis of dendritic cell development and homeostasis. *Science,* 324**,** 392-7.

LIU, K., WASKOW, C., LIU, X., YAO, K., HOH, J. & NUSSENZWEIG, M. 2007. Origin of dendritic cells in peripheral lymphoid organs of mice. *Nat Immunol,* 8**,** 578-83.

LLOPIZ, D., DOTOR, J., ZABALETA, A., LASARTE, J. J., PRIETO, J., BORRÁS-CUESTA, F. & SAROBE, P. 2008. Combined immunization with adjuvant molecules poly(I:C) and anti-CD40 plus

a tumor antigen has potent prophylactic and therapeutic antitumor effects. *Cancer Immunol Immunother,* 57**,** 19-29.

LUND, F. E. & RANDALL, T. D. 2010. Effector and regulatory B cells: modulators of CD4+ T cell immunity. *Nat Rev Immunol,* 10**,** 236-47.

LUTZ, M. B., KUKUTSCH, N., OGILVIE, A. L., RÖSSNER, S., KOCH, F., ROMANI, N. & SCHULER, G. 1999. An advanced culture method for generating large quantities of highly pure dendritic cells from mouse bone marrow. *J Immunol Methods,* 223**,** 77-92.

LUTZ, M. B., SCHNARE, M., MENGES, M., ROSSNER, S., ROLLINGHOFF, M., SCHULER, G. & GESSNER, A. 2002. Differential functions of IL-4 receptor types I and II for dendritic cell maturation and IL-12 production and their dependency on GM-CSF. *J Immunol,* 169**,** 3574-80.

LYONS, A. B. 2000. Analysing cell division in vivo and in vitro using flow cytometric measurement of CFSE dye dilution. *J Immunol Methods,* 243**,** 147-54.

LYONS, A. B. & PARISH, C. R. 1994. Determination of lymphocyte division by flow cytometry. *J Immunol Methods,* 171**,** 131-7.

MAC SHARRY, J., SHALABY, K. H., MARCHICA, C., FARAHNAK, S., CHIEH-LI, T., LAPTHORNE, S., QURESHI, S. T., SHANAHAN, F. & MARTIN, J. G. 2014. Concomitant exposure to ovalbumin and endotoxin augments airway inflammation but not airway hyperresponsiveness in a murine model of asthma. *PLoS One,* 9**,** e98648.

MACKEY, M. F., GUNN, J. R., TING, P. P., KIKUTANI, H., DRANOFF, G., NOELLE, R. J. & BARTH, R. J. 1997. Protective immunity induced by tumor vaccines requires interaction between CD40 and its ligand, CD154. *Cancer Res,* 57**,** 2569-74.

MACLEOD, M. K., MCKEE, A. S., DAVID, A., WANG, J., MASON, R., KAPPLER, J. W. & MARRACK, P. 2011. Vaccine adjuvants aluminum and monophosphoryl lipid A provide distinct signals to generate protective cytotoxic memory CD8 T cells. *Proc Natl Acad Sci U S A,* 108**,** 7914-9.

MAISONNEUVE, C., BERTHOLET, S., PHILPOTT, D. J. & DE GREGORIO, E. 2014. Unleashing the potential of NOD- and Toll-like agonists as vaccine adjuvants. *Proc Natl Acad Sci U S A,* 111**,** 12294-9.

MALONEY, D. G., LILES, T. M., CZERWINSKI, D. K., WALDICHUK, C., ROSENBERG, J., GRILLO-LOPEZ, A. & LEVY, R. 1994. Phase I clinical trial using escalating single-dose infusion of chimeric anti-CD20 monoclonal antibody (IDEC-C2B8) in patients with recurrent B-cell lymphoma. *Blood,* 84**,** 2457-66.

MALYNN, B. A., ROMEO, D. T. & WORTIS, H. H. 1985. Antigen-specific B cells efficiently present low doses of antigen for induction of T cell proliferation. *J Immunol,* 135**,** 980-8.

MARCUS, R., IMRIE, K., BELCH, A., CUNNINGHAM, D., FLORES, E., CATALANO, J., SOLAL-CELIGNY, P., OFFNER, F., WALEWSKI, J., RAPOSO, J., JACK, A. & SMITH, P. 2005. CVP chemotherapy plus rituximab compared with CVP as first-line treatment for advanced follicular lymphoma. *Blood,* 105**,** 1417-23.

MARICHAL, T., OHATA, K., BEDORET, D., MESNIL, C., SABATEL, C., KOBIYAMA, K., LEKEUX, P., COBAN, C., AKIRA, S., ISHII, K. J., BUREAU, F. & DESMET, C. J. 2011. DNA released from dying host cells mediates aluminum adjuvant activity. *Nat Med,* 17**,** 996-1002.

MAROUN, C. R. & JULIUS, M. 1994. Distinct roles for CD4 and CD8 as co-receptors in T cell receptor signalling. *Eur J Immunol,* 24**,** 959-66.

MARRACK, P., SHIMONKEVITZ, R., HANNUM, C., HASKINS, K. & KAPPLER, J. 1983. The major histocompatibility complex-restricted antigen receptor on T cells. IV. An antiidiotypic antibody predicts both antigen and I-specificity. *Journal of Experimental Medicine,* 158**,** 1635-1646.

MATZINGER, P. 1994. Tolerance, danger, and the extended family. *Annu Rev Immunol,* 12**,** 991-1045.

MAURER, T., HEIT, A., HOCHREIN, H., AMPENBERGER, F., O'KEEFFE, M., BAUER, S., LIPFORD, G. B., VABULAS, R. M. & WAGNER, H. 2002. CpG-DNA aided cross-presentation of soluble antigens by dendritic cells. *Eur J Immunol,* 32**,** 2356-64.

MAXFIELD, F. R. & YAMASHIRO, D. J. 1987. Endosome acidification and the pathways of receptor-mediated endocytosis. *Adv Exp Med Biol,* 225**,** 189-98.

MCGEE, J. P., DAVIS, S. S. & O'HAGAN, D. T. 1994. The immunogenicity of a model protein entrapped in poly(lactide-co-glycolide) microparticles prepared by a novel phase separation technique. *Journal of Controlled Release,* 31**,** 55-60.

MELERO, I., GAUDERNACK, G., GERRITSEN, W., HUBER, C., PARMIANI, G., SCHOLL, S., THATCHER, N., WAGSTAFF, J., ZIELINSKI, C., FAULKNER, I. & MELLSTEDT, H. 2014. Therapeutic vaccines for cancer: an overview of clinical trials. *Nat Rev Clin Oncol,* 11**,** 509-24.

MELLMAN, I., COUKOS, G. & DRANOFF, G. 2011. Cancer immunotherapy comes of age. *Nature,* 480**,** 480-9.

MERCK 2011a. Gardasil® . Prescribing information.

MERCK 2011b. Recombivax HB® . Prescribing information.

MICONNET, I., KOENIG, S., SPEISER, D., KRIEG, A., GUILLAUME, P., CEROTTINI, J. C. & ROMERO, P. 2002. CpG are efficient adjuvants for specific CTL induction against tumor antigen-derived peptide. *J Immunol,* 168**,** 1212-8.

MILES, D., ROCHÉ, H., MARTIN, M., PERREN, T. J., CAMERON, D. A., GLASPY, J., DODWELL, D., PARKER, J., MAYORDOMO, J., TRES, A., MURRAY, J. L., IBRAHIM, N. K. & GROUP, T. S. 2011. Phase III multicenter clinical trial of the sialyl-TN (STn)-keyhole limpet hemocyanin (KLH) vaccine for metastatic breast cancer. *Oncologist,* 16**,** 1092-100.

MILLER, R. A., MALONEY, D. G., WARNKE, R. & LEVY, R. 1982. Treatment of B-cell lymphoma with monoclonal anti-idiotype antibody. *N Engl J Med,* 306**,** 517-22.

MOCIKAT, R., BRAUMÜLLER, H., GUMY, A., EGETER, O., ZIEGLER, H., REUSCH, U., BUBECK, A., LOUIS, J., MAILHAMMER, R., RIETHMÜLLER, G., KOSZINOWSKI, U. & RÖCKEN, M. 2003. Natural killer cells activated by MHC class I(low) targets prime dendritic cells to induce protective CD8 T cell responses. *Immunity,* 19**,** 561-9.

MOND, J. J., LEES, A. & SNAPPER, C. M. 1995. T cell-independent antigens type 2. *Annu Rev Immunol,* 13**,** 655-92.

MOORE, M. W., CARBONE, F. R. & BEVAN, M. J. 1988. Introduction of soluble protein into the class I pathway of antigen processing and presentation. *Cell,* 54**,** 777-85.

MORGAN, D. A., RUSCETTI, F. W. & GALLO, R. 1976. Selective in vitro growth of T lymphocytes from normal human bone marrows. *Science,* 193**,** 1007-8.

MORIS, P., VAN DER MOST, R., LEROUX-ROELS, I., CLEMENT, F., DRAMÉ, M., HANON, E., LEROUX-ROELS, G. G. & VAN MECHELEN, M. 2011. H5N1 influenza vaccine formulated with AS03 A induces strong cross-reactive and polyfunctional CD4 T-cell responses. *J Clin Immunol,* 31**,** 443-54.

MOSER, C., AMACKER, M., KAMMER, A. R., RASI, S., WESTERFELD, N. & ZURBRIGGEN, R. 2007. Influenza virosomes as a combined vaccine carrier and adjuvant system for prophylactic and therapeutic immunizations. *Expert Rev Vaccines,* 6**,** 711-21.

MOSER, M. & LEO, O. 2010. Key concepts in immunology. *Vaccine,* 28 Suppl 3**,** C2-13.

MOSMANN, T. R., CHERWINSKI, H., BOND, M. W., GIEDLIN, M. A. & COFFMAN, R. L. 1986. Two types of murine helper T cell clone. I. Definition according to profiles of lymphokine activities and secreted proteins. *J Immunol,* 136**,** 2348-57.

MOYLE, P. M. & TOTH, I. 2013. Modern subunit vaccines: development, components, and research opportunities. *ChemMedChem,* 8**,** 360-76.

MURPHY, K., WALPORT, M. & TRAVERS, P. 2008. *Janeway's Immunobiology.,* 7th edition. New York and London, *Taylor & Francis* Ltd.

MURPHY, R. F., POWERS, S. & CANTOR, C. R. 1984. Endosome pH measured in single cells by dual fluorescence flow cytometry: rapid acidification of insulin to pH 6. *J Cell Biol,* 98**,** 1757-62.

MUTINI, C., FALZONI, S., FERRARI, D., CHIOZZI, P., MORELLI, A., BARICORDI, O. R., COLLO, G., RICCIARDI-CASTAGNOLI, P. & DI VIRGILIO, F. 1999. Mouse dendritic cells express the P2X7 purinergic receptor: characterization and possible participation in antigen presentation. *J Immunol,* 163**,** 1958-65.

MYERS, K. R., TRUCHOT, A. T., WARD, J., HUDSON, Y. & ULRICH, J. T. 1990. Cellular and Molecular Aspects of Endotoxin Reactions. *In:* NOWOTNY, A., SPITZER, J. J. & ZIEGLER, E. J. (eds.). Amsterdam: Elsevier Science.

NAKAE, S., NAMBU, A., SUDO, K. & IWAKURA, Y. 2003. Suppression of immune induction of collagen-induced arthritis in IL-17-deficient mice. *J Immunol,* 171**,** 6173-7.

NATHAN, C. F., MURRAY, H. W., WIEBE, M. E. & RUBIN, B. Y. 1983. Identification of interferon-gamma as the lymphokine that activates human macrophage oxidative metabolism and antimicrobial activity. *J Exp Med,* 158**,** 670-89.

NESTLE, F. O., ALIJAGIC, S., GILLIET, M., SUN, Y., GRABBE, S., DUMMER, R., BURG, G. & SCHADENDORF, D. 1998. Vaccination of melanoma patients with peptide- or tumor lysate-pulsed dendritic cells. *Nat Med,* 4**,** 328-32.

NETEA, M. G., SUTMULLER, R., HERMANN, C., VAN DER GRAAF, C. A., VAN DER MEER, J. W., VAN KRIEKEN, J. H., HARTUNG, T., ADEMA, G. & KULLBERG, B. J. 2004. Toll-like receptor 2 suppresses immunity against Candida albicans through induction of IL-10 and regulatory T cells. *J Immunol,* 172**,** 3712-8.

NINOMIYA, A., OGASAWARA, K., KAJINO, K., TAKADA, A. & KIDA, H. 2002. Intranasal administration of a synthetic peptide vaccine encapsulated in liposome together with an anti-CD40 antibody induces protective immunity against influenza A virus in mice. *Vaccine,* 20**,** 3123-9.

NUCHTERN, J. G., BIDDISON, W. E. & KLAUSNER, R. D. 1990. Class II MHC molecules can use the endogenous pathway of antigen presentation. *Nature,* 343**,** 74-6.

O'HAGAN, D. T. & DE GREGORIO, E. 2009. The path to a successful vaccine adjuvant--'the long and winding road'. *Drug Discov Today,* 14**,** 541-51.

O'KEEFFE, M., HOCHREIN, H., VREMEC, D., SCOTT, B., HERTZOG, P., TATARCZUCH, L. & SHORTMAN, K. 2003. Dendritic cell precursor populations of mouse blood: identification of the murine homologues of human blood plasmacytoid pre-DC2 and CD11c+ DC1 precursors. *Blood,* 101**,** 1453-9.

OANCEA, G., O'MARA, M. L., BENNETT, W. F., TIELEMAN, D. P., ABELE, R. & TAMPÉ, R. 2009. Structural arrangement of the transmission interface in the antigen ABC transport complex TAP. *Proc Natl Acad Sci U S A,* 106**,** 5551-6.

OHTEKI, T., FUKAO, T., SUZUE, K., MAKI, C., ITO, M., NAKAMURA, M. & KOYASU, S. 1999. Interleukin 12-dependent interferon gamma production by CD8alpha+ lymphoid dendritic cells. *J Exp Med,* 189**,** 1981-6.

OTT, G., BARCHFELD, G. L., CHERNOFF, D., RADHAKRISHNAN, R., VAN HOOGEVEST, P. & VAN NEST, G. 1995. MF59. Design and evaluation of a safe and potent adjuvant for human vaccines. *Pharm Biotechnol,* 6**,** 277-96.

OWENS, M. L., BRIDSON, W. E., SMITH, S. L., MYERS, J. A., FOX, T. L. & WELLS, T. M. 1998. Percutaneous penetration of Aldara cream, 5% during the topical treatment of genital and perianal warts. *Prim Care Update Ob Gyns,* 5**,** 151.

PAPE, K. A., CATRON, D. M., ITANO, A. A. & JENKINS, M. K. 2007. The humoral immune response is initiated in lymph nodes by B cells that acquire soluble antigen directly in the follicles. *Immunity,* 26**,** 491-502.

PARK, H., LI, Z., YANG, X. O., CHANG, S. H., NURIEVA, R., WANG, Y. H., WANG, Y., HOOD, L., ZHU, Z., TIAN, Q. & DONG, C. 2005. A distinct lineage of CD4 T cells regulates tissue inflammation by producing interleukin 17. *Nat Immunol,* 6**,** 1133-41.

PARK, H. J. & NEELAPU, S. S. 2008. Developing idiotype vaccines for lymphoma: from preclinical studies to phase III clinical trials. *Br J Haematol,* 142**,** 179-91.

PARRA, D., RIEGER, A. M., LI, J., ZHANG, Y. A., RANDALL, L. M., HUNTER, C. A., BARREDA, D. R. & SUNYER, J. O. 2012. Pivotal advance: peritoneal cavity B-1 B cells have phagocytic and microbicidal capacities and present phagocytosed antigen to CD4+ T cells. *J Leukoc Biol,* 91**,** 525-36.

PASTEUR, L. 1880. De l'attenuation du virus du cholera des poules. *Comptes Rendus de l'Académie des Sciences Paris,* 91**,** 673-680.

PASTEUR, L. 1885. Méthode pour prévenir la rage après morsure. *Comptes Rendus de l'Académie des Sciences Paris,* 101.

PASTEUR, M. 1881. An Address on Vaccination in Relation to Chicken Cholera and Splenic Fever. *Br Med J,* 2**,** 283-4.

PATEL, K. G. & SWARTZ, J. R. 2011. Surface functionalization of virus-like particles by direct conjugation using azide-alkyne click chemistry. *Bioconjug Chem,* 22**,** 376-87.

PERFETTO, S. P., CHATTOPADHYAY, P. K., LAMOREAUX, L., NGUYEN, R., AMBROZAK, D., KOUP, R. A. & ROEDERER, M. 2006. Amine reactive dyes: an effective tool to discriminate live and dead cells in polychromatic flow cytometry. *J Immunol Methods,* 313**,** 199-208.

PERNIS, B., CHIAPPINO, G. & ROWE, D. S. 1966. Cells producing IgD immunoglobulins in human spleen. *Nature,* 211**,** 424-5.

PETERS, P. J., NEEFJES, J. J., OORSCHOT, V., PLOEGH, H. L. & GEUZE, H. J. 1991. Segregation of MHC class II molecules from MHC class I molecules in the Golgi complex for transport to lysosomal compartments. *Nature,* 349**,** 669-76.

PHYTHIAN-ADAMS, A. T., COOK, P. C., LUNDIE, R. J., JONES, L. H., SMITH, K. A., BARR, T. A., HOCHWELLER, K., ANDERTON, S. M., HÄMMERLING, G. J., MAIZELS, R. M. & MACDONALD, A. S. 2010. CD11c depletion severely disrupts Th2 induction and development in vivo. *J Exp Med,* 207**,** 2089-96.

PLANTINGA, M., GUILLIAMS, M., VANHEERSWYNGHELS, M., DESWARTE, K., BRANCO-MADEIRA, F., TOUSSAINT, W., VANHOUTTE, L., NEYT, K., KILLEEN, N., MALISSEN, B., HAMMAD, H. & LAMBRECHT, B. N. 2013. Conventional and monocyte-derived CD11b(+) dendritic cells initiate and maintain T helper 2 cell-mediated immunity to house dust mite allergen. *Immunity,* 38**,** 322-35.

PLOTKIN, S. & PLOTKIN, S. 2008. A short history of vaccination. *In:* SA, P., W, O. & PAUL, O. (eds.) *Vaccines.* 5th ed. New York: Elsevier.

PLOTKIN, S. A. 2005. Vaccines: past, present and future. *Nat Med,* 11**,** S5-11.

PLOTKIN, S. A. 2010. Correlates of protection induced by vaccination. *Clin Vaccine Immunol,* 17**,** 1055-65.

PLOTKIN, S. A., FARQUHAR, J. D., KATZ, M. & BUSER, F. 1969. Attenuation of RA 27-3 rubella virus in WI-38 human diploid cells. *Am J Dis Child,* 118**,** 178-85.

PRESKY, D. H., MINETTI, L. J., GILLESSEN, S., GUBLER, U., CHIZZONITE, R., STERN, A. S. & GATELY, M. K. 1996. Evidence for multiple sites of interaction between IL-12 and its receptor. *Ann N Y Acad Sci,* 795**,** 390-3.

PROKOPOWICZ, Z. M., ARCE, F., BIEDROŃ, R., CHIANG, C. L., CISZEK, M., KATZ, D. R., NOWAKOWSKA, M., ZAPOTOCZNY, S., MARCINKIEWICZ, J. & CHAIN, B. M. 2010. Hypochlorous acid: a natural adjuvant that facilitates antigen processing, cross-priming, and the induction of adaptive immunity. *J Immunol,* 184**,** 824-35.

PULENDRAN, B., KUMAR, P., CUTLER, C. W., MOHAMADZADEH, M., VAN DYKE, T. & BANCHEREAU, J. 2001. Lipopolysaccharides from distinct pathogens induce different classes of immune responses in vivo. *J Immunol,* 167**,** 5067-76.

PÉREZ-MELGOSA, M., HOLLENBAUGH, D. & WILSON, C. B. 1999. Cutting edge: CD40 ligand is a limiting factor in the humoral response to T cell-dependent antigens. *J Immunol,* 163**,** 1123-7.

RAMACHANDRA, L., SIMMONS, D. & HARDING, C. V. 2009. MHC molecules and microbial antigen processing in phagosomes. *Curr Opin Immunol,* 21**,** 98-104.

RAMESH, N., FULEIHAN, R. & GEHA, R. 1994. Molecular pathology of X-linked immunoglobulin deficiency with normal or elevated IgM (HIGMX-1). *Immunol Rev,* 138**,** 87-104.

RAMESH, N., RAMESH, V., GUSELLA, J. F. & GEHA, R. 1993. Chromosomal localization of the gene for human B-cell antigen CD40. *Somat Cell Mol Genet,* 19**,** 295-8.

RANDALL, T. D., HEATH, A. W., SANTOS-ARGUMEDO, L., HOWARD, M. C., WEISSMAN, I. L. & LUND, F. E. 1998. Arrest of B lymphocyte terminal differentiation by CD40 signaling: mechanism for lack of antibody-secreting cells in germinal centers. *Immunity,* 8**,** 733-42.

RAPPUOLI, R. & ADEREM, A. 2011. A 2020 vision for vaccines against HIV, tuberculosis and malaria. *Nature,* 473**,** 463-9.

REED, S. G., ORR, M. T. & FOX, C. B. 2013. Key roles of adjuvants in modern vaccines. *Nat Med,* 19**,** 1597-608.

REIS E SOUSA, C., STAHL, P. D. & AUSTYN, J. M. 1993. Phagocytosis of antigens by Langerhans cells in vitro. *J Exp Med,* 178**,** 509-19.

RICHARDS, R. L., RAO, M., WASSEF, N. M., GLENN, G. M., ROTHWELL, S. W. & ALVING, C. R. 1998. Liposomes containing lipid A serve as an adjuvant for induction of antibody and cytotoxic T-cell responses against RTS,S malaria antigen. *Infect Immun,* 66**,** 2859-65.

RIMANIOL, A. C., GRAS, G., VERDIER, F., CAPEL, F., GRIGORIEV, V. B., PORCHERAY, F., SAUZEAT, E., FOURNIER, J. G., CLAYETTE, P., SIEGRIST, C. A. & DORMONT, D. 2004. Aluminum hydroxide adjuvant induces macrophage differentiation towards a specialized antigen-presenting cell type. *Vaccine,* 22**,** 3127-35.

ROBERTSON, J. M., JENSEN, P. E. & EVAVOLD, B. D. 2000a. DO11.10 and OT-II T cells recognize a C-terminal ovalbumin 323-339 epitope. *J Immunol,* 164**,** 4706-12.

ROBERTSON, J. M., JENSEN, P. E. & EVAVOLD, B. D. 2000b. DO11.10 and OT-II T cells recognize a C-terminal ovalbumin 323-339 epitope. *Journal of Immunology,* 164**,** 4706-12.

ROLPH, M. S. & KAUFMANN, S. H. 2001. CD40 signaling converts a minimally immunogenic antigen into a potent vaccine against the intracellular pathogen Listeria monocytogenes. *J Immunol,* 166**,** 5115-21.

ROMANI, N., KOIDE, S., CROWLEY, M., WITMER-PACK, M., LIVINGSTONE, A. M., FATHMAN, C. G., INABA, K. & STEINMAN, R. M. 1989. Presentation of exogenous protein antigens by dendritic cells to T cell clones. Intact protein is presented best by immature, epidermal Langerhans cells. *J Exp Med,* 169**,** 1169-78.

ROOZENDAAL, R., MEMPEL, T. R., PITCHER, L. A., GONZALEZ, S. F., VERSCHOOR, A., MEBIUS, R. E., VON ANDRIAN, U. H. & CARROLL, M. C. 2009. Conduits mediate transport of low-molecular-weight antigen to lymph node follicles. *Immunity,* 30**,** 264-76.

RUDD, C. E., TAYLOR, A. & SCHNEIDER, H. 2009. CD28 and CTLA-4 coreceptor expression and signal transduction. *Immunol Rev,* 229**,** 12-26.

RUSSELL, C. A. & VINDELOV, L. L. 1998. Optimization and comparison of the MTT assay and the 3H-TdR assay for the detection of IL-2 in helper T cell precursor assays. *J Immunol Methods,* 217**,** 165-75.

SABIN, A. B., HENNESSEN, W. A. & WINSSER, J. 1954. Studies on variants of poliomyelitis virus. I. Experimental segregation and properties of avirulent variants of three immunologic types. *J Exp Med,* 99**,** 551-76.

SALK, J., VAN WEZEL, A. L., STOECKEL, P., VAN STEENIS, G., SCHLUMBERGER, M., MEYRAN, M., REY, J. L., LAPINLEIMU, K., BÖTTIGER, M. & COHEN, H. 1981. Theoretical and practical

considerations in the application of killed poliovirus vaccine for the control of paralytic poliomyelitis. *Dev Biol Stand,* 47**,** 181-98.

SALK, J. E. 1955. Considerations in the preparation and use of poliomyelitis virus vaccine. *J Am Med Assoc,* 158**,** 1239-48.

SALLUSTO, F., CELLA, M., DANIELI, C. & LANZAVECCHIA, A. 1995. Dendritic cells use macropinocytosis and the mannose receptor to concentrate macromolecules in the major histocompatibility complex class II compartment: downregulation by cytokines and bacterial products. *J Exp Med,* 182**,** 389-400.

SALLUSTO, F. & LANZAVECCHIA, A. 1994. Efficient presentation of soluble antigen by cultured human dendritic cells is maintained by granulocyte/macrophage colony-stimulating factor plus interleukin 4 and downregulated by tumor necrosis factor alpha. *J Exp Med,* 179**,** 1109-18.

SANDERSON, S. & SHASTRI, N. 1994. LacZ inducible, antigen/MHC-specific T cell hybrids. *Int Immunol,* 6**,** 369-76.

SARMA, V., LIN, Z., CLARK, L., RUST, B. M., TEWARI, M., NOELLE, R. J. & DIXIT, V. M. 1995. Activation of the B-cell surface receptor CD40 induces A20, a novel zinc finger protein that inhibits apoptosis. *J Biol Chem,* 270**,** 12343-6.

SAUTER, B., ALBERT, M. L., FRANCISCO, L., LARSSON, M., SOMERSAN, S. & BHARDWAJ, N. 2000. Consequences of cell death: exposure to necrotic tumor cells, but not primary tissue cells or apoptotic cells, induces the maturation of immunostimulatory dendritic cells. *J Exp Med,* 191**,** 423-34.

SCHLENNER, S. M., MADAN, V., BUSCH, K., TIETZ, A., LÄUFLE, C., COSTA, C., BLUM, C., FEHLING, H. J. & RODEWALD, H. R. 2010. Fate mapping reveals separate origins of T cells and myeloid lineages in the thymus. *Immunity,* 32**,** 426-36.

SCHNEERSON, R., BARRERA, O., SUTTON, A. & ROBBINS, J. B. 1980. Preparation, characterization, and immunogenicity of Haemophilus influenzae type b polysaccharide-protein conjugates. *J Exp Med,* 152**,** 361-76.

SCHNEERSON, R., ROBBINS, J. B., PARKE, J. C., BELL, C., SCHLESSELMAN, J. J., SUTTON, A., WANG, Z., SCHIFFMAN, G., KARPAS, A. & SHILOACH, J. 1986. Quantitative and qualitative analyses of serum antibodies elicited in adults by Haemophilus influenzae type b and pneumococcus type 6A capsular polysaccharide-tetanus toxoid conjugates. *Infect Immun,* 52**,** 519-28.

SCHNEIDER, L. C. 2000. X-linked hyper IgM syndrome. *Clin Rev Allergy Immunol,* 19**,** 205-15.

SCHOENBERGER, S. P., TOES, R. E., VAN DER VOORT, E. I., OFFRINGA, R. & MELIEF, C. J. 1998. T-cell help for cytotoxic T lymphocytes is mediated by CD40-CD40L interactions. *Nature,* 393**,** 480-3.

SCHULZ, H., BOHLIUS, J. F., TRELLE, S., SKOETZ, N., REISER, M., KOBER, T., SCHWARZER, G., HEROLD, M., DREYLING, M., HALLEK, M. & ENGERT, A. 2007. Immunochemotherapy with rituximab and overall survival in patients with indolent or mantle cell lymphoma: a systematic review and meta-analysis. *J Natl Cancer Inst,* 99**,** 706-14.

SCHUSTER, S. J., NEELAPU, S. S., GAUSE, B. L., JANIK, J. E., MUGGIA, F. M., GOCKERMAN, J. P., WINTER, J. N., FLOWERS, C. R., NIKCEVICH, D. A., SOTOMAYOR, E. M., MCGAUGHEY, D. S., JAFFE, E. S., CHONG, E. A., REYNOLDS, C. W., BERRY, D. A., SANTOS, C. F., POPA, M. A., MCCORD, A. M. & KWAK, L. W. 2011. Vaccination with patient-specific tumor-derived antigen in first remission improves disease-free survival in follicular lymphoma. *J Clin Oncol,* 29**,** 2787-94.

SCHUSTER, S. J., NEELAPU, S. S., GAUSE, B. L., MUGGIA, F. M., GOCKERMAN, J. P., SOTOMAYOR, E. M., WINTER, J. N., FLOWERS, C. R., STERGIOU, A. M. & KWAK, L. W. 2009. Idiotype vaccine therapy (BiovaxID) in follicular lymphoma in first complete remission: phase III clinical trial results. *Journal of Clinical Oncology,* 27.

SCHWARTZ, R. H. 1990. A cell culture model for T lymphocyte clonal anergy. *Science,* 248**,** 1349-56.

SCHWARTZENTRUBER, D. J., LAWSON, D. H., RICHARDS, J. M., CONRY, R. M., MILLER, D. M., TREISMAN, J., GAILANI, F., RILEY, L., CONLON, K., POCKAJ, B., KENDRA, K. L., WHITE, R. L., GONZALEZ, R., KUZEL, T. M., CURTI, B., LEMING, P. D., WHITMAN, E. D., BALKISSOON, J., REINTGEN, D. S., KAUFMAN, H., MARINCOLA, F. M., MERINO, M. J., ROSENBERG, S. A., CHOYKE, P., VENA, D. & HWU, P. 2011. gp100 peptide vaccine and interleukin-2 in patients with advanced melanoma. *N Engl J Med,* 364**,** 2119-27.

SEDER, R. A. & AHMED, R. 2003. Similarities and differences in CD4+ and CD8+ effector and memory T cell generation. *Nat Immunol,* 4**,** 835-42.

SEDER, R. A., PAUL, W. E., DAVIS, M. M. & FAZEKAS DE ST GROTH, B. 1992. The presence of interleukin 4 during in vitro priming determines the lymphokine-producing potential of CD4+ T cells from T cell receptor transgenic mice. *J Exp Med,* 176**,** 1091-8.

SELIGMAN, S. J. & GOULD, E. A. 2004. Live flavivirus vaccines: reasons for caution. *Lancet,* 363**,** 2073-5.

SERBINA, N. V., SALAZAR-MATHER, T. P., BIRON, C. A., KUZIEL, W. A. & PAMER, E. G. 2003. TNF/iNOS-producing dendritic cells mediate innate immune defense against bacterial infection. *Immunity,* 19**,** 59-70.

SERCARZ, E. E., LEHMANN, P. V., AMETANI, A., BENICHOU, G., MILLER, A. & MOUDGIL, K. 1993. Dominance and crypticity of T cell antigenic determinants. *Annu Rev Immunol,* 11**,** 729-66.

SERWOLD, T. & SHASTRI, N. 1999. Specific proteolytic cleavages limit the diversity of the pool of peptides available to MHC class I molecules in living cells. *J Immunol,* 162**,** 4712-9.

SEUBERT, A., MONACI, E., PIZZA, M., O'HAGAN, D. T. & WACK, A. 2008. The adjuvants aluminum hydroxide and MF59 induce monocyte and granulocyte chemoattractants and enhance monocyte differentiation toward dendritic cells. *J Immunol,* 180**,** 5402-12.

SHAH, J. A., DARRAH, P. A., AMBROZAK, D. R., TURON, T. N., MENDEZ, S., KIRMAN, J., WU, C. Y., GLAICHENHAUS, N. & SEDER, R. A. 2003. Dendritic cells are responsible for the capacity of CpG oligodeoxynucleotides to act as an adjuvant for protective vaccine immunity against Leishmania major in mice. *J Exp Med,* 198**,** 281-91.

SHASTRI, N. & GONZALEZ, F. 1993. Endogenous generation and presentation of the ovalbumin peptide/Kb complex to T cells. *J Immunol,* 150**,** 2724-36.

SHIMONKEVITZ, R., COLON, S., KAPPLER, J. W., MARRACK, P. & GREY, H. M. 1984. Antigen recognition by H-2-restricted T cells. II. A tryptic ovalbumin peptide that substitutes for processed antigen. *J Immunol,* 133**,** 2067-74.

SHIROTA, H., SANO, K., HIRASAWA, N., TERUI, T., OHUCHI, K., HATTORI, T. & TAMURA, G. 2002. B cells capturing antigen conjugated with CpG oligodeoxynucleotides induce Th1 cells by elaborating IL-12. *J Immunol,* 169**,** 787-94.

SHIROTA, H., SANO, K., KIKUCHI, T., TAMURA, G. & SHIRATO, K. 2000. Regulation of murine airway eosinophilia and Th2 cells by antigen-conjugated CpG oligodeoxynucleotides as a novel antigen-specific immunomodulator. *J Immunol,* 164**,** 5575-82.

SKENE, C. D. & SUTTON, P. 2006. Saponin-adjuvanted particulate vaccines for clinical use. *Methods,* 40**,** 53-9.

SMITH, K. A. 2012. Louis pasteur, the father of immunology? *Front Immunol,* 3**,** 68.

SOARES, M. M., MEHTA, V. & FINN, O. J. 2001. Three different vaccines based on the 140-amino acid MUC1 peptide with seven tandemly repeated tumor-specific epitopes elicit distinct immune effector mechanisms in wild-type versus MUC1-transgenic mice with different potential for tumor rejection. *J Immunol,* 166**,** 6555-63.

SOLLINGER, D., EIßLER, R., LORENZ, S., STRAND, S., CHMIELEWSKI, S., AOQUI, C., SCHMADERER, C., BLUYSSEN, H., ZICHA, J., WITZKE, O., SCHERER, E., LUTZ, J.,

HEEMANN, U. & BAUMANN, M. 2014. Damage-associated molecular pattern activated Toll-like receptor 4 signalling modulates blood pressure in L-NAME-induced hypertension. *Cardiovasc Res,* 101**,** 464-72.

SON, Y. I., EGAWA, S., TATSUMI, T., REDLINGER, R. E., KALINSKI, P. & KANTO, T. 2002. A novel bulk-culture method for generating mature dendritic cells from mouse bone marrow cells. *J Immunol Methods,* 262**,** 145-57.

STEVENSON, G. T. & STEVENSON, F. K. 1975. Antibody to a molecularly-defined antigen confined to a tumour cell surface. *Nature,* 254**,** 714-6.

STEWART, V. A., MCGRATH, S. M., WALSH, D. S., DAVIS, S., HESS, A. S., WARE, L. A., KESTER, K. E., CUMMINGS, J. F., BURGE, J. R., VOSS, G., DELCHAMBRE, M., GARÇON, N., TANG, D. B., COHEN, J. D. & HEPPNER, D. G. 2006. Pre-clinical evaluation of new adjuvant formulations to improve the immunogenicity of the malaria vaccine RTS,S/AS02A. *Vaccine,* 24**,** 6483-92.

STOUTE, J. A., SLAOUI, M., HEPPNER, D. G., MOMIN, P., KESTER, K. E., DESMONS, P., WELLDE, B. T., GARÇON, N., KRZYCH, U. & MARCHAND, M. 1997. A preliminary evaluation of a recombinant circumsporozoite protein vaccine against Plasmodium falciparum malaria. RTS,S Malaria Vaccine Evaluation Group. *N Engl J Med,* 336**,** 86-91.

SULLIVAN, B. M., JUEDES, A., SZABO, S. J., VON HERRATH, M. & GLIMCHER, L. H. 2003. Antigen-driven effector CD8 T cell function regulated by T-bet. *Proc Natl Acad Sci U S A,* 100**,** 15818-23.

SUN, H., POLLOCK, K. G. & BREWER, J. M. 2003. Analysis of the role of vaccine adjuvants in modulating dendritic cell activation and antigen presentation in vitro. *Vaccine,* 21**,** 849-55.

SUZUKI, K., GRIGOROVA, I., PHAN, T. G., KELLY, L. M. & CYSTER, J. G. 2009. Visualizing B cell capture of cognate antigen from follicular dendritic cells. *J Exp Med,* 206**,** 1485-93.

TAKADA, H. & KOTANI, S. 1989. Structural requirements of lipid A for endotoxicity and other biological activities. *Crit Rev Microbiol,* 16**,** 477-523.

TAKAYAMA, K., QURESHI, N., RIBI, E. & CANTRELL, J. L. 1984. Separation and characterization of toxic and nontoxic forms of lipid A. *Rev Infect Dis,* 6**,** 439-43.

TAKAYAMA, K., RIBI, E. & CANTRELL, J. L. 1981. Isolation of a nontoxic lipid A fraction containing tumor regression activity. *Cancer Res,* 41**,** 2654-7.

TANIGUCHI, T., MATSUI, H., FUJITA, T., TAKAOKA, C., KASHIMA, N., YOSHIMOTO, R. & HAMURO, J. 1983. Structure and expression of a cloned cDNA for human interleukin-2. *Nature,* 302**,** 305-10.

TAO, X., GRANT, C., CONSTANT, S. & BOTTOMLY, K. 1997. Induction of IL-4-producing CD4+ T cells by antigenic peptides altered for TCR binding. *J Immunol,* 158**,** 4237-44.

TAYLOR, A., VERHAGEN, J., BLASER, K., AKDIS, M. & AKDIS, C. A. 2006. Mechanisms of immune suppression by interleukin-10 and transforming growth factor-beta: the role of T regulatory cells. *Immunology,* 117**,** 433-42.

TIGHE, H., TAKABAYASHI, K., SCHWARTZ, D., VAN NEST, G., TUCK, S., EIDEN, J. J., KAGEY-SOBOTKA, A., CRETICOS, P. S., LICHTENSTEIN, L. M., SPIEGELBERG, H. L. & RAZ, E. 2000. Conjugation of immunostimulatory DNA to the short ragweed allergen amb a 1 enhances its immunogenicity and reduces its allergenicity. *J Allergy Clin Immunol,* 106**,** 124-34.

TIMMERMAN, J. M., CASPAR, C. B., LAMBERT, S. L., SYRENGELAS, A. D. & LEVY, R. 2001. Idiotype-encoding recombinant adenoviruses provide protective immunity against murine B-cell lymphomas. *Blood,* 97**,** 1370-7.

TOMURA, M., HATA, A., MATSUOKA, S., SHAND, F. H., NAKANISHI, Y., IKEBUCHI, R., UEHA, S., TSUTSUI, H., INABA, K., MATSUSHIMA, K., MIYAWAKI, A., KABASHIMA, K., WATANABE, T. & KANAGAWA, O. 2014. Tracking and quantification of dendritic cell migration and antigen trafficking between the skin and lymph nodes. *Sci Rep,* 4**,** 6030.

TOPALIAN, S. L., DRAKE, C. G. & PARDOLL, D. M. 2012. Targeting the PD-1/B7-H1(PD-L1) pathway to activate anti-tumor immunity. *Curr Opin Immunol,* 24**,** 207-12.

TURLEY, S. J., INABA, K., GARRETT, W. S., EBERSOLD, M., UNTERNAEHRER, J., STEINMAN, R. M. & MELLMAN, I. 2000. Transport of peptide-MHC class II complexes in developing dendritic cells. *Science,* 288**,** 522-7.

TUTT, A. L., O'BRIEN, L., HUSSAIN, A., CROWTHER, G. R., FRENCH, R. R. & GLENNIE, M. J. 2002. T cell immunity to lymphoma following treatment with anti-CD40 monoclonal antibody. *J Immunol,* 168**,** 2720-8.

UNDERHILL, D. M., BASSETTI, M., RUDENSKY, A. & ADEREM, A. 1999. Dynamic interactions of macrophages with T cells during antigen presentation. *J Exp Med,* 190**,** 1909-14.

VALLÉ, A., ZUBER, C. E., DEFRANCE, T., DJOSSOU, O., DE RIE, M. & BANCHEREAU, J. 1989. Activation of human B lymphocytes through CD40 and interleukin 4. *Eur J Immunol,* 19**,** 1463-7.

VAN KOOTEN, C. & BANCHEREAU, J. 2000. CD40-CD40 ligand. *J Leukoc Biol,* 67**,** 2-17.

VELDHOEN, M., HOCKING, R. J., ATKINS, C. J., LOCKSLEY, R. M. & STOCKINGER, B. 2006. TGFbeta in the context of an inflammatory cytokine milieu supports de novo differentiation of IL-17-producing T cells. *Immunity,* 24**,** 179-89.

VELLA, P. P., MARBURG, S., STAUB, J. M., KNISKERN, P. J., MILLER, W., HAGOPIAN, A., IP, C., TOLMAN, R. L., RUSK, C. M. & CHUPAK, L. S. 1992. Immunogenicity of conjugate vaccines consisting of pneumococcal capsular polysaccharide types 6B, 14, 19F, and 23F and a meningococcal outer membrane protein complex. *Infect Immun,* 60**,** 4977-83.

VERDIJK, P., VAN VEELEN, P. A., DE RU, A. H., HENSBERGEN, P. J., MIZUNO, K., KOERTEN, H. K., KONING, F., TENSEN, C. P. & MOMMAAS, A. M. 2004. Morphological changes during dendritic cell maturation correlate with cofilin activation and translocation to the cell membrane. *European journal of immunology,* 34**,** 156-64.

VERMAELEN, K. Y., CARRO-MUINO, I., LAMBRECHT, B. N. & PAUWELS, R. A. 2001. Specific migratory dendritic cells rapidly transport antigen from the airways to the thoracic lymph nodes. *J Exp Med,* 193**,** 51-60.

VESIKARI, T., GROTH, N., KARVONEN, A., BORKOWSKI, A. & PELLEGRINI, M. 2009. MF59-adjuvanted influenza vaccine (FLUAD) in children: safety and immunogenicity following a second year seasonal vaccination. *Vaccine,* 27**,** 6291-5.

VILLADANGOS, J. A. 2001. Presentation of antigens by MHC class II molecules: getting the most out of them. *Mol Immunol,* 38**,** 329-46.

VITETTA, E. S., OHARA, J., MYERS, C. D., LAYTON, J. E., KRAMMER, P. H. & PAUL, W. E. 1985. Serological, biochemical, and functional identity of B cell-stimulatory factor 1 and B cell differentiation factor for IgG1. *J Exp Med,* 162**,** 1726-31.

VONDERHEIDE, R. H., FLAHERTY, K. T., KHALIL, M., STUMACHER, M. S., BAJOR, D. L., HUTNICK, N. A., SULLIVAN, P., MAHANY, J. J., GALLAGHER, M., KRAMER, A., GREEN, S. J., O'DWYER, P. J., RUNNING, K. L., HUHN, R. D. & ANTONIA, S. J. 2007. Clinical activity and immune modulation in cancer patients treated with CP-870,893, a novel CD40 agonist monoclonal antibody. *J Clin Oncol,* 25**,** 876-83.

VONDERHEIDE, R. H. & GLENNIE, M. J. 2013. Agonistic CD40 antibodies and cancer therapy. *Clin Cancer Res,* 19**,** 1035-43.

VREDEN, S. G., VERHAVE, J. P., OETTINGER, T., SAUERWEIN, R. W. & MEUWISSEN, J. H. 1991. Phase I clinical trial of a recombinant malaria vaccine consisting of the circumsporozoite repeat region of Plasmodium falciparum coupled to hepatitis B surface antigen. *Am J Trop Med Hyg,* 45**,** 533-8.

WAKITA, T., PIETSCHMANN, T., KATO, T., DATE, T., MIYAMOTO, M., ZHAO, Z., MURTHY, K., HABERMANN, A., KRÄUSSLICH, H. G., MIZOKAMI, M., BARTENSCHLAGER, R. & LIANG,

T. J. 2005. Production of infectious hepatitis C virus in tissue culture from a cloned viral genome. *Nat Med,* 11**,** 791-6.

WALSH, K. P. & MILLS, K. H. 2013. Dendritic cells and other innate determinants of T helper cell polarisation. *Trends Immunol,* 34**,** 521-30.

WANG, J. Y., HARLEY, R. H. & GALEN, J. E. 2013. Novel methods for expression of foreign antigens in live vector vaccines. *Hum Vaccin Immunother,* 9**,** 1558-64.

WANG, Y., RAHMAN, D. & LEHNER, T. 2012. A comparative study of stress-mediated immunological functions with the adjuvanticity of alum. *J Biol Chem,* 287**,** 17152-60.

WASKOW, C., LIU, K., DARRASSE-JÈZE, G., GUERMONPREZ, P., GINHOUX, F., MERAD, M., SHENGELIA, T., YAO, K. & NUSSENZWEIG, M. 2008. The receptor tyrosine kinase Flt3 is required for dendritic cell development in peripheral lymphoid tissues. *Nat Immunol,* 9**,** 676-83.

WATANABE, J., MIYAZAKI, Y., ZIMMERMAN, G. A., ALBERTINE, K. H. & MCINTYRE, T. M. 2003. Endotoxin contamination of ovalbumin suppresses murine immunologic responses and development of airway hyper-reactivity. *J Biol Chem,* 278**,** 42361-8.

WELLS, J. W., DARLING, D., FARZANEH, F. & GALEA-LAURI, J. 2005. Influence of interleukin-4 on the phenotype and function of bone marrow-derived murine dendritic cells generated under serum-free conditions. *Scand J Immunol,* 61**,** 251-9.

WENZEL, J., UERLICH, M., HALLER, O., BIEBER, T. & TUETING, T. 2005. Enhanced type I interferon signaling and recruitment of chemokine receptor CXCR3-expressing lymphocytes into the skin following treatment with the TLR7-agonist imiquimod. *J Cutan Pathol,* 32**,** 257-62.

WEST, M. A., WALLIN, R. P., MATTHEWS, S. P., SVENSSON, H. G., ZARU, R., LJUNGGREN, H. G., PRESCOTT, A. R. & WATTS, C. 2004. Enhanced dendritic cell antigen capture via toll-like receptor-induced actin remodeling. *Science,* 305**,** 1153-7.

WHITMIRE, J. K., TAN, J. T. & WHITTON, J. L. 2005. Interferon-gamma acts directly on CD8+ T cells to increase their abundance during virus infection. *J Exp Med,* 201**,** 1053-9.

WHO 2006. WHO position paper on Haemophilus influenzae type b conjugate vaccines. (Replaces WHO position paper on Hib vaccines previously published in the Weekly Epidemiological Record. *Wkly Epidemiol Rec,* 81**,** 445-52.

WHO. 2014. Fact sheet number 114 - Poliomyelitis. Available: http://www.who.int/mediacentre/factsheets/fs114/en/.

WHO. 2013. Haemophilus influenzae type b (Hib) Vaccination Position Paper - July 2013. *Releve epidemiologique hebdomadaire / Section d'hygiene du Secretariat de la Societe des Nations = Weekly epidemiological record / Health Section of the Secretariat of the League of Nations,* 88**,** 413-26.

WIEDERMANN, G., AMBROSCH, F., KOLLARITSCH, H., HOFMANN, H., KUNZ, C., D'HONDT, E., DELEM, A., ANDRÉ, F. E., SAFARY, A. & STÉPHENNE, J. 1990. Safety and immunogenicity of an inactivated hepatitis A candidate vaccine in healthy adult volunteers. *Vaccine,* 8**,** 581-4.

WILLE-REECE, U., FLYNN, B. J., LORÉ, K., KOUP, R. A., KEDL, R. M., MATTAPALLIL, J. J., WEISS, W. R., ROEDERER, M. & SEDER, R. A. 2005. HIV Gag protein conjugated to a Toll-like receptor 7/8 agonist improves the magnitude and quality of Th1 and CD8+ T cell responses in nonhuman primates. *Proc Natl Acad Sci U S A,* 102**,** 15190-4.

WILSCHUT, J. 2009. Influenza vaccines: the virosome concept. *Immunol Lett,* 122**,** 118-21.

WILSON, N. S., EL-SUKKARI, D., BELZ, G. T., SMITH, C. M., STEPTOE, R. J., HEATH, W. R., SHORTMAN, K. & VILLADANGOS, J. A. 2003. Most lymphoid organ dendritic cell types are phenotypically and functionally immature. *Blood,* 102**,** 2187-94.

WILSON, N. S., EL-SUKKARI, D. & VILLADANGOS, J. A. 2004. Dendritic cells constitutively present self antigens in their immature state in vivo and regulate antigen presentation by controlling the rates of MHC class II synthesis and endocytosis. *Blood,* 103**,** 2187-95.

WONG, C. K., HO, C. Y., KO, F. W., CHAN, C. H., HO, A. S., HUI, D. S. & LAM, C. W. 2001. Proinflammatory cytokines (IL-17, IL-6, IL-18 and IL-12) and Th cytokines (IFN-gamma, IL-4, IL-10 and IL-13) in patients with allergic asthma. *Clin Exp Immunol,* 125**,** 177-83.

WORKMAN, P., ABOAGYE, E. O., BALKWILL, F., BALMAIN, A., BRUDER, G., CHAPLIN, D. J., DOUBLE, J. A., EVERITT, J., FARNINGHAM, D. A., GLENNIE, M. J., KELLAND, L. R., ROBINSON, V., STRATFORD, I. J., TOZER, G. M., WATSON, S., WEDGE, S. R., ECCLES, S. A. & INSTITUTE, C. O. T. N. C. R. 2010. Guidelines for the welfare and use of animals in cancer research. *Br J Cancer,* 102**,** 1555-77.

WRIGHT, A. E. & SEMPLE, D. 1897. Remarks on Vaccination against Typhoid Fever. *Br Med J,* 1**,** 256-9.

WRIGHT, T. C., BOSCH, F. X., FRANCO, E. L., CUZICK, J., SCHILLER, J. T., GARNETT, G. P. & MEHEUS, A. 2006. Chapter 30: HPV vaccines and screening in the prevention of cervical cancer; conclusions from a 2006 workshop of international experts. *Vaccine,* 24 Suppl 3**,** S3/251-61.

WU, D., JI, S. & HU, T. 2013. Development of pneumococcal polysaccharide conjugate vaccine with long spacer arm. *Vaccine,* 31**,** 5623-6.

XU, J., FOY, T. M., LAMAN, J. D., ELLIOTT, E. A., DUNN, J. J., WALDSCHMIDT, T. J., ELSEMORE, J., NOELLE, R. J. & FLAVELL, R. A. 1994. Mice deficient for the CD40 ligand. *Immunity,* 1**,** 423-31.

YANG, Y., HUANG, C. T., HUANG, X. & PARDOLL, D. M. 2004. Persistent Toll-like receptor signals are required for reversal of regulatory T cell-mediated CD8 tolerance. *Nat Immunol,* 5**,** 508-15.

YOSHINO, N., ENDO, M., KANNO, H., MATSUKAWA, N., TSUTSUMI, R., TAKESHITA, R. & SATO, S. 2013. Polymyxins as novel and safe mucosal adjuvants to induce humoral immune responses in mice. *PLoS One,* 8**,** e61643.

ZEPP, F. 2010. Principles of vaccine design-Lessons from nature. *Vaccine,* 28 Suppl 3**,** C14-24.

ZHANG, J., RAPER, A., SUGITA, N., HINGORANI, R., SALIO, M., PALMOWSKI, M. J., CERUNDOLO, V. & CROCKER, P. R. 2006. Characterization of Siglec-H as a novel endocytic receptor expressed on murine plasmacytoid dendritic cell precursors. *Blood,* 107**,** 3600-8.

ZHOU, Q., HO, A. W., SCHLITZER, A., TANG, Y., WONG, K. H., WONG, F. H., CHUA, Y. L., ANGELI, V., MORTELLARO, A., GINHOUX, F. & KEMENY, D. M. 2014. GM-CSF-licensed CD11b+ lung dendritic cells orchestrate Th2 immunity to Blomia tropicalis. *J Immunol,* 193**,** 496-509.